MULTIMODALITY IMAGING IN CHRONIC CORONARY SYNDROME

EDITED BY: Joao Bicho Augusto, Steffen Erhard Petersen, Gianluca Pontone and Bernhard L. Gerber
PUBLISHED IN: Frontiers in Cardiovascular Medicine

frontiers Research Topics

frontiers

ISSN 1664-8714
ISBN 978-2-88976-676-5
DOI 10.3389/978-2-88976-676-5

About Frontiers

Frontiers is more than just an open-access publisher of scholarly articles: it is a pioneering approach to the world of academia, radically improving the way scholarly research is managed. The grand vision of Frontiers is a world where all people have an equal opportunity to seek, share and generate knowledge. Frontiers provides immediate and permanent online open access to all its publications, but this alone is not enough to realize our grand goals.

Frontiers Journal Series

The Frontiers Journal Series is a multi-tier and interdisciplinary set of open-access, online journals, promising a paradigm shift from the current review, selection and dissemination processes in academic publishing. All Frontiers journals are driven by researchers for researchers; therefore, they constitute a service to the scholarly community. At the same time, the Frontiers Journal Series operates on a revolutionary invention, the tiered publishing system, initially addressing specific communities of scholars, and gradually climbing up to broader public understanding, thus serving the interests of the lay society, too.

Dedication to Quality

Each Frontiers article is a landmark of the highest quality, thanks to genuinely collaborative interactions between authors and review editors, who include some of the world's best academicians. Research must be certified by peers before entering a stream of knowledge that may eventually reach the public - and shape society; therefore, Frontiers only applies the most rigorous and unbiased reviews.
Frontiers revolutionizes research publishing by freely delivering the most outstanding research, evaluated with no bias from both the academic and social point of view. By applying the most advanced information technologies, Frontiers is catapulting scholarly publishing into a new generation.

What are Frontiers Research Topics?

Frontiers Research Topics are very popular trademarks of the Frontiers Journals Series: they are collections of at least ten articles, all centered on a particular subject. With their unique mix of varied contributions from Original Research to Review Articles, Frontiers Research Topics unify the most influential researchers, the latest key findings and historical advances in a hot research area! Find out more on how to host your own Frontiers Research Topic or contribute to one as an author by contacting the Frontiers Editorial Office: frontiersin.org/about/contact

MULTIMODALITY IMAGING IN CHRONIC CORONARY SYNDROME

Topic Editors:
Joao Bicho Augusto, Barts Heart Centre, United Kingdom
Steffen Erhard Petersen, Queen Mary University of London, United Kingdom
Gianluca Pontone, Monzino Cardiology Center (IRCCS), Italy
Bernhard L. Gerber, Cliniques Universitaires Saint-Luc, Belgium

Citation: Augusto, J. B., Petersen, S. E., Pontone, G., Gerber, B. L., eds. (2022). Multimodality Imaging in Chronic Coronary Syndrome. Lausanne: Frontiers Media SA. doi: 10.3389/978-2-88976-676-5

Table of Contents

05 ***A LASSO-Derived Risk Model for Subclinical CAC Progression in Asian Population With an Initial Score of Zero***
Yun-Ju Wu, Guang-Yuan Mar, Ming-Ting Wu and Fu-Zong Wu

15 ***Vasodilator Myocardial Perfusion Cardiac Magnetic Resonance Imaging Is Superior to Dobutamine Stress Echocardiography in the Detection of Relevant Coronary Artery Stenosis: A Systematic Review and Meta-Analysis on Their Diagnostic Accuracy***
Sebastian M. Haberkorn, Sandra I. Haberkorn, Florian Bönner, Malte Kelm, Gareth Hopkin and Steffen E. Petersen

28 ***Commentary: Vasodilator Myocardial Perfusion Cardiac Magnetic Resonance Imaging Is Superior to Dobutamine Stress Echocardiography in the Detection of Relevant Coronary Artery Stenosis: A Systematic Review and Meta-Analysis on Their Diagnostic Accuracy***
Attila Kardos, Roxy Senior and Harald Becher

30 ***What Is the Clinical Impact of Stress CMR After the ISCHEMIA Trial?***
Théo Pezel, Luis Miguel Silva, Adriana Aparecia Bau, Adherbal Teixiera, Michael Jerosch-Herold and Otávio R. Coelho-Filho

41 ***Agreement in Left Ventricular Function Measured by Echocardiography and Cardiac Magnetic Resonance in Patients With Chronic Coronary Total Occlusion***
Jiahui Li, Lijun Zhang, Yueli Wang, Huijuan Zuo, Rongchong Huang, Xueyao Yang, Ye Han, Yi He and Xiantao Song

49 ***Coronary Magnetic Resonance Angiography in Chronic Coronary Syndromes***
Reza Hajhosseiny, Camila Munoz, Gastao Cruz, Ramzi Khamis, Won Yong Kim, Claudia Prieto and René M. Botnar

66 ***Non-invasive Imaging in Patients With Chronic Total Occlusions of the Coronary Arteries—What Does the Interventionalist Need for Success?***
Johannes Kersten, Nina Eberhardt, Vikas Prasad, Mirjam Keßler, Sinisa Markovic, Johannes Mörike, Nicoleta Nita, Tilman Stephan, Marijana Tadic, Temsgen Tesfay, Wolfgang Rottbauer and Dominik Buckert

78 ***Artificial Intelligence Based Multimodality Imaging: A New Frontier in Coronary Artery Disease Management***
Riccardo Maragna, Carlo Maria Giacari, Marco Guglielmo, Andrea Baggiano, Laura Fusini, Andrea Igoren Guaricci, Alexia Rossi, Mark Rabbat and Gianluca Pontone

96 ***Clinical Application of Dynamic Contrast Enhanced Perfusion Imaging by Cardiovascular Magnetic Resonance***
Russell Franks, Sven Plein and Amedeo Chiribiri

109 ***Non-invasive Ischaemia Testing in Patients With Prior Coronary Artery Bypass Graft Surgery: Technical Challenges, Limitations, and Future Directions***
Andreas Seraphim, Kristopher D. Knott, Joao B. Augusto, Katia Menacho, Sara Tyebally, Benjamin Dowsing, Sanjeev Bhattacharyya, Leon J. Menezes, Daniel A. Jones, Rakesh Uppal, James C. Moon and Charlotte Manisty

128 ***Non-invasive Multimodality Imaging of Coronary Vulnerable Patient***
Marjorie Canu, Alexis Broisat, Laurent Riou, Gerald Vanzetto, Daniel Fagret, Catherine Ghezzi, Loic Djaileb and Gilles Barone-Rochette

136 ***The Role of Multimodality Imaging for Percutaneous Coronary Intervention in Patients With Chronic Total Occlusions***
Eleonora Melotti, Marta Belmonte, Carlo Gigante, Vincenzo Mallia, Saima Mushtaq, Edoardo Conte, Danilo Neglia, Gianluca Pontone, Carlos Collet, Jeroen Sonck, Luca Grancini, Antonio L. Bartorelli and Daniele Andreini

frontiers in Cardiovascular Medicine

ORIGINAL RESEARCH
published: 15 January 2021
doi: 10.3389/fcvm.2020.619798

A LASSO-Derived Risk Model for Subclinical CAC Progression in Asian Population With an Initial Score of Zero

Yun-Ju Wu[1,2], *Guang-Yuan Mar*[3], *Ming-Ting Wu*[1,4] *and Fu-Zong Wu*[1,4,5]*

[1] Department of Radiology, Kaohsiung Veterans General Hospital, Kaohsiung, Taiwan, [2] Department of Health Care Administration, Chang Jung Christian University, Tainan, Taiwan, [3] Physical Examination Center, Kaohsiung Veterans General Hospital, Kaohsiung, Taiwan, [4] Faculty of Medicine, School of Medicine, National Yang-Ming University, Taipei, Taiwan, [5] Department of Medical Imaging and Radiology, Shu-Zen Junior College of Medicine and Management, Kaohsiung, Taiwan

Background: This study is aimed at developing a prediction nomogram for subclinical coronary atherosclerosis in an Asian population with baseline zero score, and to compare its discriminatory ability with Framingham risk score (FRS) and atherosclerotic cardiovascular disease (ASCVD) models.

Methods: Clinical characteristics, physical examination, and laboratory profiles of 830 subjects were retrospectively reviewed. Subclinical coronary atherosclerosis in term of Coronary artery calcification (CAC) progression was the primary endpoint. A nomogram was established based on a least absolute shrinkage and selection operator (LASSO)-derived logistic model. The discrimination and calibration ability of this nomogram was evaluated by Hosmer–Lemeshow test and calibration curves in the training and validation cohort.

Results: Of the 830 subjects with baseline zero score with the average follow-up period of 4.55 ± 2.42 year in the study, these subjects were randomly placed into the training set or validation set at a ratio of 2.8:1. These study results showed in the 612 subjects with baseline zero score, 145 (23.69%) subjects developed CAC progression in the training cohort ($N = 612$), while in the validation cohort ($N = 218$), 51 (23.39%) subjects developed CAC progression. This LASSO-derived nomogram included the following 10 predictors: "sex," age," "hypertension," "smoking habit," "Gamma-Glutamyl Transferase (GGT)," "C-reactive protein (CRP)," "high-density lipoprotein cholesterol (HDL-C)," "cholesterol," "waist circumference," and "follow-up period." Compared with the FRS and ASCVD models, this LASSO-derived nomogram had higher diagnostic performance and lower Akaike information criterion (AIC) and Bayesian information criterion (BIC) value. The discriminative ability, as determined by the area under receiver operating characteristic curve was 0.780 (95% confidence interval: 0.731–0.829) in the training cohort and 0.836 (95% confidence interval: 0.761–0.911) in the validation cohort. Moreover, satisfactory calibration was confirmed by Hosmer–Lemeshow test with *P*-values of 0.654 and 0.979 in the training cohort and validation cohort.

OPEN ACCESS

Edited by:
Steffen Erhard Petersen, Queen Mary University of London, United Kingdom

Reviewed by:
Riccardo Liga, Pisana University Hospital, Italy
Nay Aung, Queen Mary University of London, United Kingdom

***Correspondence:**
Fu-Zong Wu
cmvwu1029@gmail.com

Specialty section:
This article was submitted to Cardiovascular Imaging, a section of the journal Frontiers in Cardiovascular Medicine

Received: *21 October 2020*
Accepted: *11 December 2020*
Published: *15 January 2021*

Citation:
Wu Y-J, Mar G-Y, Wu M-T and Wu F-Z (2021) A LASSO-Derived Risk Model for Subclinical CAC Progression in Asian Population With an Initial Score of Zero. Front. Cardiovasc. Med. 7:619798. doi: 10.3389/fcvm.2020.619798

Conclusions: This validated nomogram provided a useful predictive value for subclinical coronary atherosclerosis in subjects with baseline zero score, and could provide clinicians and patients with the primary preventive strategies timely in individual-based preventive cardiology.

Keywords: zero score, CAC progression, subclinical atherosclerosis, prediction model, nomogram

INTRODUCTION

Subclinical atherosclerosis is a chronic, progressive, and inflammatory disease of the arterial wall with a long-term asymptomatic phase (1–3). In recent years, non-invasive imaging modalities have been proposed to help early detect and monitor the burden of subclinical atherosclerosis. The introduction of several non-invasive imaging modalities has given the possibility to diagnose subclinical atherosclerosis easily in asymptomatic subjects, including carotid ultrasonography and coronary calcium assessment by computed tomography (CT). Coronary artery calcification (CAC) could be considered a surrogate marker of subclinical coronary atherosclerotic burden (2). Agatston score of zero is known to be a powerful negative cardiovascular event predictor with a long-term warranty period ("the power of zero") (4–8). PESA study has demonstrated that male, age, high-density lipoprotein cholesterol (LDL-C), hemoglobin A1c ($HbA1_c$), vascular cell adhesion molecule-1 (VCAM) and cystatin are significant biologic predictors associated with subclinical atherosclerotic lesions in Western asymptomatic population with low cardiovascular risk (9). Previous studies have investigated the risk factors associated with the warrant period of zero score in Asian population (8, 10, 11). To the best of our knowledge, no previous studies have evaluated early preventive models for predicting the risk of subclinical coronary atherosclerosis in term of CAC progression in Asian population with baseline zero score. Therefore, we aim to develop a LASSO (least absolute shrinkage and selection operator)-based risk model for the prediction of subclinical CAC progression with an initial score of zero in a hospital-based dataset, and to compare its discriminatory ability with other prediction models, such as Framingham risk score (FRS) and atherosclerotic cardiovascular disease (ASCVD) score.

Abbreviations: CT, computed tomography; CAC, coronary artery calcification; LDL-C, low-density lipoprotein cholesterol; HDL-C, high-density lipoprotein cholesterol; HbA1c, hemoglobin A1c; VCAM, vascular cell adhesion molecule-1; FRS, Framingham risk score; ASCVD, atherosclerotic cardiovascular disease; BMI, Body mass index; SBP, systolic blood pressure; DBP, diastolic blood pressure; CRP, C-reactive protein; GGT, Gamma-Glutamyl Transferase; CTA, CT angiography; SCCT, Society of Cardiovascular Computed Tomography; LASSO, least absolute shrinkage and selection operator; AIC, Akaike information criterion; BIC, Bayesian information criterion; CAD-RADS^{TM}, Coronary Artery Disease Reporting and Data System; OR, odds ratio; CVHI, cardiovascular health index; CIMT, carotid intima-media thickness; MetS, metabolic syndrome.

METHODS

Study Population and Baseline Characteristics

Eight hundred and thirty consecutive subjects were included in this study from April 2005 to December 2018 according to the inclusion criteria. The inclusion criteria for this study are as follows: (1) all subjects with medical check-ups underwent two consecutive scans (CAC scan and coronary CT angiography) during the follow-up period; (2) all subjects must meet the criteria of zero score in the baseline scan. Because we did not use any human subjects or personally identifiable records in our study, informed consent was waived. The study protocol was approved by the institutional review boards of Kaohsiung Veterans General Hospital in accordance with the Declaration of Helsinki (IRB: VGHKS19-CT6–02). Clinical characteristics, physical examination, and laboratory profiles were retrospectively obtained from the patients' electronic medical records and reviewed by a trained study coordinator. Laboratory profiles were performed at the same day as the baseline CT scans. Clinical demographic characteristics included age, gender, BMI, current smoking habit, pack-year, hypertension, diabetes mellitus and follow-up period collected by patients' electronic medical records or questionnaire. A physical examination was also conducted to collect data on body mass index (BMI), systolic blood pressure (SBP), diastolic blood pressure (DBP), body-fat percentage, and waist circumference. Laboratory profiles were collected to obtain biochemical variables, including uric acid, Gamma-Glutamyl Transferase (GGT), fasting glucose, hemoglobin A1c (HbA1c), C-reactive protein (CRP), low-density lipoprotein cholesterol (LDL-C), high-density lipoprotein cholesterol (HDL-C), total cholesterol, and triglycerides level. Hypertension was defined as systolic blood pressure (SBP) $>$ 140 mmHg, diastolic blood pressure (DBP) $>$90 mmHg, or subjects with anti-hypertensive medications. Diabetes mellitus was diagnosed in subjects with additional oral anti-diabetic or insulin medications. Framingham risk score (%) in the first round, CAD-RADS categories in the first and final round, and CAC score in the final round were also recorded.

CT Imaging Acquisition

All subjects retrospectively underwent two consecutive scans in the first round and final round during the mean follow-up period of 4.55 $\pm$ 2.42 years. In brief, a non-contrast CAC scan was performed before the cardiac CT angiography on a 256 $\times$ 0.625-mm detector row CT system (Revolution CT, GE Healthcare,

Milwaukee, USA) or a 64 × 0.5-mm detector row CT system (Aquilion 64; Toshiba Medical Systems). CT acquisition protocol includes two sequential acquisitions.

First, a non-contrast CAC scan was performed with the following acquisition parameters: fixed tube voltage 120-kVp with reconstructed at 3 mm slice thickness. Secondly, a prospectively ECG-triggered cardiac CT angiography (CTA) was performed with the following parameters: fixed tube voltage of 120 kV, tube current modulation (mA modulation). CAC scoring was performed using the Agatston method with GE AW analysis software (12). Prior to cardiac CT angiography imaging, oral beta-blockers (metoprolol 100 mg) and sublingual nitroglycerin (nitrostat one tablet, 0.6 mg) were administered to all subjects without contraindication if the heart rate exceeded 65 beats per min. Intravenous contrast (Iopamidol 370) was administered at 5 mL/second followed by 40 mL 0.9% saline flush. Images were acquired and reconstructed at diastole (75–81% of the R-R interval) or at systole (37–43% of the R-R interval). All CT scans were reported by accredited cardiac radiologists. The severity of obstructive CAD with standardized reporting of individual segmental coronary stenosis was reported according to Coronary Artery Disease Reporting and Data System (CAD-RADS™), published in 2016 by the Society of Cardiovascular Computed Tomography (SCCT) (13).

Three Prediction Models for Subclinical CAC Progression

LASSO-Derived Prediction Model

We extracted 10 features through lasso regression to construct the new prediction model with the optimal value of lambda that minimizes the cross-validation error, and compares its prediction accuracy and discriminatory ability with other different prediction models, such as FRS model and ASCVD

TABLE 1 | Clinical features of the training and validation sets.

	Total patient cohort (n = 830)	Training set (n = 612)	Validation set (n = 218)	P-value
Age (years)	51.17 ± 8.24	51.26 ± 8.26	50.90 ± 8.19	0.576
Sex, *n* (%)				0.381
Male	555 (66.9%)	404 (66%)	151 (69.3%)	
Female	275 (33.1%)	208 (34%)	67 (30.7%)	
BMI (kg/m²)	24.72 ± 3.42	24.83 ± 3.40	24.41 ± 3.44	0.120
SBP (mmHg)	123.90 ± 16.99	124.23 ± 17.05	122.98 ± 16.84	0.355
DBP (mmHg)	78.13 ± 11.14	78.33 ± 11.14	77.58 ± 11.16	0.403
Hypertension, *n* (%)	245 (29.5%)	188 (30.7%)	57 (26.2%)	0.185
Smoking, *n* (%)	270 (32.5%)	194 (31.6%)	76 (34.9%)	0.303
DM, *n* (%)	104 (12.5%)	82 (13.4%)	22 (10.1%)	0.213
Uric acid (mg/dL)	6.37 ± 2.32	6.37 ± 2.52	6.39 ± 1.64	0.907
GGT (U/L)	42.18 ± 77.92	42.11 ± 72.26	42.36 ± 92.07	0.973
Fasting glucose (mg/dL)	99.85 ± 22.43	100.30 ± 22.76	98.57 ± 21.46	0.334
CRP (mg/dL)	0.21 ± 0.43	0.21 ± 0.48	0.18 ± 0.23	0.383
LDL-C (mg/dL)	116.29 ± 29.12	116.31 ± 29.22	116.25 ± 28.90	0.981
HDL-C (mg/dL)	47.16 ± 13.27	47.41 ± 13.33	46.47 ± 13.11	0.377
Cholesterol (mg/dL)	205.96 ± 37.48	206.76 ± 37.24	203.70 ± 38.15	0.306
Triglycerides (mg/dL)	151.98 ± 102.11	153.05 ± 100.21	148.96 ± 107.46	0.615
HbA1c (%)	5.88 ± 0.79	5.90 ± 0.83	5.83 ± 0.67	0.295
Body fat percentage (%)	23.97 ± 5.93	24.20 ± 5.82	23.34 ± 6.19	0.097
Waist circumference (cm)	85.70 ± 9.31	85.98 ± 9.29	84.93 ± 9.36	0.200
Follow-up period (year)	4.55 ± 2.42	4.59 ± 2.42	4.43 ± 2.41	0.416
First CAD-RADS categories (%)				0.260
0	682 (82.2%)	508 (84%)	174 (80%)	
≧ 1	143 (17.2%)	100 (16%)	43 (20%)	
Final CAD-RADS categories (%)				0.668
0	480 (58.1%)	356 (58.6%)	124 (56.9%)	
≧ 1	346 (41.9%)	252 (41.4%)	94 (43.1%)	
Framingham risk score (%)	12.79 ± 8.90	12.94 ± 9.00	12.40 ± 8.62	0.452
CAC score in the final round	5.17 ± 21.41	5.56 ± 23.59	4.05 ± 13.47	0.370

BMI, body mass index; SBP, systolic blood pressure; DBP, diastolic blood pressure; DM, diabetes mellitus; GGT, gamma-glutamyl transferase; CRP, c-reactive protein; LDL-C, low-density lipoprotein cholesterol; HDL-C, high-density lipoprotein cholesterol; HbA1c, hemoglobin A1c; CAD-RADS, the coronary artery disease - reporting and data system; CAC, coronary artery calcification.

model. In addition, we evaluated the discriminatory ability of different prediction models by using c-statistic, Akaike information criterion (AIC) and Bayesian information criterion (BIC). Higher c-statistic and lower AIC and BIC values were considered to indicate a more discriminatory model. Previous literature reviews have shown that original purpose of FRS and ASCVD models in 10-year cardiovascular event prediction (14, 15). However, there are some scientific merits of FRS and ASCVD models in subclinical atherosclerosis prediction according to recent studies (16, 17).

Framingham Risk Score (FRS) Model

FRS is the scoring system that is most commonly used to predict the 10-year cardiovascular events. The components of the FRS include age, sex, total cholesterol, HDL-C, systolic BP, DM, and smoking habit. A total FRS score was calculated for each eligible subject according to the algorithm developed by D'Agostini et al. (14). Current clinical guidelines recommend categorizing asymptomatic individuals into low (FRS < 10%), intermediate (10–20%), and high-risk subgroups (> 20%) for risk stratification.

Atherosclerotic Cardiovascular Disease (ASCVD) Model

The ASCVD score includes predictors as age, sex, race, smoking habit, systolic blood pressure, diastolic blood pressure, and diabetes for prediction 10-year fatal outcome in individuals aged 40 to 65 years (15). Individuals were classified into low-risk (ASCVD <7.5%), and high-risk (ASCVD≧7.5%) subgroups for ASCVD risk stratification (18).

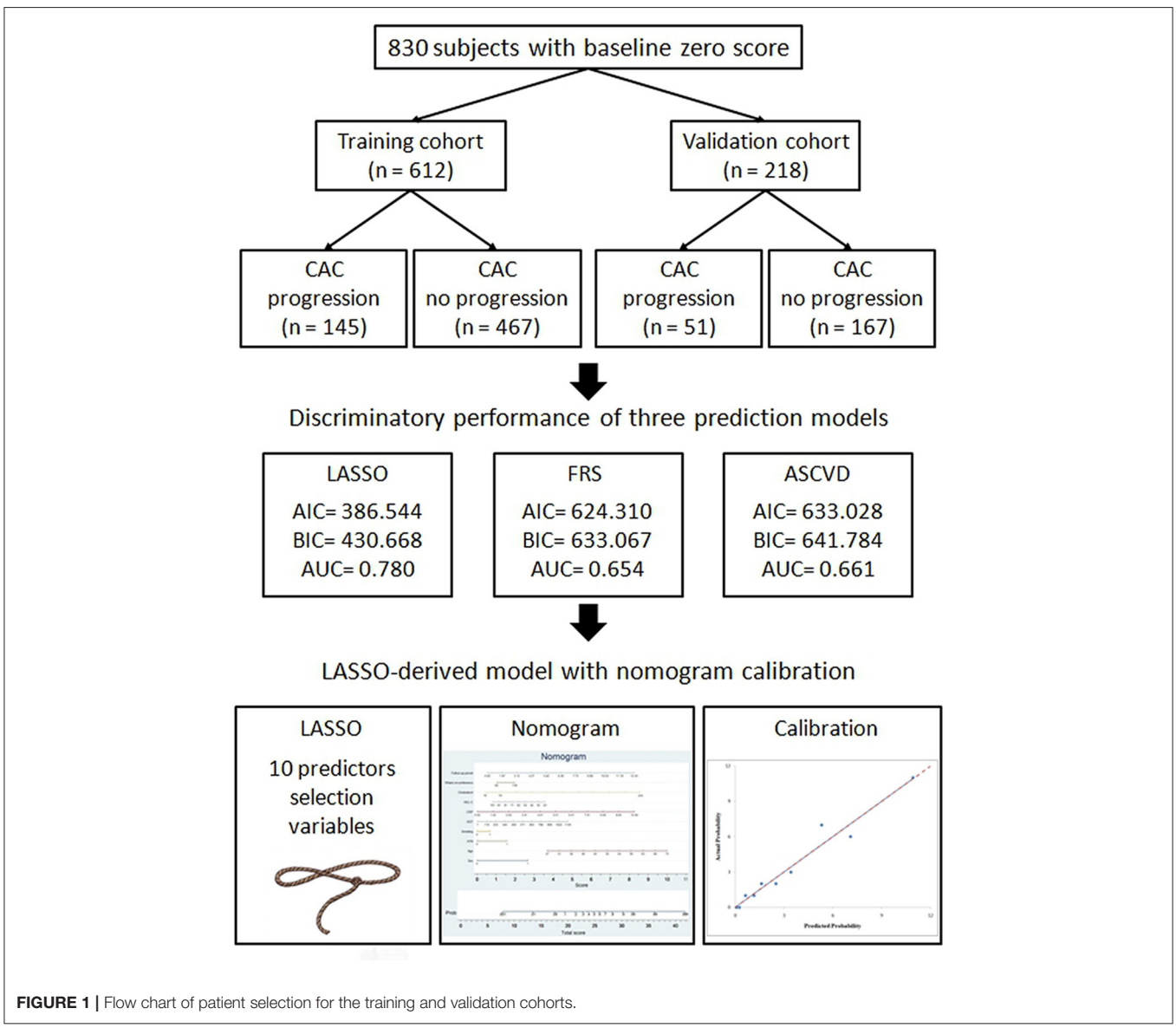

FIGURE 1 | Flow chart of patient selection for the training and validation cohorts.

Statistical Analysis

The clinical characteristics and demographic profiles of the subjects in the training and validation cohorts were compared by Student *t*-test for continuous variables and chi-square test/Fisher exact text for categorical variables. The primary study outcome was to develop a LASSO-based prediction nomogram (Optimal lambda selection) for CAC progression in Asian population with baseline zero-score (19). The multivariable logistic regression model was used to estimate the odds ratio (OR) and 95% CI. We evaluate and compare the discriminatory ability of three predictive models by using the c-statistic (area under the ROC curve, AUC), Bayesian information criterion (BIC) and Akaike information criterion (AIC). Higher c-statistic and lower AIC/BIC values were considered to indicate a more discriminatory model (20). The values of the c-statistic range from 0.5 (no ability to discriminate) to 1.0 (full ability to discriminate). Calibration was assessed by the Hosmer–Lemeshow goodness-of-fit statistic and by calibration graphs plotting predicted CAC progression against the observed rates in deciles of predicted risk (21). A nomogram was established based on the LASSO-derived parameters in the training cohort. The statistical significance for all tests was set at $P < 0.05$. All statistical analyses were performed using SPSS 22.0 for Windows (SPSS Inc., Chicago, IL) and Stata version 13.0 (Stata Corp, College Station, TX, USA).

RESULTS

The Study Population Characteristics

Of the 830 subjects with baseline zero score in our study, of whom 555 were men and 275 were women, 196 had CAC progression events and 634 did not have the events.

The prevalence of CAC progression in the total study cohort was 23.61%.

In the study cohort of 830 subjects, about 17.2 subjects have non-calcified plaques in the baseline scan. In the final round, about 41.9% subjects have non-calcified or calcified plaques formation during follow up period of 4.55 ± 2.42 year shown in **Table 1**. These subjects were randomly placed into the training set or validation set at a ratio of 2.8:1. 612 and 218 subjects with baseline zero score were included in the training and validation cohorts, respectively, shown in **Figure 1**. **Table 1** summarizes the subjects' characteristics in the training and validation cohort. Our study included 830 subjects with baseline zero score in this study cohort. The basic clinical characteristics for the training cohort (612 subjects, mean age 51.26 ± 8.26, 66% male) and the validation cohort (218 subjects, mean age 50.90 ± 8.19, 69.3% male) are list in **Table 1**. In the training cohort, 145 subjects (23.69%) developed CAC progression, while in the validation cohort, 51 subjects (23.39%) developed CAC progression. There were no significant differences between the two groups (the train cohort and the validation cohort) in terms of all parameters of clinical characteristics, physical examination, and laboratory profiles.

LASSO-Derived Predictor for Subclinical CAC Progression

We conducted logistic regression with the least absolute shrinkage and selection operator (LASSO) penalization to help reduce the dimensions of feature selection through a 10-fold cross validation for subclinical CAC progression prediction. Finally, ten of the original 20 variables were selected in the prediction model developing. The finial LASSO model with optimal lambda included the following 10 non-zero variables: "sex," "age," "hypertension," "smoking habit," "GGT," "CRP," "HDL-C," "cholesterol," "waist circumference," and "follow-up period." We carried out the multivariate analyses in the training cohort to establish the prediction model for subclinical CAC progression. Ten of the original 20 variables were included in the prediction model. The results of the multivariate logistic regression analysis are summarized in **Table 2**. The LASSO-derived prediction model including 10 selected variables also has showed its good performance in **Table 2**.

Development of the Nomogram

The probability of subclinical CAC progression in the study training cohort with the baseline zero score according to the multivariable logistic regression model including ten potential predictive factors (sex, age, hypertension, smoking habit, GGT, CRP, HDL-C, cholesterol, waist circumference, and follow-up period). A nomogram was further generated to predict subclinical CAC progression based on the multivariable logistic regression results shown in **Figure 2**. By adding up these scores identified on the points scale for each parameter, we were easily able to draw a straight line down to establish the estimated individual probability score of subclinical CAC progression in the training cohort with baseline zero score. As an example to better explain the nomogram model, if the male subject is age

TABLE 2 | LASSO-derived multivariable logistic regression for predicting CAC progression in subjects with baseline zero score.

	Coefficient	OR	95% CI	*P*-value
LASSO-selected 10 variable				
Sex (%)	1.086	2.962	1.387–6.325	0.005
Age (year)	0.056	1.057	1.020–1.095	0.002
Hypertension (%)	0.639	1.896	1.099–3.269	0.021
Smoking (%)	0.276	1.318	0.738–2.353	0.350
GGT (U/L)	0.002	1.002	0.999–1.005	0.250
CRP (mg/dL)	0.336	1.399	0.923–2.123	0.114
HDL-C (mg/dL)	−0.014	0.986	0.961–1.011	0.260
Cholesterol (mg/dL)	0.009	1.009	1.002–1.016	0.009
Waist circumference (cm)	0.007	1.007	0.973–1.041	0.697
Follow-up period (year)	0.272	1.313	1.186–1.454	<0.001
LASSO-derived model				
Prediction model	5.256	191.667	47.062–780.597	<0.001

LASSO, least absolute shrinkage and selection operator; CAC, coronary artery calcium; GGT, gamma-glutamyl transferase; CRP, c-reactive protein; HDL-C, high-density lipoprotein cholesterol; OR, odds ratio; CI, confidence interval.

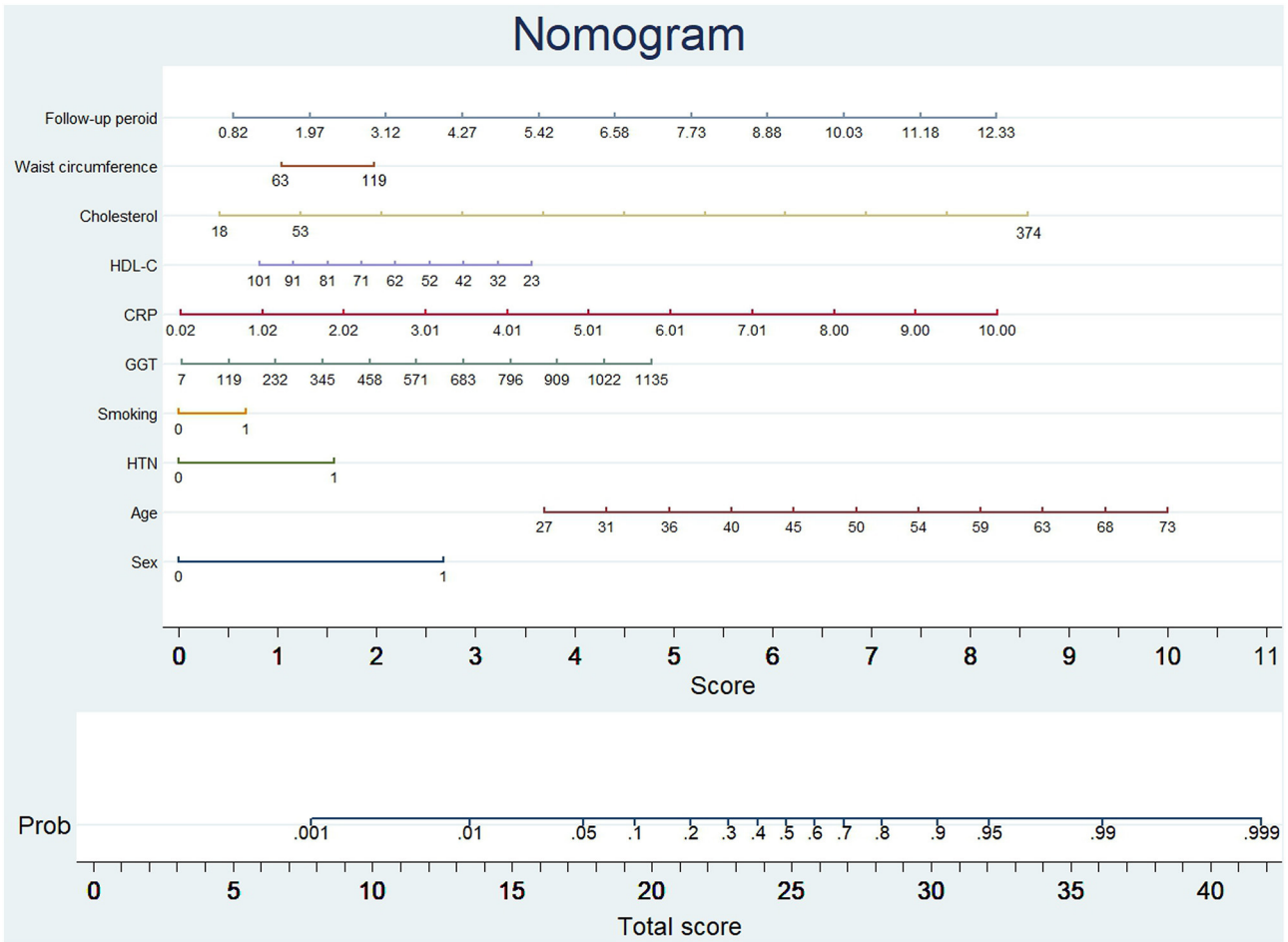

FIGURE 2 | Nomogram to predict CAC progression in subjects with baseline zero score. (Figure was created by Stata 13, nomolog). To use the nomogram, an individual participant's value is located on each variable axis, and a line is drawn upward to determine the number of points received for each variable value. The sum of these numbers is located on the total points axis to determine the possibility of CAC progression.

of 58, Hypertension (+), smoking (−), GGT of 465 u/L, CRP of 9 mg/dl, HDL-C of 40 mmol/L, cholesterol of 374 mmol/L, waist circumference of 119 cm, and follow-up period of 8.8 year, the probability of subclinical CAC progression is estimated to be 99%.

Internal and External Validation of the LASSO-Derived Nomogram

A 10-fold cross-validation method was applied to validate the nomogram model.

The pooled area under ROC curve of the nomogram was 0.780 (95% confidence interval: 0.731–0.829) in the training cohort and 0.836 (95% confidence interval: 0.761–0.911) in the validation cohort. The ROC showed the resulting model had quite good discrimination in the training and validation cohorts. Good calibration was also demonstrated by non-statistical significance obtained in the Hosmer–Lemeshow test in both the training and validation cohorts ($p = 0.654$ in the training cohort; $p = 0.979$ in the validation cohort), as displayed by calibration curves shown in **Figures 3**, **4**.

Comparison of LASSO-Derived, FRS and ASCVD Models

Table 3 presents a summary of the discriminatory ability and diagnostic performance of the three prediction models, including LASSO-derived, FRS, and ASCVD models.

In addition, the comparison and difference of three predictive models are summarized in **Table 4**. Our study result demonstrated that LASSO-based model has significantly superior discriminatory ability, higher c-statistic, and the lower AIC and BIC over other two predictive models. Compared with FRS and ASCVD model, the novel LASSO-derived nomogram model shows better diagnostic performance with an AUC of 0.780 (95% CI, 0.731 to 0.829) for detection subclinical CAC progression in Asian population with baseline zero score with balanced sensitivity (78.49%) and specificity (67.62%).

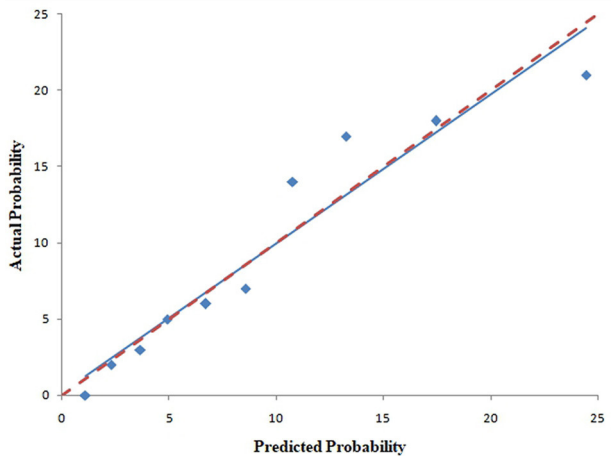

FIGURE 3 | Calibration curves of the nomogram for predicting CAC progression from the training cohort. The Hosmer–Lemeshow test had a *p*-value of 0.654 in the training cohort.

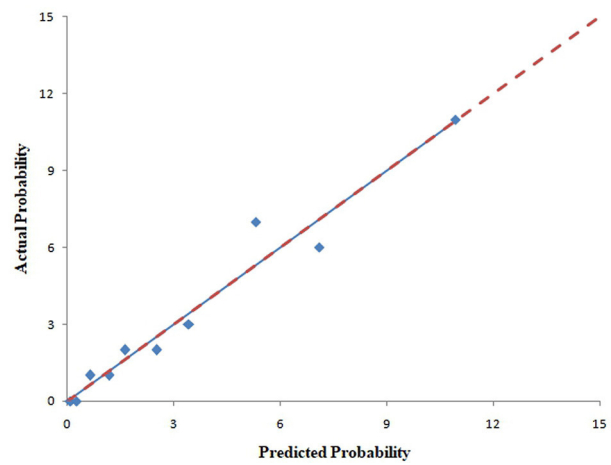

FIGURE 4 | Calibration curves of the nomogram for predicting CAC progression from the validation cohort. The Hosmer–Lemeshow test had a *p*-value of 0.979 in the validation cohort.

DISCUSSION

We built up and assessed a nomogram model for individually predicting subclinical CAC progression in subjects with baseline zero score. The predictive nomogram model incorporates clinical characteristics, physical examination and laboratory profiles for guiding individual subclinical coronary atherosclerosis prediction. To the best of our knowledge, this is a first predictive nomogram for subclinical CAC progression prediction in Asian population. In this study, we demonstrated three major findings. The first one is that we developed a LASSO-derived novel nomogram prediction model based on clinical characteristics, physical examination and laboratory profiles to predict subclinical atherosclerosis with baseline zero score, and

TABLE 3 | Prediction performance of LASSO, FRS, and ASCVD models, $n = 612$.

	AIC	BIC	AUC (95% CI)	Cut-point	Sensitivity	95% CI	Specificity	95% CI	+LR	95% CI	–LR	95% CI	+PV	95% CI	–PV	95% CI
LASSO model	386.5443	430.6682	0.780 (0.731–0.829)	>0.2205	78.49	68.8–86.3	67.62	62.1–72.8	2.42	2.1–2.8	0.32	0.2–0.5	41.7	34.3–49.4	91.4	87.1–94.7
FRS model	624.3103	633.0672	0.654 (0.605–0.702)	> 11.1	71.22	62.9–78.6	57.78	53.1–62.4	1.69	1.5–1.9	0.5	0.4–0.7	34.3	28.8–40.0	86.7	82.3–90.3
ASCVD model	633.0280	641.7848	0.661 (0.612–0.709)	>5.5	69.78	61.4–77.3	57.78	53.1–62.4	1.65	1.4–1.9	0.52	0.4–0.7	33.8	28.3–39.6	86.1	81.7–89.8

LASSO, least absolute shrinkage and selection operator; FRS, Framingham risk score; ASCVD, atherosclerotic cardiovascular disease; AIC, Akaike information criterion; BIC, Bayesian information criterion; AUC, area under the ROC curve; CI, confidence interval; LR, likelihood ratio; PV, predictive value.

TABLE 4 | Comparison of discriminatory ability in three predictive models.

	Difference between areas	SE	95% CI	*P*-value
LASSO vs. FRS	0.1000	0.0276	0.0459–0.154	<0.001
LASSO vs. ASCVD	0.0952	0.0288	0.0387–0.152	0.001
FRS vs. ASCVD	0.0048	0.0088	−0.0125–0.022	0.587

LASSO, least absolute shrinkage and selection operator; FRS, Framingham risk score; ASCVD, atherosclerotic cardiovascular disease; SE, standard error; CI, confidence interval.

demonstrated that it provides a good level of performance for predicting subclinical CAC progression in an Asian cohort. Second, compared with FRS and ASCVD model, the LASSO-derived model exhibited a significantly better discriminatory ability and lowest AIC and BIC. Third, the LASSO-derived risk prediction model exhibited good discrimination and calibration ability in the training and validation cohort.

In this study, we consecutively selected and analyzed 830 subjects with baseline zero score, which randomly divided into the training cohort and validation cohort. In the mean follow-up period of 4.55 ± 2.42 year, finally about 196 (23.61%) had CAC progression events in the study cohort. For subclinical CAC progression, LASSO-derived model with an optimal cut-off value of <0.2205 (probability score) may be an ideal screening tool to help rule out subclinical CAC progression within the 5 years of the warranty period in the middle-age Asian population with low to intermediate risk (sensitivity of 78.49%; specificity of 67.62%). Our study findings are consistent with a growing body of literature about the natural course of CAC progression in population with zero score (4–8). The evidences from previous studies have demonstrated that zero CAC score at the baseline scan could provide the 5 year- warranty period of beneficial effect on the future cardiac event in both Western and Asian asymptomatic population with low to intermediate cardiovascular risk. In addition, we developed and validated a new novel nomogram that integrated clinical characteristics, physical examination and laboratory profiles. This nomogram can more efficiently predict the subclinical CAC progression, compared with FRS or ASCVD model. Sarah et al. previously reported that CVHI (cardiovascular health index) score had most sensitive (94%) but least specific (14.9%) in identifying individuals with subclinical atherosclerosis assessed with non-invasive carotid intima-media thickness (CIMT) measurement, compared with FRS and MetS (metabolic syndrome) score (22). Our previous study has demonstrated that FRS score had poor to fair diagnostic performance for subclinical CAC progression prediction in individuals with baseline zero score (8). Compared with FRS and ASCVD model, the novel LASSO-derived nomogram model shows better performance with an AUC of 0.780 (95% CI, 0.731 to 0.829) for detection subclinical CAC progression in Asian population with baseline zero score with balanced sensitivity (78.49%) and specificity (67.62%). Our LASSO-derived model is feasible to predict subclinical CAC progression with high relative high sensitivity for rule out this clinical scenario in subjects with baseline zero score. Early detection of coronary atherosclerosis in its subclinical stage could impact on the primary prevention of cardiovascular events, and allow the prompt implementation of primary prevention strategies (1–3). The PESA study demonstrated that the high prevalence of subclinical atherosclerosis (44%) in term of the iliac-femoral district in asymptomatic middle-aged population (23, 24). Therefore, healthy lifestyle strategies such as lifelong attention to diet, exercise habit, smoking abstinence or statins treatment in the subgroup with CAC >100 through promoting patient-centered shared decision making are crucial for maintaining and prolong cardiovascular health and to slow the progression of coronary atherosclerosis in preventive cardiology (1–3, 25).

STRENGTHS AND LIMITATIONS

The study has two main strengths. First, a strength of the present study was its longitudinal nature which allowed us to clearly identify the correct sequence of time events, identify changes over time, eliminate recall bias and provide insight into cause-and-effect relationships. Second, this study investigates on the unique Asian population cohort. However, there is no population-based study focusing on the prediction model for subclinical coronary atherosclerosis among Asian population. Therefore, this study could investigate risk factors of subclinical coronary arthrosclerosis associated with the racial difference.

There are some limitations in this study. First, this is a single-center retrospective study focused on Asian population. Therefore, the generalizability of the prediction model result to the western population is limited. Second, we did not investigate the clinical cardiovascular event for primary outcome analysis due to small sample size limitation and low to intermediate FRS risk (FRS% 12.79 ± 8.90, $N = 830$). Therefore, the cost-benefit analysis of predicting subclinical coronary atherosclerosis is still uncertain (26, 27). Subclinical coronary atherosclerosis has become a threatening public health issue in the world due to behavioral, environmental and genetic factors (28, 29). There is increasing trend in the USA that people died suddenly from cardiovascular events at low risk according to Framingham risk stratification (1, 2, 30). Therefore, to pay more attention on subclinical coronary atherosclerosis is mandatory in this age with high prevalence of subclinical atherosclerosis stage. Early detection with primary prevention such as health promotion with lifestyle behavior modification (diet, physical activity, stop smoking, etc.) is a very important way to slow or reverse the progression of subclinical coronary atherosclerosis (31, 32). Third, our relatively short follow-up period is a potential limitation. Therefore, longer follow-up studies are warranted to investigate the natural course of CAC progression in the 10-year period. Fourth in this study we aimed to investigate a specific form of subclinical coronary atherosclerosis in term of coronary calcification. Therefore, other forms of subclinical atherosclerosis such as development of non-calcified coronary plaques or subclinical atherosclerosis in carotid, aorta and iliac arteries could not be assessed in this study (23, 24, 33). In addition, previous studies have demonstrated that statin therapy

may influence coronary plaque calcification (34). However, the retrospective study design did not collect complete history of the lipid-lowering drugs. Further studies are warranted to assess multiterritorial subclinical atherosclerosis in Asian population.

CONCLUSION

In summary, we developed and validated successfully a LASSO-derived prediction nomogram based on 10 routine clinical parameters conveniently including "sex," age," "hypertension," "smoking habit," "GGT," "CRP," "HDL-C," "cholesterol," "waist circumference," and "follow-up period," and demonstrated that it provides a good level of performance for predicting subclinical coronary atherosclerosis in subjects with baseline zero score. This nomogram could help clinicians to identify subclinical coronary atherosclerosis in subjects at low to intermediate risk for guidance for the primary preventive strategies in individual-based preventive cardiology.

DATA AVAILABILITY STATEMENT

The raw data supporting the conclusions of this article will be made available by the authors, without undue reservation.

ETHICS STATEMENT

The studies involving human participants were reviewed and approved by Institutional review boards of Kaohsiung Veterans General Hospital. Written informed consent for participation was not required for this study in accordance with the national legislation and the institutional requirements. Written informed consent was not obtained from the individual(s) for the publication of any potentially identifiable images or data included in this article.

AUTHOR CONTRIBUTIONS

F-ZW prepared the manuscript. All authors contributed to the data collection and analyses, edited the draft manuscript, and approved the final manuscript.

FUNDING

This study was supported by Grants from Kaohsiung Veterans General Hospital, VGHKS103-015, VGHKS104-048, VGHKS105-064, VGHKS108-159, MOST108-2314-B-075B-008-, and MOST 109-2314-B-075B-006 -Taiwan, R.O.C.

REFERENCES

1. Toth PP. Subclinical atherosclerosis: what it is, what it means and what we can do about it. *Int J Clin Pract.* (2008) 62:1246–54. doi: 10.1111/j.1742-1241.2008.01804.x
2. Shah PK. Screening Asymptomatic Subjects for Subclinical Atherosclerosis. *J. Am Coll Cardiol.* (2010) 56:98. doi: 10.1016/j.jacc.2009.09.081
3. Gatto L, Prati F. Subclinical atherosclerosis: how and when to treat it? *Eur Heart J. Suppl.* (2020) 22:E87–90. doi: 10.1093/eurheartj/suaa068
4. Gopal A, Nasir K, Liu ST, Flores FR, Chen L, Budoff MJ. Coronary calcium progression rates with a zero initial score by electron beam tomography. *Int J Cardiol.* (2007) 117:227–31. doi: 10.1016/j.ijcard.2006.04.081
5. Min JK, Lin FY, Gidseg DS, Weinsaft JW, Berman DS, Shaw LJ, et al. Determinants of coronary calcium conversion among patients with a normal coronary calcium scan: what is the "warranty period" for remaining normal? *J Am College Cardiol.* (2010) 55:1110–7. doi: 10.1016/j.jacc.2009.08.088
6. Koulaouzidis G, Charisopoulou D, Maffrett S, Tighe M, Jenkins PJ, Mcarthur T. Coronary artery calcification progression in asymptomatic individuals with initial score of zero. *Angiology*. (2012) 64:494–7. doi: 10.1177/0003319712459213
7. Lehmann N, Erbel R, Mahabadi AA, Rauwolf M, Möhlenkamp S, Moebus S, et al. Value of progression of coronary artery calcification for risk prediction of coronary and cardiovascular events. *Circulation*. (2018) 137:665–79. doi: 10.1161/CIRCULATIONAHA.116.027034
8. Shen YW, Wu YJ, Hung YC, Hsiao CC, Chan SH, Mar GY, et al. Natural course of coronary artery calcium progression in Asian population with an initial score of zero. *BMC Cardiovasc Disord.* (2020) 20:212. doi: 10.1186/s12872-020-01498-x
9. Fernandez-Friera L, Beatriz LM, Oliva B, Mocoroa A, Mendiguren JM, Pocock S, et al. SUBCLINICAL ATHEROSCLEROSIS IN THE ABSENCE OF CARDIOVASCULAR RISK FACTORS: PRE-RISK STATUS IN THE PESA (PROGRESSION OF EARLY SUBCLINICAL ATHEROSCLEROSIS) STUDY. *J Am College Cardiol.* (2017) 69:2027. doi: 10.1016/S0735-1097(17)35416-5
10. Lee JH, Han D, Hartaigh B, Rizvi A, Gransar H, Park H-B, et al. Warranty period of zero coronary artery calcium score for predicting all-cause mortality according to cardiac risk burden in asymptomatic Korean adults. *Circ. J.* (2016) 80:2356–61. doi: 10.1253/circj.CJ-16-0731
11. Lee W, Yoon YE, Kwon O, Lee H, Park HE, Chun EJ, et al. Evaluation of coronary artery calcium progression in asymptomatic individuals with an initial score of zero. *Korean Circ J.* (2019) 49:448–57. doi: 10.4070/kcj.2018.0318
12. Agatston AS, Janowitz WR, Hildner FJ, Zusmer NR, Viamonte M, Detrano R. Quantification of coronary artery calcium using ultrafast computed tomography. *J Am College Cardiol.* (1990) 15:827–32. doi: 10.1016/0735-1097(90)90282-T
13. Cury RC, Abbara S, Achenbach S, Agatston A, Berman DS, Budoff MJ, et al. CAD-RADS^{TM} Coronary Artery Disease – Reporting and Data System. An expert consensus document of the Society of Cardiovascular Computed Tomography (SCCT), the American College of Radiology (ACR) and the North American Society for Cardiovascular Imaging (NASCI). Endorsed by the American College of Cardiology. *J Cardiovasc Comp Tomography*. (2016) 10:269–81. doi: 10.1016/j.jcct.2016.04.005
14. D'agostino RB Sr, Vasan RS, Pencina MJ, Wolf PA, Cobain M, Massaro JM, et al. General cardiovascular risk profile for use in primary care: the Framingham Heart Study. *Circulation*. (2008) 117:743–53. doi: 10.1161/CIRCULATIONAHA.107.699579
15. Gluckman TJ, Kovacs RJ, Stone NJ, Damalas D, Mullen JB, Oetgen WJ. The ASCVD risk estimator app: from concept to the current state. *J Am College Cardiol.* (2016) 67:350–2. doi: 10.1016/j.jacc.2015.10.068
16. Kandula NR, Kanaya AM, Liu K, Lee JY, Herrington D, Hulley SB, et al. Association of 10-year and lifetime predicted cardiovascular disease risk with subclinical atherosclerosis in South Asians: findings from the Mediators of Atherosclerosis in South Asians Living in America (MASALA) study. *J Am Heart Association*. (2014) 3:e001117. doi: 10.1161/JAHA.114.001117
17. Fernández-Alvira JM, Fuster V, Pocock S, Sanz J, Fernández-Friera L, Laclaustra M, et al. Predicting subclinical atherosclerosis in low-risk Individuals. *J Am College Cardiol.* (2017) 70:2463–73. doi: 10.1016/j.jacc.2017.09.032
18. Goff DC, Lloyd-Jones DM, Bennett G, Coady S, D'agostino RB, Gibbons R, et al. 2013 ACC/AHA guideline on the assessment of cardiovascular risk. *Circulation*. (2014) 129:S49–73. doi: 10.1161/01.cir.0000437741.48606.98

19. Tibshirani R. Regression Shrinkage and Selection via the Lasso. *J Royal Statistical Soc Series B.* (1996) 58:267–88. doi: 10.1111/j.2517-6161.1996.tb02080.x
20. Molodianovitch K, Faraggi D, Reiser B. Comparing the areas under two correlated ROC curves: parametric and non-parametric approaches. *Biometrical J.* (2006) 48:745–57. doi: 10.1002/bimj.200610223
21. Lemeshow S, Hosmer DW Jr. A review of goodness of fit statistics for use in the development of logistic regression models1. *Am J Epidemiol.* (1982) 115:92–106. doi: 10.1093/oxfordjournals.aje.a113284
22. Singh SS, Pilkerton CS, Shrader CD Jr, Frisbee SJ. Subclinical atherosclerosis, cardiovascular health, and disease risk: is there a case for the Cardiovascular Health Index in the primary prevention population? *BMC Public Health*. (2018) 18:429. doi: 10.1186/s12889-018-5263-6
23. Fernández-Ortiz A, Jiménez-Borreguero LJ, Peñalvo JL, Ordovás JM, Mocoroa A, Fernández-Friera L, et al. The progression and early detection of subclinical atherosclerosis (PESA) study: rationale and design. *Am Heart J.* (2013) 166:990–8. doi: 10.1016/j.ahj.2013.08.024
24. Fernández-Friera L, Peñalvo JL, Fernández-Ortiz A, Ibañez B, López-Melgar B, Laclaustra M, et al. Prevalence, vascular distribution, and multiterritorial extent of subclinical atherosclerosis in a middle-aged cohort. *Circulation*. (2015) 131:2104–13. doi: 10.1161/CIRCULATIONAHA.114.014310
25. Mitchell JD, Fergestrom N, Gage BF, Paisley R, Moon P, Novak E, et al. Impact of statins on cardiovascular outcomes following coronary artery calcium scoring. *J Am College Cardiol.* (2018) 72:3233–42. doi: 10.1016/j.jacc.2018.09.051
26. Shaw LJ, Raggi P, Berman DS, Callister TQ. Cost effectiveness of screening for cardiovascular disease with measures of coronary calcium. *Progress Cardiovasc Dis*. (2003) 46:171–84. doi: 10.1016/S0033-0620(03)00085-9
27. Simon A, Chironi G, Levenson J. Comparative performance of subclinical atherosclerosis tests in predicting coronary heart disease in asymptomatic individuals. *Eur Heart J.* (2007) 28:2967–71. doi: 10.1093/eurheartj/ehm487
28. Boland LL, Folsom AR, Sorlie PD, Taylor HA, Rosamond WD, Chambless LE, et al. Occurrence of unrecognized myocardial infarction in subjects aged 45 to 65 years (the ARIC study). *Am J Cardiol*. (2002) 90:927–31. doi: 10.1016/S0002-9149(02)02655-3
29. Berger JS, Jordan CO, Lloyd-Jones D, Blumenthal RS. Screening for cardiovascular risk in asymptomatic patients. *J Am College Cardiol.* (2010) 55:1169–77. doi: 10.1016/j.jacc.2009.09.066
30. Schlendorf KH, Nasir K, Blumenthal RS. Limitations of the framingham risk score are now much clearer. *Preventive Med.* (2009) 48:115–6. doi: 10.1016/j.ypmed.2008.12.002
31. Hu FB, Willett WC. Optimal diets for prevention of coronary heart disease. *JAMA*. (2002) 288:2569–78. doi: 10.1001/jama.288.20.2569
32. Spring B, Moller AC, Colangelo LA, Siddique J, Roehrig M, Daviglus ML, et al. Healthy lifestyle change and subclinical atherosclerosis in young adults: Coronary Artery Risk Development in Young Adults (CARDIA) study. *Circulation*. (2014) 130:10–7. doi: 10.1161/CIRCULATIONAHA.113.005445
33. López-Melgar B, Fernández-Friera L, Oliva B, García-Ruiz JM, Sánchez-Cabo F, Bueno H, et al. Short-term progression of multiterritorial subclinical atherosclerosis. *J Am College Cardiol.* (2020) 75:1617. doi: 10.1016/j.jacc.2020.02.026
34. Nakazato R, Gransar H, Berman DS, Cheng VY, Lin FY, Achenbach S, et al. Statins use and coronary artery plaque composition: results from the International Multicenter CONFIRM registry. *Atherosclerosis*. (2012) 225:148–53. doi: 10.1016/j.atherosclerosis.2012.08.002

Conflict of Interest: The authors declare that the research was conducted in the absence of any commercial or financial relationships that could be construed as a potential conflict of interest.

frontiers in Cardiovascular Medicine

SYSTEMATIC REVIEW
published: 12 March 2021
doi: 10.3389/fcvm.2021.630846

Vasodilator Myocardial Perfusion Cardiac Magnetic Resonance Imaging Is Superior to Dobutamine Stress Echocardiography in the Detection of Relevant Coronary Artery Stenosis: A Systematic Review and Meta-Analysis on Their Diagnostic Accuracy

Sebastian M. Haberkorn[1], Sandra I. Haberkorn[1], Florian Bönner[1], Malte Kelm[1], Gareth Hopkin[2] and Steffen E. Petersen[3,4]*

[1] Department of Cardiology, Pneumology and Angiology, University Hospital Düsseldorf, Düsseldorf, Germany, [2] Department of Health Policy, London School of Economics and Political Science, London, United Kingdom, [3] William Harvey Research Institute, Queen Mary University of London, London, United Kingdom, [4] Barts Heart Center, St. Bartholomew's Hospital, Barts Health NHS (National Health Service) Trust, London, United Kingdom

OPEN ACCESS

Edited by:
Constantinos Anagnostopoulos, Biomedical Research Foundation of the Academy of Athens (BRFAA), Greece

Reviewed by:
Alexios Antonopoulos, National and Kapodistrian University of Athens, Greece
Alessia Gimelli, Gabriele Monasterio Tuscany Foundation (CNR), Italy

***Correspondence:**
Sebastian M. Haberkorn
sebastian.haberkorn@med.uni-duesseldorf.de

Specialty section:
This article was submitted to Cardiovascular Imaging, a section of the journal Frontiers in Cardiovascular Medicine

Received: 18 November 2020
Accepted: 15 February 2021
Published: 12 March 2021

Citation:
Haberkorn SM, Haberkorn SI, Bönner F, Kelm M, Hopkin G and Petersen SE (2021) Vasodilator Myocardial Perfusion Cardiac Magnetic Resonance Imaging Is Superior to Dobutamine Stress Echocardiography in the Detection of Relevant Coronary Artery Stenosis: A Systematic Review and Meta-Analysis on Their Diagnostic Accuracy. Front. Cardiovasc. Med. 8:630846. doi: 10.3389/fcvm.2021.630846

Objectives: Guideline recommendations for patients with either a high or a low risk of obstructive coronary artery disease (CAD) are clear. However, the evidence for initial risk stratification in patients with an intermediate risk of CAD is still unclear, despite the availability of multiple non-invasive assessment strategies. The aim of this study was to synthesize the evidence for this population to provide more informed recommendations.

Background: A meta-analysis was performed to systematically assess the diagnostic accuracy of vasodilator myocardial perfusion cardiovascular magnetic resonance imaging (pCMR) and dobutamine stress echocardiography (DSE) for the detection of relevant CAD. In contrast to previous work, this meta-analysis follows rigorous selection criteria in regards to the risk stratification and a narrowly prespecified definition of their invasive reference tests, resulting in unprecedentedly informative results for this reference group.

Data Collection and Analysis: From the 5,634 studies identified, 1,306 relevant articles were selected after title screening and further abstract screening left 865 studies for full-text review. Of these, 47 studies fulfilled all inclusion criteria resulting in a total sample size of 4,742 patients.

Results: pCMR studies showed a superior sensitivity [0.88 (95% confidence interval (CI): 0.85–0.90) vs. 0.72 (95% CI: 0.61–0.81)], diagnostic odds ratio (DOR) [38 (95% CI: 29–49) vs. 20 (95% CI: 9–46)] and an augmented post-test probability [negative likelihood ratio (LR) of 0.14 (95% CI: 0.12–0.18) vs. 0.31 (95% CI: 0.21, 0.46)] as compared to

DSE. Specificity was statistically indifferent [0.84 (95% CI: 0.81–0.87) vs. 0.89 (95% CI: 0.83–0.93)].

Conclusion: The results of this systematic review and meta-analysis suggest that pCMR has a superior diagnostic test accuracy for relevant CAD compared to DSE. In patients with intermediate risk of CAD only pCMR can reliably rule out relevant stenosis. In this risk cohort, pCMR can be offered for initial risk stratification and guidance of further invasive treatment as it also rules in relevant CAD.

Keywords: meta-analysis, systematic (literature) review, dobutamine stress echocardiography, diagnostic test accuracy, cardiac imaging, coronary artery disease, cardiac MR, myocardial perfusion MR

KEY POINTS

- *Question:* Which imaging modality for initial risk stratification of patients with an intermediate pre-test probability of CAD is superior?
- *Findings:* In this systematic review and meta-analysis the diagnostic accuracy of pCMR and DSE was systematically assessed in 47 studies reporting data from 4,742 patients. The findings suggest that pCMR has a superior test accuracy compared to DSE in the detection of relevant CAD (sensitivity 0.88 vs. 0.72, specificity 0.84 vs. 0.89).
- *Meaning:* Despite the widespread use of DSE, the evidence at hand favors pCMR in the risk stratification of patients with an intermediate risk of CAD.

INTRODUCTION

Myocardial ischemia in the form of relevant coronary artery stenosis is strongly associated with adverse outcomes, such as myocardial infarctions (MIs) and death (1). An early and accurate identification of myocardial ischemia has consequently been highlighted as a priority in current international guidelines (2, 3). Conventional coronary angiography (CCA) or a fractional flow reserve (FFR)-based assessment is the reference standard for diagnosis of CAD in patients with a high pre-test probability. An non-invasive assessment with multi-detector CT-angiography (MDCT) is the preferred approach in patients with a low pre-test probability of CAD (3).

However, in the large number of patients with an intermediate pre-test probability, guidance is underdeveloped on which of the different non-invasive imaging modalities is to prefer and clear recommendations are not yet available (2, 3). Myocardial perfusion cardiovascular magnetic resonance imaging (pCMR), dobutamine stress echocardiography (DSE), or alternative techniques can be performed equivalently for a non-invasive functional assessment of myocardial ischemia in this risk cohort (4). Therefore, there is a strong need to identify the best diagnostic alternative for these patients.

In this systematic review and meta-analysis, pCMR and DSE have been selected because they are the only imaging modalities without radiation and are frequently operated by cardiologists alone. Moreover, a diagnostic superiority over Single Photon Emission Computed Tomography (SPECT) in the detection of relevant coronary stenosis, for instance, has already been shown in several meta-analyses (4, 5), and trials, such as the CE-MARC, MR-IMPACT I, and II (6, 7). Most recently, the MR-INFORM trial even suggested that pCMR is "*non-inferior to FFR with respect to major adverse cardiac events*" in stable patients with high risk of CAD, underlining its significance in the non-invasive assessment of CAD (8).

Several systematic reviews and meta-analyses have been published on the diagnostic accuracy of various imaging approaches (4, 5, 9). However, the ability of these meta-analyses to support clinical decission making is potentially limited due to considerable heterogeneity between their included studies. This heterogeneity is due to broad eligibility criteria, varying reference tests and comparators, and vague definitions of "*significant coronary artery stenosis*" (5). Most importantly though, heterogeneity is due to individual patient risk for CAD in the included study cohorts, such as age, sex, and different risk factors. Studies with verification bias and studies from unsystematic literature searches are included in some of these analyses, which influences their applicability. Finally, previous meta-analyses have not employed systematic search methods, resulting in an incomplete or invalid identification of the available evidence. Each of these limitations of existing evidence reduces their ability to make recommendations for specific populations in the context of guideline development and as such there are still evidence gaps in the literature.

To address these existing evidence gaps, we performed a systematic review and meta-analysis with rigorous eligibility criteria on risk stratification and reference procedures, ascertaining the diagnosis of hemodynamically significant CAD. We focused on pCMR and DSE with the aim of providing resilient recommendations for the large number of patients with an intermediate risk of CAD.

Abbreviations: CAD, coronary artery disease; CCA, conventional coronary angiography; CI, confidence interval (CI); DSE, dobutamine stress echocardiography; DTA, diagnostic test accuracy; DOR, diagnostic odds ratio; FFR, fractional flow reserve; FP, false positive; FN, false negative; LR, likelihood ratio; MDCT, multi-detector computer-tomography; pCMR, perfusion cardiovascular magnetic resonance; HSROC, hierarchical summary receiver operating characteristic; SPECT, single-photon emission computed tomography; MDCT, multidetector computed tomography; MI, myocardial infarction; TP, true positive; TN, true negative; QUADAS, Quality Assessment of Diagnostic Accuracy Studies tool.

METHODS

Registration

This systematic review and meta-analysis was prospectively registered in PROSPERO under the registration number CRD42018105535. Reporting of the systematic review has been performed according to the PRISMA statements (10) and the Cochrane Handbook for Systematic Reviews of Diagnostic Test Accuracy (DTA) (11). The search was conducted in July 2018 and the latest included study was published in May 2018.

Inclusion and Exclusion Criteria

Peer-reviewed studies were included in the analysis if pCMR and/or DSE were used to identify relevant coronary artery stenosis in patients at the age of 18 years and above with non-diagnosed or stable, asymptomatic CAD without ischemia-associated ECG abnormalities (right/left bundle branch block) and preserved left-ventricular ejection fraction. Only studies that included CCA and/or FFR as the reference test have been selected and sufficient detail to reconstruct a contingency table [e.g., true positive (TP), false positive (FP), false negative (FN), and true negative (TN) findings] was also needed. For pCMR, studies needed to use either adenosine or regadenoson perfusion with a qualitative or semi-quantitative approach and reports of CMR with dobutamine were not included. For DSE only studies with transthoracic assessment evaluating wall motion abnormalities were included.

Studies on animals, studies with fewer than 20 patients, and studies reporting data on patients with unstable angina, acute or subacute MI, heart transplantation, acute coronary revascularization, congenital or ischemic heart disease were excluded. Any studies using only physical stress, echo perfusion imaging or non-visual assessment were excluded. Studies with a different definition of relevant CAD determined by CCA and FFR were excluded, such as grade of stenosis $<70\%$ or a value >0.80 on FFR recordings (2). Studies on microvascular disease were also excluded. Studies in a language other than English, French or German were excluded.

Search Methods for Identification of Studies

For the systematic review, MEDLINE (1946 to July 29, 2018), EMBASE (1974 to July 29, 2018) and Cochrane Library (Cochrane Database of Systematic Reviews: Issue 7 of 12, July 2018) databases were searched for articles that met inclusion criteria. Additionally, references of other meta-analyses published on the topic have been screened for further studies.

We developed a sensitive search strategy for MEDLINE (Ovid Web), EMBASE (Ovid Web) and the Cochrane Library (Wiley Online Library) as recommended in the Cochrane Handbook for Systematic reviews of DTA. The search strategy is shown in full in the **Supplementary Material**.

Data Collection and Analysis

Selection of Studies

Two investigators (SMH and SIH) independently reviewed first article titles, then abstracts and finally the full text for eligibility. Discrepancies were resolved by discussion and consequent consensus.

Data Extraction and Management

For each study, both investigators (SMH and SIH) independently extracted information on author, year of publication, imaging technique, study size, demographic characteristics of participants (mean age, percentage male), magnetic field strength, type of stressor, type of assessment (qualitative or quantitative), definition of relevant CAD, prevalence of CAD and the presence of risk factors (diabetes, hypertension), the clinical settings considered (suspected or known CAD), as well as the numbers of TP, FP, FN, and TN. Discrepancies between investigators extraction were resolved by consensus after discussion.

If studies reported data for multiple CAD definitions (for instance at >50, >70, and $>90\%$ stenosis), only the sensitivity of the cut-off point that was the closest to our definition (e.g., $>70\%$) was extracted. If a study reported sensitivity and specificity measures of multiple observers, the mean values were used. Patient characteristics extracted from all studies included in this meta-analysis are weight-adjusted averages; the weights have been based on the study size.

Assessment of Methodological Quality

The *Quality Assessment of Diagnostic Accuracy Studies* (QUADAS) tool (12), recommended in the modified version suggested by the *Cochrane Handbook for Systematic reviews of DTA* (13) was used to assess the quality of included studies. Two investigators (SMH and SIH) independently examined the study quality of the included reports. Disagreement was resolved by discussion and subsequent consensus.

Statistical Analysis and Data Synthesis

For all included studies sensitivity, specificity, positive likelihood ratio (LR), negative LR, and diagnostic odds ratio (DOR) with 95% confidence interval (CI) were calculated from the TP, FP, FN, and TN results. Hierarchical models, recommended by the *Cochrane DTA reviews* (14), include the interdependence of sensitivity and specificity observed across studies which may alter their true effect size. Since an explicit cut-off point for relevant coronary artery stenosis was pre-defined in this meta-analysis, the *Bivariate model* by Reitsma (13) has been applied to produce summary operating points of sensitivity and specificity directly.

Statistical analysis was performed with Stata software version 15.0 (StataCorp LLC, College Station, Texas, USA). A two-tailed p-value of <0.05 was considered to be significant, unless otherwise stated.

Investigations of Heterogeneity

One major cause of heterogeneity in test accuracy studies is the threshold effect (9). Therefore, only studies with the same reference value of relevant coronary stenosis are incorporated in this meta-analysis. Regardless, a meta-regression analysis has been facilitated to study potential reasons of heterogeneity in form of sex, age, sample size, MRI field strength, demographic patient characteristics, prevalence of CAD and

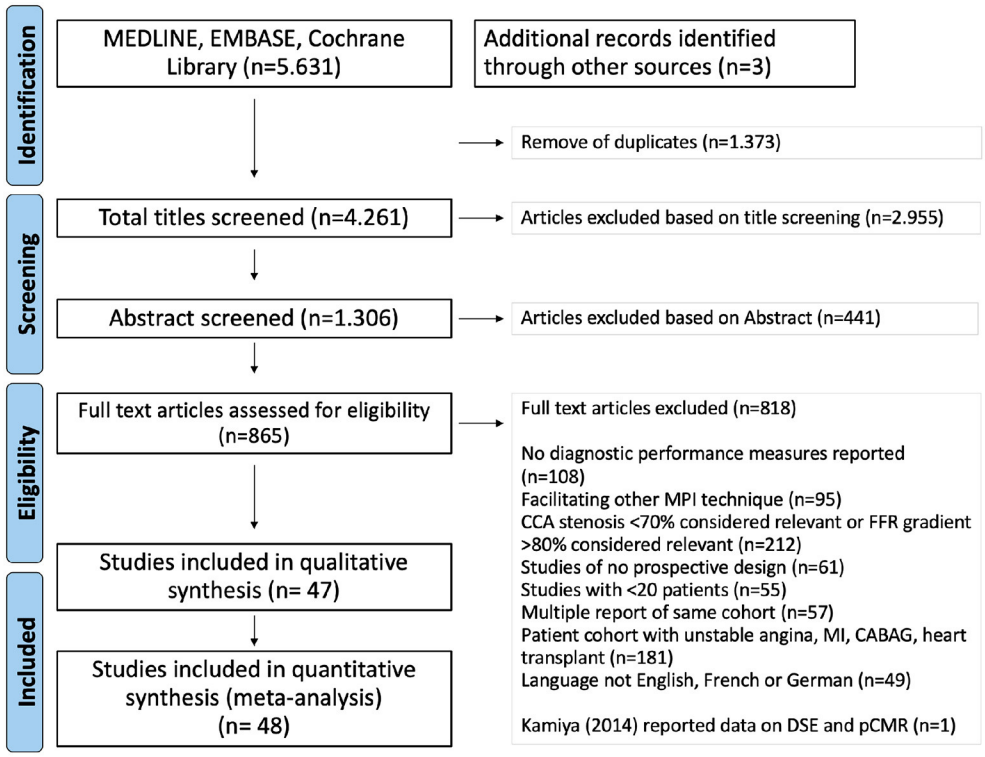

FIGURE 1 | Flowchart of study selection process. Kamiya et al. (18) reported results for DSE and pCMR, so that it contributed with two sets of data to the quantitative, but only once to the qualitative assessment.

several cardiovascular risk factors, as well as the reference method (CCA vs. FFR).

In-between study heterogeneity has been evaluated using the Cochrane-Q test (with a p-value of <0.10 contemplating significant heterogeneity) and the I^2 statistic (15).

Sensitivity Analysis

Pooled estimates of sensitivity and specificity with a 95% CI have been combined independently across all studies using a random effect meta-analysis that takes into account the possibility that these estimates may actually differ in-between studies, as a result of clinical and methodological differences (15). The value of LRs allows to compute the post-test probability based on Bayes' theorem (16).

Assessment of Reporting Bias

To explore publication bias, a funnel plot of the natural logarithm of the diagnostic odds ratio was constructed and a regression test for asymmetry was performed weighted to the study size (17). The threshold of significance was set to a p-value <0.10 for this method.

RESULTS

Literature Search

The systemic search identified 5,634 potentially relevant articles. After removal of duplicates and screening study titles, 1,306 articles were retained. These articles were screened by abstract and after 441 articles were excluded, the full texts of 865 articles were reviewed. Of these, forty-seven studies were judged as eligible for the meta-analysis.

The flowchart of the article search and selection process is illustrated in **Figure 1**.

Methodological Quality of Included Studies

Quality assessments using the QUADAS tool assessment can be found in the **Supplementary Figure A1**.

Study Characteristics

A total of 47 studies with 4,742 patients, published between 1993 and 2018, were included in this meta-analysis: 39 pCMR (4,115 patients), 9 DSE (652 patients). One of these 47 studies, Kamiya et al. (18) reported both pCMR and DSE results, thus both sets of data contribed to the quantitative assessment. The systematic literature search initially identified more DSE studies (3,752 vs. 2,174) on the topic, however, the rigor of study design was generally inferior, so that only 0.2% as compared to 1.8% for pCMR studies fulfilled all of our strict inclusion criteria. The sample size varied from 24 to 676 patients. Results showed that 50% of patients (2,359 of 4,692) had hemodynamic relevant CAD (**Table 1**). The study populations had a mean age of 61 years and the majority of patients were men (64% of all patients). In most studies patients were hypertensive (60% of all patients) with

TABLE 1 | Study characteristics.

	Study	Imaging modality	MRI field strength	Study size	Data acquisition per	Reference test	CAD status	Mean age	Prevalence of CAD	Percentage male	Prevalence of diabetes	Prevalence of hypertension
1	Hoffmann (1993)	DSE		64	Person	CCA	S	57	76%	77%	n/s	n/s
2	Dagianti (1995)	DSE		64	Person	CCA	S	55	39%	70%	n/s	n/s
3	Sochowski (1995)	DSE		46	Person	CCA	S	58	52%	67%	n/s	n/s
4	Bartunek (1996)	DSE		75	Person	FFR	S&K	57	72%	89%	n/s	n/s
5	Santoro (1998)	DSE		60	Person	CCA	S	n/s	55%	52%	n/s	n/s
6	Rieber (2004)	DSE		46	Person	FFR	S&K	64	65%	60%	21%	69%
7	Jung (2008)	DSE		70	Person	FFR	S&K	65	41%	64%	20%	76%
8	Kamiya (2014)	DSE		25	Vessel	FFR	S&K	68	41%	56%	60%	64%
9	Kim (2016)	DSE		202	Person	CCA	S	58	21%	0%	17%	43%
10	Nagel (2003)	pCMR	1.5	84	Person	CCA	S	63	51%	81%	0%	0%
11	Paetsch (2004)	pCMR	1.5	79	Person	CCA	S&K	61	38%	66%	24%	78%
12	Pons Lladó (2004)	pCMR	1.5	32	Vessel	CCA	S	65	72%	81%	31%	53%
13	Wolff (2004)	pCMR	1.5	75	Person	CCA	S&K	57	62%	83%	n/s	n/s
14	Plein (2005)	pCMR	1.5	92	Person	CCA	S&K	58	64%	74%	9%	33%
15	Klem (2006)	pCMR	1.5	92	Person	CCA	S	58	40%	49%	23%	64%
16	Pilz (2006)	pCMR	1.5	171	Person	CCA	S&K	62	66%	63%	27%	61%
17	Costa (2007)	pCMR	1.5	30	Vessel	FFR	n/s	65	47%	53%	23%	80%
18	Kühl (2007)	pCMR	1.5	28	Vessel	FFR	S&K	63	68%	61%	25%	64%
19	Merkle (2007)	pCMR	1.5	228	Person	CCA	S&K	61	67%	79%	20%	69%
20	Klem (2008)	pCMR	1.5	136	Person	CCA	S	63	27%	0%	22%	68%
21	Meyer (2008)	pCMR	3.0	60	Person	CCA	S	59	60%	63%	23%	65%
22	Watkins (2009)	pCMR	1.5	101	Person	FFR	S	60	77%	74%	16%	62%
23	Klumpp (2010)	pCMR	3.0	57	Vessel	CCA	S&K	62	72%	82%	25%	68%
24	Scheffel (2010)	pCMR	1.5	43	Vessel	CCA	S	64	65%	79%	19%	72%
25	Kirschbaum (2011)	pCMR	1.5	50	Vessel	FFR	S	64	n/s	76%	18%	50%
26	Lockie (2011)	pCMR	3.0	42	Vessel	FFR	S&K	57	52%	79%	19%	48%
27	Huber (2012)	pCMR	1.5	31	Vessel	FFR	S	67	55%	87%	23%	35%
28	Jogiya (2012)	pCMR	3.0	53	Vessel	FFR	S&K	64	61%	77%	30%	66%
29	Khoo (2012)	pCMR	1.5	241	Person	CCA	S&K	65	71%	n/s	n/s	n/s
30	Manka (2012)	pCMR	1.5	120	Person	FFR	S&K	64	58%	75%	26%	73%
31	Bernhardt (2013)	pCMR	3.0	34	Person	FFR	S	62	62%	76%	15%	79%
32	Bettencourt (2013)	pCMR	1.5	101	Person	FFR	S	62	44%	67%	39%	72%
33	Chiribiri (2013)	pCMR	3.0	67	Person	FFR	S&K	61	82%	79%	25%	48%
34	Ebersberger (2013)	pCMR	3.0	116	Person	FFR	S&K	63	78%	61%	26%	60%
35	Groothuis (2013)	pCMR	1.5	88	Person	FFR	S	56	30%	50%	12%	38%
36	Pereira (2013)	pCMR	1.5	80	Person	FFR	S	61	46%	68%	44%	72%
37	Walcher (2013)	pCMR	3.0	52	Vessel	CCA	S	62	52%	71%	19%	79%

(Continued)

TABLE 1 | Continued

	Study	Imaging modality	MRI field strength	Study size	Data acquisition per	Reference test	CAD status	Mean age	Prevalence of CAD	Percentage male	Prevalence of diabetes	Prevalence of hypertension
8	Kamiya (2014)	pCMR	3.0	25	Vessel	FFR	S&K	68	41%	56%	60%	64%
38	Ponte (2014)	pCMR	1.5	95	Person	FFR	S	62	43%	68%	39%	75%
39	Greulich (2015)	pCMR	1.5	72	Person	CCA	S	70	14%	46%	28%	81%
40	Manka (2015)	pCMR	3.0	150	Person	FFR	S	63	57%	70%	18%	73%
41	Pan (2015)	pCMR	3.0	71	Vessel	FFR	S&K	60	57%	80%	31%	8%
42	Ripley (2015)	pCMR	1.5	676	Person	CCA	S	60	33%	62%	13%	51%
43	Papanastasiou (2016)	pCMR	3.0	24	Person	FFR	S&K	63	67%	83%	13%	54%
44	Foley (2017)	pCMR	1.5	54	Person	CCA	S&K	65	50%	53%	19%	54%
45	Hamada (2017)	pCMR	Mixed	357	Person	FFR	S&K	63	48%	85%	22%	76%
46	Biglands (2018)	pCMR	1.5	128	Person	CCA	S	61	33%	60%	13%	51%
47	Hsu (2018)	pCMR	1.5	80	Person	CCA	S&K	58	44%	70%	20%	69%

n/s, not stated; S, suspected; S&K, suspected & known.

TABLE 2 | Summary of findings table.

Parameter	*pCMR*		*DSE*	
	Estimate	**95% CI**	**Estimate**	**95% CI**
Number of studies included	**39**		**9**	
Number of patients included	**4.115**		**652**	
Sensitivity	**0.88**	[0.85–0.90]	**0.72**	[0.61–0.81]
Q	113.2	$p < 0.1$	24.9	$p < 0.01$
I^2	66	[55–78]	68	[45–90]
Specificity	**0.84**	[0.81–0.87]	**0.89**	[0.83–0.93]
Q	140.6	$p < 0.01$	21.1	$p < 0.01$
I^2	73	[64–82]	62	[34–90]
Positive LR	**5.5**	[4.7–6.5]	**6.3**	[3.8–10.4]
Negative LR	**0.14**	[0.12–0.18]	**0.31**	[0.21–0.46]
DOR	**38**	[29–49]	**20**	[9–46]
Positive post-test probability				
At 25% pre-test	65%		68%	
At 50% pre-test	85%		86%	
At 75% pre-test	94%		95%	
Negative post-test probability				
At 25% pre-test	5%		9%	
At 50% pre-test	13%		24%	
At 75% pre-test	30%		49%	
Deek's funnel plot *p*-value	**0.95**		**0.74**	

DOR, diagnostic odds ratio; I^2, the percentage of variation across studies that is due to heterogeneity rather than chance; LR, likelihood ratio; Q, Cochran's Q measure of heterogeneity.

some having additional risk factors, such as diabetes (21% of all patients).

Diagnostic Accuracy

Pooled estimates of sensitivity, specificity, positive and negative LR, as well as DOR are summarized in **Table 2**. The data of all studies are summarized in forest plots (**Figures 2**, **3**) and summary estimates of sensitivity and specificity for pCMR and DSE are stated with a 95% CI.

At the patient level, pCMR (0.88, 95% CI: 0.85–0.90) had higher sensitivity compared to DSE (0.72, 95% CI: 0.61–0.81). Conversely, specificity of DSE (0.89, 95% CI: 0.83–0.93) was statistically non-superior compared to pCMR (0.84, 95% CI: 0.81–0.87), as described in **Figures 2**, **3**. The DOR was highest for pCMR (38, 95% CI: 29–49) as compared to DSE (20, 95% CI: 9–46) (see **Table 2**). At a low clinical likelihood (pre-test probability 25%), both test fail to sufficiently rule-in (defined as post-test probability >85%) obstructive CAD (pCMR 65% CI: 63–67% vs. DSE 68% CI: 62–74%) (**Figure 4A**). In a patient with a very high likelihood (pre-test probability 75%) of CAD on the other hand, ruling out relevant stenosis (defined as post-test probability <15%) becomes challenging when post-test probability ranges from CI: 26–35% for pCMR and CI: 39–58% for DSE studies (**Figure 4B**). In the intermediate risk cohort, however, with a pre-test probability of 50%, solemly an pCMR-based assessment could sufficiently rule-in and rule-out obstructive CAD with a post-test probability of 85% (CI: 83–86%), respectivley 13% (CI:

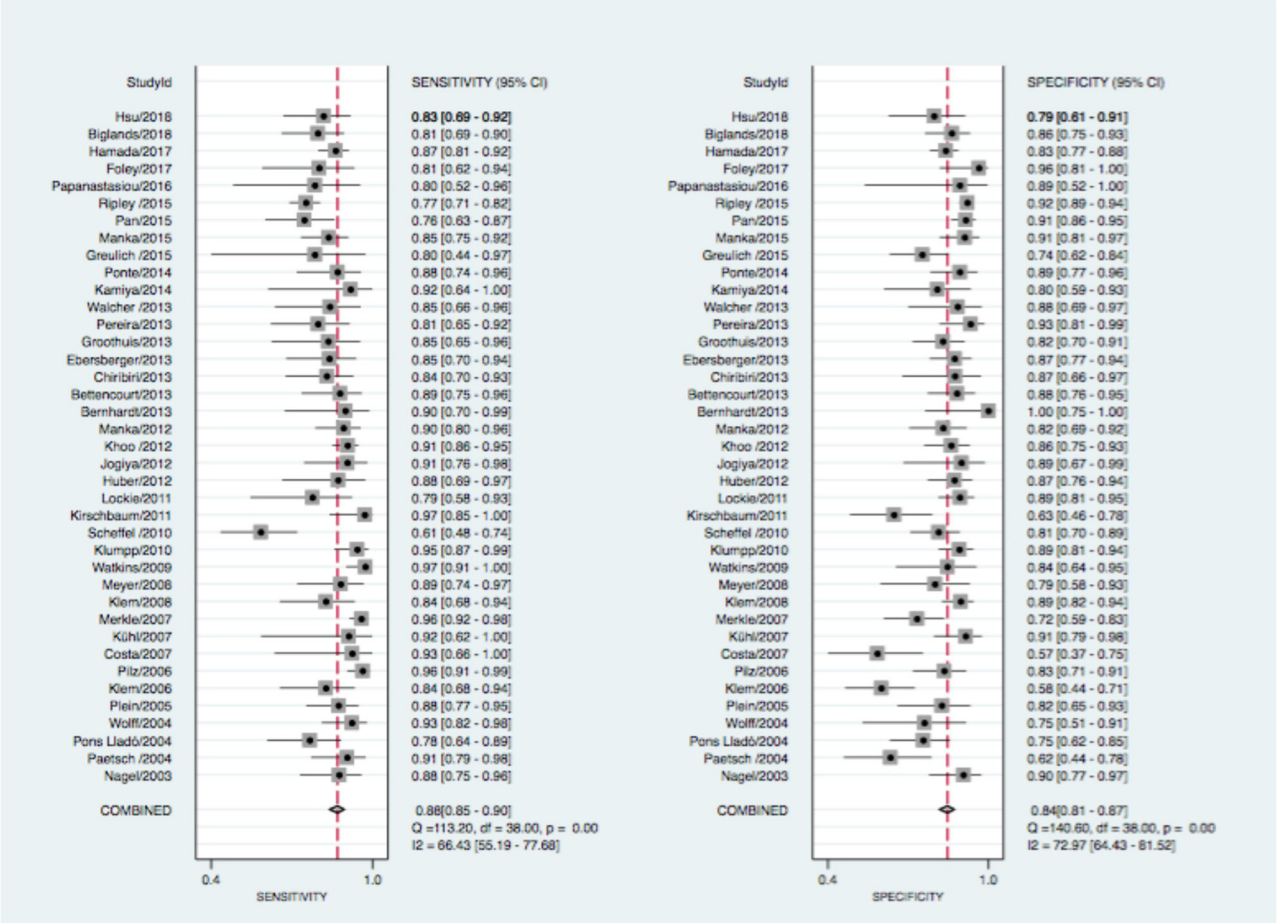

FIGURE 2 | Forrest plot for pCMR with sensitivity (left) and specificity (right) estimates. CI, confidence intervall; I^2, the percentage of variation across studies that is due to heterogeneity rather than chance; Q, Cochran's Q measure of heterogeneity.

12–14%), compared to DSE-based assessment with 86% (CI: 83–90%), and 24% (CI: 21–28%) (**Figure 4C**).

Hints for heterogeneity were found for the sensitivity of pCMR (Q = 113.2, $p < 0.01$; $I^2 = 66$, 95% CI: 55–78), and for the specificity results across studies (Q = 140.6, $p < 0.01$; $I^2 = 73$, 95% CI: 64–82). DSE also showed heterogeneity for sensitivity (Q = 24.9, $p < 0.01$; $I^2 = 68$, 95% CI: 45–90) and for specificity (Q = 21.1, $p < 0.01$; $I^2 = 72$, 95% CI: 34–90) (see **Figures 2**, **3**). The forest plots further highlights three potential outliers for pCMR studies Klem (2006), Costa (2007), Scheffel (2010), and a single potential outlier, Santoro (1998), for DSE studies. A sensitivity analysis is shown in the **Supplementary Figures A2, A3** in which the influence of these studies on the summary estimates is assessed.

Heterogeneity Assessment

The meta-regression analysis was used in order to reveal factors impacting heterogeneity incorporated sex, age, MRI field strength, prevalence of CAD and cardiovascular risk factors, as well as the reference method (FFR vs. CCA). No parameter was identified as a significant predictor of heterogeneity for pCMR studies. For DSE studies, meta-regression analysis suggested that the prevalence of diabetes ($p < 0.01$) was an independent predictor of heterogeneity (see **Figure 5**).

In a subgroup analysis to identify reasons for in-between study variation and to investigate if the distribution of specific study characteristics biased the comparison of the two imaging methods, no significant effect of study and test characteristics was found on the DTA performance. A trend toward a lower diagnostic accuracy of pCMR studies performed at 1.5 T as compared to 3.0 T scanners was seen but was not significant. For DSE, studies with a higher prevalence of diabetes were associated with a worse diagnostic performance. The diagnostic accuracy of pCMR in comparison to DSE remained unaffected in the majority of subgroup analyses (see **Figure 5**). Surprisingly, the diagnostic accuracy of pCMR studies was not affected by the reference method, whereas DSE studies showed a tendency toward a lower sensitivity when using FFR rather than CCA as reference. This might hint an advantage of pCMR for the hemodynamic assessment of coronary stenosis over DSE, even though the differences did not reach a statistical significant level (*see* **Figure 5**).

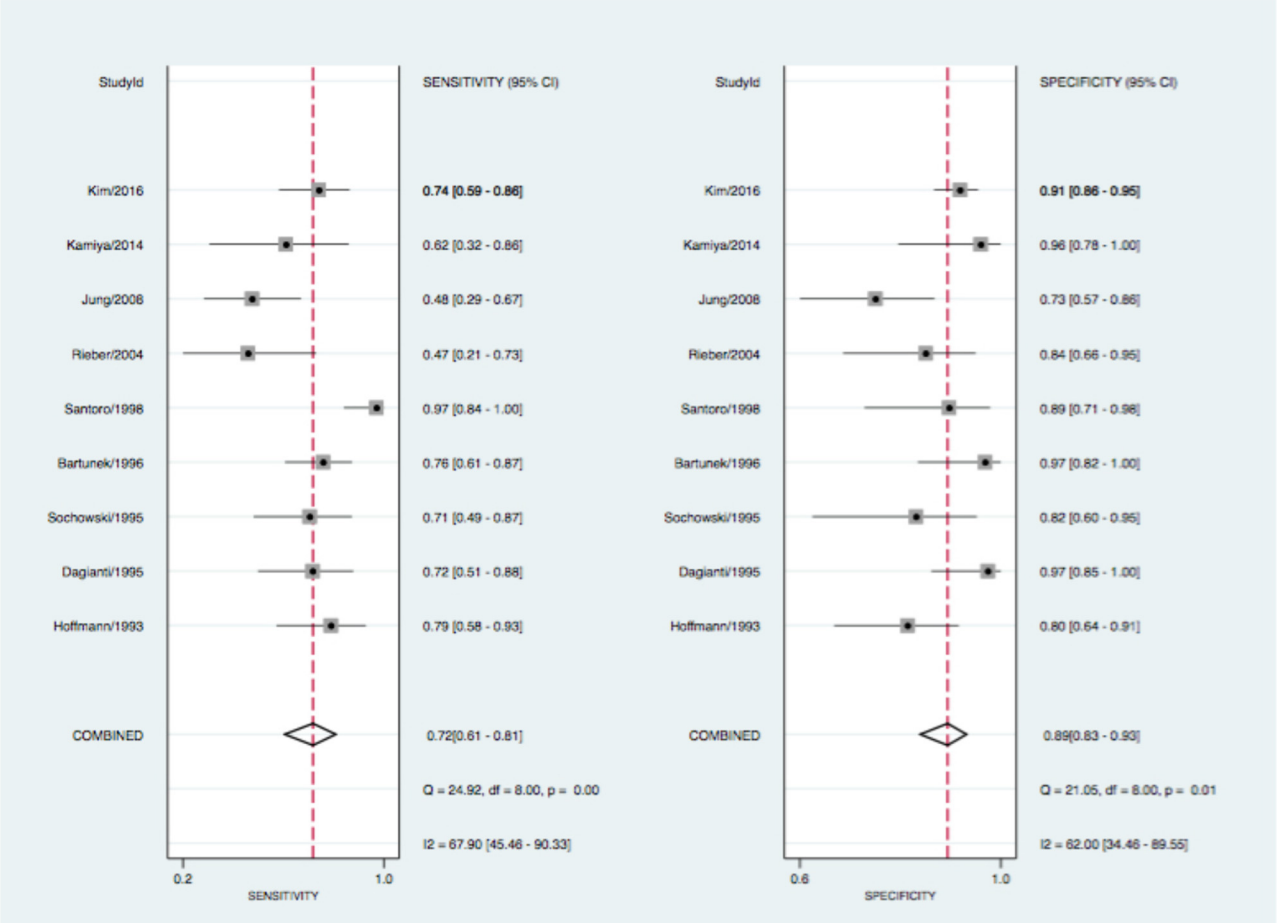

FIGURE 3 | Forrest plot for DSE with sensitivity (left) and specificity (right) estimates. CI, confidence intervall; I^2, the percentage of variation across studies that is due to heterogeneity rather than chance; Q, Cochran's Q measure of heterogeneity.

A more in depth analysis of heterogeneity can be in the **Supplementary Figure A4**.

Bias Assessment

In the assessment of publication bias, the slope coefficient for pCMR suggests symmetry in the data and therefore a low likelihood of publication bias with a statistically non-significant *p*-value of 0.95 (see **Supplementary Material**, **Figure 6A**). However, the slope in the DSE Deek's funnel plot (see **Figure 6B**) is suggestive of a bias from small studies even if the *p*-value is not significant (0.74).

DISCUSSION

Findings

The present meta-analysis demonstrates that pCMR has a significantly higher diagnostic accuracy in detecting obstructive CAD than DSE in stable patients with an intermediate risk of CAD. Here, only an assessment with pCMR can rigourusly rule-in and rule-out relevant stenosis. Therefore, this meta-analysis can inform clinical decision making regarding interventional coronary therapy in the intermediate risk cohort. Despite the presently high utilization of DSE for non-invasive assessment of CAD especially in European facilities, the evidence for that is supported by studies of inferior quality and study populations with divers risk stratification (19). From the 3,752 studies initially identified by the systematic literature review for DSE in this meta-analysis, only nine studies (0.2%) had a high quality study design and fulfilled all inclusion criteria. This is a small sample of the available evidence on DTA of one of the oldest stress tests used in clinical practice to detect obstructive CAD. However, the broad body of evidence regarding DTA of DSE is very diverse in the sense of blended with comorbidities and preconditions, that we excluded in our very precise selection process in order to perfectly depict patients with an intermediate risk of CAD (20). Most studies had varying reference standards, unclear cut-off values of relevant stenosis, limited contemporary data, fewer comparisons to FFR or did not recruit a homogenous patient collective (4, 5). Less strict inclusion criteria would have allowed a larger proportion of studies to be included in

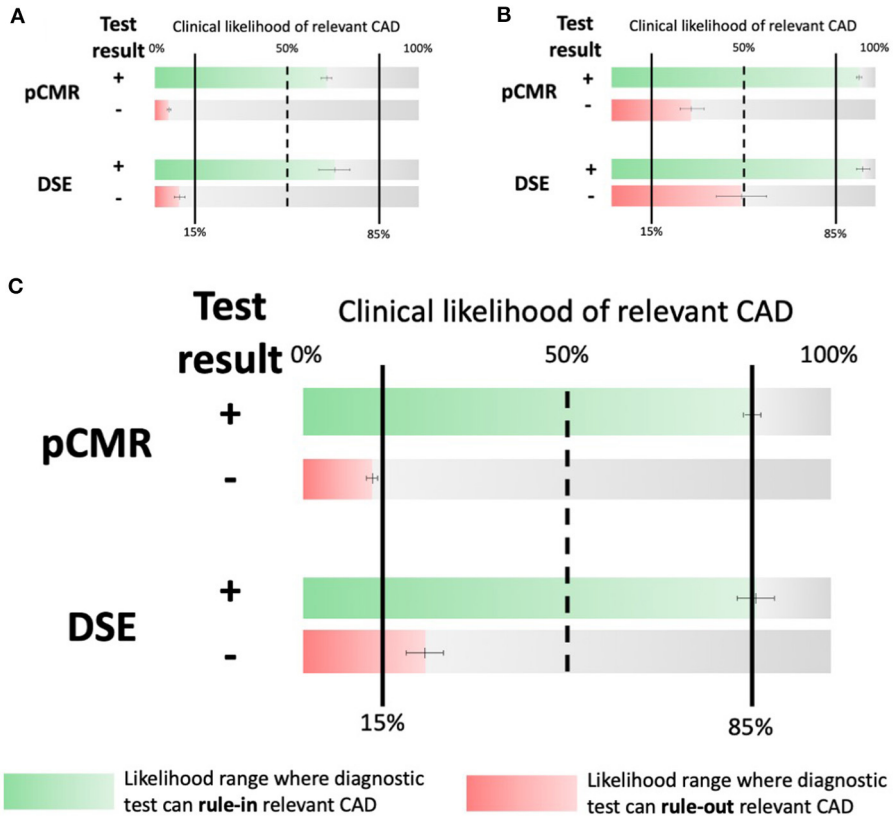

FIGURE 4 | Central Illustration. Likelihood ranges at which the respective tests can rule-in (green) and rule-out (red) obstructive CAD. **(A)** Respective likelihood ranges at a low (25% PrTP). **(B)** a high risk (75% PrTP) of obstructive CAD and **(C)** Respective likelihood ranges at an intermediate risk of CAD (50% PrTP). Note that only pCMR can rule-out relevant CAD (defined as PoTP < 15%) at an intermediate PrTP. CAD, coronary artery disease; PrTP, pre-test probability; PoTP, post-test-probability.

the assessment of DTA of DSE, leading to more heterogeneity in-between studies and thus an overall wider confidence of respective results. By focussing on DSE and excluding studies with dypiridamole and/or adenosine stress-echocardiography we choose the modality with the highest diagnostic accuracy over its competitors at the expanse of a broader base of studies to include in our meta-analysis. This results in less heterogeneity, a less diluted and thus more comparable precision of DTA. However, the novelty of this meta-analysis is the assessment of a well-defined and very precise cohort of patients with an intermediate pre-test probability of CAD. Inclusion of studies with patients of other risk cohorts would have biased the results and falsified the interpretation of DTA for patients at an intermediate risk of CAD. Consequentley, our results precisely depict the DTA of pCMR and DSE for patient at an intermediate pre-test probability of CAD and cannot automatically be generalized to patients at other risk levels. Providing higher quality evidence on DSE is critical for clinical decision making and these issues should be adressed in large scale comparative-effectiveness trials, in order to reassess diagnostic recommendations (19).

The recent results of the ISCHEMIA trial put the necessity of testing for obstructive CAD in patients with intermediate risk in question (21). Arguably, this trial rather highlights the strong medical need to identify the optimal diagnostic test modality in this risk cohort, rather than making it obsolete. Since the identification of patients, where the benefits from invasive procedures outweigh the risks is essential, the results of our meta-analysis can guide clinical decision making in patients with an intermediate risk of obstructive CAD. The reservation must be made, however, that the non-invasive assessment in the ISCEHMIA trial was facilitated by MDCT, which can be susceptible to overestimating stenosis in specific patients (22). The non-inferiority of a strictly conservative vs. an invasive management could also be explained in part by a suboptimal identification of obstructive CAD, underlining the relevance of the evidence collated in this work.

Whilst not all commonly employed perfusion tests, such as SPECT, PET, or FFR_{CT} were included in this analysis, previous meta-analyses have suggested SPECT (DOR 9.1, 15.3) is less accurate than DSE (DOR 9.5, 26.3) and pCMR (DOR 92.2, 26.4) for the detection of relevant coronary stenosis (4, 5). However, more recent results from the EVINCI study, where a comparison between wall motion and myocardial perfusion imaging was performed in patients with stable chest pain and intermediate likelihood of CAD, demonstrate that the diagnostic accuracy of the latter was similar to that of DSE (23). It should be noted that perfusion imaging is predominately performed by SPECT in the USA, comprising around 90% of stress tests anually (24).

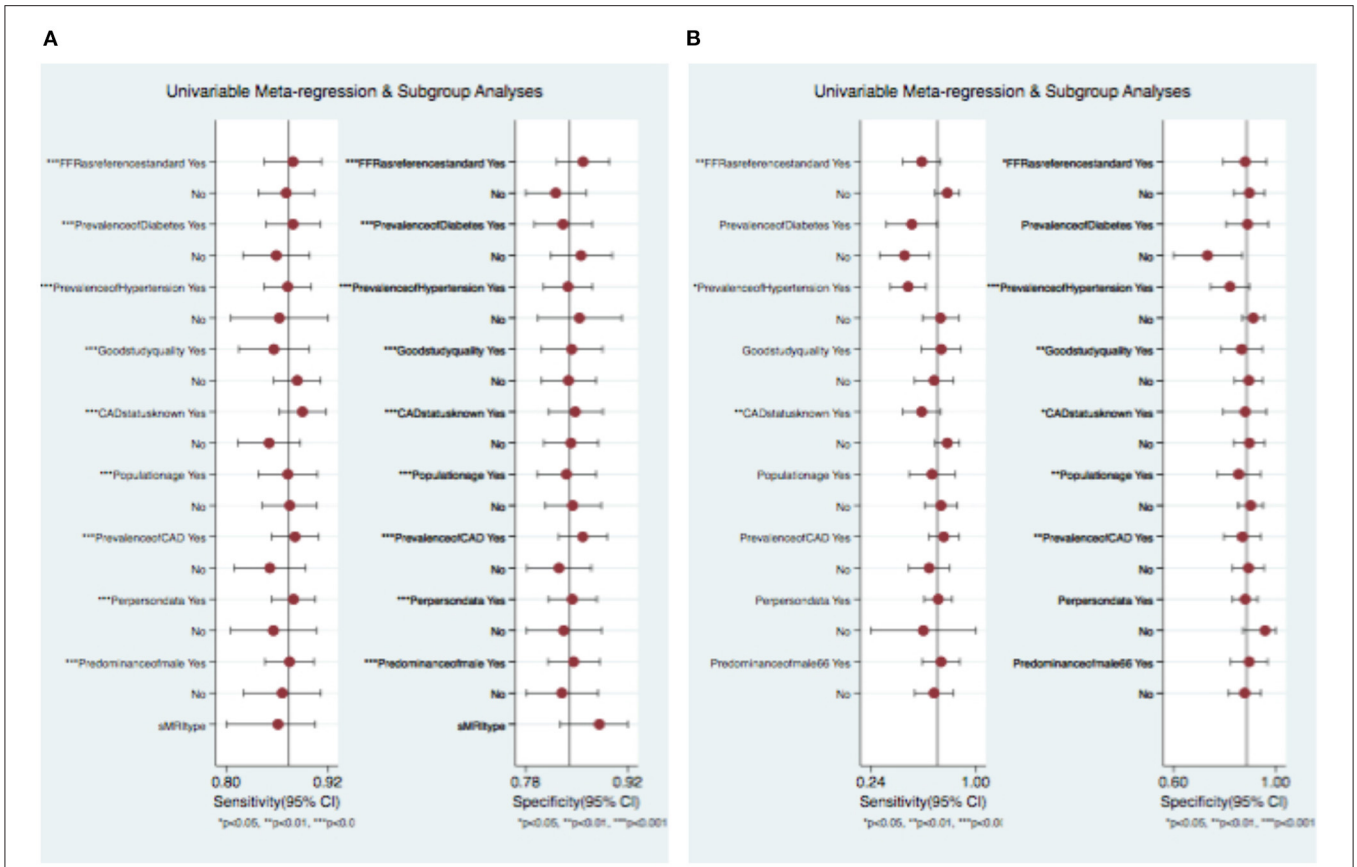

FIGURE 5 | Univariable meta-regression and subgroup analysis of **(A)** pCMR and **(B)** DSE. CI, confidence intervall.

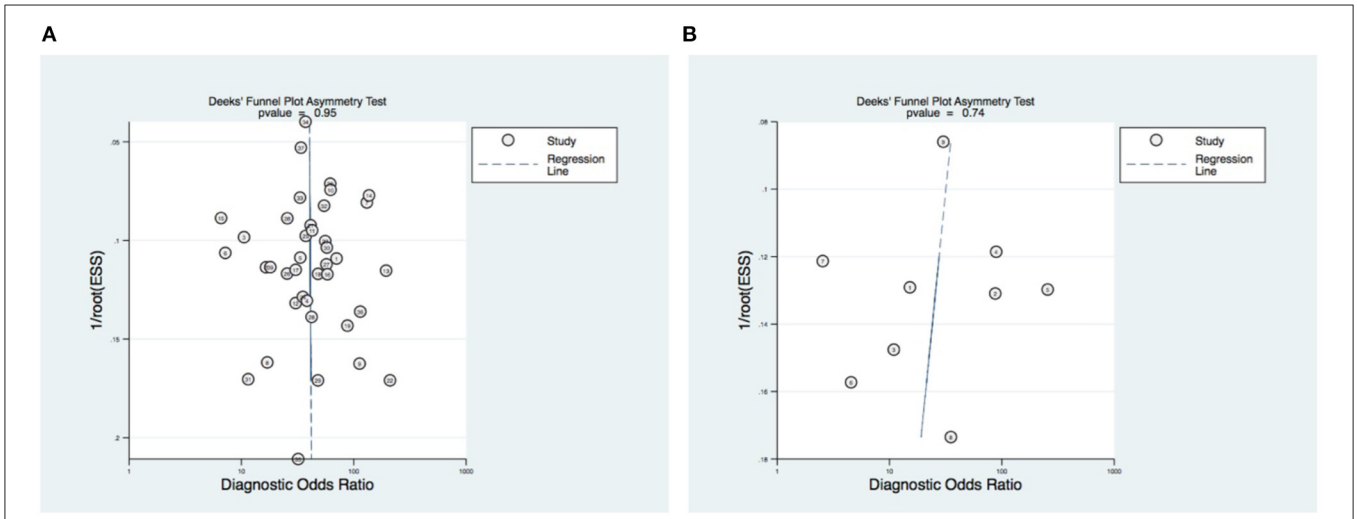

FIGURE 6 | Publication bias assessment. Deek's funnel plot of **(A)** pCMR and **(B)** DSE. The vertical axis displays the inverse of the square root of the effective sample size [1/root(ESS)]. The horizontal axis displays the DOR. *P*-values <0.10 indicate non-symmetrical funnel shapes and is suggestive of publication bias. The subimage description at the end is then obsolete (**(A)** pCMR. **(B)** DSE).

However, our findings cannot be generalized to other scenarios with patients at different pre-test probabilities or compared with myocardial perfusion tests not inlcuded in this assessment. Symptomatic patients with unstable disease or a high risk of CAD were excluded in this analysis because guidelines for this group are clear and supported by a large body of existing

evidence (2, 3). Despite, the recently published results of the MR-INFORM trial provide evidence of non-inferiority of pCMR as compared to FFR in the symptomatic patient cohort with high risk of CAD, which might even influence future guideline recommendations in favor of pCMR (8). Nevertheless, current guidelines recommand non-invasive assessment strategies with MDCT in patients at low risk of obstructive CAD, since in this cohort perfusion tests failed to sustainably rule-out obstructive disease (2, 3).

In this meta-analysis, a non-inferior diagnostic accuracy of pCMR in the subgroup of diabetic patients could hint a relevant diagnostic advantage in patients with low event rates. On the contrary, DSE studies had an inferior diagnostic performance in this subgroup, which is inline with findings from the DIAD trial (25) and the work of van der Wall et al. (26), where the screening for CAD in asymptomatic, diabetic patients was ineffective given a low event rate. Nonetheless, current guidelines for symptomatic patients with a low risk for CAD are favoring MDCT for initial assessment, even though studies provide evidence of non-inferiority only to standard care and over a limited follow-up period of 6 months (3, 22). Results from this meta-analysis confirm a statistically insufficient risk startification in patients with low event rates with an non-invasive pCMR or DSE-based assessment. In consequence, these data emphasize the role of non-invasive imaging to guide clinical decision making and highlight the indisputable need for a distinct recommendation on the diagnostic work-up of patients with an intermediate risk of CAD.

Strengths and Weaknesses of Review

The findings of this meta-analysis are novel and expand on previous studies (4, 5, 9). In contrast to previously published studies on DTA of obstructive CAD we like to emphasize that the results of our meta-analysis depict the clinically particularly relevant cohort of patients with an intermediate pre-test probability. Furthermore, we excluded studies that pre-selected their patients on the basis of angiographic findings to investigate the accuracy of the imaging modalities to identify obstructive CAD, rather than the ability to verify angiographic findings. This distinguishes our approach from the findings of the PACIFIC study for instance (27). Since the scope of our study was a patient- rather than a vessel-based assessment of DTA, our findings can be regarded as complementary to the results of the EVINCI trial, focusing on co-localization of perfusion defects with angiographic findings in patients also with an intermediate risk of CAD (23). In addition, a pre-defined, invasive cut-off value for diagnosis of relevant coronary artery stenosis has been applied so that we could compare more similar populations with less heterogenous results. This differentiates our work from previous meta-analysis. Specifically, FFR as well as CCA were used as reference standards with their respective cut-offs from international guidelines (2, 3, 28).

CCA cannot always provide sufficient information on the hemodynamic significance of a coronary artery stenosis, as the landmark trials FAME (29) as well as FAMOUS-NSTEMI (30) have shown. Nevertheless, "*diffuse coronary atherosclerosis without focal stenosis at angiography*" (31) can cause a continuous pressure fall along the vessel length, "*due to increased rest-perfusion, hence a lower flow-reserve*" (31) and this can lead to FFR values below the ischemic threshold, even in the absence of relevant CAD (31). Due to these issues, the analysis in this study was not restricted to reports that performed only FFR with the aim of avoiding confounding related to a narrow endpoint. In addition, studies that compared pCMR exclusively to FFR, sensitivity and specificity for the diagnosis of functionally relevant CAD has been significantly higher than in studies where it was compared with CCA only (32). This could be due to confounding of non-flow limiting stenosis in studies using CCA as the reference test with hemodynamically insignificant cut-off values. This meta-analysis incorporated only studies with severe definitions of significance for coronary artery stenosis (lumen narrowing of >70% in CCA) (2).

A key strength of this study is that a more comprehensive and detailed search strategy was used than in existing meta-analyses (4, 5, 9), meaning that the present study has a higher chance of identifying all available literature on the aimed risk cohort. For example, a similar published meta-analysis by Danad et al. reported data comparing several myocardial perfusion tests but did not use a systematic review of the literature nor a specific patient risk stratification (4). They included only three studies on DSE and four pCMR studies as compared to the nine DSE and 39 pCMR studies included in this review. This supports the argument that more comprehensive methods were able to identify a wider range of existing work (4). Another strength is that while prior syntheses have included studies that have been evaluated with reference tests that comprised FFR and CCA assessments at different cut-off points (5), this study reports at specific thresholds which minimizes risk of bias (14). On that note, studies that only used FFR measurements were largely single center and small trials. Patients were often pre-selected due to their angiographic findings, which may also improve sensitivity at the cost of specificity. These circumstances thus alter the generalizability of results and present another reason for incorporating both, CCA and FFR, reference standards as was done in this study. Even though a higher sensitivity but a lower specificity was seen in pCMR studies, which predominately used FFR measurements as the reference standard, the meta-regression and sub-group analysis of this report attested no confounding of preselection. To elaborate on that, reporting different cut-off values for FFR (e.g., 0.75 or 0.70) would have further limited the generalizability of results and potentially increase the risk of the threshold bias for a higher sensitivity at the expense of a lower specificity (9).

Finally, as with any meta-analysis, limitations to this method include heterogeneity in between studies and presence of publication bias. An in-depth discussion of limitations to this study can be found in the **Supplementary Material**.

CONCLUSION

This systematic review and meta-analysis concludes that pCMR is superior to DSE in the diagnosis of relevant coronary artery stenosis in patients with an intermediate pre-test probability

of CAD. Patients in this cohort might benefit from primary pCMR assessment for risk stratification and to guide further invasive procedures.

CLINICAL COMPETENCIES

The evaluation of the accuracy of pCMR and DSE for diagnosis of significant coronary artery stenosis is relevant for the appropriate management and risk stratification of patients with suspected or stable CAD. Erroneous interpretations of hemodynamic relevance of stenosis can lead to clinically unnecessary revascularizations without any prognostic benefit to patients. Moreover, the underlying systematic review revealed a discrepancy between the absolute amount of evidence on DSE assessment for CAD and its significance regarding valide risk stratification and adaquate reference methodes, which limits their clinical value.

TRANSLATIONAL OUTLOOK

Even though pCMR presented here as the superior non-invasive method, this meta-analysis does not qualify to comment on the general validity of its superiority in the assessment of CAD. A comparative cost-effectiveness analysis is needed, in order to assess efficiency. It may be possible, in certain patient groups, that pCMR has some diagnostic advantages over FFR but this was outside the scope of the current review.

DATA AVAILABILITY STATEMENT

The original contributions presented in the study are included in the article/**Supplementary Material**, further inquiries can be directed to the corresponding author/s.

AUTHOR CONTRIBUTIONS

SMH acquired the data (scanned studies for eligibility and extracted data), performed statistical analysis, conceived and designed the meta-analysis, conceptualized the key intellectual content, wrote, and drafted the manuscript. SIH scanned the studies for eligibility and extracted data to square results with SMH. GH and SP participated in the design and helped to coordination the workflow. FB, MK, GH, and SP took part in the editing of the manuscript. SP complemented also to the key intellectual content of this paper. All authors contributed to the article and approved the submitted version.

FUNDING

This manuscript was funded, in part, by a grant from the European Heart Academy of the European Society of Cardiology scholarship for the Executive M.Sc. Health Economics, Outcomes and Management in Cardiovascular Sciences in collaboration with the London School of Economics. SP would like to acknowledge support from the National Institute for Health Research Barts Biomedical Research Center (BRC).

ACKNOWLEDGMENTS

I would like to express my sincere gratitude to Elias Mossialos and Huseyin Naci for their compelling intellectual guidance during the completion of the present work.

SUPPLEMENTARY MATERIAL

The Supplementary Material for this article can be found online at: https://www.frontiersin.org/articles/10.3389/fcvm.2021.630846/full#supplementary-material

REFERENCES

1. Kumar A, Cannon CP. Acute coronary syndromes: diagnosis and management, part II. *Mayo Clin Proc.* (2009) 84:1021–36. doi: 10.1016/S0025-6196(11)60674-5
2. Fihn SD, Blankenship JC, Alexander KP, Bittl JA, Byrne JG, Fletcher BJ, et al. 2014 ACC/AHA/AATS/PCNA/SCAI/STS focused update of the guideline for the diagnosis and management of patients with stable ischemic heart disease: a report of the American College of Cardiology/American Heart Association Task Force on Practice Guidelines, and the American Association for Thoracic Surgery, Preventive Cardiovascular Nurses Association, Society for Cardiovascular Angiography and Interventions, and Society of Thoracic Surgeons. *Circulation.* (2014) 130:1749–67. doi: 10.1161/CIR.0000000000000095
3. Knuuti J, Wijns W, Saraste A, Capodanno D, Barbato E, Funck-Brentano C, et al. 2019 ESC Guidelines for the diagnosis and management of chronic coronary syndromes. *Eur Heart J.* (2020) 41:407–77. doi: 10.1093/eurheartj/ehz425
4. Danad I, Szymonifka J, Twisk JWR, Norgaard BL, Zarins CK, Knaapen P, et al. Diagnostic performance of cardiac imaging methods to diagnose ischaemia-causing coronary artery disease when directly compared with fractional flow reserve as a reference standard: a meta-analysis. *Eur Heart J.* (2017) 38:991–8. doi: 10.1093/eurheartj/ehw095
5. Jaarsma C, Leiner T, Bekkers SC, Crijns HJ, Wildberger JE, Nagel E, et al. Diagnostic performance of noninvasive myocardial perfusion imaging using single-photon emission computed tomography, cardiac magnetic resonance, and positron emission tomography imaging for the detection of obstructive coronary artery disease: a meta-analysis. *J Am Coll Cardiol.* (2012) 59:1719–28. doi: 10.1016/j.jacc.2011.12.040
6. Greenwood JP, Maredia N, Younger JF, Brown JM, Nixon J, Everett CC, et al. Cardiovascular magnetic resonance and single-photon emission computed tomography for diagnosis of coronary heart disease (CE-MARC): a prospective trial. *Lancet.* (2012) 379:453–60. doi: 10.1016/S0140-6736(11)61335-4
7. Schwitter J, Wacker CM, Wilke N, Al-Saadi N, Sauer E, Huettle K, et al. MR-IMPACT II: magnetic resonance imaging for myocardial perfusion assessment in coronary artery disease trial: perfusion-cardiac magnetic resonance vs. single-photon emission computed tomography for the detection of coronary artery disease: a comparative multicentre, multivendor trial. *Eur Heart J.* (2013) 34:775–81. doi: 10.1093/eurheartj/ehs022
8. Nagel E, Greenwood JP, McCann GP, Bettencourt N, Shah AM, Hussain ST, et al. Magnetic resonance perfusion or fractional flow reserve in coronary disease. *N Engl J Med.* (2019) 380:2418–28. doi: 10.1056/NEJMoa1716734
9. Jiang B, Cai W, Lv X, Liu H. Diagnostic performance and clinical utility of myocardial perfusion MRI for coronary artery disease with fractional flow reserve as the standard reference: a meta-analysis. *Heart Lung Circ.* (2016) 25:1031–8. doi: 10.1016/j.hlc.2016.02.018

10. Liberati A, Altman DG, Tetzlaff J, Mulrow C, Gotzsche PC, Ioannidis JP, et al. The PRISMA statement for reporting systematic reviews and meta-analyses of studies that evaluate healthcare interventions: explanation and elaboration. *BMJ.* (2009) 339:b2700. doi: 10.1136/bmj.b2700
11. Deeks JJ, Wisniewski S, Davenport C. *Chapter 4: Guide to the Contents of a Cochrane Diagnostic Test Accuracy Protocol: The Cochrane Collaboration.* (2013). Available online at: http://srdta.cochrane.org/ (accessed June 29, 2018).
12. Whiting P, Rutjes AW, Reitsma JB, Bossuyt PM, Kleijnen J. The development of QUADAS: a tool for the quality assessment of studies of diagnostic accuracy included in systematic reviews. *BMC Med Res Methodol.* (2003) 3:25. doi: 10.1186/1471-2288-3-25
13. Reitsma JB, Rutjes AWS, Whiting P, Vlassov VV, Leeflang MMG, Deeks JJ. *Chapter 9: Assessing Methodological Quality*. Version 1.0.0, 2009. The Cochrane Collaboration (2009). Available online at: http://srdta.cochrane.org/ (accessed June 29, 2018).
14. Macaskill P, Gatsonis C, Deeks JJ, Harbord RM, Takwoingi Y. *Chapter 10: Analysing and Presenting Results*. The Cochrane Collaboration (2010). Available online at: http://srdta.cochrane.org/
15. Higgins JP, Thompson SG, Deeks JJ, Altman DG. Measuring inconsistency in meta-analyses. *BMJ.* (2003) 327:557–60. doi: 10.1136/bmj.327.7414.557
16. Gelijns AC. *An Introduction to a Bayesian Method for Meta-Analysis: The Confidence Profile Method*. Washington, DC: National Academies Press (US) (1990).
17. Deeks JJ, Macaskill P, Irwig L. The performance of tests of publication bias and other sample size effects in systematic reviews of diagnostic test accuracy was assessed. *J Clin Epidemiol.* (2005) 58:882–93. doi: 10.1016/j.jclinepi.2005.01.016
18. Kamiya K, Sakakibara M, Asakawa N, Yoshitani T, Iwano H, Komatsu H, et al. Cardiac magnetic resonance performs better in the detection of functionally significant coronary artery stenosis compared to single-photon emission computed tomography and dobutamine stress echocardiography. *Circ J.* (2014) 78:2468–76. doi: 10.1253/circj.CJ-13-1454
19. Shaw LJ, Phillips LM, Nagel E, Newby DE, Narula J, Douglas PS. Comparative effectiveness trials of imaging-guided strategies in stable ischemic heart disease. *JACC Cardiovasc Imaging.* (2017) 10:321–34. doi: 10.1016/j.jcmg.2016.10.016
20. Martin TW, Seaworth JF, Johns JP, Pupa LE, Condos WR. Comparison of adenosine, dipyridamole, and dobutamine in stress echocardiography. *Ann Intern Med.* (1992) 116:190–6. doi: 10.7326/0003-4819-116-3-190
21. Maron DJ, Hochman JS, Reynolds HR, Bangalore S, O'Brien SM, Boden WE, et al. Initial invasive or conservative strategy for stable coronary disease. *N Engl J Med.* (2020) 382:1395–407. doi: 10.1056/NEJMoa1915922
22. Hulten E, Pickett C, Bittencourt MS, Villines TC, Petrillo S, Di Carli MF, et al. Outcomes after coronary computed tomography angiography in the emergency department: a systematic review and meta-analysis of randomized, controlled trials. *J Am Coll Cardiol.* (2013) 61:880–92. doi: 10.1016/j.jacc.2012.11.061
23. Liga R, Vontobel J, Rovai D, Marinelli M, Caselli C, Pietila M, et al. Multicentre multi-device hybrid imaging study of coronary artery disease: results from the EValuation of INtegrated Cardiac Imaging for the Detection and Characterization of Ischaemic Heart Disease (EVINCI) hybrid imaging population. *Eur Heart J Cardiovasc Imaging.* (2016) 17:951–60. doi: 10.1093/ehjci/jew038
24. Benjamin EJ, Virani SS, Callaway CW, Chamberlain AM, Chang AR, Cheng S, et al. Heart disease and stroke statistics—2018 update: a report from the American Heart Association. *Circulation.* (2018) 137:e67–492. doi: 10.1161/CIR.0000000000000558
25. Young LH, Wackers FJT, Chyun DA, Davey JA, Barrett EJ, Taillefer R, et al. Cardiac outcomes after screening for asymptomatic coronary artery disease in patients with type 2 diabetes: the DIAD study: a randomized controlled trial. *JAMA.* (2009) 301:1547–55. doi: 10.1001/jama.2009.476
26. van der Wall EE, Scholte AJ, Holman ER, Bax JJ. Stress imaging in patients with diabetes; routine practice? *Int J Cardiovasc Imaging.* (2011) 27:939–42. doi: 10.1007/s10554-010-9639-7
27. Danad I, Raijmakers PG, Driessen RS, Leipsic J, Raju R, Naoum C, et al. Comparison of coronary CT angiography, SPECT, PET, and hybrid imaging for diagnosis of ischemic heart disease determined by fractional flow reserve. *JAMA Cardiol.* (2017) 2:1100–7. doi: 10.1001/jamacardio.2017.2471
28. Neumann FJ, Sousa-Uva M, Ahlsson A, Alfonso F, Banning AP, Benedetto U, et al. 2018 ESC/EACTS Guidelines on myocardial revascularization. *Eur Heart J.* (2019) 40:87–165. doi: 10.1093/eurheartj/ehy394
29. Tonino PA, Fearon WF, De Bruyne B, Oldroyd KG, Leesar MA, Ver Lee PN, et al. Angiographic versus functional severity of coronary artery stenoses in the FAME study fractional flow reserve versus angiography in multivessel evaluation. *J Am Coll Cardiol.* (2010) 55:2816–21. doi: 10.1016/j.jacc.2009.11.096
30. Layland J, Oldroyd KG, Curzen N, Sood A, Balachandran K, Das R, et al. Fractional flow reserve vs. angiography in guiding management to optimize outcomes in non-ST-segment elevation myocardial infarction: the British Heart Foundation FAMOUS-NSTEMI randomized trial. *Eur Heart J.* (2015) 36:100–11. doi: 10.1093/eurheartj/ehu338
31. De Bruyne B, Hersbach F, Pijls NH, Bartunek J, Bech JW, Heyndrickx GR, et al. Abnormal epicardial coronary resistance in patients with diffuse atherosclerosis but "Normal" coronary angiography. *Circulation.* (2001) 104:2401–6. doi: 10.1161/hc4501.099316
32. Watkins S, McGeoch R, Lyne J, Steedman T, Good R, McLaughlin MJ, et al. Validation of magnetic resonance myocardial perfusion imaging with fractional flow reserve for the detection of significant coronary heart disease. *Circulation.* (2009) 120:2207–13. doi: 10.1161/CIRCULATIONAHA.109.872358

Conflict of Interest: SP provides consultancy to, owns stock and has also received research support for unrelated research to this article from Circle Cardiovascular Imaging, Inc., Calgary, Alberta, Canada.

The remaining authors declare that the research was conducted in the absence of any commercial or financial relationships that could be construed as a potential conflict of interest.

frontiers in Cardiovascular Medicine

GENERAL COMMENTARY
published: 10 June 2021
doi: 10.3389/fcvm.2021.694323

Commentary: Vasodilator Myocardial Perfusion Cardiac Magnetic Resonance Imaging Is Superior to Dobutamine Stress Echocardiography in the Detection of Relevant Coronary Artery Stenosis: A Systematic Review and Meta-Analysis on Their Diagnostic Accuracy

Attila Kardos[1,2]*, *Roxy Senior*[3] and *Harald Becher*[4]

[1] Department of Cardiology, Milton Keynes University Hospital, Milton Keynes, United Kingdom, [2] School of Sciences and Medicine, University of Buckingham, Buckingham, United Kingdom, [3] Imperial College, National Heart and Lung Institute, London, United Kingdom, [4] ABACUS, Mazankowski Alberta Heart Institute, University of Alberta Hospital, Edmonton, AB, Canada

Keywords: stress echocardiography, cardiac MRI, chronic coronary syndrome, diagnostic accuracy and yield, discussion points

OPEN ACCESS

Edited by:
Gianluca Pontone, Monzino Cardiology Center (IRCCS), Italy

Reviewed by:
Grigorios Korosoglou, GRN Klinik Weinheim, Germany

***Correspondence:**
Attila Kardos
attila.kardos@cardiov.ox.ac.uk

Specialty section:
This article was submitted to Cardiovascular Imaging, a section of the journal Frontiers in Cardiovascular Medicine

Received: *12 April 2021*
Accepted: *05 May 2021*
Published: *10 June 2021*

Citation:
Kardos A, Senior R and Becher H (2021) Commentary: Vasodilator Myocardial Perfusion Cardiac Magnetic Resonance Imaging Is Superior to Dobutamine Stress Echocardiography in the Detection of Relevant Coronary Artery Stenosis: A Systematic Review and Meta-Analysis on Their Diagnostic Accuracy. Front. Cardiovasc. Med. 8:694323. doi: 10.3389/fcvm.2021.694323

A Commentary on

Vasodilator Myocardial Perfusion Cardiac Magnetic Resonance Imaging Is Superior to Dobutamine Stress Echocardiography in the Detection of Relevant Coronary Artery Stenosis: A Systematic Review and Meta-Analysis on Their Diagnostic Accuracy
by Haberkorn, S. M., Haberkorn, S. I., Bönner, F., Kelm, M., Hopkin, G., and Petersen, S. E. (2021). Front. Cardiovasc. Med. 8:630846. doi: 10.3389/fcvm.2021.630846

We are grateful to the authors for sharing the results of this very precise and detailed analysis of comparing the diagnostic performance of perfusion cardiac magnetic resonance (pCMR) and dobutamine stress echocardiography (DSE) for the detection of coronary artery stenosis with the scientific readership as the two functional test modalities without associated harmful radiation (1). The authors found higher sensitivity for pCMR vs. DSE (0.88 vs. 0.720) with a negative likelihood ratio of 0.14 vs. 0.31, respectively. There was no difference in specificity. We acknowledge the precise nature of the work. However, we would like to raise some points that may be worthwhile considering.

(1) This meta-analysis takes historical studies into account using either DSE or pCMR that compared the functional test results to that of invasive or coronary CT angiography (CCTA) or invasive fractional flow reserve. Albeit these are the only data available for comparison, it may question the legitimacy of comparing two functional tests with different principles to address coronary artery disease (CAD) severity detection. With this in mind, one would look for studies that are comparing the effect of the same stressor (e.g., coronary vasodilators) that investigates the

accuracy of the imaging modality, i.e., echocardiography vs. CMR in detecting inducible ischemia and significant CAD. One such methodological comparison was showing no difference in the accuracy between echocardiography vs. CMR using vasodilator stress test in the same patients' cohort (2).

(2) The majority of the included DSE studies were performed before 2000 without using ultrasound-enhancing contrast agents (UECAs). Not until 2009, the European Association of Cardiovascular Imaging recommended UECA to be used regularly during echocardiography where >2 segments of the left ventricle are not delineated properly (3). This certainly was a major step forward in improving interpretability and increasing operator confidence during stress echocardiography. However, recent comparisons of contrast-enhanced stress echocardiography with coronary angiography mainly used vasodilator stress test. Further randomized, prospective studies with contemporary imaging techniques and modalities, e.g., contrast-enhanced stress echocardiography, may help our understanding of the strength and weaknesses of those modalities.

(3) Although the diagnostic accuracy is essential, the prediction of outcome and/or risk stratification following a test is probably more important. In this respect, both pCMR (4–6) and DSE (7–9) have robust data, although with no head-to-head comparative studies. Stress echocardiography has consistently shown that a normal study identifies a low-risk cohort who needs no further testing, while significant ischemia identifies a high-risk group. In addition, the Mayo Clinic group has shown the same outcome in patients with abnormal stress echo findings regardless of the degree of coronary artery stenosis by Invasive Coronary Angiography (10). This meta-analysis did not evaluate outcome prediction nor risk stratification.

(4) Thus, current European Society of Cardiology and American Heart Association guidelines for chest pain assessment in chronic coronary syndrome patients with intermediate pretest probability recommend a non-invasive functional test [stress echocardiography, single-photon emission computed tomography, CMR] as well as an anatomical test, such as CCTA as the initial test, guided by the local expertise and infrastructure (11). In order to recommend CMR as a first-line diagnostic test, further comparative studies on risk stratification, management-based outcome, and cost-effectiveness need to be demonstrated.

AUTHOR CONTRIBUTIONS

All authors listed have made a substantial, direct and intellectual contribution to the work, and approved it for publication.

REFERENCES

1. Haberkorn SM, Haberkorn SI, Bönner F, Kelm M, Hopkin G, Petersen SE. Vasodilator myocardial perfusion cardiac magnetic resonance imaging is superior to dobutamine stress echocardiography in the detection of relevant coronary artery stenosis: a systematic review and meta-analysis on their diagnostic accuracy. *Front Cardiovasc Med.* (2021) 8:630846. doi: 10.3389/fcvm.2021.630846
2. Arnold JR, Karamitsos TD, Pegg TJ, Francis JM, Olszewski R, Searle N, et al. Adenosine stress myocardial contrast echocardiography for the detection of coronary artery disease: a comparison with coronary angiography and cardiac magnetic resonance. *JACC Cardiovasc Imaging.* (2010) 3:934–43. doi: 10.1016/j.jcmg.2010.06.011
3. Senior R, Becher H, Monaghan M, Agati L, Zamorano J, Vanoverschelde JL, et al. Contrast echocardiography: evidence-based recommendations by European Association of Echocardiography. *Eur J Echocardiogr.* (2009) 10:194–212. doi: 10.1093/ejechocard/jep005
4. Heitner JF, Kim RJ, Kim HW, Klem I, Shah DJ, Debs D, et al. Prognostic value of vasodilator stress cardiac magnetic resonance imaging: a multicenter study with 48,000 patient-years of follow-up. *JAMA Cardiol.* (2019) 4:256–64. doi: 10.1001/jamacardio.2019.0035
5. Kwong RY, Ge Y, Steel K, Bingham S, Abdullah S, Fujikura K, et al. Cardiac magnetic resonance stress perfusion imaging for evaluation of patients with chest pain. *J Am Coll Cardiol.* (2019) 74:1741–55. doi: 10.1016/j.jacc.2019.07.074
6. Pezel T, Hovasse T, Kinnel M, Unterseeh T, Champagne S, Toupin S, et al. Prognostic value of stress cardiovascular magnetic resonance in asymptomatic patients with known coronary artery disease. *J Cardiovasc Magn Reson.* (2021) 23:19. doi: 10.1186/s12968-021-00721-8
7. Marwick TH, Case C, Sawada S, Vasey C, Short L, Lauer M. Use of stress echocardiography to predict mortality in patients with diabetes and known or suspected coronary artery disease. *Diabetes Care.* (2002) 25:1042–8. doi: 10.2337/diacare.25.6.1042
8. Yao SS, Bangalore S, Chaudhry FA. Prognostic implications of stress echocardiography and impact on patient outcomes: an effective gatekeeper for coronary angiography and revascularization. *J Am Soc Echocardiogr.* (2010) 23:832–9. doi: 10.1016/j.echo.2010.05.004
9. Cortigiani L, Borelli L, Raciti M, Bovenzi F, Picano E, Molinaro S, et al. Prediction of mortality by stress echocardiography in 2835 diabetic and 11 305 nondiabetic patients. *Circ Cardiovasc Imaging.* (2015) 8:e002757. doi: 10.1161/CIRCIMAGING.114.002757
10. From AM, Kane G, Bruce C, Pellikka PA, Scott C, McCully RB. Characteristics and outcomes of patients with abnormal stress echocardiograms and angiographically mild coronary artery disease (<50% stenoses) or normal coronary arteries. *J Am Soc Echocardiogr.* (2010) 23:207–14. doi: 10.1016/j.echo.2009.11.023
11. Knuuti J, Wijns W, Saraste A, Capodanno D, Barbato E, Funck-Brentano C, et al. 2019 ESC guidelines for the diagnosis and management of chronic coronary syndromes. *Eur Heart J.* (2020) 41:407–77. doi: 10.1093/eurheartj/ehz425

Conflict of Interest: The authors declare that the research was conducted in the absence of any commercial or financial relationships that could be construed as a potential conflict of interest.

frontiers in Cardiovascular Medicine

REVIEW
published: 04 June 2021
doi: 10.3389/fcvm.2021.683434

What Is the Clinical Impact of Stress CMR After the ISCHEMIA Trial?

Théo Pezel[1,2], *Luis Miguel Silva*[3], *Adriana Aparecia Bau*[3], *Adherbal Teixiera*[3], *Michael Jerosch-Herold*[4] *and Otávio R. Coelho-Filho*[3]*

[1] Division of Cardiology, Department of Medicine, Johns Hopkins University, Baltimore, MD, United States, [2] Department of Cardiology, Lariboisiere Hospital, University of Paris, Inserm, UMRS 942, Paris, France, [3] Discipline of Cardiology, Faculty of Medical Science – State University of Campinas – UNICAMP, Campinas, São Paulo, Brazil, [4] Noninvasive Cardiovascular Imaging Program and Department of Radiology, Brigham and Women's Hospital, Boston, MA, United States

After progressively receding for decades, cardiovascular mortality due to coronary artery disease has recently increased, and the associated healthcare costs are projected to double by 2030. While the 2019 European Society of Cardiology guidelines for chronic coronary syndromes recommend non-invasive cardiac imaging for patients with suspected coronary artery disease, the impact of non-invasive imaging strategies to guide initial coronary revascularization and improve long-term outcomes is still under debate. Recently, the ISCHEMIA trial has highlighted the fundamental role of optimized medical therapy and the lack of overall benefit of early invasive strategies at a median follow-up of 3.2 years. However, sub-group analyses excluding procedural infarctions with longer follow-ups of up to 5 years have suggested that patients undergoing revascularization had better outcomes than those receiving medical therapy alone. A recent sub-study of ISCHEMIA in patients with heart failure or reduced left ventricular ejection fraction (LVEF<45%) indicated that revascularization improved clinical outcomes compared to medical therapy alone. Furthermore, other large observational studies have suggested a favorable prognostic impact of coronary revascularization in patients with severe inducible ischemia assessed by stress cardiovascular magnetic resonance (CMR). Indeed, some data suggest that stress CMR-guided revascularization assessing the extent of the ischemia could be useful in identifying patients who would most benefit from invasive procedures such as myocardial revascularization. Interestingly, the MR-INFORM trial has recently shown that a first-line stress CMR-based non-invasive assessment was non-inferior in terms of outcomes, with a lower incidence of coronary revascularization compared to an initial invasive approach guided by fractional flow reserve in patients with stable angina. In the present review, we will discuss the current state-of-the-art data on the prognostic value of stress CMR assessment of myocardial ischemia in light of the ISCHEMIA trial results, highlighting meaningful sub-analyses, and still unanswered opportunities of this pivotal study. We will also review the available evidence for the potential clinical application of quantifying the extent of ischemia to stratify cardiovascular risk and to best guide invasive and non-invasive treatment strategies.

Keywords: cardiovascular magnetic resonance, stress testing, myocardial ischemia, cardiovascular events, coronary revascularization, stable coronary disease

OPEN ACCESS

Edited by:
Bernhard L. Gerber, Cliniques Universitaires Saint-Luc, Belgium

Reviewed by:
Ali Yilmaz, University Hospital Münster, Germany
Florian Bönner, Heinrich Heine University of Düsseldorf, Germany

***Correspondence:**
Otávio R. Coelho-Filho
orcfilho@unicamp.br; tavicocoelho@gmail.com

Specialty section:
This article was submitted to Cardiovascular Imaging, a section of the journal Frontiers in Cardiovascular Medicine

Received: *21 March 2021*
Accepted: *12 May 2021*
Published: *04 June 2021*

Citation:
Pezel T, Silva LM, Bau AA, Teixiera A, Jerosch-Herold M and Coelho-Filho OR (2021) What Is the Clinical Impact of Stress CMR After the ISCHEMIA Trial? Front. Cardiovasc. Med. 8:683434. doi: 10.3389/fcvm.2021.683434

INTRODUCTION

After progressively dropping for decades, cardiovascular (CV) mortality due to coronary artery disease (CAD) has recently increased, and the associated healthcare costs are projected to double by 2030 (1). Although the current European and American guidelines for chronic coronary syndromes recommend non-invasive cardiac imaging for patients with suspected CAD (2, 3), the impact of non-invasive imaging strategies to guide initial coronary revascularization and improve long-term outcomes is still under debate (4). Indeed, the International Study of Comparative Health Effectiveness with Medical and Invasive Approaches (ISCHEMIA) trial has recently shown the lack of benefit to an initial revascularization strategy as compared to optimal medical therapy (5).

Cardiovascular magnetic resonance (CMR) imaging is an accurate technique to assess ventricular function, the extent of myocardial scar and viability, and inducible myocardial ischemia (6–9). Furthermore, the diagnostic accuracy (10–14), cost-effectiveness (15), and prognostic value (8, 9, 16, 17) of stress CMR compare favorably to other functional non-invasive tests, such as nuclear perfusion or stress echocardiography. A recent study has even demonstrated (18) that a first-line stress CMR-based non-invasive strategy was non-inferior in terms of outcomes, with a lower incidence of coronary revascularization, compared to an initial invasive approach guided by fractional flow reserve (FFR) in patients with stable angina. Consistently, several studies have underlined the high negative predictive value of stress CMR to detect CAD (6–9). Therefore, it can be hypothesized that myocardial ischemia detected by stress CMR could be helpful in guiding coronary revascularization and optimizing the management of these patients (19).

In the present review, we will discuss the current state-of-the-art data on the prognostic value of stress CMR assessment of myocardial ischemia in light of the ISCHEMIA trial results, highlighting some sub-analyses and still unanswered questions of this pivotal study. We will also review the available evidence for the potential clinical application of assessing the extent of ischemia to stratify CV risk and to best guide invasive and non-invasive treatment strategies.

LESSONS FROM THE ISCHEMIA TRIAL

Before the ISCHEMIA trial, the BARI 2D (Bypass Angioplasty Revascularization Investigation 2 Diabetes) (20) and COURAGE (Clinical Outcomes Utilizing Revascularization and Aggressive Drug Evaluation) (21) trials failed to demonstrate any significant benefit from coronary revascularization compared to medical treatment in the occurrence of all-cause death or CV outcomes in patients with angiographic evidence of obstructive CAD. The ISCHEMIA trial is to-date the largest well-designed trial comparing an invasive strategy to optimal medical therapy in patients, 5,179 in total, with moderate or severe ischemia on stress tests. The presence of at least moderate ischemia on stress tests was defined as follow: (i) $\geq$5% myocardium ischemic for nuclear perfusion; (ii) $\geq$2/16 segments with stress-induced severe hypokinesis or akinesis for echocardiography; (iii) $\geq$12% myocardium ischemic, and/or wall motion $\geq$3/16 segments with stress-induced severe hypokinesis or akinesis for CMR; and (iv) as compared to the baseline ECG tracing, additional exercise-induced horizontal or downsloping ST- segment depression $\geq$1.5 mm in 2 leads or $\geq$2.0 mm in any lead; ST-segment elevation $\geq$1 mm in a non-infarct territory for exercise test without imaging (5). Among the 5,179 patients randomized, 45% had a moderate ischemia defined by an extent of ischemia <10%. Therefore, ISCHEMIA trial was a mix of patients with moderate or severe ischemia which limits the extrapolation of these data. However, some larges studies suggest that the threshold of $\geq$10% ischemic myocardium could be the exact threshold to define revascularisation benefit (22). Notably, more severe ischemia was diagnosed with exercise test in 25% of patients.

This study highlighted the crucial role of optimized medical therapy and the lack of benefit to an initial invasive strategy (5) (**Figure 1**). This trial had several strengths. First, it was a randomized clinical trial with a rigorous design requiring the documentation of obstructive CAD evaluated on coronary computed tomography angiography (CCTA) prior to randomization assessed by an independent core laboratory. Moreover, this trial was not industry funded, and the rate of patients lost to follow-up was very low (<1%). The primary outcome was a composite of cardiovascular death, myocardial infarction (MI), or hospitalization for unstable angina, heart failure, or resuscitated cardiac arrest. Beyond the usual CV outcomes, the study performed a rigorous evaluation of quality-of-life measures. Finally, control of CV risk factors was optimal in the entire cohort, based on systolic blood pressure and LDL cholesterol levels. Consistently, follow-up appeared to be very good with excellent adherence to medical treatment in both groups (about 80% at the end of follow-up) (5).

Despite these important strengths, some aspects warrant further attention. While the ISCHEMIA trial, which included procedural infarctions, showed the lack of benefit of initial coronary revascularization at a median follow-up of 3.2 years, a sub-analysis that excluded procedural infarctions suggested that initial coronary revascularization could improve outcomes at 5 years of follow-up (5). Indeed, during the first 6 months of follow-up, the estimated cumulative CV events rate was 5.3% in the invasive group and 3.4% in the medical treatment group (difference: 1.9%; 95% CI: 0.8–3.0). However, at 5 years, the cumulative event rate was 16.4% in the invasive group and 18.2% in the medical treatment group (difference, −1.8%; 95% CI, −4.7 to −1.0). This result suggests that initial coronary revascularization could improve outcomes at 5 years of follow-up. A similar finding was described for the composite outcome including CV death or MI and angina-related quality of life with a cumulative event rate of 14.2% in the invasive group and 16.5% in the medical treatment group (difference: −2.3%; 95% CI: −5.0 to −0.4) (5). This is consistent with another secondary analysis suggesting greater improvement in health status scores for patients in the invasive group compared to patients in the medical treatment group. Moreover, previous large observational cohort studies also suggested a clinical benefit to early coronary revascularization in patients with inducible ischemia at a mean follow-up of 4.6–5.5 years (23, 24). Therefore,

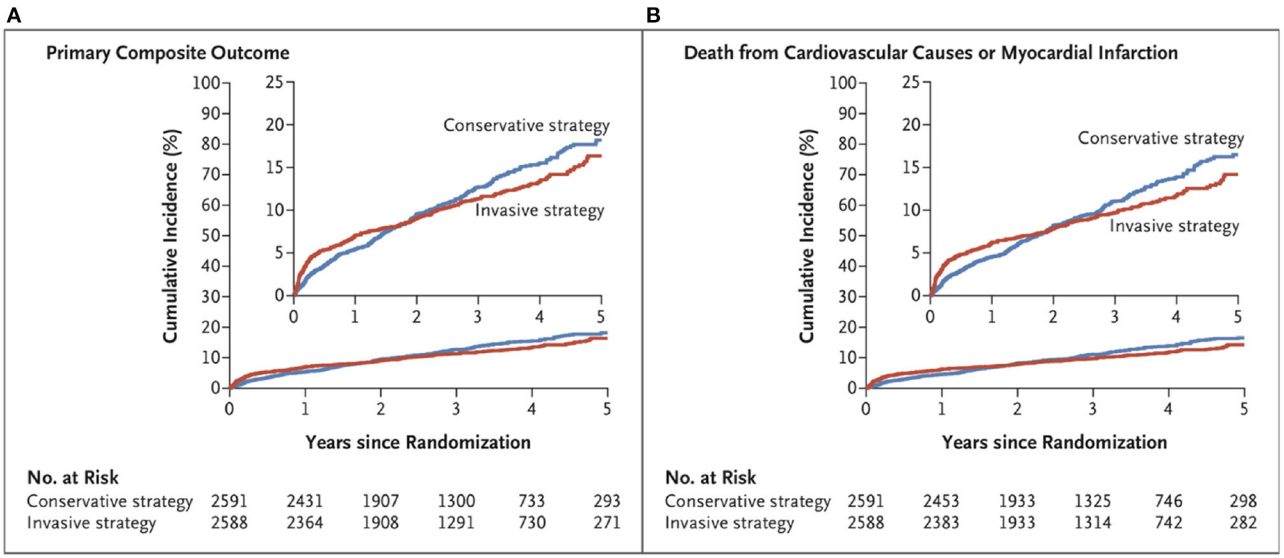

FIGURE 1 | Cumulative incidence curves for the primary composite outcome and other outcomes, from ISCHEMIA trial (5). **(A)** shows the cumulative incidence of the primary composite outcome of death from cardiovascular causes, myocardial infarction, or hospitalization for unstable angina, heart failure, or resuscitated cardiac arrest in the conservative-strategy group and the invasive- strategy group. **(B)** shows the cumulative incidence of death from cardiovascular causes or myocardial infarction.

the extended follow-up of the ISCHEMIA trial will provide more information since survival curves have crossed through the study period.

Regarding the presence of symptoms, 35% of participants had no angina, 44% had angina <3 times a month, and only 20% had daily or weekly angina. In addition, the Seattle Angina Questionnaire score was 73 ± 19 in the invasive strategy group and 75 ± 19 in the medical treatment group (5). This indicates that the majority of participants in both groups were asymptomatic or only mildly symptomatic at baseline. Therefore, these findings suggest that the optimal medical treatment in asymptomatic or mildly symptomatic patients may be the best initial strategy without the benefit of coronary revascularization. However, in symptomatic patients with frequent angina episodes, and a fortiori in cases of severe ischemia, an invasive strategy would be a reasonable complementary approach to the optimal medical treatment for effective angina relief, in line with the current guidelines (2, 3). Therefore, one major message of the ISCHEMIA trial was the excellent capability of coronary revascularisation to relief symptoms. In addition, all patients with left main stenosis of at least 50% were excluded from the ISCHEMIA trial, although left main stenosis is the most severe CAD involvement in terms of ischemia extent and risk of cardiovascular events (5). However, these patients would likely benefit most from coronary revascularization. Furthermore, because coronary angiography was performed before the randomization, patients with coronary anatomy that might be associated with a very high risk for adverse outcomes were likely not randomized but sent directly to invasive revascularization. Although 54.8% of patients had severe ischemia, 45.2% had mild to moderate ischemia after core laboratory analysis (5). Notably, the ISCHEMIA trial was not designed for assessing the clinical value of ischemia testing because there was no control group without ischemia testing or with a negative stress test.

DIAGNOSTIC PERFORMANCE OF STRESS CMR COMPARED TO OTHER METHODS

Although the American guidelines published in 2012 advise using stress CMR to detect obstructive CAD with a class II recommendation (level of evidence B), while other imaging methods had a class I recommendation (3), stress CMR has recently been added as a class I imaging technique for chronic coronary syndromes assessment (level B of evidence) in the current European guidelines, published in 2019 (2) (**Table 1**). Indeed, in these guidelines, stress CMR is recommended to guide coronary revascularization and to stratify symptomatic patients with intermediate risk of CAD (I, B), alongside other stress imaging approaches (2). Interestingly, these guidelines advocate quantitative perfusion CMR as a means of helping to identify patients with coronary microvascular disease, assigning it the same class of recommendation and level of evidence as PET (IIb, B). The adaptation of these European guidelines took into account recent data from a compilation of 26 studies, including more than 11,000 patients, a predicted sensitivity of 89%, and a specificity of 80% in the detection of CAD by stress CMR (11). A very recent meta-analysis has shown the superiority of stress CMR regarding the diagnostic test accuracy for detecting obstructive CAD compared to dobutamine stress

TABLE 1 | Comparison between European and American guidelines regarding the use of stress CMR.

	Recommendation for the use of stress CMR	Class (Level)
European Guidelines Knuuti et al. (2) ESC Guidelines for the diagnosis and management of chronic coronary syndromes.	**All non-invasive functional stress testing** including Stress echocardiography, SPECT and Stress CMR, are recommended as the initial test to diagnose CAD in symptomatic patients.	**I** (B)
American Guidelines Fihn et al. (3)	**Pharmacological stress with CMR** can be useful for patients with an intermediate to high pretest probability of obstructive CAD.	**II** (B)
ACCF/AHA/ACP/AATS/PCNA/SCAI/STS guideline for the diagnosis and management of patients with stable ischemic heart diseases.	Exercise stress with **nuclear imaging** or **echocardiography** is recommended for patients with an intermediate to high pretest probability of obstructive CAD.	**I** (B)

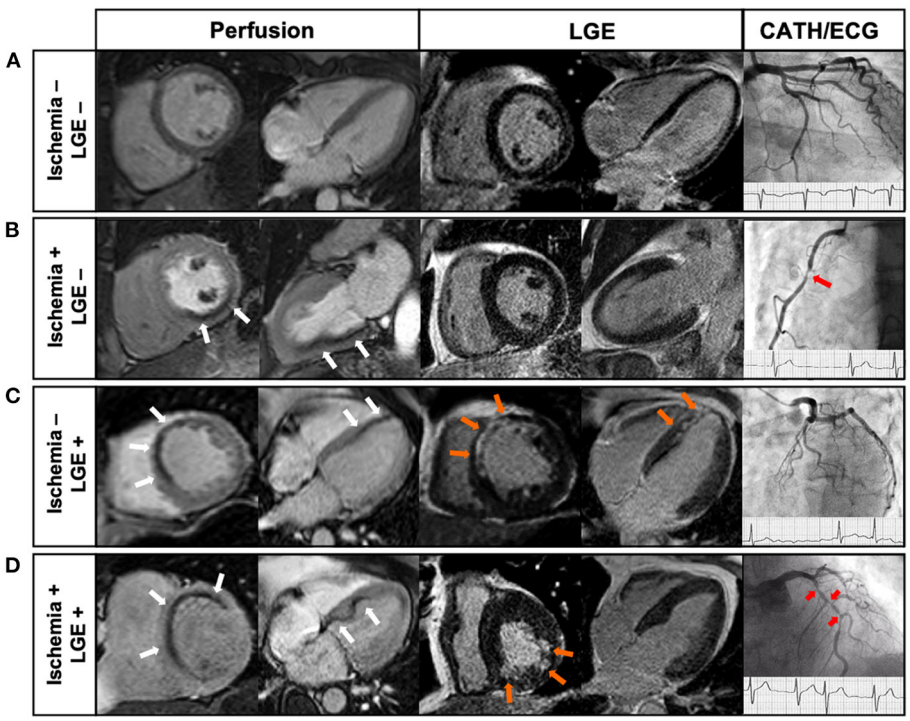

FIGURE 2 | Examples of Clinical cases of stress CMR (26). **(A)** 68-year old male with atypical chest pain. Stress CMR revealed no perfusion defect and LGE was negative, ruling out the diagnosis of CAD. **(B)** 71-year old male with dyspnea on exertion. First-pass myocardial stress perfusion images revealed a reversible perfusion defect of the inferior wall (3 segments) (*white arrows*) without LGE, indicative of myocardial ischemia suggestive of significant RCA stenosis, confirmed by coronary angiography (*red arrow*). **(C)** 62-year old female with prior anterior STEMI treated by PCI 4 years before, referred for atypical chest pain. CMR showed a subendocardial anteroseptal scar on LGE (*orange arrows*), with a colocalization of the perfusion defect (*white arrows*), and therefore no inducible ischemia. Coronary angiography confirmed the absence of significant stenosis. **(D)** 69-year old male with AF and a history of inferior NSTEMI treated by PCI 8 years before, presenting with dyspnea on exertion. CMR showed a subendocardial scar on the inferior wall on LGE sequences (*orange arrows*), and a perfusion defect of the antero-septo-basal wall (4 segments) (*white arrows*) on first-pass perfusion images, indicative of inducible myocardial ischemia. Coronary angiography showed several high-grade stenoses of the LAD (*red arrows*). CAD, coronary artery disease; CMR, cardiac magnetic resonance; LAD, left anterior descending; LGE, late gadolinium enhancement; MI, myocardial infarction; NSTEMI, non ST-segment elevation myocardial infarction; PCI, percutaneous coronary intervention; RCA, right coronary artery; STEMI, ST-segment elevation myocardial infarction.

echocardiography (25). Some clinical cases of stress CMR are illustrated in **Figure 2**.

Regarding single photon emission computed tomography (SPECT), the MR-IMPACT II trial has demonstrated non-inferior performance of stress CMR in the presence of at least one diseased vessel and superior performance in multi-vessel disease (14). This is consistent with the CE-MARC study, which also reported the superiority of stress CMR in single-vessel disease compared to SPECT related to the higher spatial resolution of CMR than SPECT. Moreover, it seems those with multi-vessel disease stand to benefit the most from CAD diagnosis by CMR due to the better spatial resolution (12, 27), and particularly using

quantitative stress CMR imaging (28). Recent meta-analyses (10, 11) comparing all non-invasive stress test methods to FFR confirmed the diagnostic accuracy of stress CMR compared to other methods. The MR IMPACT II trial ($n = 533$) showed stress CMR is a good and efficient alternative to SPECT with greater sensitivity (0.67 vs. 0.59, $p = 0.024$), but lower specificity (0.61 vs. 0.72, $p = 0.038$) (14). The CE-MARC study ($n = 752$), on the other hand, demonstrated greater sensitivity (87 vs. 67%, $p < 0.0001$) and negative predictive value (91 vs. 79%, $p < 0.0001$) for CMR vs. SPECT, while specificity (83% vs. 83%, $p = 0.916$) and positive predictive value (77 vs. 71%, $p = 0.061$) were similar (12). In a sex-specific analysis from the CE-MARC study, CMR had greater sensitivity in women and men (89 vs. 86%, $p = 0.57$) than SPECT (51 vs. 71%, $p = 0.007$) in identifying coronary angiography significant stenosis without a significant difference between sexes (27).

Beyond the traditional non-invasive stress-test methods, computed tomography with fractional flow reserve (FFR-CT) is a new non-invasive technique that has developed significantly in recent years (29). Recently, a study compared the diagnostic performance of FFR-CT and stress perfusion CMR in 110 patients with stable chest pain referred to invasive coronary angiography (30). Interestingly, both methods presented similar overall diagnostic accuracy. Sensitivity for prediction of obstructive CAD was highest for FFR-CT (97%), whereas specificity was highest for stress CMR (88%).

PROGNOSTIC VALUE OF STRESS CMR

The long-term prognostic value of stress CMR is well-established in large studies (8, 9, 16, 17). In the Euro-CMR registry (27,000 consecutive CMR studies in 15 European countries), 1,706 patients with suspected CAD presenting with a normal stress CMR had a low CV event rate (1%/year) (31). Another large multicenter study, assessing 9,151 patients with a median follow-up of 5 years, showed that stress CMR is independently associated with all-cause death (9). While the annual death rate of patients with a normal stress CMR in this study was 1.4% per year, it increased to 4.0% per year in patients with an abnormal stress CMR. Moreover, a meta-analysis (19 studies, 11,636 patients, mean follow-up of 2.7 years) supported the excellent negative prognostic value of stress CMR, describing an annualized rate of CV outcomes of 4.9% per year for patients with an abnormal stress CMR vs. only 0.8% per year for a normal stress CMR (16). A more recent meta-analysis (165 studies, 122,721 patients, mean follow-up of 2.7 years) studied all non-invasive cardiac modalities to detect myocardial ischemia and demonstrated that the annual event rates for CV death and non-fatal MI have been consistently reported as < 1% for patients with a normal stress CMR (32). Regarding sex difference, Coelho-Filho et al. showed that stress CMR myocardial perfusion imaging is an effective and robust risk-stratifying tool for patients of either sex presenting with ischemia (33). However, among individuals with a negative stress CMR, some data demonstrate lower rates of CV events in women than in men, with annualized CV event rates of 0.3% in women vs. 1.1% in men (33).

Recently, the SPINS (Stress CMR Perfusion Imaging in the United States) study investigated the prognostic value of stress CMR in the largest CMR retrospective cohort of patients with stable chest pain in the US (8). In this study, patients with intermediate pre-test probability of CAD who had both negative ischemia and late gadolinium enhancement (LGE) (67% of the patients) experienced a low annualized rate of CV death or non-fatal myocardial infarction (0.6%) (8). On the other hand, patients with both positive ischemia and LGE had an annual event rate of 4.5% per year. In addition, several recent studies have shown that the prognostic value of stress CMR was also observed in subgroups challenging to evaluate using other non-invasive methods, such as patients with obesity (26, 34), prior CABG, or (35) atrial fibrillation during stress testing (36, 37), and very elderly individuals (38). Beyond the presence of ischemia, a sub-study of SPINS has recently shown that the presence of unrecognized or recognized MI portended an equally significant risk for CV events, even after adjustment for the presence of ischemia (37). These findings highlight the importance of using both ischemia and myocardial scar detected by stress CMR to stratify the risk of CV events.

In addition, several studies have emphasized that the extent of inducible ischemia assessing by the number of ischemic segments was a strong and independent predictor of MACE and CV mortality (39, 40), in both patient without (41) or with known CAD (42).

Beyond the prognostic value, it could be worthwhile to assess the incremental prognostic value of the stress CMR over traditional risk factors or comorbidities. In a cohort of 513 patients, Jahnke et al. described an incremental prognostic value of stress CMR, either by perfusion or by wall motion, over traditional factors such as age, sex, smoking, and diabetes, in predicting CV death and non-fatal myocardial infarction (43). Moreover, another study assessing 815 consecutive patients referred for CAD detection demonstrated that stress CMR results in a better reclassification to predict CV outcomes beyond traditional risk factors, specifically in patients at moderate to high pre-test clinical risk and in patients with previous CAD (44). All these findings are in agreement with myocardial perfusion SPECT or echocardiographic studies, which have shown the incremental prognostic value of ischemia in predicting CV mortality (45, 46).

SUBGROUPS WITH SPECIFIC BENEFIT OF REVASCULARISATION: HEART FAILURE PATIENTS

Coronary artery disease is the main risk factor for heart failure and accounts for more than two-thirds of heart failure cases with reduced left ventricular ejection fraction (LVEF) (47). Knowing that myocardial ischemia may represent a treatable cause of LV dysfunction (48), current guidelines recommend invasive or non-invasive assessment for obstructive CAD in all newly diagnosed heart failure cases (49, 50). Indeed, coronary revascularization in patients with ischemic cardiomyopathy and reduced LVEF may improve LV dysfunction by reducing ischemia in a viable

hibernating myocardium (2, 49, 50). Interestingly, a large multicenter registry has shown that the presence of inducible ischemia assessed by stress CMR was an independent predictor of all-cause mortality in patients with LVEF < 55% (adjusted hazard ratio 1.8, $p < 0.001$) (9). A more recent stress CMR study has suggested that both the presence and extent of inducible ischemia were independent and strong predictors of a higher incidence of CV outcomes in a cohort of 1,053 patients with heart failure and LVEF < 40% (51).

Although the ISCHEMIA trial has described the overall lack of benefit to early revascularization, it was not designed to investigate the population of patients with reduced LVEF. Indeed, the large majority of patients had LVEF ≥ 50% (median [IQR] = 60 [55–65]%) (5). Interestingly, a recent ancillary study of ISCHEMIA assessing only the subgroup of patients with LVEF 35–45% suggested a better event-free survival rate after an initial invasive strategy (52) (**Figure 3**). However, initial studies assessing the potential interest of coronary revascularization in patients with reduced LVEF did not suggest any benefit in terms of CV outcomes. For example, the results of the randomized STICH (comparison of surgical and medical treatment for congestive HF and CAD) and HEART (HF revascularization trial) studies, evaluating the prognostic value of coronary artery bypass graft (CABG) in patients with reduced LVEF, were negative at 5 years (48, 53).

However, the extended follow-up of STICH (median 9.8 years) has recently shown that surgical revascularization in addition to medical therapy resulted in a significant benefit for all-cause mortality and CV outcomes (54). Moreover, some non-randomized studies have also demonstrated the potential benefit of percutaneous coronary intervention (PCI) compared to medical treatment alone in patients with reduced LVEF (55). Therefore, all of these studies seem to show a real benefit to coronary revascularization in patients with both ischemia and reduced LVEF.

SUBGROUPS WITH SPECIFIC BENEFIT OF REVASCULARISATION: PATIENTS WITH SEVERE ISCHEMIA

Assessment of ischemia extent by stress CMR was previously described as a strong and independent prognostic factor in many cohort studies (39, 40). A prospective stress CMR study assessing 1,024 consecutive patients with suspected CAD suggested that simple quantification of the number of ischemic segments provides a good prognostic value to stratify the CV risk of patients (39). Indeed, this study suggested that patients with ≥1.5 ischemic segments presented a worse prognosis with a higher incidence of CV death, non-fatal myocardial infarction, or late coronary revascularization. More recently, Marcos-Garces et al. have shown that an extensive ischemic burden, assessed by number of ischemic segments using stress CMR, was related to a higher risk of long-term, all-cause mortality after a median follow-up of 6 years in a cohort of 6,389 consecutive patients with suspected CAD (40). Furthermore, the authors demonstrated that the long-term risk of all-cause mortality increased in parallel with the extent of ischemia, with a risk of death at 6 years of 8% in patients with <2 ischemic segments vs. 27% in those with a large ischemic burden, defined as >9 ischemic segments. Coronary revascularization was associated with a protective effect only in the restricted subset of patients with extensive CMR-related ischemia, defined as >5 ischemic segments. Moreover, the extension of myocardial ischemic burden using SPECT was also described as stratifying all-cause mortality in a large cohort of patients with suspected CAD. Indeed, this study demonstrated both short- and long-term survival benefits associated with revascularization in patients with significant (>10%) ischemic myocardium (56, 57). All these findings are in line with a previous functional imaging sub-study of the COURAGE trial. In the subset of patients who underwent serial functional testing with scintigraphy, PCI with a treatment target of ≥5% ischemia reduction resulted in improved outcomes and a greater reduction in ischemia compared with medical therapy alone (58).

Therefore, all of these studies suggest that there is a potential benefit to coronary revascularization for severe ischemia, i.e., an ischemia of more than 5 ischemic segments. However, the ISCHEMIA trial assessed only 54.8% of patients had severe ischemia after core laboratory analysis (5). One could thus imagine an interest in a new randomized controlled trial assessing the benefit of coronary revascularization, but only in patients with severe ischemia.

THE POTENTIAL INTEREST OF QUANTITATIVE PERFUSION CMR

Nuclear imaging with SPECT is most commonly used for clinical myocardial perfusion imaging, whereas PET is the gold-standard for the quantification of myocardial perfusion (59). More recently, technical improvements to the quantification of pathophysiological parameters of myocardial ischaemia in the CMR field allow to assess the myocardial perfusion using stress CMR without any exposure to ionizing radiation (59). Currently, the analysis of stress CMR perfusion scans is overwhelmingly based on a visual, observer-dependent assessment of contrast enhancement. Thus, an accurate and reproducible quantification of the burden of ischemia, such as quantification of myocardial blood flow (MBF) by CMR, may be useful in improving the assessment of the optimal medical therapy. Quantitative perfusion analysis provides incremental prognostic value over semiquantitative and qualitative data analysis, with an area under the receiver operating characteristic curve (AUC) of 0.85 vs. 0.75 (59, 60). MBF quantification techniques have been validated against coronary sinus flow (61) and PET MBF in healthy volunteers (62). Interestingly, there are different models for quantification of MBF including: tracer-kinetic modeling using blood-tissue exchange models (63), Fermi deconvolution analysis (64), and model-independent analysis (65). However, absolute measures remain variable with these techniques because they are tightly connected to the CMR sequence, and a lack of standardization exists between systems (59). Although not currently part of clinical practice, MBF quantification could allow for identification of multi-vessel coronary disease (28) and give

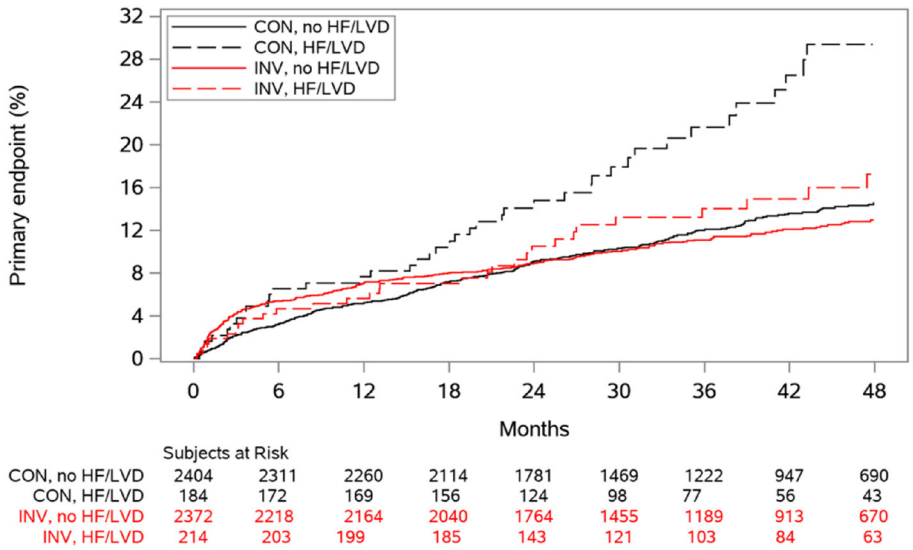

FIGURE 3 | Cumulative incidence curves for the primary composite outcome according to randomized treatment and history of heart failure (HF) or left ventricular dysfunction (LVD), from ISCHEMIA trial (52). CON indicates conservative strategy; and INV, invasive strategy.

a very accurate assessment of the extent of the ischemia, and not just the detection of microvascular disease, as previously mentioned (2).

Beyond obstructive CAD, invasive coronary flow reserve (CFR) or FFR evaluation emphasize the importance of detecting microvascular dysfunction. Indeed, a recent randomized controlled trial showed that in patients without obstructive CAD, personalized treatment guided by the results of CFR reduced anginal symptoms compared to conventional medical treatment (66). Current European guidelines suggest that CFR and/or microcirculatory resistance measurements should be considered in patients with persistent symptoms, but coronary arteries that are either angiographically normal or have moderate stenoses with preserved FFR (level IIa) (2). Notably, several studies have shown the excellent correlation between quantitative perfusion CMR and the diagnosis of microvascular dysfunction using invasive measurement (67). Indeed, microvascular disease may appear as a subendocardial concentric perfusion defect. Because this perfusion defect may not respect coronary territories, its diagnosis could be difficult. Quantification of MBF by CMR can be useful in such cases. Therefore, we could imagine a role for quantitative perfusion CMR to perform large therapeutic randomized controlled trials in this population, for which no treatment is recommended.

CLINICAL AND COST-EFFECTIVENESS IMPACT OF STRESS CMR-RELATED CORONARY REVASCULARIZATION

Beyond diagnostic performance and prognostic value in patients with suspected CAD, a randomized controlled trial—the MR-INFORM study—has recently demonstrated that a diagnostic strategy based on stress CMR was non-inferior in terms of incidence of death, non-fatal myocardial infarction, or target-vessel revascularization compared to an invasive strategy with fractional flow reserve but with a lower use of coronary revascularization (18). Indeed, despite a similar pre-test probability of CAD of 75% in both groups, only 36% of patients who underwent invasive angiography in the stress CMR group required index coronary revascularization, as opposed to 45% in the FFR group (18).

Beyond the potential benefit of coronary revascularization, some recent studies have shown promising new therapy strategies targeting coagulation (68) and inflammation (69, 70) to decrease the risk CV outcomes in patients with CAD. However, these new therapies are associated with some side effects, such as an increased risk of bleeding and a risk of infection. Thus, this is crucial to be able to identify accurately the patients who will benefit most from these treatments in terms of the benefit/risk balance. Based on the studies showing an incremental prognostic value of stress CMR above traditional risk factors (8, 9, 43, 44), we can assume that an improved risk stratification using stress CMR could allow for the identification of high-risk patients who could benefit from treatment intensification, new therapy and/or revascularization.

Based on published average national payment rates from the Medicare Hospital Outpatient Prospective Payment System (71), the cost of stress CMR is usually lower than that of SPECT techniques and only slightly higher than stress echo, which makes it a cost-effective approach owing to its complementary diagnostic capabilities. Indeed, the SPINS study has shown that patients without ischemia or LGE experienced a very low incidence of CV events, little need for coronary revascularization, and low financial expenditure on subsequent ischemia testing in the US (8). Moreover, the lower cost of stress CMR compared

to nuclear stress techniques or initial coronary angiography has recently been confirmed in a dedicated cost-effectiveness report from the SPINS study (15). Hypothetically, combining data from the public health systems of Europe (Germany, the UK, and Switzerland) and the US, the stress CMR approach—as opposed to coronary angiography as a single test—could result in a cost savings of up to 51% (72). All of these findings suggest that stress CMR could be helpful in reducing the costs of downstream testing, mainly due to a high negative predictive value. Therefore, stress CMR emerges as a highly attractive method for non-invasive risk stratification and further referral of high-risk patients.

FUTURE DIRECTIONS AFTER THE ICHEMIA TRIAL

Although ischemia trial underlined the fundamental role of optimized medical therapy, the invasive approach clearly has benefits. Invasive therapy reduces symptomatic angina, with greater advantage in more symptomatic patients. It also reduces late MI and hospitalizations for unstable angina in ISCHEMIA trial (5). Indeed, while including procedural infarctions, the ISCHEMIA trial showed the lack of benefit of revascularisation, a sub-analysis that excluded procedural infarctions suggested better outcome in the invasive strategy group (5). In addition, another sub-analysis of ISCHEMIA at 5-year follow-up suggested that coronary revascularization could be beneficial in the subgroup of patients with inducible ischemia. Therefore, a longer-term follow-up of ISCHEMIA is important to understand these late benefits and early risks more fully. Moreover, approximately 8% of patients screened were found to have significant left main disease and were not randomized in ISCHEMIA trial. However, patients with left main disease have historically greater risks of cardiovascular events than other subgroups and theoretically derive greater benefits from coronary revascularization. Thus, for these patients, invasive management remains recommended (2). Moreover, a role for quantitative stress CMR can be hypothesized to accurately assess invasive approaches and then propose new prognostic stratification tools after an invasive approach has been performed. This review detailed the good results of stress CMR compared to other ischemia assessment methods in terms of diagnostic performance (10, 11), prognostic value (8, 16), and clinical impact compared to an invasive FFR strategy (18). However, among the 5,176 patients included in ISCHEMIA trial, stress CMR was performed in only 257 patients (5%) whereas the myocardial SPECT was carried out in 2,567 patients (49.6%). Knowing the superiority of stress CMR compared to SPECT (12), the ISCHEMIA trial probably does not accurately assess the prognostic value of stress CMR-based coronary revascularization guided by myocardial ischemia. Notably, the initial inclusion criterion for SPECT, which was the extent of the myocardial ischemia >10%, was modified during the study to >5% of the ischemic myocardium. Knowing the rather low spatial resolution of SPECT, a threshold of only 5% of the ischemic myocardium does not allow to identify accurately severe ischemia. Thus, one may wonder about the results of a new randomized controlled trial evaluating the interest of revascularization, in line with the design of the ISCHEMIA trial, but including patients with inducible ischemia defined only by stress CMR. Interestingly, a recent study assessing the external applicability of the ISCHEMIA trial has shown that only 4% of patients from a large registry fulfilled ISCHEMIA inclusion criteria (73), which suggests a very limited applicability of these findings to other patient cohorts.

SAFETY AND LIMITATIONS OF STRESS CMR

The excellent safety profile of stress CMR was demonstrated in a large registry of 11,984 patients using dipyridamole or dobutamine (74) and in the EuroCMR registry assessing 10,228 patients referred for stress CMR (31). The incidence of severe complications and non-severe complications was low, at 0.08 and 1.5%, respectively (74) and 0.07 and 7.3%, respectively (31). Nephrogenic systemic fibrosis related to gadolinium contrast appears to be rare, with fewer than 1,000 cases reported. Of note, this complication was limited to patients with severe renal failure with a low glomerular filtration rate (< 30 ml/min/1.73 m^2) (75). Regarding potential device issues, MR-conditional implantable electronic devices have improved CMR compatibility with no changes in thresholds and pacemaker parameters (76). Although the impact on image quality should be considered, some studies demonstrated that patients with non-conditional devices can safely undergo the exam given proper protocols are used (77, 78).

CONCLUSION

Despite some discussion to the contrary, the ISCHEMIA trial provides several crucial findings regarding the contemporary management of CAD and the clinical impact of coronary revascularization. In accordance with current guidelines (2, 3), both conservative and invasive strategies remain useful in the management of patients with CAD.

Among the non-invasive stress methods, stress CMR is recognized as an accurate technique to detect inducible myocardial ischemia and infarction with high sensitivity and specificity. Moreover, several large studies have shown its excellent prognostic value for predicting CV events. Recently, a first-line stress CMR-based strategy was shown to be non-inferior in terms of outcomes compared to an invasive approach with FFR in patients with stable angina. Given that stress CMR was used in only 5% of the patients from the ISCHEMIA trial, we may wonder about the results of a new randomized controlled trial including patients with severe ischemia defined only by stress CMR. The use of the optimal medical treatment in asymptomatic or mildly symptomatic patients who fit the profile of the ISCHEMIA trial (5) may be the best initial strategy without the benefit of coronary revascularization. However, in symptomatic patients with frequent angina episodes, or in patients with severe ischemia, an invasive strategy may be a reasonable complementary approach to the optimal medical treatment for effective angina relief. Indeed, the ischemic

burden quantified with imaging modalities is crucial for guiding coronary revascularisation and improve the cardiovascular risk stratification.

AUTHOR CONTRIBUTIONS

TP, MJ-H, and OC-F: made substantial contributions to conception and design, acquisition of data, or analysis and interpretation of data, and drafted the article. TP, LS, AB, AT, MJ-H, and OC-F: reviewed it critically for important intellectual content and given final approval of the version to be published. All authors contributed to the article and approved the submitted version.

FUNDING

OC-F was supported by grants from The São Paulo Research Foundation (2015/15402-2, 2016/26209-1, and 2017/03708-5).

REFERENCES

1. Benjamin EJ, Muntner P, Alonso A, Bittencourt MS, Callaway CW, Carson AP, et al. Heart disease and stroke statistics-2019 update: a report from the American Heart Association. *Circulation.* (2019) 139:e56–528. doi: 10.1161/CIR.0000000000000659
2. Knuuti J, Wijns W, Saraste A, Capodanno D, Barbato E, Funck-Brentano C, et al. 2019 ESC guidelines for the diagnosis and management of chronic coronary syndromes. *Eur Heart J.* (2020) 41:407–77. doi: 10.1093/eurheartj/ehz425
3. Fihn SD, Gardin JM, Abrams J, Berra K, Blankenship JC, Dallas AP, et al. 2012 ACCF/AHA/ACP/AATS/PCNA/SCAI/STS guideline for the diagnosis and management of patients with stable ischemic heart disease: a report of the American College of Cardiology Foundation/American Heart Association task force on practice guidelines, and the American College of Physicians, American Association for Thoracic Surgery, Preventive Cardiovascular Nurses Association, Society for Cardiovascular Angiography and Interventions, and Society of Thoracic Surgeons. *Circulation.* (2012) 126:e354–471. doi: 10.1161/CIR.0b013e318277d6a0
4. Katritsis DG, Mark DB, Gersh BJ. Revascularization in stable coronary disease: evidence and uncertainties. *Nat Rev Cardiol.* (2018) 15:408–19. doi: 10.1038/s41569-018-0006-z
5. Maron DJ, Hochman JS, Reynolds HR, Bangalore S, O'Brien SM, Boden WE, et al. Initial invasive or conservative strategy for stable coronary disease. *N Engl J Med.* (2020) 382:1395–407. doi: 10.1056/NEJMoa1915922
6. Knuuti J, Ballo H, Juarez-Orozco LE, Saraste A, Kolh P, Rutjes AWS, et al. The performance of non-invasive tests to rule-in and rule-out significant coronary artery stenosis in patients with stable angina: a meta-analysis focused on post-test disease probability. *Eur Heart J.* (2018) 39:3322–30. doi: 10.1093/eurheartj/ehy267
7. Danad I, Szymonifka J, Twisk JWR, Norgaard BL, Zarins CK, Knaapen P, et al. Diagnostic performance of cardiac imaging methods to diagnose ischaemia-causing coronary artery disease when directly compared with fractional flow reserve as a reference standard: a meta-analysis. *Eur Heart J.* (2017) 38:991–8. doi: 10.1093/eurheartj/ehw095
8. Kwong RY, Ge Y, Steel K, Bingham S, Abdullah S, Fujikura K, et al. Cardiac magnetic resonance stress perfusion imaging for evaluation of patients with chest pain. *J Am College Cardiol.* (2019) 74:1741–55. doi: 10.1016/j.jacc.2019.07.074
9. Heitner JF, Kim RJ, Kim HW, Klem I, Shah DJ, Debs D, et al. Prognostic value of vasodilator stress cardiac magnetic resonance imaging: a multicenter study with 48 000 patient-years of follow-up. *JAMA Cardiol.* (2019) 4:256–64. doi: 10.1001/jamacardio.2019.0035
10. Nandalur KR, Dwamena BA, Choudhri AF, Nandalur MR, Carlos RC. Diagnostic performance of stress cardiac magnetic resonance imaging in the detection of coronary artery disease: a meta-analysis. *J Am Coll Cardiol.* (2007) 50:1343–53. doi: 10.1016/j.jacc.2007.06.030
11. Hamon M, Fau G, Née G, Ehtisham J, Morello R, Hamon M. Meta-analysis of the diagnostic performance of stress perfusion cardiovascular magnetic resonance for detection of coronary artery disease. *J Cardiovasc Magn Reson.* (2010) 12:29. doi: 10.1186/1532-429X-12-29
12. Greenwood JP, Maredia N, Younger JF, Brown JM, Nixon J, Everett CC, et al. Cardiovascular magnetic resonance and single-photon emission computed tomography for diagnosis of coronary heart disease (CE-MARC): a prospective trial. *Lancet.* (2012) 379:453–60. doi: 10.1016/S0140-6736(11)61335-4
13. Schwitter J, Wacker CM, van Rossum AC, Lombardi M, Al-Saadi N, Ahlstrom H, et al. MR-IMPACT: comparison of perfusion-cardiac magnetic resonance with single-photon emission computed tomography for the detection of coronary artery disease in a multicentre, multivendor, randomized trial. *Eur Heart J.* (2008) 29:480–9. doi: 10.1093/eurheartj/ehm617
14. Schwitter J, Wacker CM, Wilke N, Al-Saadi N, Sauer E, Huettle K, et al. MR-IMPACT II: magnetic resonance imaging for myocardial perfusion assessment in coronary artery disease trial: perfusion-cardiac magnetic resonance vs. single-photon emission computed tomography for the detection of coronary artery disease: a comparative multicentre, multivendor trial. *Eur Heart J.* (2013) 34:775–81. doi: 10.1093/eurheartj/ehs022
15. Ge Y, Pandya A, Steel K, Bingham S, Jerosch-Herold M, Chen Y-Y, et al. Cost-effectiveness analysis of stress cardiovascular magnetic resonance imaging for stable chest pain syndromes. *JACC Cardiovasc Imaging.* (2020) 13:1505–17. doi: 10.1016/j.jcmg.2020.02.029
16. Lipinski MJ, McVey CM, Berger JS, Kramer CM, Salerno M. Prognostic value of stress cardiac magnetic resonance imaging in patients with known or suspected coronary artery disease: a systematic review and meta-analysis. *J Am Coll Cardiol.* (2013) 62:826–38. doi: 10.1016/S0735-1097(13)60809-8
17. Bodi V, Sanchis J, Lopez-Lereu MP, Nunez J, Mainar L, Monmeneu JV, et al. Prognostic value of dipyridamole stress cardiovascular magnetic resonance imaging in patients with known or suspected coronary artery disease. *J Am Coll Cardiol.* (2007) 50:1174–9. doi: 10.1016/j.jacc.2007.06.016
18. Nagel E, Greenwood JP, McCann GP, Bettencourt N, Shah AM, Hussain ST, et al. Magnetic resonance perfusion or fractional flow reserve in coronary disease. *N Engl J Med.* (2019) 380:2418–28. doi: 10.1056/NEJMoa1716734
19. Greenwood JP, Walker S. Stress CMR imaging for stable chest pain syndromes. *JACC.* (2020) 13:1518–20. doi: 10.1016/j.jcmg.2020.04.006
20. BARI 2D Study Group, Frye RL, August P, Brooks MM, Hardison RM, Kelsey SF, et al. A randomized trial of therapies for type 2 diabetes and coronary artery disease. *N Engl J Med.* (2009) 360:2503–15. doi: 10.1056/NEJMoa0805796
21. Boden WE, O'Rourke RA, Teo KK, Hartigan PM, Maron DJ, Kostuk WJ, et al. Optimal medical therapy with or without PCI for stable coronary disease. *N Engl J Med.* (2007) 356:1503–16. doi: 10.1056/NEJMoa070829
22. Patel KK, Spertus JA, Chan PS, Sperry BW, Thompson RC, Al Badarin F, et al. Extent of myocardial ischemia on positron emission tomography and survival benefit with early revascularization. *J Am Coll Cardiol.* (2019) 74:1645–54. doi: 10.1016/j.jacc.2019.07.055
23. Gada H, Kirtane AJ, Kereiakes DJ, Bangalore S, Moses JW, Généreux P, et al. Meta-analysis of trials on mortality after percutaneous coronary intervention compared with medical therapy in patients with stable coronary heart disease and objective evidence of myocardial ischemia. *Am J Cardiol.* (2015) 115:1194–9. doi: 10.1016/j.amjcard.2015.01.556
24. Czarnecki A, Qiu F, Elbaz-Greener G, Cohen EA, Ko DT, Roifman I, et al. Variation in revascularization practice and outcomes in asymptomatic stable ischemic heart disease. *JACC Cardiovasc Interv.* (2019) 12:232–41. doi: 10.1016/j.jcin.2018.10.049
25. Haberkorn SM, Haberkorn SI, Bönner F, Kelm M, Hopkin G, Petersen SE. Vasodilator myocardial perfusion cardiac magnetic resonance imaging is superior to dobutamine stress echocardiography in the detection

of relevant coronary artery stenosis: a systematic review and meta-analysis on their diagnostic accuracy. *Front Cardiovasc Med.* (2021) 8:630846. doi: 10.3389/fcvm.2021.630846
26. Kinnel M, Garot J, Pezel T, Hovasse T, Unterseeh T, Champagne S, et al. Prognostic value of vasodilator stress perfusion CMR in morbidly obese patients (BMI ≥40 kg/m2) without known CAD. *JACC Cardiovasc Imaging.* (2020) 13:1276–7. doi: 10.1016/j.jcmg.2019.12.002
27. Greenwood JP, Motwani M, Maredia N, Brown JM, Everett CC, Nixon J, et al. Comparison of cardiovascular magnetic resonance and single-photon emission computed tomography in women with suspected coronary artery disease from the Clinical Evaluation of Magnetic Resonance Imaging in Coronary Heart Disease (CE-MARC) trial. *Circulation.* (2014) 129:1129–38. doi: 10.1161/CIRCULATIONAHA.112.000071
28. Patel AR, Antkowiak PF, Nandalur KR, West AM, Salerno M, Arora V, et al. Assessment of advanced coronary artery disease: advantages of quantitative cardiac magnetic resonance perfusion analysis. *J Am Coll Cardiol.* (2010) 56:561–9. doi: 10.1016/j.jacc.2010.02.061
29. Min JK, Leipsic J, Pencina MJ, Berman DS, Koo B-K, van Mieghem C, et al. Diagnostic accuracy of fractional flow reserve from anatomic CT angiography. *JAMA.* (2012) 308:1237–45. doi: 10.1001/2012.jama.11274
30. Rønnow Sand NP, Nissen L, Winther S, Petersen SE, Westra J, Christiansen EH, et al. Prediction of coronary revascularization in stable angina: comparison of FFRCT with CMR Stress Perfusion Imaging. *JACC Cardiovasc Imaging.* (2020) 13:994–1004. doi: 10.1016/j.jcmg.2019.06.028
31. Bruder O, Wagner A, Lombardi M, Schwitter J, van Rossum A, Pilz G, et al. European Cardiovascular Magnetic Resonance (EuroCMR) registry–multi national results from 57 centers in 15 countries. *J Cardiovasc Magn Reson.* (2013) 15:9. doi: 10.1186/1532-429X-15-9
32. Smulders MW, Jaarsma C, Nelemans PJ, Bekkers SCAM, Bucerius J, Leiner T, et al. Comparison of the prognostic value of negative non-invasive cardiac investigations in patients with suspected or known coronary artery disease-a meta-analysis. *Eur Heart J Cardiovasc Imaging.* (2017) 18:980–7. doi: 10.1093/ehjci/jex014
33. Coelho-Filho OR, Seabra LF, Mongeon F-P, Abdullah SM, Francis SA, Blankstein R, et al. Stress myocardial perfusion imaging by CMR provides strong prognostic value to cardiac events regardless of patient's sex. *JACC Cardiovasc Imaging.* (2011) 4:850–61. doi: 10.1016/j.jcmg.2011.04.015
34. Ge Y, Steel K, Antiochos P, Bingham S, Abdullah S, Mikolich JR, et al. Stress CMR in patients with obesity: insights from the Stress CMR Perfusion Imaging in the United States (SPINS) registry. *Eur Heart J Cardiovasc Imaging.* (2020) 20:1321–31. doi: 10.1093/ehjci/jeaa281
35. Kinnel M, Sanguineti F, Pezel T, Unterseeh T, Hovasse T, Toupin S, et al. Prognostic value of vasodilator stress perfusion CMR in patients with previous coronary artery bypass graft. *Eur Heart J Cardiovasc Imaging.* (2020) jeaa316. doi: 10.1093/ehjci/jeaa316. [Epub ahead of print].
36. Pezel T, Sanguineti F, Kinnel M, Landon V, Toupin S, Unterseeh T, et al. Feasibility and prognostic value of vasodilator stress perfusion CMR in patients with atrial fibrillation. *JACC Cardiovasc Imaging.* (2020) 16:233–70. doi: 10.1093/ehjci/ehaa946.0251
37. Kanagala P, Cheng ASH, Singh A, McAdam J, Marsh A-M, Arnold JR, et al. Diagnostic and prognostic utility of cardiovascular magnetic resonance imaging in heart failure with preserved ejection fraction – implications for clinical trials. *J Cardiovasc Magn Reson.* (2018) 20:4. doi: 10.1186/s12968-017-0424-9
38. Pezel T, Sanguineti F, Kinnel M, Hovasse T, Garot P, Unterseeh T, et al. Prognostic value of dipyridamole stress perfusion cardiovascular magnetic resonance in elderly patients >75 years with suspected coronary artery disease. *Eur Heart J Cardiovasc Imaging.* (2020) jeaa193. doi: 10.1093/ehjci/jeaa193. [Epub ahead of print].
39. Vincenti G, Masci PG, Monney P, Rutz T, Hugelshofer S, Gaxherri M, et al. Stress perfusion CMR in patients with known and suspected CAD. *JACC: Cardiovascular Imaging.* (2017) 10:526–37. doi: 10.1016/j.jcmg.2017.02.006
40. Marcos-Garces V, Gavara J, Monmeneu JV, Lopez-Lereu MP, Bosch MJ, Merlos P, et al. Vasodilator stress CMR and all-cause mortality in stable ischemic heart disease: a large retrospective registry. *JACC Cardiovasc Imaging.* (2020) 13:1674–86. doi: 10.1016/j.jcmg.2020.02.027
41. Pezel T, Unterseeh T, Kinnel M, Hovasse T, Sanguineti F, Toupin S, et al. Long-term prognostic value of stress perfusion cardiovascular magnetic resonance in patients without known coronary artery disease. *J Cardiovasc Magn Reson.* (2021) 23:43. doi: 10.1186/s12968-021-00737-0
42. Pezel T, Hovasse T, Kinnel M, Unterseeh T, Champagne S, Toupin S, et al. Prognostic value of stress cardiovascular magnetic resonance in asymptomatic patients with known coronary artery disease. *J Cardiovasc Magn Reson.* (2021) 23:19. doi: 10.1186/s12968-021-00721-8
43. Jahnke C, Nagel E, Gebker R, Kokocinski T, Kelle S, Manka R, et al. Prognostic value of cardiac magnetic resonance stress tests: adenosine stress perfusion and dobutamine stress wall motion imaging. *Circulation.* (2007) 115:1769–76. doi: 10.1161/CIRCULATIONAHA.106.652016
44. Shah R, Heydari B, Coelho-Filho O, Murthy VL, Abbasi S, Feng JH, et al. Stress cardiac magnetic resonance imaging provides effective cardiac risk reclassification in patients with known or suspected stable coronary artery disease. *Circulation.* (2013) 128:605–14. doi: 10.1161/CIRCULATIONAHA.113.001430
45. Berman DS, Kang X, Hayes SW, Friedman JD, Cohen I, Abidov A, et al. Adenosine myocardial perfusion single-photon emission computed tomography in women compared with men. impact of diabetes mellitus on incremental prognostic value and effect on patient management. *J Am Coll Cardiol.* (2003) 41:1125–33. doi: 10.1016/S1062-1458(03)00284-8
46. Neglia D, Liga R, Caselli C, Carpeggiani C, Lorenzoni V, Sicari R, et al. Anatomical and functional coronary imaging to predict long-term outcome in patients with suspected coronary artery disease: the EVINCI-outcome study. *Eur Heart J Cardiovasc Imaging.* (2019) 21:1273–82. doi: 10.1093/ehjci/jez248
47. Gheorghiade M, Sopko G, De Luca L, Velazquez EJ, Parker JD, Binkley PF, et al. Navigating the crossroads of coronary artery disease and heart failure. *Circulation.* (2006) 114:1202–13. doi: 10.1161/CIRCULATIONAHA.106.623199
48. Velazquez EJ, Lee KL, Deja MA, Jain A, Sopko G, Marchenko A, et al. Coronary-artery bypass surgery in patients with left ventricular dysfunction. *N Engl J Med.* (2011) 364:1607–16. doi: 10.1056/NEJMoa1100356
49. Yancy CW, Jessup M, Bozkurt B, Butler J, Casey DE, Drazner MH, et al. 2013 ACCF/AHA guideline for the management of heart failure: a report of the American College of Cardiology Foundation/American Heart Association task force on practice guidelines. *J Am Coll Cardiol.* (2013) 62:e147–239. doi: 10.1016/j.jacc.2013.05.019
50. Ponikowski P, Voors AA, Anker SD, Bueno H, Cleland JGF, Coats AJS, et al. 2016 ESC guidelines for the diagnosis treatment of acute chronic heart failure: The Task Force for the diagnosis treatment of acute chronic heart failure of the European Society of Cardiology (ESC)Developed with the special contribution of the Heart Failure Association (HFA) of the ESC. *Eur Heart J.* (2016) 37:2129–200. doi: 10.1093/eurheartj/ehw128
51. Pezel T, Sanguineti F, Kinnel M, Landon V, Bonnet G, Garot P, et al. Safety and prognostic value of vasodilator stress cardiovascular magnetic resonance in patients with heart failure and reduced ejection fraction. *Circ Cardiovasc Imaging.* (2020) 13:e010599. doi: 10.1161/CIRCIMAGING.120.010599
52. Lopes RD, Alexander KP, Stevens SR, Reynolds HR, Stone GW, Piña IL, et al. Initial invasive versus conservative management of stable ischemic heart disease in patients with a history of heart failure or left ventricular dysfunction: insights from the ISCHEMIA Trial. *Circulation.* (2020) 142:1725–35. doi: 10.1161/CIR.0000000000000927
53. Cleland JGF, Calvert M, Freemantle N, Arrow Y, Ball SG, Bonser RS, et al. The Heart Failure Revascularisation trial (HEART). *Eur J Heart Fail.* (2011) 13:227–33. doi: 10.1093/eurjhf/hfq230
54. Velazquez EJ, Lee KL, Jones RH, Al-Khalidi HR, Hill JA, Panza JA, et al. Coronary-artery bypass surgery in patients with ischemic cardiomyopathy. *N Engl J Med.* (2016) 374:1511–20. doi: 10.1056/NEJMoa1602001
55. Trikalinos TA, Alsheikh-Ali AA, Tatsioni A, Nallamothu BK, Kent DM. Percutaneous coronary interventions for non-acute coronary artery disease: a quantitative 20-year synopsis and a network meta-analysis. *Lancet.* (2009) 373:911–8. doi: 10.1016/S0140-6736(09)60319-6
56. Hachamovitch R, Rozanski A, Shaw LJ, Stone GW, Thomson LEJ, Friedman JD, et al. Impact of ischaemia and scar on the therapeutic benefit derived from myocardial revascularization vs. medical therapy among patients undergoing stress-rest myocardial perfusion scintigraphy. *Eur Heart J.* (2011) 32:1012–24. doi: 10.1093/eurheartj/ehq500
57. Hachamovitch R, Hayes SW, Friedman JD, Cohen I, Berman DS. Comparison of the short-term survival benefit associated with

revascularization compared with medical therapy in patients with no prior coronary artery disease undergoing stress myocardial perfusion single photon emission computed tomography. *Circulation.* (2003) 107:2900–7. doi: 10.1161/01.CIR.0000072790.23090.41
58. Shaw LJ, Berman DS, Maron DJ, Mancini GBJ, Hayes SW, Hartigan PM, et al. Optimal medical therapy with or without percutaneous coronary intervention to reduce ischemic burden: results from the Clinical Outcomes Utilizing Revascularization and Aggressive Drug Evaluation (COURAGE) trial nuclear substudy. *Circulation.* (2008) 117:1283–91. doi: 10.1161/CIRCULATIONAHA.107.743963
59. Dewey M, Siebes M, Kachelrieß M, Kofoed KF, Maurovich-Horvat P, Nikolaou K, et al. Clinical quantitative cardiac imaging for the assessment of myocardial ischaemia. *Nat Rev Cardiol.* (2020) 17:427–50. doi: 10.1038/s41569-020-0341-8
60. Sammut EC, Villa ADM, Di Giovine G, Dancy L, Bosio F, Gibbs T, et al. Prognostic value of quantitative stress perfusion cardiac magnetic resonance. *JACC Cardiovasc Imaging.* (2018) 11:686–94. doi: 10.1016/j.jcmg.2017.07.022
61. Ichihara T, Ishida M, Kitagawa K, Ichikawa Y, Natsume T, Yamaki N, et al. Quantitative analysis of first-pass contrast-enhanced myocardial perfusion MRI using a Patlak plot method and blood saturation correction. *Magn Reson Med.* (2009) 62:373–83. doi: 10.1002/mrm.22018
62. Fritz-Hansen T, Hove JD, Kofoed KF, Kelbaek H, Larsson HBW. Quantification of MRI measured myocardial perfusion reserve in healthy humans: a comparison with positron emission tomography. *J Magn Reson Imaging.* (2008) 27:818–24. doi: 10.1002/jmri.21306
63. Kroll K, Wilke N, Jerosch-Herold M, Wang Y, Zhang Y, Bache RJ, et al. Modeling regional myocardial flows from residue functions of an intravascular indicator. *Am J Physiol.* (1996) 271:H1643–55. doi: 10.1152/ajpheart.1996.271.4.H1643
64. Jerosch-Herold M, Swingen C, Seethamraju RT. Myocardial blood flow quantification with MRI by model-independent deconvolution. *Med Phys.* (2002) 29:886–97. doi: 10.1118/1.1473135
65. Quinaglia T, Jerosch-Herold M, Coelho-Filho OR. State-of-the-art quantitative assessment of myocardial ischemia by stress perfusion cardiac magnetic resonance. *Magn Reson Imaging Clin N Am.* (2019) 27:491–505. doi: 10.1016/j.mric.2019.04.002
66. Ford TJ, Stanley B, Good R, Rocchiccioli P, McEntegart M, Watkins S, et al. Stratified medical therapy using invasive coronary function testing in angina: the CorMicA trial. *J Am Coll Cardiol.* (2018) 72:2841–55. doi: 10.1016/j.jacc.2018.09.006
67. Kotecha T, Martinez-Naharro A, Boldrini M, Knight D, Hawkins P, Kalra S, et al. Automated pixel-wise quantitative myocardial perfusion mapping by CMR to detect obstructive coronary artery disease and coronary microvascular dysfunction: validation against invasive coronary physiology. *JACC Cardiovasc Imaging.* (2019) 12:1958–69. doi: 10.1016/j.jcmg.2018.12.022
68. Eikelboom JW, Connolly SJ, Bosch J, Dagenais GR, Hart RG, Shestakovska O, et al. Rivaroxaban with or without aspirin in stable cardiovascular disease. *N Engl J Med.* (2017) 377:1319–30. doi: 10.1056/NEJMoa1709118
69. Tardif J-C, Kouz S, Waters DD, Bertrand OF, Diaz R, Maggioni AP, et al. Efficacy and safety of low-dose colchicine after myocardial infarction. *N Engl J Med.* (2019) 381:2497–505. doi: 10.1056/NEJMoa1912388
70. Ridker PM, Everett BM, Thuren T, MacFadyen JG, Chang WH, Ballantyne C, et al. Antiinflammatory therapy with canakinumab for atherosclerotic disease. *N Engl J Med.* (2017) 377:1119–31. doi: 10.1056/NEJMoa1707914
71. *Medicare Hospital Outpatient Prospective Payment System*. Available online at: https://www.medicareinteractive.org/glossary/outpatient-prospective-payment-system-opps (accessed May 20, 2021).
72. Moschetti K, Petersen SE, Pilz G, Kwong RY, Wasserfallen J-B, Lombardi M, et al. Cost-minimization analysis of three decision strategies for cardiac revascularization: results of the "suspected CAD" cohort of the european cardiovascular magnetic resonance registry. *J Cardiovasc Magn Reson.* (2016) 18:3. doi: 10.1186/s12968-015-0222-1
73. De Luca L, Uguccioni M, Meessen J, Temporelli PL, Tomai F, De Rosa FM, et al. External applicability of the ISCHEMIA trial: an analysis of a prospective, nationwide registry of patients with stable coronary artery disease. *EuroIntervention.* (2020) 16:e966–73. doi: 10.4244/EIJ-D-20-00610
74. Monmeneu Menadas JV, Lopez-Lereu MP, Estornell Erill J, Garcia Gonzalez P, Igual Muñoz B, Maceira Gonzalez A. Pharmacological stress cardiovascular magnetic resonance: feasibility and safety in a large multicentre prospective registry. *Eur Heart J Cardiovasc Imaging.* (2016) 17:308–15. doi: 10.1093/ehjci/jev153
75. Fraum TJ, Ludwig DR, Bashir MR, Fowler KJ. Gadolinium-based contrast agents: a comprehensive risk assessment. *J Magn Reson Imaging.* (2017) 46:338–53. doi: 10.1002/jmri.25625
76. Gimbel JR, Bello D, Schmitt M, Merkely B, Schwitter J, Hayes DL, et al. Randomized trial of pacemaker and lead system for safe scanning at 1.5 Tesla. *Heart Rhythm.* (2013) 10:685–91. doi: 10.1016/j.hrthm.2013.01.022
77. Indik JH, Gimbel JR, Abe H, Alkmim-Teixeira R, Birgersdotter-Green U, Clarke GD, et al. 2017 HRS expert consensus statement on magnetic resonance imaging and radiation exposure in patients with cardiovascular implantable electronic devices. *Heart Rhythm.* (2017) 14:e97–153. doi: 10.1016/j.hrthm.2017.04.025
78. Nazarian S, Hansford R, Rahsepar AA, Weltin V, McVeigh D, Gucuk Ipek E, et al. Safety of magnetic resonance imaging in patients with cardiac devices. *N Engl J Med.* (2017) 377:2555–64. doi: 10.1056/NEJMoa1604267

Conflict of Interest: The authors declare that the research was conducted in the absence of any commercial or financial relationships that could be construed as a potential conflict of interest.

frontiers in Cardiovascular Medicine

ORIGINAL RESEARCH
published: 15 June 2021
doi: 10.3389/fcvm.2021.675087

Agreement in Left Ventricular Function Measured by Echocardiography and Cardiac Magnetic Resonance in Patients With Chronic Coronary Total Occlusion

Jiahui Li[1], Lijun Zhang[2], Yueli Wang[3], Huijuan Zuo[4], Rongchong Huang[5], Xueyao Yang[1], Ye Han[2‡], Yi He[2†‡] and Xiantao Song[1†]*

[1] Ward 1 of Coronary Heart Disease Center, Beijing Institute of Heart Lung and Blood Vessel Disease, Beijing Anzhen Hospital, Capital Medical University, Beijing, China, [2] Department of Radiology, Beijing Institute of Heart Lung and Blood Vessel Disease, Beijing Anzhen Hospital, Capital Medical University, Beijing, China, [3] Department of Echocardiology, Beijing Institute of Heart Lung and Blood Vessel Disease, Beijing Anzhen Hospital, Capital Medical University, Beijing, China, [4] Department of Community Health Research, Beijing Institute of Heart Lung and Blood Vessel Disease, Beijing Anzhen Hospital, Capital Medical University, Beijing, China, [5] Department of Cardiology, Beijing Friendship Hospital, Capital Medical University, Beijing, China

Aims: To determine the agreement between two-dimensional transthoracic echocardiography (2DTTE) and cardiovascular magnetic resonance (CMR) in left ventricular (LV) function [including end-systolic volume (LVESV), end-diastolic volume (LVEDV), and ejection fraction (LVEF)] in chronic total occlusion (CTO) patients.

Methods: Eighty-eight CTO patients were enrolled in this study. All patients underwent 2DTTE and CMR within 1 week. The correlation and agreement of LVEF, LVESV, and LVEDV as measured by 2DTTE and CMR were assessed using Pearson correlation, Kappa analysis, and Bland–Altman method.

Results: The mean age of patients enrolled was 57 ± 10 years. There was a strong correlation ($r = 0.71$, 0.90, and 0.80, respectively, all $P < 0.001$) and a moderately strong agreement (Kappa = 0.62, $P < 0.001$) between the two modalities in measurement of LV function. The agreement in patients with EF ≧50% was better than in those with an EF <50%. CTO patients without echocardiographic wall motion abnormality (WMA) had stronger intermodality correlations ($r = 0.84$, 0.96, and 0.87, respectively) and smaller biases in LV function measurement.

Conclusions: The difference in measurement between 2DTTE and CMR should be noticed in CTO patients with EF <50% or abnormal ventricular motion. CMR should be considered in these conditions.

Keywords: magnetic resonance imaging, transthoracic echocardiography, left ventricular function, chronic total occlusion, agreement

OPEN ACCESS

Edited by:
Gianluca Pontone, Monzino Cardiology Center (IRCCS), Italy

Reviewed by:
Maria Aurora Morales, National Research Council (CNR), Italy
Saima Mushtaq, Monzino Cardiology Center (IRCCS), Italy

***Correspondence:**
Xiantao Song
songxiantao0929@qq.com

[†] These authors have contributed equally to this work

[‡] Present address:
Ye Han, Department of Radiology, Beijing Friendship Hospital, Capital Medical University, Beijing, China
Yi He, Department of Radiology, Beijing Friendship Hospital, Capital Medical University, Beijing, China

Specialty section:
This article was submitted to Cardiovascular Imaging, a section of the journal Frontiers in Cardiovascular Medicine

Received: *02 March 2021*
Accepted: *04 May 2021*
Published: *15 June 2021*

Citation:
Li J, Zhang L, Wang Y, Zuo H, Huang R, Yang X, Han Y, He Y and Song X (2021) Agreement in Left Ventricular Function Measured by Echocardiography and Cardiac Magnetic Resonance in Patients With Chronic Coronary Total Occlusion. Front. Cardiovasc. Med. 8:675087. doi: 10.3389/fcvm.2021.675087

INTRODUCTION

For patients with coronary chronic total occlusion (CTO), left ventricular (LV) function assessment before revascularization is crucial for clinical decision-making and has reference value in evaluating the improvement of cardiac function status after revascularization (1, 2). LV function can be measured by several non-invasive cardiac imaging modalities, including echocardiography, cardiac magnetic resonance (CMR), and cardiac computed tomography. Many studies regarding the comparison among these techniques have been reported. However, most of them enroll healthy subjects or patients with different cardiac diseases. Data about the agreement in ventricular function determined by these different modalities in CTO patients are still sparse.

The aim of this study was to determine the agreement between two-dimensional transthoracic echocardiography (2DTTE) and CMR in the assessment of LV function in CTO patients.

MATERIALS AND METHODS

Study Population

A total of 137 consecutive CTO patients, diagnosed by coronary angiography (CAG) from May 2015 to June 2017, were enrolled in this study. As shown in **Figure 1**, patients were excluded due to the contradictions of CMR ($N = 33$) or incomplete CMR data ($N = 1$). The rest of the patients were referred to echocardiography examination and further excluded due to poor-quality images ($N = 5$), incomplete 2DTTE data ($N = 4$), or lack of 2DTTE images ($N = 6$), leaving 88 patients eligible for the study. All enrolled patients underwent both echocardiography and CMR imaging within the same week. Coronary artery interventions were not performed until both types of imaging were finished. The coronary occlusion duration was divided into three levels: certain, likely, and undetermined, as previously described (3). The study was approved by Beijing Anzhen Hospital Ethics Committee, and the informed consent was waived.

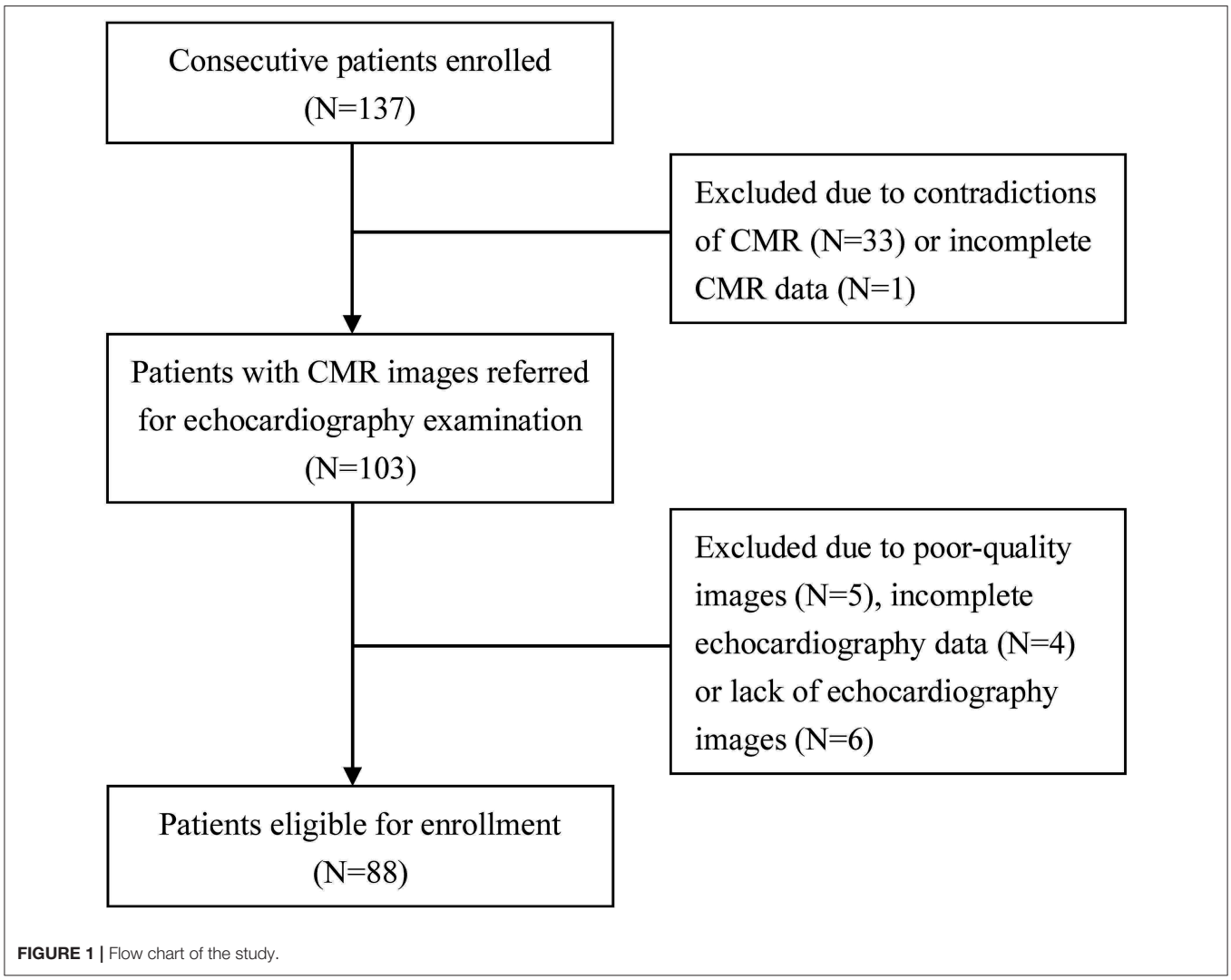

FIGURE 1 | Flow chart of the study.

Transthoracic Echocardiography

Transthoracic echocardiography was assessed using standard clinical 2-dimensional imaging platforms: 56 patients with IE33 XMatrix (Philips, Amsterdam, Netherlands) and 32 patients with Vivid 7 (General Electric Medical Systems, Boston, USA). All images were recorded and analyzed by an experienced echocardiologist, who was blinded to clinical data and CMR results.

In each subject, assessments of LV function [including end-systolic volume (LVESV), end-diastolic volume (LVEDV), and ejection fraction (LVEF)] were performed according to the recommendations of the American Society of Echocardiography (4) following the Modified Simpson's rule (5). At end-diastole and end-systole stages, in apical four- and two-chamber views, the LV endocardial interface between myocardium and LV cavity was traced contiguously from one side of the mitral annulus to the other side, including papillary muscles as part of the LV cavity. The contour was finished after a straight line connected the two edges of mitral annular ring. LVEF, LVESV, and LVEDV were calculated using the biplane Simpson's formula.

For each patient, regional wall motion was assessed using a 17-segment LV model. The level of endocardial wall motion of each segment was scored according to previous guideline: score 1, normal or hyperkinetic; score 2, hypokinetic; score 3, akinetic; and score 4, dyskinetic (4). The wall motion score index (WMSI) was calculated by averaging the scores of 17 segments. Based on WMSI findings, two groups were identified: wall motion abnormality (WMA) group (WMSI = 1) and non-WMA group (WMSI > 1).

Cardiac Magnetic Resonance Imaging

CMR imaging was performed using a 3-T whole-body scanner (Siemens, Munich, Germany) with a 32-element matrix coil. Images were obtained using steady-state and breath-hold cines in three long-axis planes and sequential short-axis slices extending from the mitral valve plane to just below the LV apex. End-diastolic and end-systolic volumes were obtained by manual delineation of the endocardial borders. Short-axis slices with ≧50% of the LV circumference surrounded by the myocardium were included in the process of volume calculation (6). The basal and apical slices were ensured on long-axis views. In every short-axis slice, the endocardial contour was traced at end-diastole and end-systole stages, with inclusion of papillary muscle and trabeculae as part of the LV cavity. Imaging analysis was performed by an experienced radiologist, who was blinded to the study. LVEF, LVESV, and LVEDV were calculated with commercially available software (CVI42 version5.9.1, Circle Cardiovascular Imaging, Calgary, AB, Canada). CMR was used as the reference standard for comparing with echocardiography.

Statistical Analysis

All analyses were performed using SPSS (Version 20.0, IBM Corporation, Armonk, NY, USA). For continuous variables, a Shapiro–Wilk test was used for normal distribution tests. Normally distributed values were expressed as means ± standard deviation (SD) and compared using Student's *t*-test. Non-normally distributed ones were expressed as a median with interquartile range (IQR) and compared using the Mann–Whitney *U*-test. Categorical variables were expressed as percentages and compared using the chi-squared test. The intermodality correlation and agreement were tested using Pearson correlation, Kappa analysis, and Bland–Altman method, respectively. Bias and limits of agreement (LOA) were expressed as the mean and 95% confidence interval of the differences in normally distributed values and as median and 2.5th−97.5th percentiles of the differences in non-normally distributed values. All statistical tests were two-sided, and statistical significance was defined as $P < 0.05$.

RESULTS

Patient Characteristics

A total of 88 patients (mean age, 57 ± 10 years; 83% male) with 90 CTO vessels were included in this study. Among them, 76

TABLE 1 | Baseline characteristics.

	All patients *N* = 88
Age (years)	57 ± 10
Male	73 (83.0)
Clinical presentations	
Asymptomatic	7 (8.0)
Stable angina	8 (9.1)
Unstable angina	68 (77.3)
NSTEMI	5 (5.7)
Duration of coronary occlusion	
Certain	45 (51.1)
Likely	10 (11.4)
Undetermined	33 (37.5)
Hypertension	49 (55.7)
Diabetes	18 (20.5)
Dyslipidemia	32 (36.4)
Prior myocardial infarction	24 (27.3)
Prior PCI	31 (35.2)
Smoking	47 (53.4)
Number of CTO vessels	90
CTO location	
LAD	36 (40.0)
LCX	14 (15.6)
RCA	40 (44.4)
WMSI >1	40 (45.5)
Interval between 2DTTE and CMR (days)	1 (0–2)
Echocardiography	
EF (%)	60.0 (54.3–63.9)
ESV (ml)	38.9 (32.0–53.8)
EDV (ml)	100.3 (82.5–123.9)
CMR	
EF (%)	58.4 (50.3–66.5)
ESV (ml)	45.0 (28.8–56.8)
EDV (ml)	106.7 (83.3–130.3)

Data are expressed as mean ± standard deviation or median with interquartile range. CMR, cardiac magnetic resonance; CTO, chronic total occlusion; EF, ejection fraction; EDV, end-diastolic volume; ESV, end-systolic volume; NSTEMI, non-ST-segment elevated myocardial infarction; LAD, left ascending branch; LCX, left circumflex branch; PCI, percutaneous coronary intervention; RCA, right coronary artery; WMSI, wall motion score index; 2DTTE, two-dimensional transthoracic echocardiography.

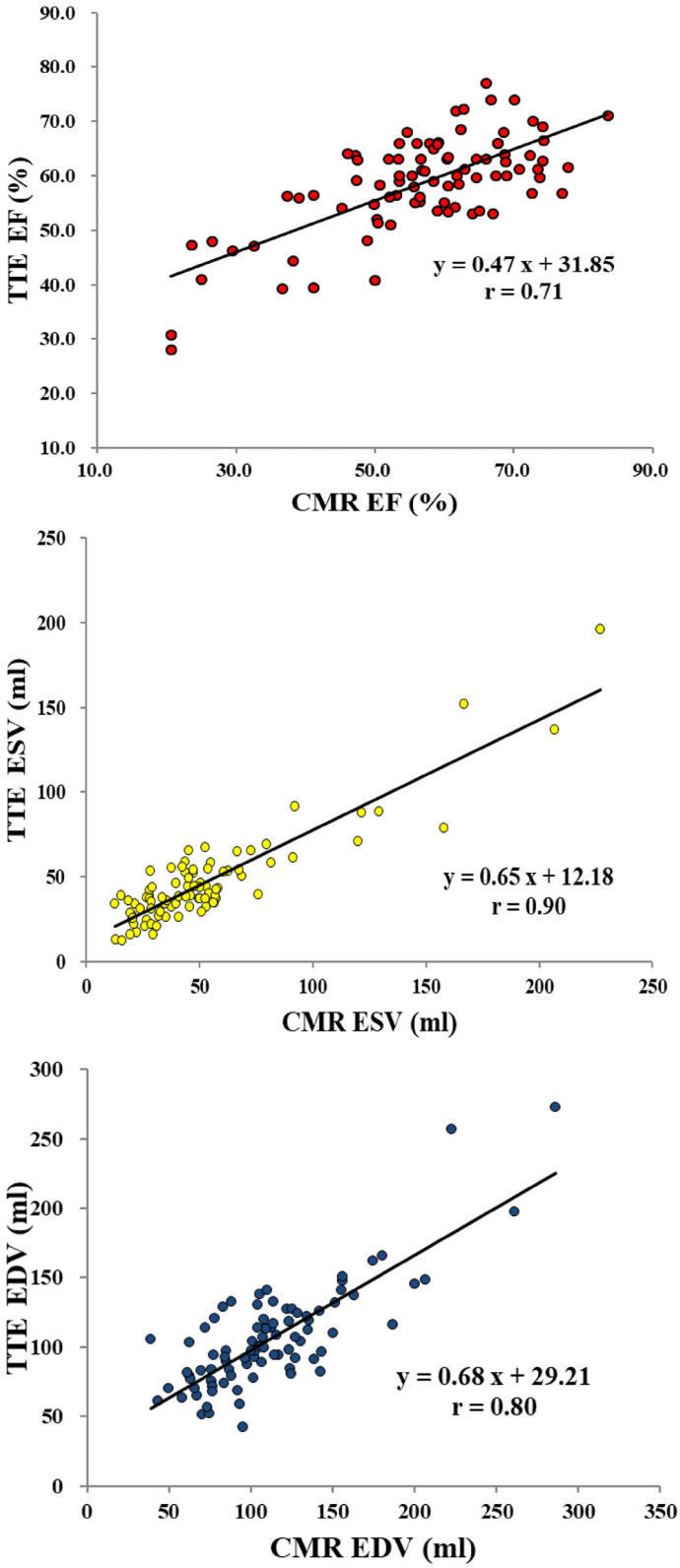

FIGURE 2 | Linear regression analysis for left ventricular functions between echocardiography and CMR (reference standard). EF, ejection fraction; ESV, end-systolic volume; EDV, end-diastolic volume; CMR, cardiovascular magnetic resonance; TTE, transthoracic echocardiography.

patients had presentation of angina (86.4%), 5 were diagnosed as non-ST-segment elevated myocardial infarction (NSTEMI) (5.7%), and 7 were asymptomatic (8.0%). Most of CTO lesions located in the right coronary artery (RCA) (44.4%), followed by left ascending branch (LAD) (40.0%) and left circumflex branch (LCX) (15.6%). The median interval between 2DTTE and CMR was 1 day. Further clinical data and LV functions are presented in **Table 1**.

Correlation and Agreement in 2DTTE and CMR Measurements of LV Function

In all 88 patients, correlation coefficients between 2DTTE and CMR for LVEF, LVESV, and LVEDV were 0.71, 0.90, and 0.80, respectively ($P < 0.001$ for all). (**Figure 2**, **Table 2**) The Bland–Altman analysis, bias, and 95% LOA between two modalities (with CMR as reference standard) were +2.0 (−16.7, 20.6)% for LVEF, −4.2 (−65.2, 22.8) ml for LVESV, and −6.4 (−57.9, 45.2) ml for LVEDV (**Figure 3**, **Table 2**). According to the heart failure guidelines (7), an LVEF of 50% was chosen as the threshold when assessing the agreement between 2DTTE and CMR. The intermodality agreement was moderately strong ($k = 0.62$, $P < 0.001$). In detail, 78 patients had the same classification when measured by 2DTTE and CMR, and 67 of them (85.9%) had an EF≧50%. 2DTTE reclassified 10 of the total 88 patients (11.4%). Furthermore, in 9 of the 10 instances (90.0%) of reclassification, 2DTTE-derived EF values were overestimated (≥50%) than CMR-derived EF (**Table 3**).

Agreement of Measurement for LV Functions in Patients With and Without Regional Wall Motion Abnormality

Based on 2DTEE findings, non-WMA group had 48 patients, and WMA group included 40 patients with 43 segments of abnormal wall motion. Most of segmental WMAs occur in the inferior wall of LV, and the distribution of WMA was in consistence with dominant area of occluded coronary arteries (**Table 4**). Among the five NSTEMI patients, only one had WMA in inferolateral wall of LV, rather than the dominant area of the CTO vessel (LAD).

TABLE 2 | Correlation and agreement analysis for 2DTTE and CMR.

	Pearson r*	Linear regression equation	Bias§	limits of agreement†
EF	0.71	y = 0.47x + 31.85	2.0%	(−16.7, 20.6)%
ESV	0.90	y = 0.65x + 12.18	−4.2 ml	(−65.2, 22.8) ml
EDV	0.80	y = 0.68x + 29.21	−6.4 ml	(−57.9, 45.2) ml

CMR, cardiac magnetic resonance; EF, ejection fraction; EDV, end-diastolic volume; ESV, end-systolic volume; 2DTTE, two-dimensional transthoracic echocardiography.
**All P values were <0.001.*
§Bias in EF and EDV were expressed as the mean of the differences, as median of the differences in ESV.
†Limits of agreement in EF and EDV were expressed as the 95% confidence interval of the differences, as 2.5th−97.5th percentiles of the differences in ESV.

Compared with the WMA group, the non-WMA group had significantly higher CMR-derived EF (59.0 ± 10.4 vs. 54.9 ± 16.1%) (**Table 5**) and higher intermodality correlations for LVEF, LVESV, and LVEDV (0.84 vs. 0.66, 0.96 vs. 0.87, and 0.87 vs. 0.75, respectively). Additionally, bias in LVEF, LVESV, and LVEDV were all greater in WMA group (8.2 vs. 4.8%, −7.3 vs. −3.3 ml, and −12.3 vs. −10.6 ml, respectively) (**Table 6**).

DISCUSSION

In this study, the results suggested that (a) there were strong correlations between 2DTTE and CMR for LV volume measurement in CTO patients; (b) for CTO patients with LVEF<50%, the strength of intermodality agreement might be lower and the EF was overestimated by 2DTTE; and (c) CTO patients with WMA had lower intermodality correlation and greater bias in LV evaluation.

Both echocardiography and CMR are important non-invasive cardiac techniques for accurate and practical cardiac function assessment. CMR is considered as the gold standard for volumetric and EF assessment, with better tissue characterization and endocardium definition (7). Previous studies had shown a strong correlation and agreement between 2DTTE and CMR in LV measurement (8), which was further confirmed in this study. However, the strength of intermodality correlation for LVEF ($r = 0.71$) was found to be lower than that in prior studies (9, 10). The Bland–Altman analysis also showed a small bias in LV measurements but with a large range of agreement. These findings might result from worse ventricular functions in enrolled subjects. Due to long-term ischemic impairment, minimal infarction and restructure in local myocardium are more common in CTO patients, leading to abnormalities in cardiac structure and function (11) and affecting the myocardium mapping during measurement.

In a previous study investigating the agreement between 2DTTE and CMR, 44% of enrolled patients differed in LVEF classification (≦35, 35–50, >50%) when comparing the two modalities (12). Another study including patients with ST-elevation myocardial infarction showed low sensitivity (52%) and positive predictive values (54%) to detect LVEF <50% using 2DTTE (13). In our study, in patients with the same classification detected by 2DTTE and CMR, the majority had an EF ≧50%. On the other hand, most of the patients who were reclassified by 2DTTE had a CMR-derived EF <50%. This implied that the intermodality agreement might be better in patients with normal EF and the necessity of CMR for further accurate assessment of LV function in patients with EF <50%.

For patients in early stage of acute myocardial infarction, WMA can be observed due to temporary ventricular dysfunction. Among the five NSTEMI patients in this study, four of them had no transient or persistent WMA. Only one NSTEMI patient had WMA in inferolateral wall, which was more likely to be related to previous history of inferior myocardial infarction. Although the distribution of WMA was basically in consistence with occluded coronary arteries, no WMA was detected in the dominant area of CTO vessels in these five NSTEMI patients. The reason

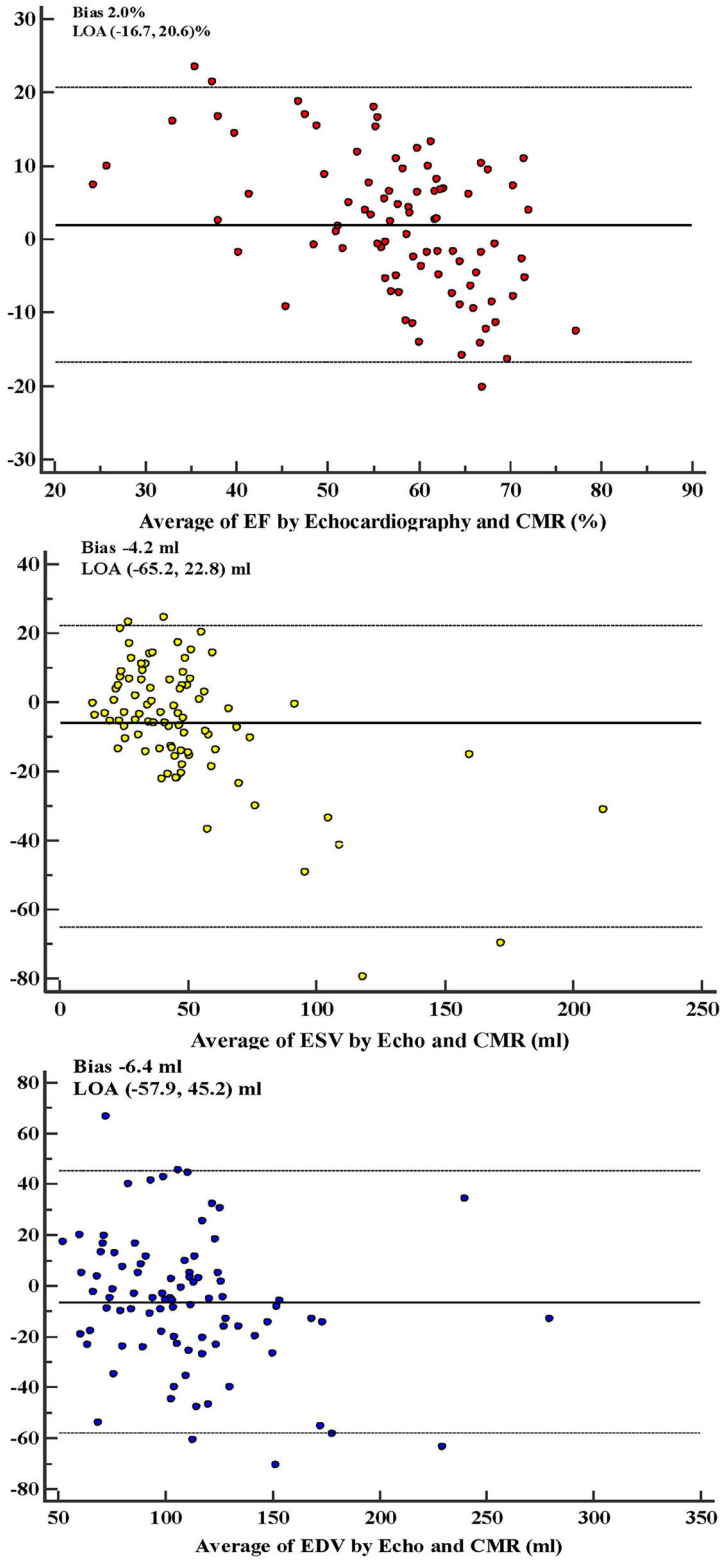

FIGURE 3 | Bland–Altman analysis for left ventricular functions between echocardiography and CMR. Bias and 95% LOA were expressed as the mean and 95% confidence interval of the differences in normally distributed values (i.e., EF and EDV), as median and 2.5th–97.5th percentiles of the differences in non-normally distributed values (i.e., ESV). EF, ejection fraction; ESV, end-systolic volume; EDV, end-diastolic volume; CMR, cardiovascular magnetic resonance; LOA, limits of agreement.

TABLE 3 | Patients assessed by echocardiography and CMR at EF 50% threshold.

		CMR EF		
		≥50%	<50%	Total
Echocardiographic EF	≥50%	67	9	76
	<50%	1	11	12
Total		68	20	88

Kappa = 0.62, P < 0.001. CMR, cardiac magnetic resonance; EF, ejection fraction.

TABLE 4 | CTO vessels and the distribution of wall motion abnormalities.

	LAD	LCX	RCA	Total
Anterior	7	0	0	7
Anteroseptal	3	0	0	3
Anterolateral	4	3	0	7
Inferior	0	0	10	10
Inferoseptal	1	0	5	6
Inferolateral	1	2	7	10
Total	16	5	22	43

CMR, cardiac magnetic resonance; CTO, chronic total occlusion; LAD, left ascending branch; LCX, left circumflex branch; RCA, right coronary artery.

for the inconsistency was that timely revascularization avoids further ischemic impairment and ensured myocardial viability and normal ventricular motion.

Besides, no significant difference was found in the history of myocardial infarction in comparison of patients with and without WMA. This suggests that WMA is not appropriate for diagnosis of myocardial infarction existence. In patients with cardiac microcirculation dysfunction or with equivocal evidence of cardiac ischemia, they may present with tiny or unrecognized infarction and undetectable WMA in echocardiography. In this condition, late gadolinium enhancement (LGE) performed by CMR can be better in the recognition of infarction lesions.

In addition, lower strength of intermodality correlations for LV measurements and more significant bias in LVEF were observed in WMA group. The defect in the mechanism of echocardiography measurement was the main reason for this result. During the assessment and calculation of LV function, the interface between myocardium and ventricular cavity should be mapped at the end-diastole and end-systole stages in apical four and two-chamber views. The LV model is then made into a bullet shape and becomes the basis for measurements of volumetric values and EF calculation (4). A concise mapping may avoid potential error in model making and measurement. However, in patients with WMA, asymmetry of LV cavity and irregular myocardial motion add difficulties in mapping the ventricular interface and are therefore more likely to add inaccuracies in echocardiography measurements. Although echocardiography has lower cost and is more convenient in practice, for patients with WMA or even worse cardiac function, some clinical applications such as implantable cardiac defibrillator and cardiac supplement device will be restricted or overused due to the inaccurate assessments by echocardiography. Thus, for these

TABLE 5 | Comparison of patients with and without regional wall motion abnormality detected by 2DTTE.

	WMA N = 40	Non-WMA N = 48	*P*-value
Age (years)	57 ± 10	56 ± 10	0.742
Male	33 (82.5)	40 (83.3)	0.918
Clinical presentations			
Asymptomatic	4 (10.0)	3 (6.3)	0.801
Stable angina	4 (10.0)	4 (8.3)	1.000
Unstable angina	31 (77.5)	37 (77.1)	0.963
Myocardial infarction(NSTEMI)	1 (2.5)	4 (8.3)	0.475
Hypertension	25 (62.5)	24 (50.0)	0.240
Diabetes	7 (17.5)	11 (22.9)	0.530
Dyslipidemia	15 (37.5)	17 (35.4)	0.840
Prior myocardial infarction	11 (27.5)	13 (27.1)	0.965
Prior PCI	14 (35.0)	17 (35.4)	0.968
Smoking	20 (50.0)	27 (56.2)	0.588
Interval between 2DTTE and CMR (days)	1 (0–2)	2 (0–2)	0.474
Number of CTO vessels	41	49	
Echocardiography			
EF (%)	58.7 ± 8.8	58.6 ± 9.3	0.901
ESV (ml)	38.7 (31.0–57.5)	39.0 (32.5–52.4)	0.782
EDV (ml)	109.1 ± 38.3	104.1 ± 37.0	0.890
CMR			
EF (%)	54.9 ± 16.1	59.0 ± 10.4	0.007
ESV (ml)	43.8 (28.1–58.0)	45.3 (28.8–56.5)	0.802
EDV (ml)	105.6 (79.2–123.6)	108.5 (85.0–135.3)	0.379

Data are expressed as mean ± standard deviation or median with interquartile range. CMR, cardiac magnetic resonance; CTO, chronic total occlusion; EF, ejection fraction; EDV, end-diastolic volume; ESV, end-systolic volume; NSTEMI, non-ST-segment elevated myocardial infarction; 2DTTE, two-dimensional transthoracic echocardiography.

TABLE 6 | Correlation and agreement analysis for 2DTTE and CMR in patients with and without regional wall motion abnormality.

		Pearson r*	Linear regression equation	Bias§	Limits of agreement†
WMA	EF	0.66	y = 0.39x + 39.37	8.2%	(−20.1, 23.5)%
	ESV	0.87	y = 0.55x + 16.98	−7.3 ml	(−79.1, 24.5) ml
	EDV	0.75	y = 0.60x + 42.68	−12.3 ml	(−53.5, 28.9) ml
Without	EF	0.84	y = 0.75x + 14.08	4.8%	(−19.3, 28.8)%
WMA	ESV	0.96	y = 0.80x + 5.61	−3.3 ml	(−39.0, 16.7) ml
	EDV	0.87	y = 0.79x + 13.89	−10.6 ml	(−50.1, 29.0) ml

CMR, cardiac magnetic resonance; EF, ejection fraction; EDV, end-diastolic volume; ESV, end-systolic volume; 2DTTE, two-dimensional transthoracic echocardiography; WMA, wall motion abnormality.

**All P values were <0.001.*

§Bias in EF and EDV were expressed as the mean of the differences, as median of the differences in ESV.

†Limits of agreement in EF and EDV were expressed as the 95% confidence interval of the differences, as 2.5th−97.5th percentiles of the differences in ESV.

patients, CMR should be considered for accurate and reliable ventricular evaluation.

Several limitations of this study need to be addressed. First, this was a single center study with a small number of patients. Second, only CTO patients who underwent 2DTTE and CMR were enrolled. It may be better to expand this study to newly emerging modalities, including 3D echocardiography and cardiac computed tomography. Previous studies have confirmed that 3D echocardiography is superior to the 2D method when it comes to LV function assessment (14), especially in patients with abnormal LV dilating motion or distortedly shaped LV.

DATA AVAILABILITY STATEMENT

The original contributions presented in the study are included in the article/supplementary material, further inquiries can be directed to the corresponding author/s.

ETHICS STATEMENT

The studies involving human participants were reviewed and approved by Beijing Anzhen Hospital Ethics Committee. The patients/participants provided their written informed consent to participate in this study.

AUTHOR CONTRIBUTIONS

XY and YHa collected the patient data. JL, LZ, and YW analyzed data and were major contributors in writing the manuscript. HZ, RH, YHe, and XS took the revision of the manuscript. All authors agree to be accountable for the content of the work.

FUNDING

This study was supported by Beijing Council of Science and Technology (Grant Number Z161100000516139), Beijing Lab for Cardiovascular Precision Medicine (Grant Number PXM2018_014226_000013), China Cardiovascular Disease Alliance VG Youth Fund Project (Grant Number 2017-CCA-VG-046), and Chinese National Natural Science Foundation (Grant Numbers 81671650 and 81971569).

REFERENCES

1. Grantham JA, Marso SP, Spertus J, House J, Holmes DR Jr, Rutherford BD. Chronic total occlusion angioplasty in the United States. *JACC Cardiovasc Interv*. (2009) 2:479–86. doi: 10.1016/j.jcin.2009.02.008
2. Joyal D, Afilalo J, Rinfret S. Effectiveness of recanalization of chronic total occlusions: a systematic review and meta-analysis. *Am Heart J.* (2010) 160:179–87. doi: 10.1016/j.ahj.2010.04.015
3. Tomasello SD, Boukhris M, Giubilato S, Marza F, Garbo R, Contegiacomo G, et al. Management strategies in patients affected by chronic total occlusions: results from the Italian Registry of Chronic Total Occlusions. *Eur Heart J.* (2015) 36:3189–98. doi: 10.1093/eurheartj/ehv450
4. Lang RM, Badano LP, Mor-Avi V, Afilalo J, Armstrong A, Ernande L, et al. Recommendations for cardiac chamber quantification by echocardiography in adults: an update from the American Society of Echocardiography and the European Association of Cardiovascular Imaging. *J Am Soc Echocardiogr.* (2015) 28:1–39.e14. doi: 10.1016/j.echo.2014.10.003
5. Oh JK, Velazquez EJ, Menicanti L, Pohost GM, Bonow RO, Lin G, et al. Influence of baseline left ventricular function on the clinical outcome of surgical ventricular reconstruction in patients with ischaemic cardiomyopathy. *Eur Heart J.* (2013) 34:39–47. doi: 10.1093/eurheartj/ehs021
6. Alfakih K, Plein S, Thiele H, Jones T, Ridgway JP, Sivananthan MU. Normal human left and right ventricular dimensions for MRI as assessed by turbo gradient echo and steady-state free precession imaging sequences. *J Magn Reson Imaging.* (2003) 17:323–9. doi: 10.1002/jmri.10262
7. Collins JD. Global and regional functional assessment of ischemic heart disease with cardiac MR imaging. *Radiol Clin North Am.* (2015) 53:369–95. doi: 10.1016/j.rcl.2014.11.001
8. Dorosz JL, Lezotte DC, Weitzenkamp DA, Allen LA, Salcedo EE. Performance of 3-dimensional echocardiography in measuring left ventricular volumes and ejection fraction: a systematic review and meta-analysis. *J Am Coll Cardiol.* (2012) 59:1799–808. doi: 10.1016/j.jacc.2012.01.037
9. Macron L, Lim P, Bensaid A, Nahum J, Dussault C, Mitchell-Heggs L, et al. Single-beat versus multibeat real-time 3D echocardiography for assessing left ventricular volumes and ejection fraction: a comparison study with cardiac magnetic resonance. *Circ Cardiovasc Imaging.* (2010) 3:450–5. doi: 10.1161/CIRCIMAGING.109.925966
10. Van De Heyning CM, Magne J, Pierard LA, Bruyere PJ, Davin L, De Maeyer C, et al. Assessment of left ventricular volumes and primary mitral regurgitation severity by 2D echocardiography and cardiovascular magnetic resonance. *Cardiovasc Ultrasound.* (2013) 11:46. doi: 10.1186/1476-7120-11-46
11. Yajima S, Miyagawa S, Fukushima S, Isohashi K, Watabe T, Ikeda H, et al. Microvascular dysfunction related to progressive left ventricular remodeling due to chronic occlusion of the left anterior descending artery in an adult porcine heart. *Int Heart J.* (2019) 60:715–27. doi: 10.1536/ihj.18-346
12. Chuang ML, Hibberd MG, Salton CJ, Beaudin RA, Riley MF, Parker RA, et al. Importance of imaging method over imaging modality in noninvasive determination of left ventricular volumes and ejection fraction: assessment by two- and three-dimensional echocardiography and magnetic resonance imaging. *J Am Coll Cardiol.* (2000) 35:477–84. doi: 10.1016/S0735-1097(99)00551-3
13. Hendriks T, Al Ali L, Maagdenberg CG, van Melle JP, Hummel YM, Oudkerk M, et al. Agreement of 2D transthoracic echocardiography with cardiovascular magnetic resonance imaging after ST-elevation myocardial infarction. *Eur J Radiol.* (2019) 114:6–13. doi: 10.1016/j.ejrad.2019.02.039
14. Hung J, Lang R, Flachskampf F, Shernan SK, McCulloch ML, Adams DB, et al. 3D echocardiography: a review of the current status and future directions. *J Am Soc Echocardiogr*. (2007) 20:213–33. doi: 10.1016/j.echo.2007.01.010

Conflict of Interest: The authors declare that the research was conducted in the absence of any commercial or financial relationships that could be construed as a potential conflict of interest.

frontiers in Cardiovascular Medicine

REVIEW
published: 17 August 2021
doi: 10.3389/fcvm.2021.682924

Coronary Magnetic Resonance Angiography in Chronic Coronary Syndromes

Reza Hajhosseiny[1,2], Camila Munoz[1], Gastao Cruz[1], Ramzi Khamis[2], Won Yong Kim[3], Claudia Prieto[1,4] and René M. Botnar[1,4,5]*

[1] School of Biomedical Engineering and Imaging Sciences, King's College London, London, United Kingdom, [2] National Heart and Lung Institute, Imperial College London, London, United Kingdom, [3] Department of Cardiology and Institute of Clinical Medicine, Aarhus University Hospital, Skejby, Denmark, [4] Escuela de Ingeniería, Pontificia Universidad Catolica de Chile, Santiago, Chile, [5] Instituto de Ingeniería Biologica y Medica, Pontificia Universidad Catolica de Chile, Santiago, Chile

Cardiovascular disease is the leading cause of mortality worldwide, with atherosclerotic coronary artery disease (CAD) accounting for the majority of cases. X-ray coronary angiography and computed tomography coronary angiography (CCTA) are the imaging modalities of choice for the assessment of CAD. However, the use of ionising radiation and iodinated contrast agents remain drawbacks. There is therefore a clinical need for an alternative modality for the early identification and longitudinal monitoring of CAD without these associated drawbacks. Coronary magnetic resonance angiography (CMRA) could be a potential alternative for the detection and monitoring of coronary arterial stenosis, without exposing patients to ionising radiation or iodinated contrast agents. Further advantages include its versatility, excellent soft tissue characterisation and suitability for repeat imaging. Despite the early promise of CMRA, widespread clinical utilisation remains limited due to long and unpredictable scan times, onerous scan planning, lower spatial resolution, as well as motion related image quality degradation. The past decade has brought about a resurgence in CMRA technology, with significant leaps in image acceleration, respiratory and cardiac motion estimation and advanced motion corrected or motion-resolved image reconstruction. With the advent of artificial intelligence, great advances are also seen in deep learning-based motion estimation, undersampled and super-resolution reconstruction promising further improvements of CMRA. This has enabled high spatial resolution (1 mm isotropic), 3D whole heart CMRA in a clinically feasible and reliable acquisition time of under 10 min. Furthermore, latest super-resolution image reconstruction approaches which are currently under evaluation promise acquisitions as short as 1 min. In this review, we will explore the recent technological advances that are designed to bring CMRA closer to clinical reality.

Keywords: coronary angiography, CMRA, CCS, atherosclerosis, plaque, magnetic resonance imaging

OPEN ACCESS

Edited by:
Bernhard L. Gerber, Cliniques Universitaires Saint-Luc, Belgium

Reviewed by:
David Winkel, University Hospital of Basel, Switzerland
Thoralf Niendorf, Helmholtz Association of German Research Centers (HZ), Germany

****Correspondence:***
Reza Hajhosseiny
reza.hajhosseiny@kcl.ac.uk
orcid.org/0000-0002-8116-460X

Specialty section:
This article was submitted to Cardiovascular Imaging, a section of the journal Frontiers in Cardiovascular Medicine

Received: *19 March 2021*
Accepted: *23 July 2021*
Published: *17 August 2021*

Citation:
Hajhosseiny R, Munoz C, Cruz G, Khamis R, Kim WY, Prieto C and Botnar RM (2021) Coronary Magnetic Resonance Angiography in Chronic Coronary Syndromes. Front. Cardiovasc. Med. 8:682924. doi: 10.3389/fcvm.2021.682924

INTRODUCTION

Coronary artery disease (CAD) is the leading cause of cardiovascular morbidity and mortality worldwide (1, 2). CAD is predominantly caused by coronary atherosclerosis, which initiates in the early decades of life and progresses at a variable pace depending on the intrinsic propensity of the individual in combination with lifestyle modifications and therapeutic interventions (3–5).

The clinical manifestations of CAD can present either as an acute process or a more stable but chronic deterioration of symptoms. The European Society of Cardiology has recently categorised CAD as either acute coronary syndromes (ACS) or chronic coronary syndromes (CCS) (6). Whilst cardiovascular magnetic resonance (CMR) has a clear role in the diagnosis and management of patients with ACS, this is beyond the scope of this review. We will instead focus on the role of coronary magnetic resonance angiography (CMRA) in patients with CCS with a particular emphasis on the current status quo and future directions.

Chronic coronary syndromes can present clinically in a variety of ways; symptoms of stable angina (e.g., chest pain and/or dyspnoea), symptoms of heart failure or asymptomatic left ventricular impairment, symptomatic and asymptomatic cardiac arrhythmias (6). The early detection of CCS and targeted risk stratification will facilitate the timely initiation of therapeutic interventions and monitoring of disease progression.

X-ray coronary angiography is the reference standard imaging modality for the assessment of CAD with unrivalled temporal and spatial resolution, as well as the versatility to enable real time coronary intervention for patients presenting with ACS. The addition of functional physiological assessment of CAD with pressure wiring is particularly helpful in patients presenting with CCS and has been shown to be prognostically significant (7, 8). Plaque characterisation and coronary vascular anatomy can be further complemented with intravascular imaging (9, 10). However, risk from ionising radiation, viscous iodine-containing radiocontrast agent induced acute kidney injury and its potential progression to chronic kidney disease (11) as well as potential invasive complications limit the surveillance suitability of invasive assessment for CCS beyond the initial diagnosis.

Computed tomography coronary angiography (CCTA) has emerged as a credible non-invasive alternative for the assessment of patients with CCS. It offers high diagnostic accuracy in terms of comprehensive assessment of luminal stenosis, fractional flow reserve and plaque characterisation (12–15). However, it is also limited by ionising radiation, iodinated nephrotoxic contrast agents and calcium related blooming artefacts, dampening its suitability in patients with highly calcified plaque lesions or for the longitudinal assessment of CAD.

Coronary magnetic resonance angiography could potentially offer a non-invasive alternative for the early detection and long-term monitoring of CCS, which is free of ionising radiation and iodinated nephrotoxic contrast agents. It could also be combined with volumetric assessment of left ventricular function, myocardial perfusion, myocardial tissue characterisation, valvular assessment and coronary plaque characterisation to brand CMR as one of the most comprehensive imaging modalities for cardiovascular assessment. Here we discuss the

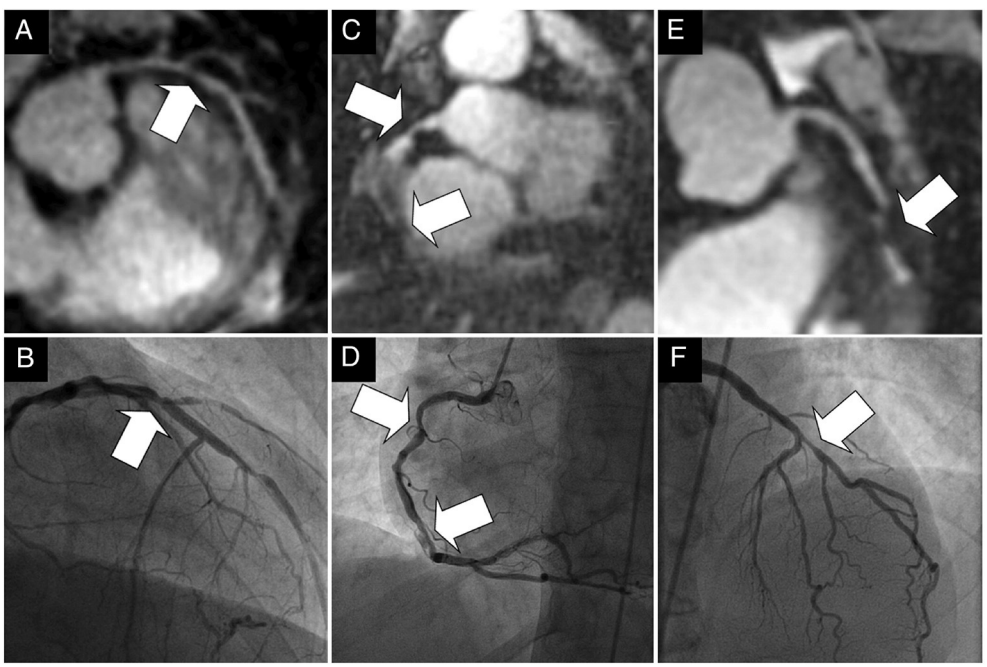

FIGURE 1 | (A–F) Examples of the comparison between multiplanar reformats of the whole-heart 1D self-navigated CMRA data sets (top row) and the corresponding x-ray coronary angiograms (bottom row) in three patients. The lesion in the proximal LAD artery and just distal to the take-off of a diagonal branch can clearly be identified in the first patient in **(A).** while this is confirmed on the x-ray angiogram in **(B)**. While the luminal narrowing of the proximal RCA in the second patient on **(C).** can clearly be identified, the further course of this artery is obscured in the region of a stent. The same in stent restenoses can be identified in **(D)**. In the third patient in **(E).** significant disease is identified in the proximal LAD artery at CMRA and is confirmed on, **(F).** the corresponding x-ray coronary angiogram. Arrows = stenoses; LAD, left anterior descending artery; RCA, right coronary artery. Adapted with permission from Piccini et al. (46).

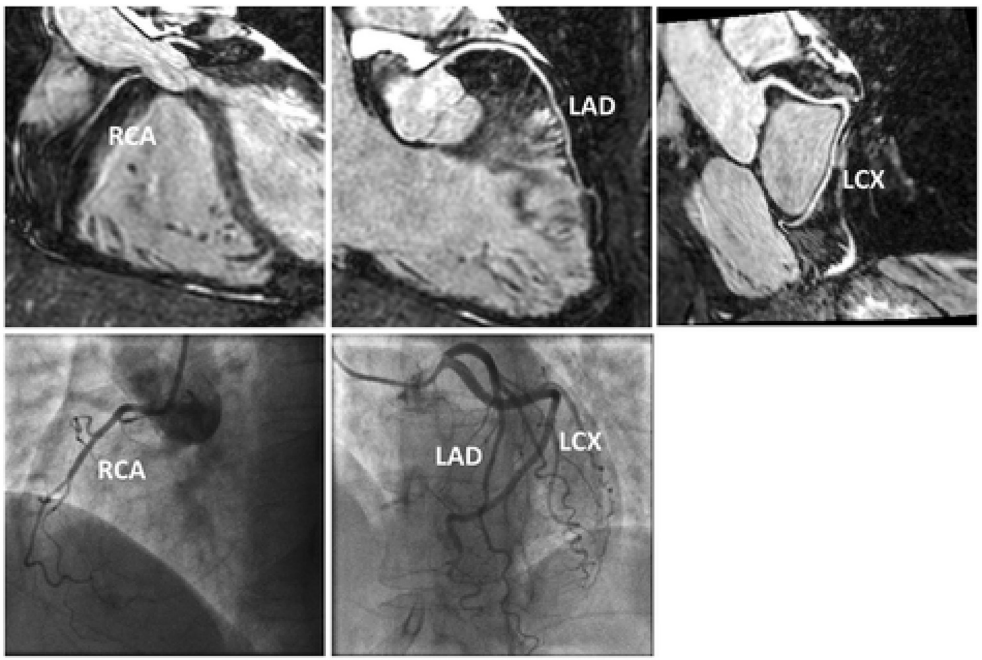

FIGURE 2 | Reformatted CMRA datasets (top row) from a patient without coronary artery disease but non dominant RCA. Coronary x-ray angiography in the same patient (bottom row). RCA, right coronary artery; LAD, left anterior descending artery; LCX, left circumflex artery. Adapted with permission from Henningsson et al. (52).

current status quo and potential future role of CMRA as a viable alternative for the assessment of patients with CCS.

CORONARY MAGNETIC RESONANCE ANGIOGRAPHY

The potential of CMRA to exclude significant CAD was first demonstrated two decades ago in a multicentre study of 109 patients, which compared non-contrast CMRA against invasive X-ray angiography (16). In this study, the sensitivity, specificity, positive and negative predictive values, and accuracy of CMRA were 93, 42, 70, 81, and 72% respectively. These findings were confirmed in a subsequent study of 127 patients comparing CMRA vs. invasive X-ray angiography (17). In this study, the sensitivity, specificity, positive and negative predictive values, and accuracy of CMRA were 88, 72, 71, 88, and 79% respectively. In a direct head-to-head comparison of CMRA vs. CCTA in patients with suspected CAD who were also assessed with invasive X-ray coronary angiography, there was no significant difference between CCTA and CMRA in terms of diagnostic accuracy, suggesting that CMRA could be used in these patients to exclude significant disease, inform revascularization and if the CMRA scan was negative the event free survival rate was comparable with CCTA (18, 19). To assess the prognostic value of CMRA, 207 patients with suspected CAD who underwent non-contrast whole-heart CMRA were followed up by Yoon et al. (20). Coronary stenosis was significantly associated with major adverse cardiac events (myocardial infarction, cardiac death, and unstable angina) and all cardiac events (which included revascularization >90 days after CMRA).

However, despite the early promise of CMRA, clinical application is currently confined to a few specialised centres within a set of niche indications e.g., suspected anomalous coronary arteries, coronary artery aneurysms and assessment of the proximal coronary arteries. Reasons for the slow uptake of CMRA in clinical practise include lower spatial resolution compared to CCTA and invasive X-ray angiography, significantly longer and unpredictable acquisition time, complicated scan planning, and motion related (cardiac and respiratory) image quality degradation.

Significant technological strides in CMR image acquisition and image processing are now enabling some of these technical challenges to be overcome. The most notable breakthroughs are in the fields of respiratory motion compensation and image acceleration. Further recent advances in deep learning-based motion correction and image reconstruction could potentially enable 3D whole-heart CMRA with similar spatial resolution and acquisition time as CCTA in the future. We will discuss some of these recent developments in the following sections.

CARDIAC AND RESPIRATORY MOTION COMPENSATION

In order to acquire a high spatial resolution 3D whole-heart CMRA, patients are required to be continuously scanned for several minutes with data acquired from numerous heat beats under free breathing. This scenario produces a challenging

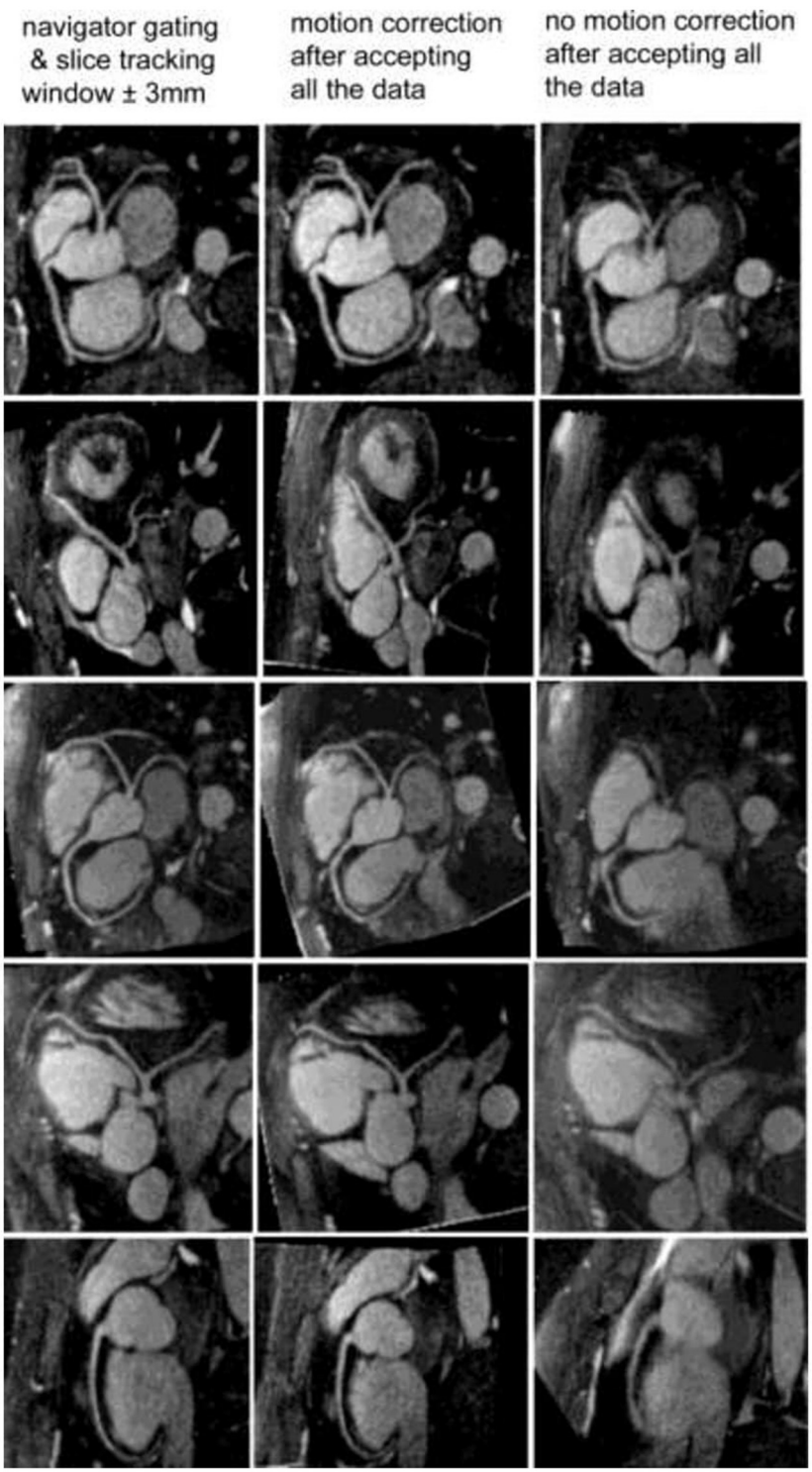

FIGURE 3 | Reformatted coronary artery images from five healthy volunteers. With the motion correction technique (middle column), coronary artery visualization is excellent and similar to the navigator gating and slice tracking approach (left column). Without any motion correction (right column), the images are blurry and the coronary artery visualization is poor. The imaging time with the motion correction technique is reduced by a factor of 2.5 to 3 compared with the navigator gating and slice tracking approach. Adapted with permission from Bhat et al. (53).

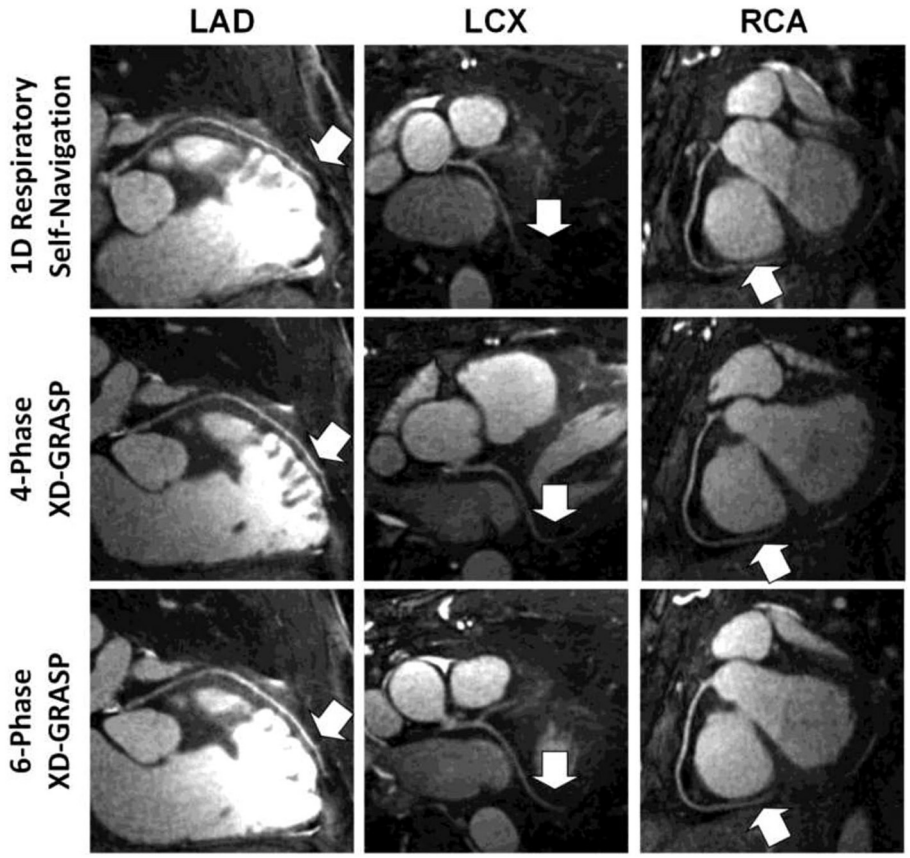

FIGURE 4 | Examples of multiplanar reformatted coronary arteries from one representative healthy adult volunteer. Although respiratory self-navigated reconstruction with 1D motion correction could achieve high image quality (top row), a clear improvement in sharpness as well as visible vessel length (arrows) can be noticed in both four-phase (middle row) and six-phase (bottom row) extradimensional golden-angle radial sparse parallel (XD-GRASP) reconstructions. Adapted with permission from Piccini et al. (54).

multi-dimensional cardiac and respiratory motion environment, which needs to be compensated through image acquisition and reconstruction techniques. Cardiac motion artefacts are typically minimised by prospective electrocardiographic (ECG) triggering to acquire data during mid-to-late diastole. However, this may be susceptible to image degradation as a result of cardiac arrhythmias, heart rate variability or user dependent estimation of the resting period. Systolic image acquisition is less sensitive to arrhythmias and heart rate variability. However, longer acquisition times may be needed due to a shorter resting period compared to diastolic imaging. Alternatively, data can be continuously acquired and then retrospectively reconstructed into multiple cardiac phases, thus selecting the phase with the minimum cardiac motion artefact, similar to CCTA (21, 22).

Various techniques have been proposed to compensate for respiratory motion artefacts during CMRA acquisition. The most rudimentary techniques utilise breath-holding to minimise respiratory motion artefacts (23–26), which enable both 2D and 3D CMRA acquisitions within a single albeit long breath-hold (27–29). However, image quality is frequently suboptimal due to diaphragmatic drift and difficulty of patients to hold their breath for a prolonged period (30, 31). As a result, clinically established 3D CMRA techniques implement free-breathing motion compensated protocols (30, 32). Initially, respiratory bellows (33) and amplitude demodulation of the ECG signal (34), which are external respiratory monitoring devices were used to enable free breathing CMRA. This is called respiratory gating as data is only acquired at end expiration when respiratory motion is minimal. However, this method is both labour intensive and time consuming to implement. Furthermore, it is not possible to estimate the true multidimensional extend of respiratory motion. As a result, respiratory navigators, incorporating the intrinsic CMR signal to track respiratory related movement of the heart became the dominant form of respiratory gating/compensation for free breathing CMRA. Here, the diaphragmatic 1D navigator (35, 36) takes advantage of the liver-diaphragm interface to perform respiratory translational motion estimation, which enables both respiratory gating and 1D (superior-inferior) motion correction. However, there is a non-linear relationship (37) between the movement of the liver/diaphragm and the heart, which is patient specific and subject to hysteresis (the motion of breathing-in is different than breathing-out). Despite

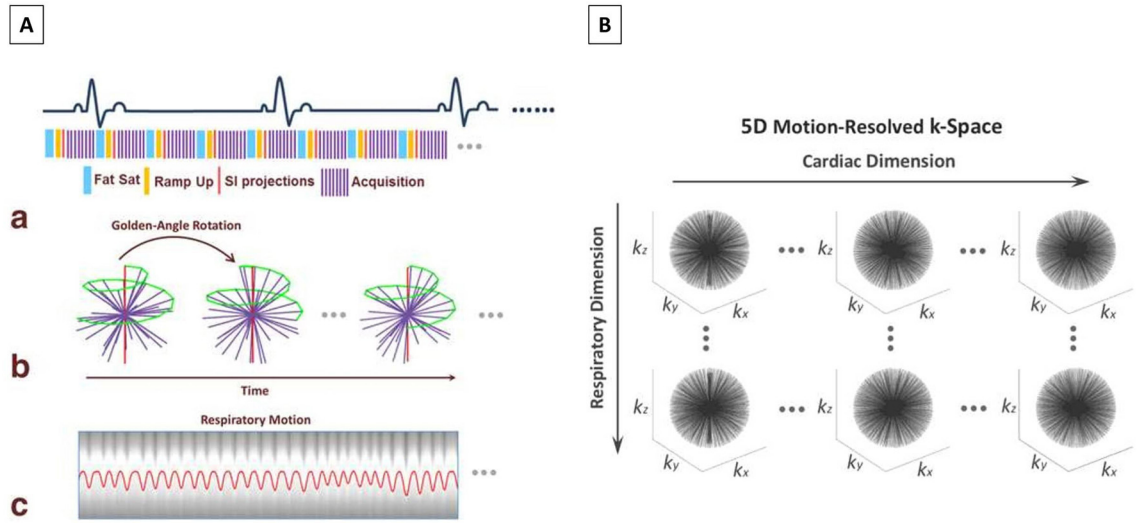

FIGURE 5 | (A) Data acquisition scheme and respiratory motion extraction for non–ECG-triggered whole-heart imaging. (a) A 3D radial b-SSFP sequence that is segmented into multiple interleaves (purple lines) is used for MR data acquisition. Each interleave starts with a spoke oriented along the superior to inferior direction for self-navigation (red lines) and is preceded by fat saturation (blue lines). Ten additional ramp-up RF pulses (yellow lines) are deployed between the fat saturation module and the data acquisition window to restore restoring steady-state at each interleave. (b) 3D radial sampling trajectory based on the spiral phyllotaxis pattern. Each interleave is rotated by the golden-angle (137.51 °) about the z-axis, starting with a self-navigation spoke (red lines) for respiratory motion extraction. (c) An extracted respiratory motion signal is superimposed to the 1D FFT of an example series of SI readouts. **(B)** The acquired k-space is sorted into a 5D dataset (k_x-k_y-k_z-cardiac phase-respiratory phase) using respiratory motion signal extracted from self-navigators and cardiac motion signal obtained from recorded ECG time stamp. The datasets are first binned into different cardiac phases with a desired temporal resolution, then each cardiac phase is further sorted into multiple respiratory motion phases spanning from end-expiration to end-inspiration. The data sorting process is performed such that the number of spokes grouped in each temporal phase is the same. SSFP, Steady State Free Precession; MR, Magnetic Resonance; RF, Radiofrequency; FFT, fast Fourier transform; SI, Superior-Inferior; ECG, Electrocardiogram. Adapted with permission from Feng et al. (55).

this, a population derived linear correction factor of 0.6 is used as an approximation of the motion between liver/diaphragm and the heart (38, 39). Furthermore, precise planning of the diaphragmatic navigator is complex and requires expertise, acquisition times are often unpredictable and reliant on the breathing pattern of patients and it is highly inefficient (∼30–50%) as data is acquired only at end expiration within a very narrow acquisition window of ±5 mm (30, 36).

Several novel respiratory motion compensation frameworks have recently been proposed to overcome some of these drawbacks, principally to deal with the 3D nature of respiratory motion, improve image quality, increase respiratory scan efficiency to 100% and therefore significantly reduce acquisition times. Using the so called "1D self-navigation" approach (40), the acquired CMR data is used to estimate displacement/movement of the heart induced by respiratory motion (40, 41), eliminating the need for the correction factor, enabling translational motion correction and acquiring data at every point of the respiratory cycle which enables 100% respiratory scan (42–45). In a cohort of 78 patients, a self-navigated CMRA framework enabled 92, 84, and 56% of proximal, middle and distal coronary segments, respectively, to be visualised, with a per vessel sensitivity and specificity for stenosis (>50%) detection of 65 and 85% compared with X-ray coronary angiography (**Figure 1**) (46).

However, with 1D self-navigation, it is difficult to separate moving (e.g., heart) from static (e.g., chest wall) tissue, which introduces artefacts (47). Image-based navigators (iNAVs) are an alternative platform to respiratory self-navigation. Whilst offering up to 100% respiratory scan efficiency, the principle aim of iNAVs is to separate moving tissue from static tissue by acquiring a low spatial resolution 2D/3D image at every heartbeat prior to the acquisition of high resolution CMRA (47–51). This framework also enables the capability to estimate respiratory motion in multiple directions to factor in the multidimensional motion of the heart. Furthermore, it eliminates additional planning as the iNAV can be derived within the same field of view (FOV) and orientation as the CMRA planning. An early version of iNAV CMRA framework demonstrated highly diagnostic image quality in the proximal, middle and distal coronary segments (98, 94, and 91, respectively) (**Figure 2**) (52). The sensitivity, specificity, and negative predictive values were 86, 83, and 95% per patient, 80, 92, and 97% per vessel and 73, 95, and 98% per segment; compared with X-ray coronary angiography.

CORONARY MAGNETIC RESONANCE ANGIOGRAPHY TECHNIQUES CURRENTLY IN DEVELOPMENT

Despite offering 100% respiratory scan efficiency, self-navigation or iNAV frameworks on their own are not sufficient. It can take up to 30 min to acquire a fully sampled high resolution (≈1 mm

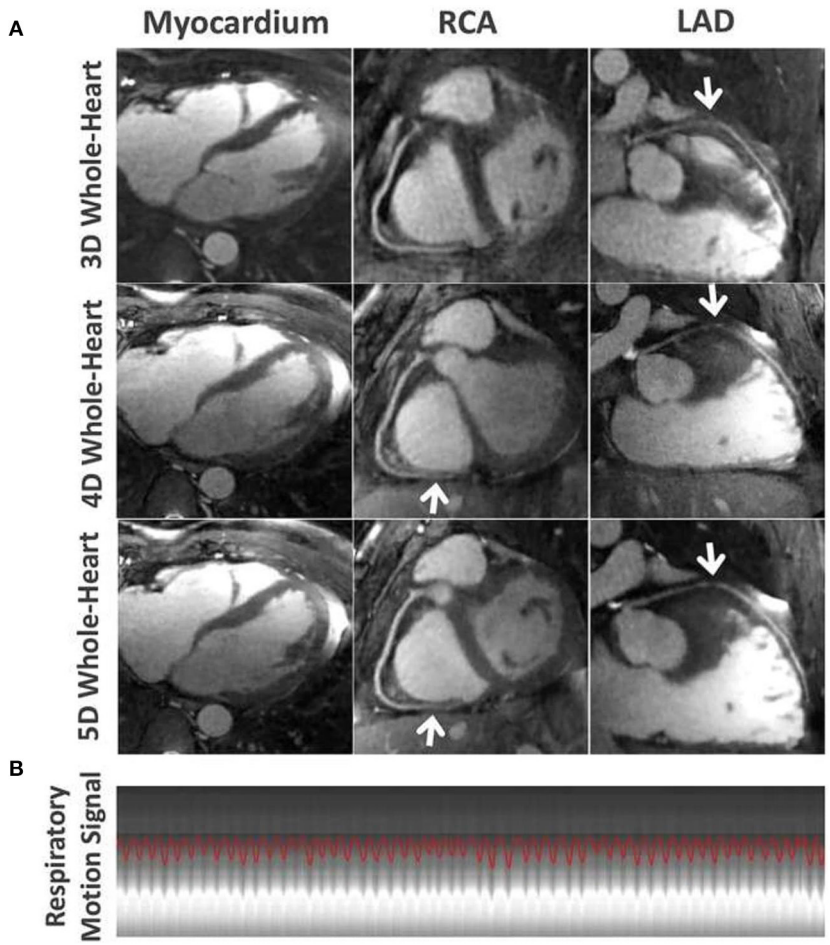

FIGURE 6 | (A) Comparison of the myocardium, the RCA and LAD coronary arteries for different imaging techniques in one subject. 5D whole-heart images (end-expiratory phase) achieved improved visual delineation of the myocardial wall and different segments of the coronary arteries (white arrows) over 4D whole-heart images, and improved delineation of the LAD over self-navigated 3D whole-heart images. **(B)** Corresponding respiratory motion pattern extracted from the continuous acquired whole-heart dataset in this subject. RCA, right coronary artery; LAD, left anterior descending artery. Adapted with permission from Feng et al. (55).

isotropic) CMRA. Here we will discuss the novel techniques in development which incorporate self-navigation or iNAV systems with a combination of image acceleration techniques (undersampled acquisition, parallel imaging, iterative non-linear reconstruction) to achieve high-spatial resolution CMRA within a clinically feasible acquisition time. We will also touch on more advanced motion correction frameworks which factor in the more complex 3D non-rigid motion of the heart within the thoracic cavity. Finally, we will briefly discuss emerging deep learning super resolution CMRA reconstruction frameworks that could potentially enable 3D whole-heart CMRA with similar spatial resolution and acquisition time as CCTA.

It is possible to combine an undersampled 3D radial trajectory acquisition with 1D navigators (diaphragmatic or self-navigation) to allocate the acquired data into specific phases in the respiratory cycle (respiratory bins). Registration algorithms subsequently assess the motion between each bin and a reference end-expiratory bin. Images from all respiratory bins are then motion corrected to the common respiratory position and averaged to produce a respiratory motion corrected image. This methodology allows for 100% respiratory scan efficiency with a drastically shorter acquisition time in comparison to respiratory gating alone with similar image quality (**Figure 3**) (22, 40, 41, 53). Respiratory resolved frameworks have been proposed to further reduce the multidirectional non-rigid motion related artefacts (**Figure 4**) (54), displaying substantial enhancement in vessel length depiction as well as vessel sharpness in comparison to 1D self-navigation frameworks. This approach has been extended to cardiac phases (so called "5D whole-heart") from free-running frameworks (**Figures 5**, **6**) (21, 55–57). However, lower signal to noise ratio and prolonged reconstruction time (with compressed sensing) are associated with radial sampling. Spiral trajectory k-space CMRA acquisitions have been proposed to improve scan efficiency, the signal to noise ratio and reduce undersampling artefacts by oversampling near the k-space origin (58–60).

FIGURE 7 | Reformatted coronary lumen images for gated, TC+GMD, TC, and NMC for subjects 1–4. Blurring present in the NMC images is reduced with TC, and sharpness is further increased with TC+GMD (magnified boxes). The distal part of both coronaries is particularly affected by motion (arrows). Note that TC and TC+GMD have image quality similar to that for gated. GMD, general matrix description; TC, translational correction; TC+GMD, two-step translational and non-rigid correction; NMC, non–motion-corrected. Adapted with permission from Cruz et al. (62).

An alternative approach is a golden-step Cartesian trajectory with spiral profile ordering k-space acquisition, which can be combined with iNAVs to enable respiratory binning as described above (61). Using the binned data, it is possible to estimate and subsequently reconstruct the 3D non-rigid respiratory motion by combining beat-to-beat 2D translational and bin-to-bin 3D non-rigid motion correction to a common reference position (**Figure 7**) (62). This approach can increase the signal to noise ratio compared with radial sampling, whilst also improving image quality compared with 2D rigid translational motion correction frameworks. To shorten acquisition times and therefore enable higher spatial resolutions, Bustin et al. (63) adapted a highly undersampled patch-based CMR reconstruction framework (64) to propose a 3D patch-based low-rank (PROST) reconstruction, enabling <1 mm^3 spatial-resolution free-breathing whole-heart 3D CMRA with <10 min

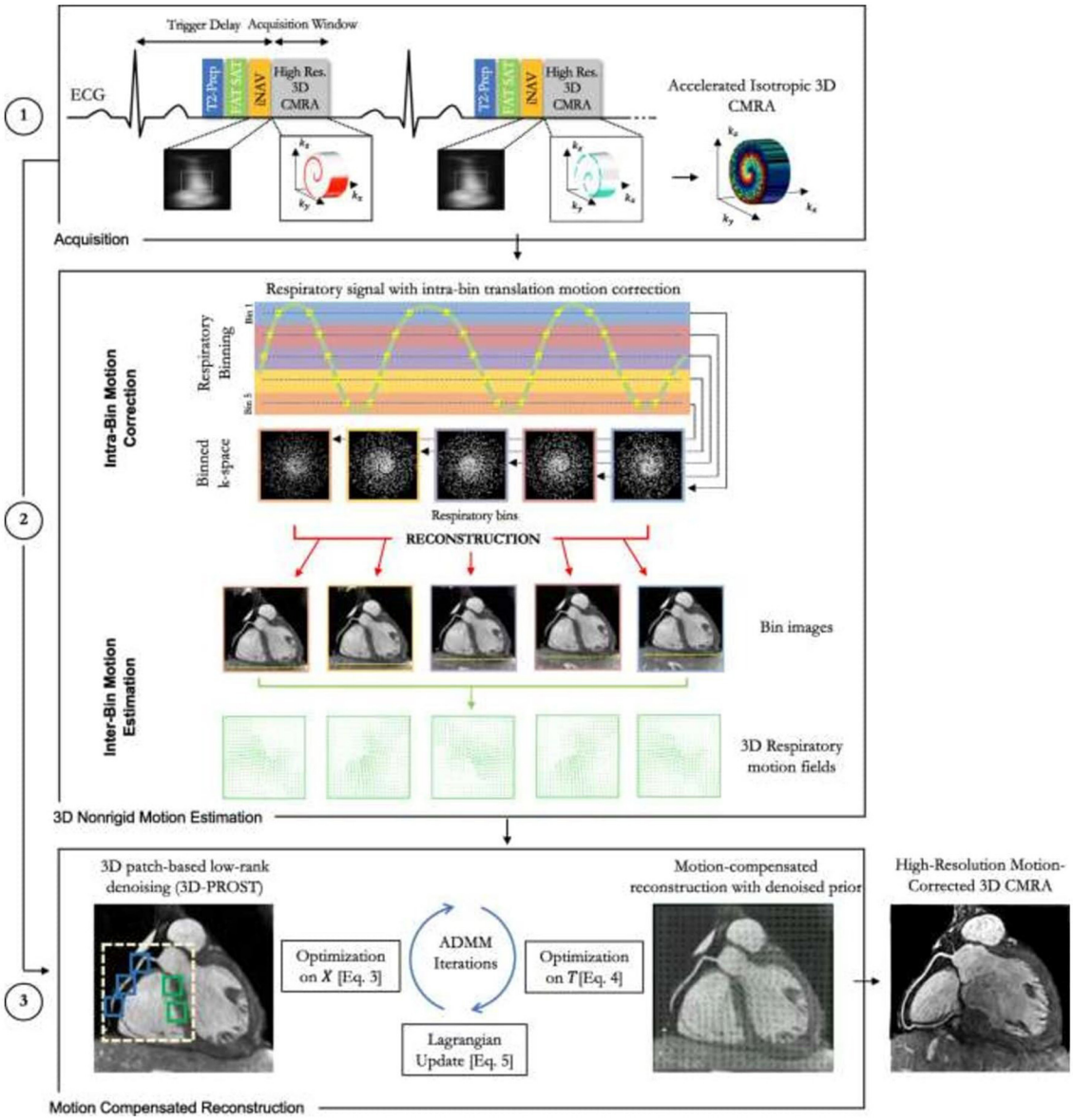

FIGURE 8 | Schematic overview of the accelerated free-breathing 3D CMRA acquisition with sub-millimeter isotropic resolution, 100% scan efficiency and non-rigid motion-compensated PROST reconstruction. (**1**) CMRA acquisition is performed with an undersampled 3D variable density spiral-like Cartesian trajectory with golden angle between spiral-like interleaves (VD-CASPR), preceded by 2D image navigators (iNAV) to allow for 100% scan efficiency and beat-to-beat translational respiratory-induced motion correction of the heart. (**2**) Foot-head respiratory signal is estimated from the 2D iNAVs and used to assign the acquired data into five respiratory bins and translation-corrected respiratory bins. Subsequent reconstruction of each bin is performed using soft-gated SENSE and 3D non-rigid motion fields are then estimated from the five reconstructed datasets. (**3**) The final 3D whole-heart motion-corrected CMRA image is obtained using the proposed 3D PROST non-rigid motion-compensated reconstruction. CMRA, coronary magnetic resonance angiography; PROST, patch-based undersampled reconstruction; ADMM, alternating direction method of multipliers. Adapted with permission from Bustin et al. (65).

predictable acquisition time with 100% scan efficiency. In a validation cohort of healthy subjects, image quality was comparable to the fully sampled acquisition and significantly improved compared to both iterative SENSE and compressed sensing reconstruction methods. This framework has been extended to include bin-to-bin non-rigid respiratory motion correction and has been compared against CCTA in patients with suspected CAD (**Figures 8**, **9**) (65). In a single centre study of 50 patients, this CMRA technique obtained diagnostic image quality in 95, 97, 97, and 90% of all, proximal, middle and distal coronary segments, respectively. Furthermore, 100, 97, 96, and 87% of left main stem, right coronary artery, left anterior descending and left circumflex artery segments, respectively on CMRA were of diagnostic image quality (**Figure 10**) (66). The sensitivity,

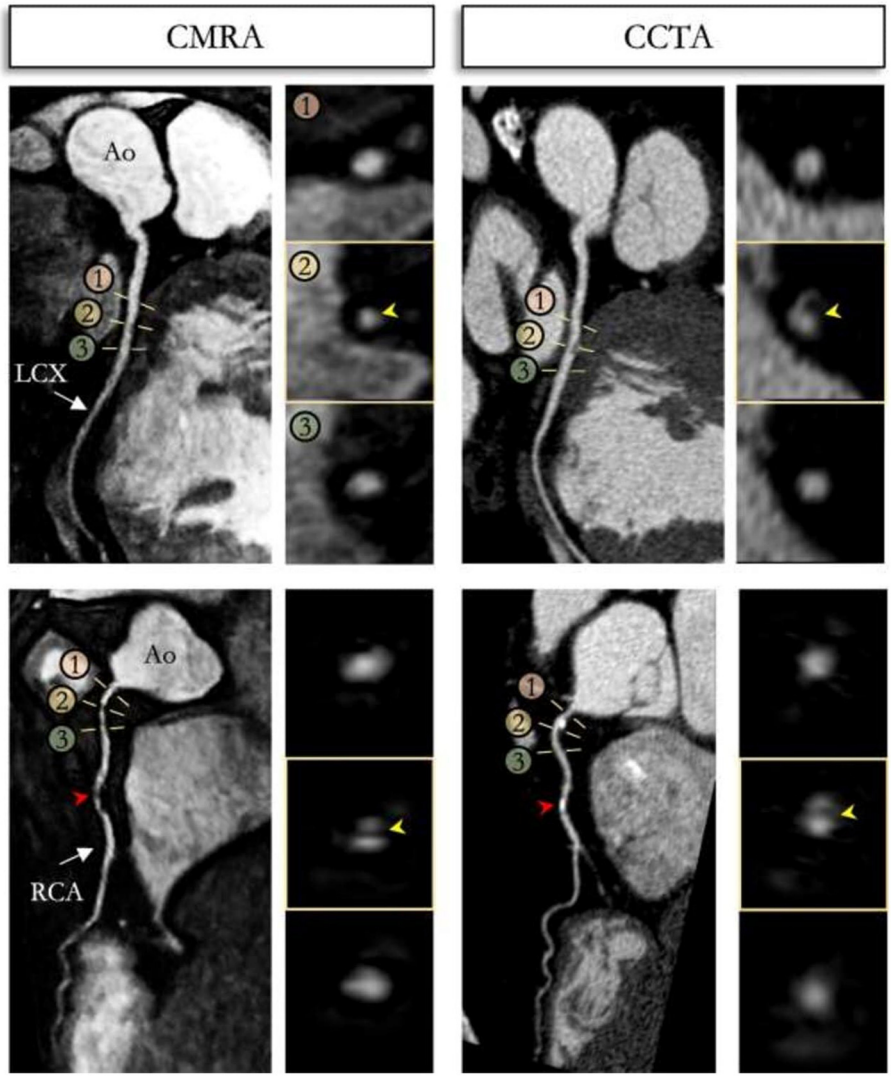

FIGURE 9 | Reformatted non-contrast whole-heart sub-millimeter isotropic CMRA (left) and CCTA (right) images along the LCX (top) and RCA (bottom) are shown for a 54 year-old male patient. The CMRA dataset was acquired in 9 min with 100% scan efficiency (heart rate of 57 bpm). The CCTA images demonstrate mild (25–49%) disease with a calcified plaque within the proximal RCA and severe disease (70–90%) with a partially calcified plaque in the mid-segment of RCA (red arrows), and minimal (0–24%) disease with calcified plaque in the mid-segment of the LCX. Luminal narrowing is seen on the cross-sectional views at the sites of coronary plaque on the CMRA images (yellow arrows). LAD, left anterior descending artery; RCA, right coronary artery; LCX, left circumflex artery; Ao, aorta. Adapted with permission from Bustin et al. (65).

specificity, positive predictive value, negative predictive value and diagnostic accuracy were as follows: per patient (100, 74, 55, 100, and 80%), per vessel (81, 88, 46, 97, and 88%) and per segment (76, 95, 44, 99, and 94%), respectively, with an average acquisition time of 10.7 min at 0.9 mm isotropic spatial resolution (66).

Whilst an acquisition time of ∼10 min for sub-1 mm isotropic spatial resolution is clinically feasible, it is nevertheless considerably longer than a full CCTA scan (even when coronary artery calcium scoring and contrast enhanced coronary angiography are combined). It is particularly disadvantageous if image quality is sub-optimal on first attempt and repeat imaging within the same scan session is required. Furthermore, reconstruction times of iterative methods are relatively long and computationally demanding, especially if combined with non-rigid motion correction or non-Cartesian trajectories. Finally, highly undersampled acquisitions are vulnerable to residual aliasing or staircasing and blurring artefacts, putting a realistic limit on the extend of conventional image acceleration methods. Recently, deep-learning based image reconstruction networks have been proposed to address some of these shortcomings (67–71). The deep neural network scheme is trained to recognise prior reconstructed data samples retrospectively, which is then adapted to prospectively reconstruct acquired images in a matter of seconds (**Figure 11**) (72). However, whilst this scheme partially

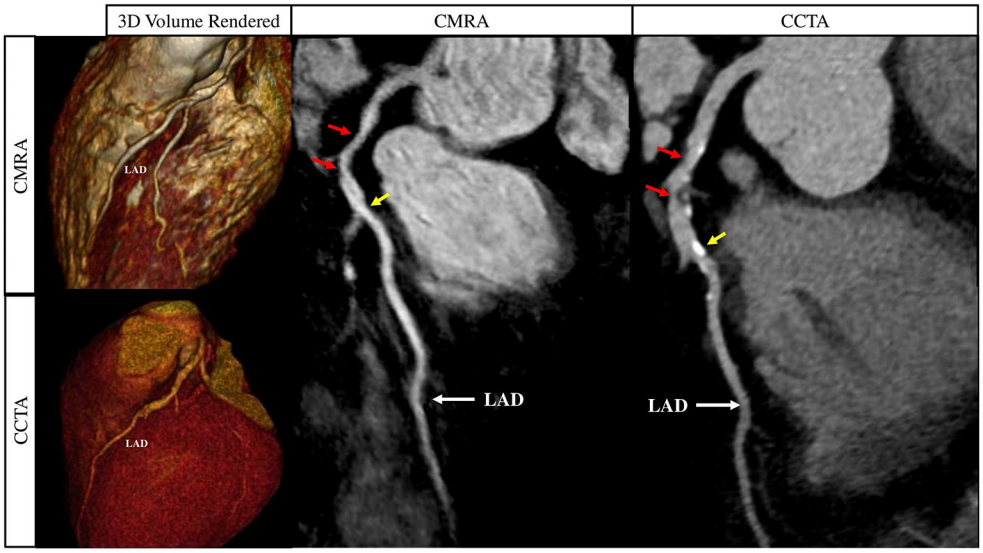

FIGURE 10 | Curved multiplanar reformat and 3D volume rendered non-contrast CMRA and contrast enhanced CCTA in a 60 year old male with >50% partially calcified stenosis in the proximal to mid LAD on either side of the first diagonal artery (red arrows). The yellow arrows represent a focal calcified <50% stenosis just distal to the second diagonal artery. CMRA, Coronary Magnetic Resonance Angiography; CCTA, Coronary Computed Tomography Angiography; LAD, Left Anterior Descending Artery. Adapted with permission from Hajhosseiny et al. (66).

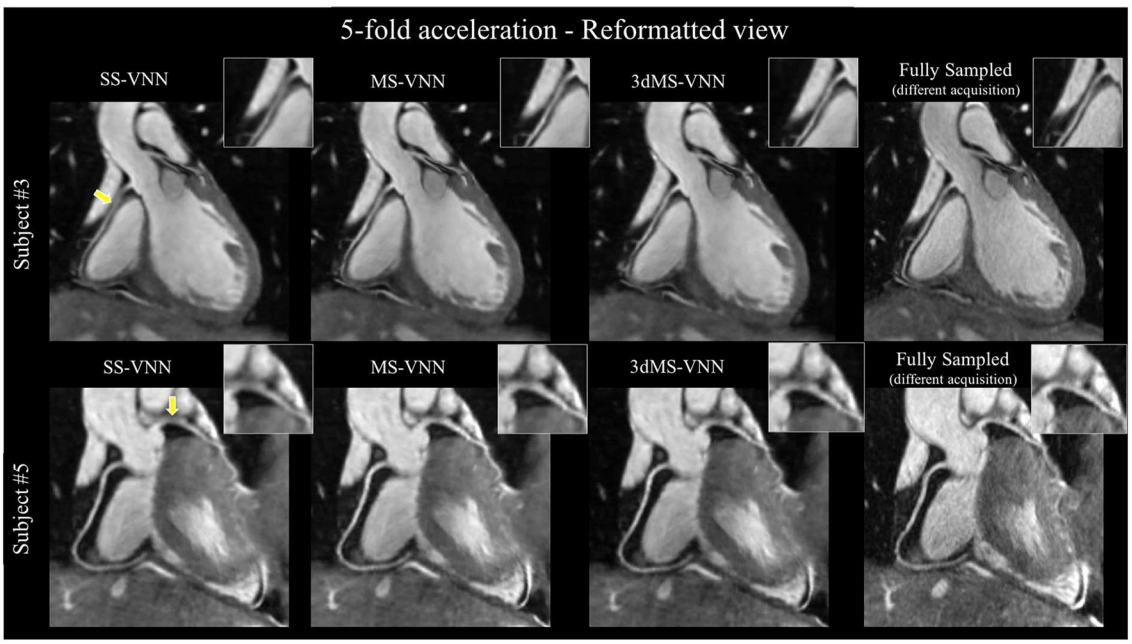

FIGURE 11 | CMRA images reconstructed with a single-scale VNN (SS-VNN), the multi-scale VNN (MS-VNN), and a pseudo 3D multi-scale VNN (3dMS-VNN). CMRA images were reformatted along the left (LAD) and right (RCA) coronary arteries, for two representative healthy subjects. Fully sampled and undersampled acquisitions with acceleration factor of 5× are shown. VNN, variational neural network. Adapted with permission from Fuin et al. (72).

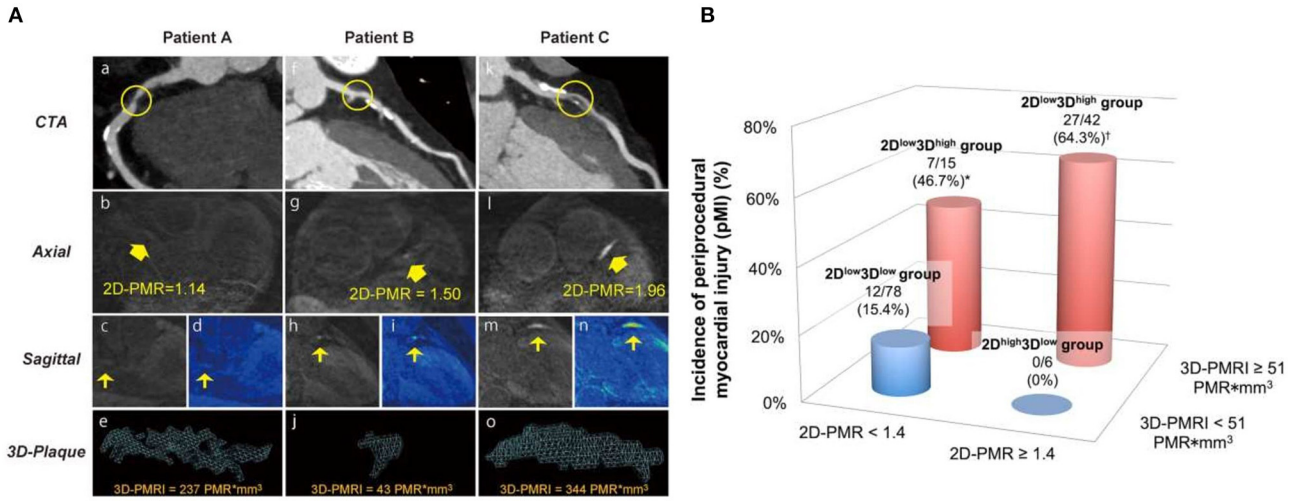

FIGURE 12 | (A) Representative 2-dimensional and 3-dimensional plaque assessment on T1-weighted imaging. Coronary plaques with $2D^{low}3D^{high}$ in the proximal right coronary artery (2D-PMR, 1.14; 3Di-PMR, 237 PMR*mm^3; Patient A: a–e), $2D^{high}3D^{low}$ in the proximal left anterior descending artery (LAD) (2D-PMR, 1.50; 3Di-PMR, 43 PMR*mm^3; Patient B: f–j), and $2D^{high}3D^{high}$ in the proximal LAD (2D-PMR, 1.96; 3Di-PMR, 344 PMR*mm^3; Patient C: k–o). Computed tomography angiography (CTA) images (a, f, k), and axial images (b, g, l), sagittal images (c, h, m), colour maps (d, l, n), and 3D region of interests (3D plaque: e, j, n) on T1w images are shown. Yellow circles indicate percutaneous coronary intervention target lesion sites on CTA. Yellow arrows indicate lesions on T1w imaging corresponding to a lesion on angiography that underwent intervention. **(B)** Incidence of periprocedural myocardial injury (pMI) based on 3Di-PMR and 2D-PMR cutoff values. The red and blue bars represent patients with 3Di-PMR $\geq$ 51 PMR*mm^3 and $<$ 51 PMR*mm^3, respectively. $P < 0.001$ based on the chi-squared test. *$P = 0.006$ vs. $2D^{high}3D^{low}$ group. $^{\dagger}P < 0.001$ vs. $2D^{low}3D^{low}$ group, and $P = 0.003$ vs. $2D^{high}3D^{low}$group. Adapted with permission from Hosoda et al. (90).

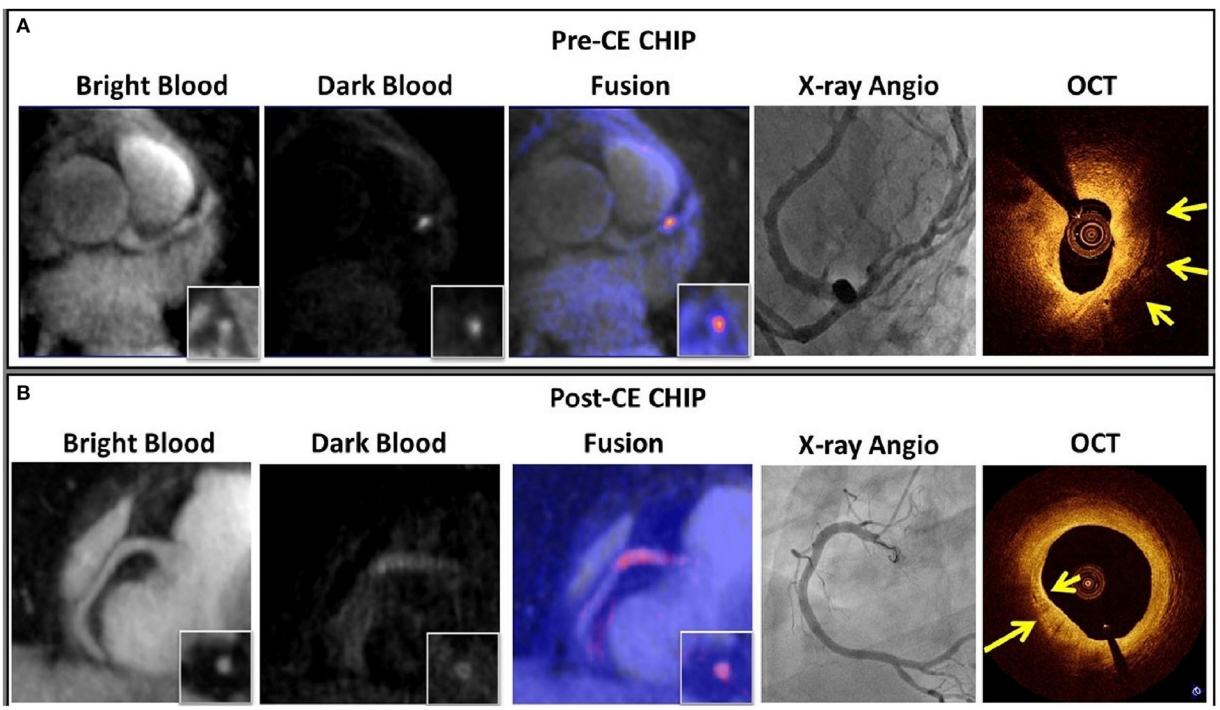

FIGURE 13 | (A) An example of pre-CE CHIP was found in the middle LAD visualised on the dark blood images and fused with the bright-blood scan. XA showed significant stenosis (70%) at that location. OCT showed large signal-poor area suggestive of possible lipid core and/or intra-plaque haemorrhage (yellow arrow). **(B)** An example of post-CE CHIP with diffuse wall enhancement at proximal RCA as localized on the bright-blood images. XA showed only mild stenosis (30%) at that location. OCT showed strong multi-focal back reflections and signal heterogeneity within the overlaying tissue suggestive of high macrophage density (yellow arrows). CE, contrast enhancement; CHIP, coronary hyper-intensive plaques; XA, X-ray angiography; OCT, optical coherence tomography. Adapted with permission from Xie et al. (96).

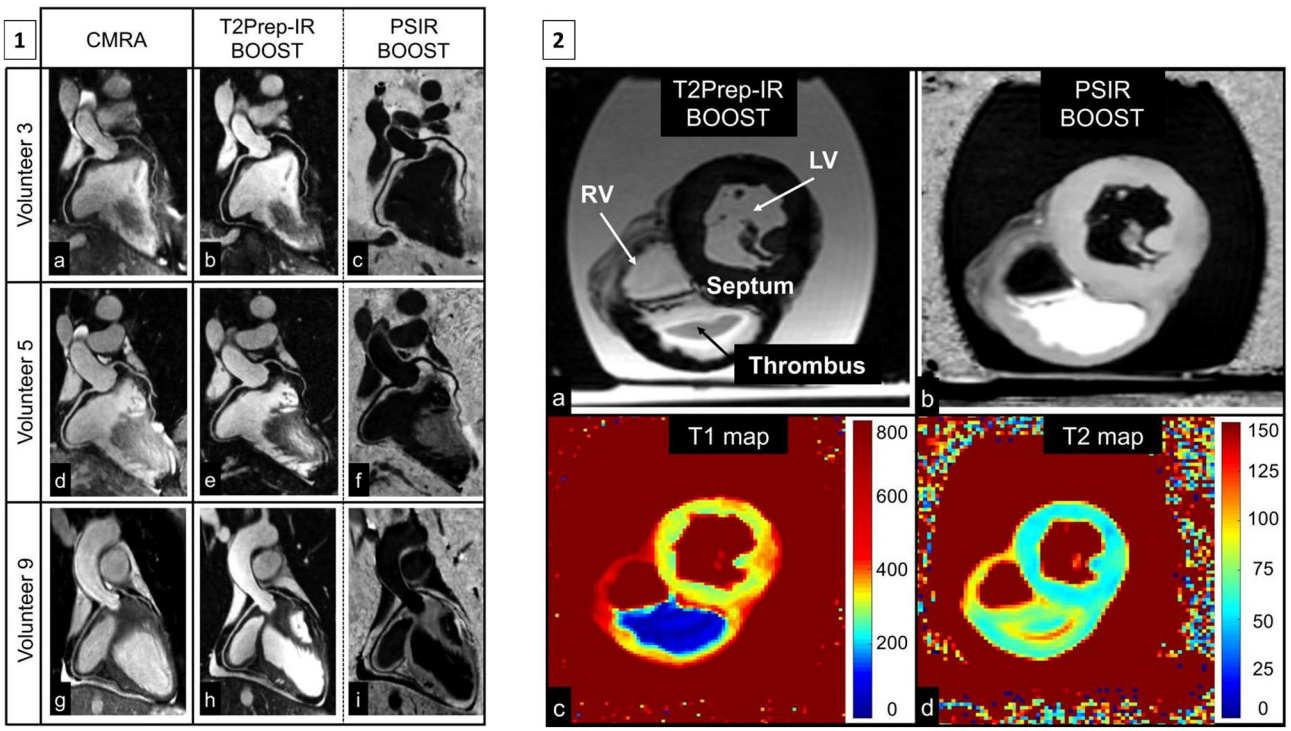

FIGURE 14 | (**1**) Reformatted coronary depiction in three representative healthy volunteers obtained with a conventional T_2-prepared bright-blood CMRA acquisition (a, d, g) and the proposed BOOST sequence for simultaneous bright-blood (T_2Prep-IR BOOST datasets in b, e, h) and black-blood (PSIR BOOST datasets in c, f, i) whole-heart MRI. Quantified $CNR_{blood-myo}$ significantly improved with the proposed T_2Prep-IR BOOST approach in comparison to the conventional CMRA, thus leading to a higher quantified coronary percentage vessel sharpness (%VS) for both right and left coronary arteries. In the PSIR BOOST images in (c, f, i), the efficacy of blood signal suppression can be appreciated along multiple portions of the coronary tree. (**2**) MRI images obtained in the *ex vivo* pig heart. All the images depict a short-axis view at the midventricular level. Images acquired with the proposed BOOST sequence are reported in (a) (bright-blood T_2Prep-IR dataset) and in (b) (black-blood PSIR-like reconstruction). RV, LV, thrombus, and interventricular septum are indicated. The black-blood reconstruction (b) clearly enhances the signal from the thrombus when compared to the bright-blood dataset (a). Furthermore, 2D T_1 (c) and T_2 (d) mapping techniques were acquired. The *ex vivo* thrombus is characterized by a relatively short T_1 and T_2. BOOST, Bright-blood and black-blOOd phase SensiTive; IR, inversion recovery; myo, myocardium; PSIR, phase-sensitive inversion recovery; T_2Prep, T_2 prepared; LV, left ventricular cavity; RV, right ventricular cavity. Adapted with permission from Ginami et al. (98).

resolves the time-consuming image reconstruction process, it still relies on a prospectively acquired high spatial resolution CMRA acquisition. Recently, deep learning based super resolution schemes have been proposed to overcome this drawback. Here, a low spatial resolution image is prospectively acquired, often with low to intermediate acceleration factors, thereby significantly shortening the time the patient is on the scanning table, whilst simultaneously employing trained deep neural networks to reconstruct to a higher target spatial resolution within a few seconds (73–82). These novel deep learning schemes have the potential to finally unlock the true potential of CMRA in the clinical setting, which require further prospective clinical validation against CCTA and invasive X-ray angiography.

MAGNETIC RESONANCE CORONARY PLAQUE IMAGING

Our understanding of CAD and CCS is rapidly evolving. The COURAGE trial highlighted the limitations of coronary luminography as a standalone prognostic measure of CAD, with no significant difference in revascularisation vs. best medical therapy on hard end point outcomes such as death or myocardial infarction in patients that were angiographically identified to have significant CAD (83). The FAME trials brought into sharp focus the prognostic benefits of functional physiological assessment of CAD, demonstrating supplementary benefits in terms of death, myocardial infarction and urgent revascularisation when coronary intervention was based on functional assessment with FFR compared with invasive angiography alone or medical therapy alone (7, 84). However, in the recently published ISCHEMIA trial of 5,179 patients with CCS, there was no prognostic or indeed symptomatic benefit of functionally guided revascularisation vs. medical therapy alone after 4 years of follow up, although patients with left main stenosis were excluded from this study (85). Therefore, academic focus is on finding a more specific marker in patients with CCS who are more likely to have a prognostically worse clinical outcome (86–88). Identification of high-risk coronary plaques by CMR has been shown to be an independent and prognostically significant marker of CAD in patients with CCS, in addition to or indeed regardless of coronary luminal stenosis

(89). It has also recently been shown to predict periprocedural myocardial injury (**Figure 12**) (90). CMR has the capability to detect vulnerable coronary plaques by taking advantage of the intrinsic T1 shortening of plaque components (e.g., intraplaque haemorrhage, thrombus, and lipid core), both with and without the need for contrast agents (91–95).

Despite this, MR coronary plaque imaging is constrained by comparable technical challenges to CMRA, e.g., respiratory motion, prohibitively long and unpredictable acquisition time, plaque to coronary artery misalignment due to the sequential nature of data acquisition. Recently, a novel framework (CATCH) has been proposed to overcome some of these limitations for MR coronary plaque imaging. This framework assembles advanced motion correction techniques outlined above to facilitate simultaneous multi contrast bright and black blood coronary artery angiography and visualisation of vulnerable coronary plaque (**Figure 13**) (96, 97). However, there is incomplete overlap of respiratory motion parameters between the bright-blood and black-blood datasets, potentially resulting in residual coronary plaque-misregistration. More recently, another framework has been proposed (BOOST) for simultaneous coronary angiography and thrombus/intraplaque haemorrhage visualisation (**Figure 14**) (98). This framework works by acquiring two differently weighted bright-blood datasets in alternate heart beats, which are subsequently processed in a phase-sensitive inversion recovery (PSIR)-like reconstruction to produce a third, black-blood dataset. The two bright-blood datasets enable respiratory motion to be independently estimated and corrected, which reduces the likelihood of misregistration artefacts. It also uses the iNAV technology with a highly undersampled golden angle Cartesian acquisition, which enables 100% respiratory scan efficiency, 2D rigid translational motion correction as well as 3D non-rigid motion estimation. Traditional reconstruction frameworks (e.g., iterative sense, compressed sensing or low rank patched based frameworks) or deep learning neural network reconstruction can be applied. These frameworks require further extensive clinical validation, ideally against intravascular imaging modalities such as intravascular ultrasound or optical coherence tomography.

It is also possible to directly target specific components of the atherosclerotic plaque (99–101). Various MR specific contrast agents are currently in development which can target molecular components that are involved in atherosclerotic plaque initiation, progression, instability and plaque rupture, such as elastin (102), tropoelastin, collagen (103, 104), fibrin (105), and matrix metalloproteinases (106). Whilst these frameworks have shown great promise in pre-clinical feasibility studies, the challenge is to safely replicate these findings in clinical validation studies.

CONCLUSIONS

Chronic coronary syndrome is a progressive and multifaceted condition associated with coronary artery atherosclerosis, which manifests clinically as either angina, heart failure and gradual left ventricular dysfunction, arrhythmia and/or acute myocardial infarction. The timely recognition of CCS enables bespoke risk assessment of patients, prompt initiation of therapeutical intervention and long-term monitoring of potential complications. Amongst a maelstrom of diagnostic imaging modalities for CAD, CMRA could potentially emerge as a viable, versatile, reproducible and non-invasive imaging modality for the assessment of CCS, which is free of ionising radiation, iodinated contrast agents and can be performed without gadolinium contrast enhancement. These characteristics would be ideally suited for repeat imaging of patients to monitor disease progression and gauge response to treatment. Furthermore, it can be combined with myocardial volumetric assessment, tissue characterisation, perfusion and coronary plaque assessment to enable comprehensive assessment of ischaemic heart disease.

AUTHOR CONTRIBUTIONS

RH drafting and editing of the manuscript. CM, GC, RK, WK, CP, and RB reviewing and editing of manuscript. All authors contributed to the article and approved the submitted version.

FUNDING

This work was supported by the following grants: (1) EPSRC EP/P032311/1, EP/P001009/1, and EP/P007619/1, (2) BHF programme grant RG/20/1/34802, (3) King's BHF Centre for Research Excellence RE/18/2/34213, (4) Wellcome EPSRC Centre for Medical Engineering (NS/A000049/1), and (5) Department of Health through the National Institute for Health Research (NIHR) comprehensive Biomedical Research Centre award to Guy's & St Thomas' NHS Foundation Trust in partnership with King's College London and King's College Hospital NHS Foundation Trust and by the NIHR MedTech Co-operative for Cardiovascular Disease at Guy's and St Thomas' NHS Foundation Trust.

REFERENCES

1. Virani SS, Alonso A, Benjamin EJ, Bittencourt MS, Callaway CW, Carson AP, et al. Heart disease and stroke statistics-−2020 update: a report from the American Heart Association. *Circulation.* (2020) 141:e33. doi: 10.1161/CIR.0000000000000746
2. Institute for Health Metrics and Evaluation (IHME). *GBD Compare*. Available online at: https://vizhub.healthdata.org/gbd-compare/ (accessed June 6, 2021).
3. Benjamin EJ, Virani SS, Callaway CW, Chamberlain AM, Chang AR, Cheng S, et al. Heart disease and stroke statistics-2018 update: a report from the American Heart Association. *Circulation.* (2018) 137:e67–492. doi: 10.1161/CIR.0000000000000573
4. Libby P. Current concepts of the pathogenesis of the acute coronary syndromes. *Circulation.* (2001) 104:365–72. doi: 10.1161/01.CIR.104.3.365
5. Ross R. The pathogenesis of atherosclerosis: a perspective for the 1990s. *Nature.* (1993) 362:801–9. doi: 10.1038/362801a0
6. Neumann FJ, Sechtem U, Banning AP, Bonaros N, Bueno H, Bugiardini R, et al. 2019 ESC Guidelines for the diagnosis and

management of chronic coronary syndromes. *Eur Heart J.* (2020) 41:407–77. doi: 10.1093/eurheartj/ehz425
7. De Bruyne B, Pijls NHJ, Kalesan B, Barbato E, Tonino PAL, Piroth Z, et al. Fractional flow reserve–guided PCI versus medical therapy in stable coronary disease. *N Engl J Med.* (2012) 367:991–1001. doi: 10.1056/NEJMoa1205361
8. Götberg M, Christiansen EH, Gudmundsdottir IJ, Sandhall L, Danielewicz M, Jakobsen L, et al. Instantaneous wave-free ratio versus fractional flow reserve to guide PCI. *N Engl J Med.* (2017) 376:1813–23. doi: 10.1056/NEJMoa1616540
9. Rathod KS, Hamshere SM, Jones DA, Mathur A. Intravascular ultrasound versus optical coherence tomography for coronary artery imaging – apples and oranges? *Interv Cardiol Rev.* (2015) 10:8–15. doi: 10.15420/icr.2015.10.1.8
10. Tian J, Dauerman H, Toma C, Samady H, Itoh T, Kuramitsu S, et al. Prevalence and characteristics of TCFA and degree of coronary artery stenosis. *J Am Coll Cardiol.* (2014) 64:672–80. doi: 10.1016/j.jacc.2014.05.052
11. Arakelyan K, Cantow K, Hentschel J, Flemming B, Pohlmann A, Ladwig M, et al. Early effects of an x-ray contrast medium on renal T(2) *T(2) MRI as compared to short-term hyperoxia, hypoxia and aortic occlusion in rats. *Acta Physiol.* (2013) 208:202–13. doi: 10.1111/apha.12094
12. Kolossváry M, Szilveszter B, Merkely B, Maurovich-Horvat P. Plaque imaging with CT-a comprehensive review on coronary CT angiography based risk assessment. *Cardiovasc Diagn Ther.* (2017) 7:489–506. doi: 10.21037/cdt.2016.11.06
13. *Non invasive Coronary Imaging With Computed Tomography*. Available online at: https://www.escardio.org/Journals/E-Journal-of-Cardiology-Practice/Volume-5/Non-Invasive-Coronary-Imaging-With-Computed-Tomography-Title-Non-Invasive-Cor (accessed August 14, 2018).
14. Alfakih K, Byrne J, Monaghan M. CT coronary angiography: a paradigm shift for functional imaging tests. *Open Hear.* (2018) 5:e000754. doi: 10.1136/openhrt-2017-000754
15. Doris MK, Newby DE. How should CT coronary angiography be integrated into the management of patients with chest pain and how does this affect outcomes? *Eur Hear J Qual Care Clin Outcomes.* (2016) 2:72–80. doi: 10.1093/ehjqcco/qcv027
16. Kim WY, Danias PG, Stuber M, Flamm SD, Plein S, Nagel E, et al. Coronary magnetic resonance angiography for the detection of coronary stenoses. *N Engl J Med.* (2001) 345:1863–69. doi: 10.1056/NEJMoa010866
17. Kato S, Kitagawa K, Ishida N, Ishida M, Nagata M, Ichikawa Y, et al. Assessment of coronary artery disease using magnetic resonance coronary angiography: a national multicenter trial. *J Am Coll Cardiol.* (2010) 56:983–91. doi: 10.1016/j.jacc.2010.01.071
18. Hamdan A, Asbach P, Wellnhofer E, Klein C, Gebker R, Kelle S, et al. A prospective study for comparison of MR and CT imaging for detection of coronary artery stenosis. *JACC Cardiovasc Imaging.* (2011) 4:50–61. doi: 10.1016/j.jcmg.2010.10.007
19. Hamdan A, Doltra A, Huppertz A, Wellnhofer E, Fleck E, Kelle S. Comparison of coronary magnetic resonance and computed tomography angiography for prediction of cardiovascular events. *JACC Cardiovasc Imaging.* (2014) 7:1063–65. doi: 10.1016/j.jcmg.2014.03.020
20. Yoon YE, Kitagawa K, Kato S, Ishida M, Nakajima H, Kurita T, et al. Prognostic value of coronary magnetic resonance angiography for prediction of cardiac events in patients with suspected coronary artery disease. *J Am Coll Cardiol.* (2012) 60:2316–22. doi: 10.1016/j.jacc.2012.07.060
21. Coppo S, Piccini D, Bonanno G, Chaptinel J, Vincenti G, Feliciano H, et al. Free-running 4D whole-heart self-navigated golden angle MRI: initial results. *Magn Reson Med.* (2015) 74:1306–16. doi: 10.1002/mrm.25523
22. Pang J, Bhat H, Sharif B, Fan Z, Thomson LEJ, LaBounty T, et al. Whole-heart coronary MRA with 100% respiratory gating efficiency: self-navigated three-dimensional retrospective image-based motion correction (TRIM). *Magn Reson Med.* (2014) 71:67–74. doi: 10.1002/mrm.24628
23. Atkinson DJ, Edelman RR. Cineangiography of the heart in a single breath hold with a segmented turboFLASH sequence. *Radiology.* (1991) 178:357–60. doi: 10.1148/radiology.178.2.1987592
24. Edelman RR, Manning WJ, Burstein D, Paulin S. Coronary arteries: breath-hold MR angiography. *Radiology.* (1991) 181:641–3. doi: 10.1148/radiology.181.3.1947074
25. Meyer CH, Hu BS, Nishimura DG, Macovski A. Fast spiral coronary artery imaging. *Magn Reson Med.* (1992) 28:202–13. doi: 10.1002/mrm.1910280204
26. Manning WJ, Li W, Edelman RR. A preliminary report comparing magnetic resonance coronary angiography with conventional angiography. *N Engl J Med.* (1993) 328:828–32. doi: 10.1056/NEJM199303253281202
27. Wielopolski PA, van Geuns RJ, de Feyter PJ, Oudkerk M. Breath-hold coronary MR angiography with volume-targeted imaging. *Radiology.* (1998) 209:209–19. doi: 10.1148/radiology.209.1.9769834
28. Li D, Carr JC, Shea SM, Zheng J, Deshpande VS, Wielopolski PA, et al. Coronary arteries: magnetization-prepared contrast-enhanced three-dimensional volume-targeted breath-hold MR angiography. *Radiology.* (2001) 219:270–7. doi: 10.1148/radiology.219.1.r01ap37270
29. Niendorf T, Hardy CJ, Giaquinto RO, Gross P, Cline HE, Zhu Y, et al. Toward single breath-hold whole-heart coverage coronary MRA using highly accelerated parallel imaging with a 32-channel MR system. *Magn Reson Med.* (2006) 56:167–76. doi: 10.1002/mrm.20923
30. Li D, Kaushikkar S, Haacke EM, Woodard PK, Dhawale PJ, Kroeker RM, et al. Coronary arteries: three-dimensional MR imaging with retrospective respiratory gating. *Radiology.* (1996) 201:857–63. doi: 10.1148/radiology.201.3.8939242
31. Danias PG, Stuber M, Botnar RM, Kissinger K V, Chuang ML, Manning WJ. Navigator assessment of breath-hold duration: impact of supplemental oxygen and hyperventilation. *Am J Roentgenol.* (1998) 171:395–7. doi: 10.2214/ajr.171.2.9694460
32. Botnar RM, Stuber M, Danias PG, Kissinger K V, Manning WJ. Improved coronary artery definition with T2-weighted, free-breathing, three-dimensional coronary MRA. *Circulation.* (1999) 99:3139–48. doi: 10.1161/01.CIR.99.24.3139
33. Runge VM, Clanton JA, Partain CL, James AE. Respiratory gating in magnetic resonance imaging at 0.5 Tesla. *Radiology.* (1984) 151:521–3. doi: 10.1148/radiology.151.2.6709928
34. Felblinger J, Boesch C. Amplitude demodulation of the electrocardiogram signal (ECG) for respiration monitoring and compensation during MR examinations. *Magn Reson Med.* (1997) 38:129–36. doi: 10.1002/mrm.1910380118
35. Ehman RL, Felmlee JP. Adaptive technique for high-definition MR imaging of moving structures. *Radiology.* (1989) 173:255–63. doi: 10.1148/radiology.173.1.2781017
36. McConnell M V, Khasgiwala VC, Savord BJ, Chen MH, Chuang ML, Edelman RR, et al. Comparison of respiratory suppression methods and navigator locations for MR coronary angiography. *Am J Roentgenol.* (1997) 168:1369–75. doi: 10.2214/ajr.168.5.9129447
37. Nehrke K, Börnert P, Manke D, Böck JC. Free-breathing cardiac MR imaging: study of implications of respiratory motion—initial results. *Radiology.* (2001) 220:810–5. doi: 10.1148/radiol.2203010132
38. Wang Y, Riederer SJ, Ehman RL. Respiratory motion of the heart: kinematics and the implications for the spatial resolution in coronary imaging. *Magn Reson Med.* (1995) 33:713–9. doi: 10.1002/mrm.1910330517
39. Nagel E, Bornstedt A, Schnackenburg B, Hug J, Oswald H, Fleck E. Optimization of realtime adaptive navigator correction for 3D magnetic resonance coronary angiography. *Magn Reson Med.* (1999) 42:408–11.
40. Stehning C, Börnert P, Nehrke K, Eggers H, Stuber M. Free-breathing whole-heart coronary MRA with 3D radial SSFP and self-navigated image reconstruction. *Magn Reson Med.* (2005) 54:476–80. doi: 10.1002/mrm.20557
41. Piccini D, Littmann A, Nielles-Vallespin S, Zenge MO. Respiratory self-navigation for whole-heart bright-blood coronary MRI: methods for robust isolation and automatic segmentation of the blood pool. *Magn Reson Med.* (2012) 68:571–9. doi: 10.1002/mrm.23247
42. Lai P, Bi X, Jerecic R, Li D. A respiratory self-gating technique with 3D-translation compensation for free-breathing whole-heart coronary MRA. *Magn Reson Med.* (2009) 62:731–8. doi: 10.1002/mrm.22058
43. Jhooti P, Gatehouse PD, Keegan J, Bunce NH, Taylor AM, Firmin DN. Phase ordering with automatic window selection (PAWS): a novel motion- resistant technique for 3D coronary imaging. *Magn Reson Med.* (2000) 43:470–80. doi: 10.1002/(SICI)1522-2594(200003)43:3<470::AID-MRM20>3.0.CO;2-U

44. Keegan J, Jhooti P, Babu-Narayan S V., Drivas P, Ernst S, Firmin DN. Improved respiratory efficiency of 3D late gadolinium enhancement imaging using the continuously adaptive windowing strategy (CLAWS). *Magn Reson Med.* (2014) 71:1064–74. doi: 10.1002/mrm.24758
45. Jhooti P, Wiesmann F, Taylor AM, Gatehouse PD, Yang GZ, Keegan J, et al. Hybrid ordered phase encoding (HOPE): an improved approach for respiratory artifact reduction. *J Magn Reson Imaging.* (1998) 8:968–80. doi: 10.1002/jmri.1880080428
46. Piccini D, Monney P, Sierro C, Coppo S, Bonanno G, van Heeswijk RB, et al. Respiratory self-navigated postcontrast whole-heart coronary MR angiography: initial experience in patients. *Radiology.* (2014) 270:378–86. doi: 10.1148/radiol.13132045
47. Henningsson M, Koken P, Stehning C, Razavi R, Prieto C, Botnar RM. Whole-heart coronary MR angiography with 2D self-navigated image reconstruction. *Magn Reson Med.* (2012) 67:437–45. doi: 10.1002/mrm.23027
48. Kawaji K, Spincemaille P, Nguyen TD, Thimmappa N, Cooper MA, Prince MR, et al. Direct coronary motion extraction from a 2D fat image navigator for prospectively gated coronary MR angiography. *Magn Reson Med.* (2014) 71:599–607. doi: 10.1002/mrm.24698
49. Scott AD, Keegan J, Firmin DN. Beat-to-beat respiratory motion correction with near 100% efficiency: a quantitative assessment using high-resolution coronary artery imaging. *Magn Reson Imaging.* (2011) 29:568–78. doi: 10.1016/j.mri.2010.11.004
50. Wu HH, Gurney PT, Hu BS, Nishimura DG, McConnell M V. Free-breathing multiphase whole-heart coronary MR angiography using image-based navigators and three-dimensional cones imaging. *Magn Reson Med.* (2013) 69:1083–93. doi: 10.1002/mrm.24346
51. Addy NO, Ingle RR, Luo J, Baron CA, Yang PC, Hu BS, Nishimura DG. 3D image-based navigators for coronary MR angiography. *Magn Reson Med.* (2017) 77:1874–83. doi: 10.1002/mrm.26269
52. Henningsson M, Shome J, Bratis K, Vieira MS, Nagel E, Botnar RM. Diagnostic performance of image navigated coronary CMR angiography in patients with coronary artery disease. *J Cardiovasc Magn Reson.* (2017) 19:68. doi: 10.1186/s12968-017-0381-3
53. Bhat H, Ge L, Nielles-Vallespin S, Zuehlsdorff S, Li D. 3D radial sampling and 3D affine transform-based respiratory motion correction technique for free-breathing whole-heart coronary MRA with 100% imaging efficiency. *Magn Reson Med.* (2011) 65:1269–77. doi: 10.1002/mrm.22717
54. Piccini D, Feng L, Bonanno G, Coppo S, Yerly J, Lim RP, et al. Four-dimensional respiratory motion-resolved whole heart coronary MR angiography. *Magn Reson Med.* (2017) 77:1473–84. doi: 10.1002/mrm.26221
55. Feng L, Coppo S, Piccini D, Yerly J, Lim RP, Masci PG, et al. 5D whole-heart sparse MRI. *Magn Reson Med.* (2018) 79:826–38. doi: 10.1002/mrm.26745
56. Pang J, Chen Y, Fan Z, Nguyen C, Yang Q, Xie Y, et al. High efficiency coronary MR angiography with nonrigid cardiac motion correction. *Magn Reson Med.* (2016) 76:1345–53. doi: 10.1002/mrm.26332
57. Di Sopra L, Piccini D, Coppo S, Stuber M, Yerly J. An automated approach to fully self-gated free-running cardiac and respiratory motion-resolved 5D whole-heart MRI. *Magn Reson Med.* (2019) 82:2118–32. doi: 10.1002/mrm.27898
58. Addy NO, Ingle RR, Wu HH, Hu BS, Nishimura DG. High-resolution variable-density 3D cones coronary MRA. *Magn Reson Med.* (2015) 74:614–21. doi: 10.1002/mrm.25803
59. Malavé MO, Baron CA, Addy NO, Cheng JY, Yang PC, Hu BS, et al. Whole-heart coronary MR angiography using a 3D cones phyllotaxis trajectory. *Magn Reson Med.* (2019) 81:1092–103. doi: 10.1002/mrm.27475
60. Malavé MO, Baron CA, Koundinyan SP, Sandino CM, Ong F, Cheng JY, et al. Reconstruction of undersampled 3D non-Cartesian image-based navigators for coronary MRA using an unrolled deep learning model. *Magn Reson Med.* (2020) 84:800–12. doi: 10.1002/mrm.28177
61. Prieto C, Doneva M, Usman M, Henningsson M, Greil G, Schaeffter T, et al. Highly efficient respiratory motion compensated free-breathing coronary mra using golden-step Cartesian acquisition. *J Magn Reson Imaging.* (2015) 41:738–46. doi: 10.1002/jmri.24602
62. Cruz G, Atkinson D, Henningsson M, Botnar RM, Prieto C. Highly efficient nonrigid motion-corrected 3D whole-heart coronary vessel wall imaging. *Magn Reson Med.* (2017) 77:1894–908. doi: 10.1002/mrm.26274
63. Bustin A, Ginami G, Cruz G, Correia T, Ismail TF, Rashid I, et al. Five-minute whole-heart coronary MRA with sub-millimeter isotropic resolution, 100% respiratory scan efficiency, and 3D-PROST reconstruction. *Magn Reson Med.* (2019) 81:102–15. doi: 10.1002/mrm.27354
64. Akçakaya M, Basha TA, Goddu B, Goepfert LA, Kissinger K V., Tarokh V, et al. Low-dimensional-structure self-learning and thresholding: regularization beyond compressed sensing for MRI reconstruction. *Magn Reson Med.* (2011) 66:756–67. doi: 10.1002/mrm.22841
65. Bustin A, Rashid I, Cruz G, Hajhosseiny R, Correia T, Neji R, et al. 3D whole-heart isotropic sub-millimeter resolution coronary magnetic resonance angiography with non-rigid motion-compensated PROST. *J Cardiovasc Magn Reson.* (2020) 22:24. doi: 10.1186/s12968-020-00611-5
66. Hajhosseiny R, Rashid I, Bustin A, Munoz C, Cruz G, Nazir MS, et al. Clinical comparison of sub-mm high-resolution non-contrast coronary CMR angiography against coronary CT angiography in patients with low-intermediate risk of coronary artery disease: a single center trial. *J Cardiovasc Magn Reson.* (2021) 23:57. doi: 10.1186/s12968-021-00758-9
67. Hyun CM, Kim HP, Lee SM, Lee S, Seo JK. Deep learning for undersampled MRI reconstruction. *Phys Med Biol.* (2018) 63:135007. doi: 10.1088/1361-6560/aac71a
68. Lin DJ, Johnson PM, Knoll F, Lui YW. Artificial intelligence for mr image reconstruction: an overview for clinicians. *J Magn Reson Imaging.* (2020) 53:1015–1028. doi: 10.1002/jmri.27078
69. Lundervold AS, Lundervold A. An overview of deep learning in medical imaging focusing on MRI. *Z Med Phys.* (2019) 29:102–27. doi: 10.1016/j.zemedi.2018.11.002
70. Hammernik K, Knoll F. Machine learning for image reconstruction. In: Zhou SK, Rueckert D, Fichtinger G, editors. *Handbook of Medical Image Computing and Computer Assisted Intervention*. London; San Diego, CA; Cambridge; Oxford: Elsevier (2020). p. 25–64.
71. Bustin A, Fuin N, Botnar RM, Prieto C. From compressed-sensing to artificial intelligence-based cardiac MRI reconstruction. *Front Cardiovasc Med.* (2020) 7:17. doi: 10.3389/fcvm.2020.00017
72. Fuin N, Bustin A, Küstner T, Oksuz I, Clough J, King AP, et al. A multi-scale variational neural network for accelerating motion-compensated whole-heart 3D coronary MR angiography. *Magn Reson Imaging.* (2020) 70:155–67. doi: 10.1016/j.mri.2020.04.007
73. Glasner D, Bagon S, Irani M. Super-resolution from a single image. In: *Proceedings of the IEEE International Conference on Computer Vision*. Kyoto (2009). p. 349–356.
74. Chen Y, Christodoulou AG, Zhou Z, Shi F, Xie Y, Li D. MRI super-resolution with GAN and 3D multi-level densenet: smaller, faster, and better. *arXiv*. (2020).
75. Shi J, Liu Q, Wang C, Zhang Q, Ying S, Xu H. Super-resolution reconstruction of MR image with a novel residual learning network algorithm. *Phys Med Biol.* (2018) 63:085011. doi: 10.1088/1361-6560/aab9e9
76. Pham C-H, Tor-Díez C, Meunier H, Bednarek N, Fablet R, Passat N, et al. Multiscale brain MRI super-resolution using deep 3D convolutional networks. *Comput Med Imaging Graph.* (2019) 77:101647. doi: 10.1016/j.compmedimag.2019.101647
77. Küstner T, Fuin N, Hammernik K, Bustin A, Qi H, Hajhosseiny R, et al. CINENet: deep learning-based 3D cardiac CINE MRI reconstruction with multi-coil complex-valued 4D spatio-temporal convolutions. *Sci Rep.* (2020) 10:13710. doi: 10.1038/s41598-020-70551-8
78. Steeden JA, Quail M, Gotschy A, Mortensen KH, Hauptmann A, Arridge S, et al. Rapid whole-heart CMR with single volume super-resolution. *J Cardiovasc Magn Reson.* (2020) 22:56. doi: 10.1186/s12968-020-00651-x
79. Xie Y, Lin R, Chen Y, Zhang Y, Shi F, Fei Y, et al. Super resolution {MRI} using 3D generative adversarial network: towards single breath-hold coronary {MR} angiography. In: *Proceedings of the Joint Annual Meeting ISMRM-ESMRMB.* Paris (2018).
80. Qi H, Cruz G, Kuestner T, Botner RM, Prieto C. Deep-learning based super-resolution reconstruction for sub-millimeter 3D isotropic coronary MR angiography in less than a minute. In: *SMRA Virtual Meeting.* (2020).
81. Küstner T, Fuin N, Bustin A, Qi H, Munoz C, Neji R, et al. Deep-learning based super-resolution reconstruction for sub-millimeter 3D isotropic coronary MR angiography. In: *ESMRMB Virtual Meeting.* (2020).

82. Chen Y, Kwan A, Yang Q, Christodoulou AG, Li DYX. Ultra-fast coronary MRA by generative adversarial super-resolution. In: *SMRA, Abstract #16 Virtual Meeting*. (2020).
83. Boden WE, O'Rourke RA, Teo KK, Hartigan PM, Maron DJ, Kostuk WJ, et al. Optimal medical therapy with or without PCI for stable coronary disease. *N Engl J Med.* (2007) 356:1503–16. doi: 10.1056/NEJMoa070829
84. Tonino PAL, De Bruyne B, Pijls NHJ, Siebert U, Ikeno F, van 't Veer M, et al. Fractional flow reserve versus angiography for guiding percutaneous coronary intervention. *N Engl J Med.* (2009) 360:213–24. doi: 10.1056/NEJMoa0807611
85. Maron DJ, Hochman JS, Reynolds HR, Bangalore S, O'Brien SM, Boden WE, et al. Initial invasive or conservative strategy for stable coronary disease. *N Engl J Med.* (2020) 382:1395–407. doi: 10.1056/NEJMoa1915922
86. Tomaniak M, Katagiri Y, Modolo R, de Silva R, Khamis RY, Bourantas C V, et al. Vulnerable plaques and patients: state-of-the-art. *Eur Heart J.* (2020) 41:2997–3004. doi: 10.1093/eurheartj/ehaa227
87. van den Berg VJ, Haskard DO, Fedorowski A, Hartley A, Kardys I, Caga-Anan M, et al. IgM anti-malondialdehyde low density lipoprotein antibody levels indicate coronary heart disease and necrotic core characteristics in the Nordic Diltiazem (NORDIL) study and the Integrated Imaging and Biomarker Study 3 (IBIS-3). *EBioMedicine.* (2018) 36:63–72. doi: 10.1016/j.ebiom.2018.08.023
88. Abdelrahman KM, Chen MY, Dey AK, Virmani R, Finn A V, Khamis RY, et al. Coronary computed tomography angiography from clinical uses to emerging technologies: JACC state-of-the-art review. *J Am Coll Cardiol.* (2020) 76:1226–43. doi: 10.1016/j.jacc.2020.06.076
89. Noguchi T, Kawasaki T, Tanaka A, Yasuda S, Goto Y, Ishihara M, et al. High-intensity signals in coronary plaques on noncontrast T1-weighted magnetic resonance imaging as a novel determinant of coronary events. *J Am Coll Cardiol.* (2014) 63:989–99. doi: 10.1016/j.jacc.2013.11.034
90. Hosoda H, Asaumi Y, Noguchi T, Morita Y, Kataoka Y, Otsuka F, et al. Three-dimensional assessment of coronary high-intensity plaques with T1-weighted cardiovascular magnetic resonance imaging to predict periprocedural myocardial injury after elective percutaneous coronary intervention. *J Cardiovasc Magn Reson.* (2020) 22:5. doi: 10.1186/s12968-019-0588-6
91. Matsumoto K, Ehara S, Hasegawa T, Sakaguchi M, Otsuka K, Yoshikawa J, et al. Localization of coronary high-intensity signals on T1-weighted MR imaging: relation to plaque morphology and clinical severity of angina pectoris. *JACC Cardiovasc Imaging.* (2015) 8:1143–52. doi: 10.1016/j.jcmg.2015.06.013
92. Ehara S, Hasegawa T, Nakata S, Matsumoto K, Nishimura S, Iguchi T, et al. Hyperintense plaque identified by magnetic resonance imaging relates to intracoronary thrombus as detected by optical coherence tomography in patients with angina pectoris. *Eur Hear J Cardiovasc Imaging.* (2012) 13:394–9. doi: 10.1093/ehjci/jer305
93. Maintz D, Ozgun M, Hoffmeier A, Fischbach R, Kim WY, Stuber M, et al. Selective coronary artery plaque visualization and differentiation by contrast-enhanced inversion prepared MRI. *Eur Heart J.* (2006) 27:1732–6. doi: 10.1093/eurheartj/ehl102
94. Yeon SB, Sabir A, Clouse M, Martinezclark PO, Peters DC, Hauser TH, et al. Delayed-enhancement cardiovascular magnetic resonance coronary artery wall imaging. *J Am Coll Cardiol.* (2007) 50:441–7. doi: 10.1016/j.jacc.2007.03.052
95. Engel L-C, Landmesser U, Gigengack K, Wurster T, Manes C, Girke G, et al. Novel Approach for *in vivo* detection of vulnerable coronary plaques using molecular 3-T CMR imaging with an albumin-binding probe. *JACC Cardiovasc Imaging.* (2018) 12:297–306. doi: 10.1016/j.jcmg.2017.10.026
96. Xie Y, Pang J, Kim Y, Yang Q, Kim J-S, Nguyen CT, et al. Coronary atherosclerosis T1-weighed Characterization with integrated anatomical reference (CATCH). *J Cardiovasc Magn Reson.* (2016) 18:O22. doi: 10.1186/1532-429X-18-S1-O22
97. Xie Y, Kim YJ, Pang J, Kim JS, Yang Q, Wei J, et al. Coronary atherosclerosis T1-weighed characterization with integrated anatomical reference: comparison with high-risk plaque features detected by invasive coronary imaging. *JACC Cardiovasc Imaging.* (2017) 10:637–48. doi: 10.1016/j.jcmg.2016.06.014
98. Ginami G, Neji R, Phinikaridou A, Whitaker J, Botnar RM, Prieto C. Simultaneous bright- and black-blood whole-heart MRI for noncontrast enhanced coronary lumen and thrombus visualization. *Magn Reson Med.* (2018) 79:1460–72. doi: 10.1002/mrm.26815
99. Hartley A, Haskard D, Khamis R. Oxidized LDL and anti-oxidized LDL antibodies in atherosclerosis - novel insights and future directions in diagnosis and therapy. *Trends Cardiovasc Med.* (2019) 29:22–6. doi: 10.1016/j.tcm.2018.05.010
100. Pandey SS, Haskard DO, Khamis RY. Developing a strategy for interventional molecular imaging of oxidized low-density lipoprotein in atherosclerosis. *Mol Imaging.* (2017) 16:1536012117723788. doi: 10.1177/1536012117723788
101. Khamis RY, Woollard KJ, Hyde GD, Boyle JJ, Bicknell C, Chang S-H, et al. Near Infrared Fluorescence (NIRF) molecular imaging of oxidized LDL with an autoantibody in experimental atherosclerosis. *Sci Rep.* (2016) 6:21785. doi: 10.1038/srep21785
102. Bary C Von, Makowski M, Preissel A, Keithahn V, Warley A, Spuentrup E, et al. MRI of coronary wall remodeling in a swine model of coronary injury using an elastin-binding contrast agent. *Circ Cardiovasc Imaging.* (2011) 4:147–5. doi: 10.1161/CIRCIMAGING.109.895607
103. Caravan P, Das B, Dumas S, Epstein FH, Helm PA, Jacques V, et al. Collagen-targeted MRI contrast agent for molecular imaging of fibrosis. *Angew Chemie Int Ed.* (2007) 46:8171–73. doi: 10.1002/anie.200700700
104. Sanders HMHF, Strijkers GJ, Mulder WJM, Huinink HP, Erich SJF, Adan OCG, et al. Morphology, binding behavior and MR-properties of paramagnetic collagen-binding liposomes. *Contrast Media Mol Imaging.* (2009) 4:81–8. doi: 10.1002/cmmi.266
105. Hellenthal FAMVI, Buurman WA, Wodzig WKWH, Schurink GWH. Biomarkers of AAA progression. Part 1: extracellular matrix degeneration. *Nat Rev Cardiol.* (2009) 6:464–74. doi: 10.1038/nrcardio.2009.80
106. Bazeli R, Coutard M, Duport BD, Lancelot E, Corot C, Laissy J-P, et al. *In vivo* evaluation of a new magnetic resonance imaging contrast agent (P947) to target matrix metalloproteinases in expanding experimental abdominal aortic aneurysms. *Invest Radiol.* (2010) 45:662–8. doi: 10.1097/RLI.0b013e3181ee5bbf

Conflict of Interest: The authors declare that the research was conducted in the absence of any commercial or financial relationships that could be construed as a potential conflict of interest.

frontiers in Cardiovascular Medicine

REVIEW
published: 30 August 2021
doi: 10.3389/fcvm.2021.713625

Non-invasive Imaging in Patients With Chronic Total Occlusions of the Coronary Arteries—What Does the Interventionalist Need for Success?

Johannes Kersten[1], Nina Eberhardt[2], Vikas Prasad[2], Mirjam Keßler[1], Sinisa Markovic[1], Johannes Mörike[1], Nicoleta Nita[1], Tilman Stephan[1], Marijana Tadic[1], Temsgen Tesfay[1], Wolfgang Rottbauer[1] and Dominik Buckert[1]*

[1] Department for Internal Medicine II, University of Ulm, Ulm, Germany, [2] Department for Nuclear Medicine, University of Ulm, Ulm, Germany

OPEN ACCESS

Edited by:
Steffen Erhard Petersen, Queen Mary University of London, United Kingdom

Reviewed by:
Alessia Gimelli, Gabriele Monasterio Tuscany Foundation (CNR), Italy
Michael Jerosch-Herold, Brigham and Women's Hospital and Harvard Medical School, United States

***Correspondence:**
Johannes Kersten
johannes.kersten@uni-ulm.de

Specialty section:
This article was submitted to Cardiovascular Imaging, a section of the journal Frontiers in Cardiovascular Medicine

Received: 23 May 2021
Accepted: 06 August 2021
Published: 30 August 2021

Citation:
Kersten J, Eberhardt N, Prasad V, Keßler M, Markovic S, Mörike J, Nita N, Stephan T, Tadic M, Tesfay T, Rottbauer W and Buckert D (2021) Non-invasive Imaging in Patients With Chronic Total Occlusions of the Coronary Arteries—What Does the Interventionalist Need for Success? Front. Cardiovasc. Med. 8:713625. doi: 10.3389/fcvm.2021.713625

Chronic total occlusion (CTO) of coronary arteries is a common finding in patients with known or suspected coronary artery disease (CAD). Although tremendous advances have been made in the interventional treatment of CTOs over the past decade, correct patient selection remains an important parameter for achieving optimal results. Non-invasive imaging can make a valuable contribution. Ischemia and viability, two major factors in this regard, can be displayed using echocardiography, single-photon emission tomography, positron emission tomography, computed tomography, and cardiac magnetic resonance imaging. Each has its own strengths and weaknesses. Although most have been studied in patients with CAD in general, there is an increasing number of studies with positive preselectional factors for patients with CTOs. The aim of this review is to provide a structured overview of the current state of pre-interventional imaging for CTOs.

Keywords: chronic total occlusion, revascularization, non-invasive imaging, hibernation, ischemia, viability

INTRODUCTION

Chronic total occlusion (CTO) of coronary arteries is a common finding in coronary angiograms of patients with known or suspected coronary artery disease (CAD). Despite their frequency, CTOs are the most reliable predictor of an incomplete revascularization. This is the result of two major factors: (a) a lack of data from randomized controlled trials regarding a benefit on mortality and (b) the lower success rate accompanied by a higher complication rate of an interventional revascularization. Large registry studies have shown that CTO percutaneous coronary interventions (PCI) can reduce mortality (1–4). The EUROCTO trial, the first randomized controlled trial on CTO, showed a benefit in terms of ischemic symptom burden rather than other hard clinical outcomes (5). In another randomized controlled trial (REVASC Trial), CTO PCI did not show an improvement in analyzed cardiovascular magnetic resonance (CMR) parameters but a reduction in major adverse cardiovascular events (6).

Current guidelines and position papers therefore recommend CTO PCI in the case of ongoing symptoms and viable myocardia in the CTO territory (7–10). However, imaging of ischemia remains controversial. On the one hand, revascularization is recommended for CAD patients with more than 10% myocardial ischemia (7, 8). However, the trial underlying this recommendation

TABLE 1 | Viability testing using different non-invasive imaging modalities.

	DSE	SPECT	FDG-PET	CT (experimental)	CMR
Sensitivity	80–84%	83–87%	88–93%	N/A	LGE: 84–95% Dobutamine: 81–84%
Specificity	78–81%	65–69%	58–73%	N/A	LGE: 51–74% Dobutamine: 82–91%
Radiation dose	None	6–24 mSv	∼7 mSv	∼7 mSv	None
Contrast agent/tracer	Not necessary	Radioactive tracer (^{99m}Tc or ^{201}Tl)	Radioactive tracer (^{18}F, ^{82}Rb)	Iodine	LGE: gadolinium Dobutamine: None
Cost	Low	Moderate	High	Moderate	High
Limitations	Very low image quality in some patients	Low resolution and high radiation dose	High cost and high radiation dose	High radiation dose and limited knowledge of viability testing	High cost and long duration
Advantages	Low cost and wide availability	Balanced cost and diagnostic accuracy	High resolution and sensitivity	Positive adjunctive information	Availability of prognostic data in CTO

Sensitivity, specificity, and radiation doses are adopted from Henzlova et al. (21), Bax et al. (22), Matsuda et al. (23), Case et al. (24), Romero et al. (25), and Schinkel et al. (26). Viability was defined as functional recovery after percutaneous coronary intervention or coronary artery bypass grafting in CAD patients.
DSE, dobutamine stress echocardiography; SPECT, single-photon emission computed tomography; FDG-PET, ^{18}F-fluoro-2-deoxy-D-glucose positron emission tomography; CT, computed tomography; CMR, cardiovascular magnetic resonance; LGE, late gadolinium enhancement.

focused on patients with CAD in general and not on CTO patients in particular (11). On the other hand, ischemia is always seen in viable CTO-related myocardia regardless of the grade of collaterals, and in most CTOs of major vessels, the degree of myocardial ischemia is above 10% (12, 13). Even though the ISCHEMIA trial found no benefit of an ischemia-driven revascularization approach, its results are not generally applicable to patients with CTOs (14, 15).

Viability is by definition present in segments with preserved systolic function. In contrast, dysfunctional segments are not a priori avital. The term "hibernation" was introduced to explain a potentially dysfunctional myocardium resulting in ischemia. Information is gained from an initial coronary angiogram where well-developed collaterals correlate with less extensive scarring, indicating a more viable myocardium (16, 17). A normal wall motion in CTO-related areas is a common finding, and extensive, transmural scarring is only observed in about 5% of CTO segments (16). Otherwise, the presence or extent of a Q wave or QS complexes in an electrocardiogram (ECG) is no proof of a vitality (18–20).

For the detection of a hibernating myocardium, a broad range of non-invasive imaging modalities is available. An overview is presented in **Table 1** with an example of their use in **Figure 1**. The selection mainly depends on local availability and expertise. This review aims to discuss the possibilities and limits of the available non-invasive imaging modalities and future trends. The review focuses on studies aiming to optimize patient selection for CTO reperfusion and its outcomes, although most findings are applicable to CAD patients in general.

ECHOCARDIOGRAPHY

Echocardiography is inexpensive and available nearly everywhere. It is the standard modality for the evaluation of global and regional cardiac function. Besides pre-interventional examinations, the bedside use of echocardiography in the catheter laboratory provides the opportunity to detect complications during interventions, such as pericardial effusions or intramural hematomas.

However, the value and validity of echocardiography depend on the investigator's experience. In CAD patients, an increase in regional contractility under dobutamine stress ("contractile reserve") can show viability and improvement of regional function after revascularization (27–29). The mostly older studies on dobutamine stress echocardiography (DSE) included small patient samples with a clear underrepresentation of women. The sensitivity of DSE in predicting an improvement of regional function ranges from 74 to 94% (30). In a relatively large trial involving 318 patients, revascularization in segments with viability on DSE was associated with reduced mortality (31). In another trial, viability assessed by DSE was associated with a relative reduction of mortality by 19.5% in patients with a severe left ventricular dysfunction (LVEF < 35%) (32). Because of its wide distribution and cost-effectiveness and the accumulated experience in clinical practice, DSE appears to be a good tool for examining patients with CTOs, provided that the image quality is good. Another advantage is the low rate of side effects of dobutamine stress (33). Other forms of myocardial stress are also possible as an alternative to dobutamine, such as dipyridamole and treadmill exercise (34).

In addition to the examination under dobutamine stress, echocardiography at rest can predict viability under certain circumstances. An end-diastolic wall thickness (EDWT) of >0.6 cm in dysfunctional segments is a marker of hibernation. In a trial involving 45 patients undergoing 2D echocardiography, DSE, and rest-redistribution thallium-201 (Tl-201) tomography before revascularization, an EDWT of >0.6 cm had 94% sensitivity and 50% specificity with a ROC curve similar to the maximum Tl-201 uptake, while DSE increased specificity to 88%

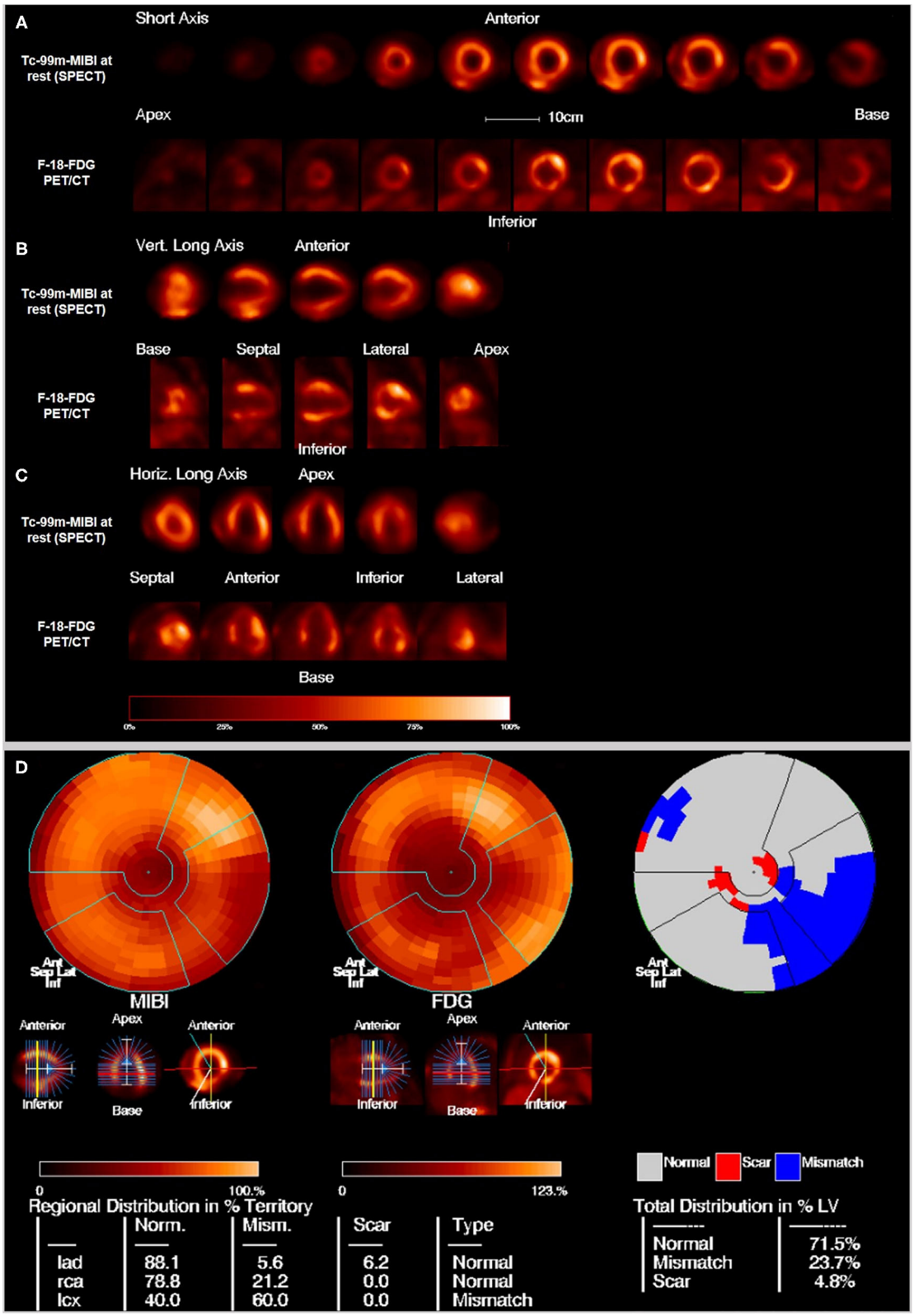

FIGURE 1 | Example of hibernating myocardium: 76 years old male with a perfusion defect on the posterolateral wall in the Tc-99m-MIBI rest scan that shows FDG uptake in the viability F-18-FDG-PET/CT scan resulting in the diagnosis of hibernating myocardium. **(A)** Short axis, **(B)** vertical long axis, and **(C)** horizontal long axis. The upper rows show the perfusion scan at rest with Tc-99m-MIBI (SPECT), the lower rows show the viability scan with F-18-FDG (PET). **(D)** Polar maps and subtraction image to visualize the mismatch between the perfusion defect on SPECT and the viability on FDG-PET/CT. 23.7% of the myocardium in the left ventricle is in hibernating status.

(33). More recent studies focusing on strain echocardiography have reported promising results (35, 36). However, the interpretation of deformation parameters depends heavily on image quality and the examiner's experience. For wider use, validation in a prospective cohort is warranted.

MYOCARDIAL PERFUSION SCINTIGRAPHY

Myocardial perfusion scintigraphy (MPS) is a nuclear medicine technique that is used for around 50 years to assess regional left ventricular myocardial perfusion, diastolic and systolic function as well as to differentiate hibernating myocardium from transmural or non-transmural infarct. Three dimension images of myocardium are acquired after injecting radiopharmaceuticals with high first pass extraction by the myocardium using the single emission computed tomography (SPECT) technique. In majority of the centers the images are additionally corrected for attenuation correction using low dose CT images acquired simultaneously with SPECT images. As radioisotopes preferentially Technetium-99m (Tc-99m), specially in Europe and rarely Thallium-201 (Tl-201) are used (21). Tl-201 as a cyclotron product is injected as Thallium-201-Chloride. The Tc-99m is eluted from a generator and is either labeled with Sestamibi (CardioliteTM) or Tetrofosmin (MyoviewTM). Nowadays Tc-99m-labeled tracers are the tracer of choice because of more favorable imaging characteristics because of higher photon energy (140 keV compared to 69–83 keV) with less attenuation by the tissues around the heart, improved image quality and less radiation exposure (6 mSv vs. 17 mSv) compared to Tl-201 because of a shorter half-life (Tc-99m = 6 h, Tl-201 = 72 h). ECG-gated perfusion images allow the simultaneous assessment of perfusion as well as global and regional function of the left ventricle and are therefore an important tool in the diagnosis and management for CAD. To assess perfusion imaging a comparison between images at rest and images after stress is required. To replicate the normal physiological effect of strenuous exercise on perfusion, radiopharmaceuticals are injected after the patients underwent either physical stress (e.g., by a treadmill) or pharmacological stress (adenosine, regadenoson or dobutamine) tests. Thereafter the resting state images are acquired at a later time point. In patients without hemodynamically relevant myocardial ischemia, both stress and rest scans show a homogeneous distribution of the perfusion tracers. In comparison, patients with hemodynamically relevant stenosis of the coronary vessels, decreased segmental or subsegmental uptake of the tracer is seen in stress which however normalizes itself in the resting phase. A scar of the myocardium shows reduced or no uptake in the scar area both during stress and in rest conditions as a fixed defect.

The rarely used Tl-201 is a potassium analog and uses the Na/K ATPase system of viable myocardial cells. Its initial myocardial uptake is proportional to blood flow and it is rapidly cleared from the blood. After that up to 4 h a re-equilibration takes place when Tl-201 concentration levels are lower in the blood. This is also called redistribution and the process is directly proportional to blood flow to the area and viable myocardial cells. If the stress and rest images show matched homogeneous normal tracer uptake there is no sign of ischemia or infarction. If the tracer uptake during stress is abnormal but with normal uptake during rest / redistribution that is a sign for ischemia. Perfusion defects on both stress and rest images usually means there is a scar. To check that area for hibernating myocardium a reinjection of Tl-201 and another image acquisition after 18–24 h can be carried out. If there is Tl-201 uptake, there is hibernating myocardium in this area. If there is a scar no tracer uptake can be detected (37, 38).

The Tc-99m-labeled radiotracers are monovalent cations that enter cells through their lipophilic characteristics. Their uptake is also dependent on blood flow but as well as on electrochemical gradients of the plasma- and mitochondrial-membranes, the cellular pH and intact energy pathways. In the myocytes they are trapped mainly in the mitochondria with minimal washout and no redistribution in the blood. After the intravenous injection these tracers are first cleared by the liver and excreted through the bile. This makes it impossible to assess the myocardial uptake of the inferior wall right after injection and leads to a delay of 15–45 min before the start of the imaging acquisition, especially for Sestamibi. Tetrofosmin allows earlier imaging acquisition because of lower hepatic uptake. Stress and rest images can be acquired in 2-day and 1-day protocols that show no significant differences (21). For the 1-day protocol the stress images should be acquired first. If there is a homogenous tracer uptake the rest images can be avoided. In the 1-day protocols the injection for the second imaging (rest) higher amount of radioactivity is injected to overcome the shine through from the remaining radioactivity after stress. With the Tc-99m-labeled radiotracers perfusion and ischemia as well as viability can be examined but not hibernating myocardium (39). As Tl-201 is associated with higher radiation exposure, hibernating myocardium are best depicted by using a combination of Tc-99m Tetrofosmin or Sestamibi perfusion scan and F-18-FDG-PET.

The accurate interpretation of the myocardial perfusion imaging with SPECT is crucial. Absolute quantification of perfusion is more common with PET than with SPECT. According to the literature the sensitivity and the specificity of gated myocardial SPECT studies to diagnose clinically significant CAD with Tc-99m tracers is 88.3 and 75.8%, respectively (40). Cutoff values for the uptake of the tracers of $>$ 50% of Tc-99m and $>$ 60% of Tl-201 are commonly associated with regional functional recovery in CAD. However, in the detection of a viable hibernating myocardium, specificity is moderate (49–69%) and can lead to an overestimation of potential functional recovery (22). The presence of an ischemic area on a SPECT scan has shown a negative predictive value for cardiac events (41). In a trial involving patients with CTO of the left anterior descending artery, perfusion defects on SPECT scans before a PCI were associated with an improvement of clinical and functional markers, such as the 6-min walk test, left ventricular volumes and ejection fraction (42). The effect was stronger in patients with reversible perfusion defects than in patients with irreversible defects.

Visual interpretation of three vessels CAD is a challenge for nuclear cardiology field. However, with the development and standardization of protocols as well as advances in the scanner types (e.g., digital scanners or the even newer C-shaped heart-specific gamma cameras) there is a remarkable improvement in the quantification of myocardial wall thickening, contraction, and dilatation as well as in measurement of ejection fraction. Left ventricular dilatation in stress in comparison to rest can be quantified as transient ischemic dilatation (TID). A TID value above 1.3 is generally considered to be significant and can be used for assessment of three vessels disease (43).

However, the comparatively low spatial resolution of SPECT images compared to that of other imaging modalities is a potential disadvantage, as it can lead to overdiagnosis of subendocardial infarctions. Nevertheless, this is not a real disadvantage in the examination of patients with CTOs since transmurality is the main question in this case. There are new predefined criteria for differentiating between transmural and non-transmural infarction in SPECT images (44).

Overall, SPECT appears to be a useful examination modality for patients with CTOs. A radiation dose of 6–24 mSv, depending on the protocol and tracer used (lower radiation doses for Tc-99m and higher radiation doses for Tl-201) (21), as well as expertise, should be taken into consideration.

POSITRON EMISSION TOMOGRAPHY

Positron emission tomography (PET) is another nuclear medicine imaging technique that is in use for around 40 years in some specialized centers with a broader use during the last years. The main advantages of PET over SPECT are higher-quality images because of high-energy emitted photons (511 keV) with improved spatial and temporal resolution and shorter half-lives of the radioisotopes (mostly some minutes) as well as less radiation exposure (45, 46). By the use of F-18-FDG it is also possible to make the myocyte glucose metabolism visible. A combination of MPS and FDG-PET is important in the detection and risk stratification of CAD. Two examples for the detection of hibernating myocardium and the differentiation to scar are seen in **Figures 1**, **2**. Additionally, perfusion PET also allows an improved functional evaluation of CAD because of a higher diagnostic accuracy and the possibility of measurements of myocardial blood flow (MBF) in absolute terms (milliliters per gram per minute). That makes it also possible to detect microvascular disease and balanced ischemia.

For the imaging with PET positron emitting radionuclides like Rubidium-82 (Rb-82), Oxygen-15 (O-15), Nitrogen-13 (N-13), and Flouride-18 (F-18) are used and incorporated into biochemical molecules. Rb-82 is a generator product, the other named radioisotopes are cyclotron products and for O-15 and N-13 with very short half-lives of 2 and 10 min, respectively, making an onsite cyclotron necessary. For perfusion imaging O-15 water, N-13 Ammonia, Rb-82 and F-18 Flurpiridaz are used with stress and rest imaging as in MPS. O-15 water is ideal for quantification of MBF in absolute terms. It can be seen as a one-compartment tracer kinetic model as it has no barrier effect form cellular membranes. Because of its very short half-life and poor contrast images between blood pool and the myocardium its use is limited. N-13 Ammonia is cationic and its first-pass extraction is related to blood flow for low flow rates. It reaches the cytosols via passive diffusion or active transport and is incorporated into the amino acid pool or diffuses back into the blood. Rb-82 is a potassium analog with a very short half-life of 75 s. During first-pass its extraction is not very high and builds a plateau with higher blood flow rates. F-18 Flurpiridaz is a novel PET mitochondrial complex-1 inhibitor in preparation with a half-life of 120 min. It has a high extraction rate with high flow and therefore makes absolute quantification of blood flow possible (47). As for SPECT tracer uptake between stress and rest images are compared to detect ischemia and scars.

For the differentiation of a perfusion defect in both stress and rest between a scar region and ischemic but viable region F-18-Fluorodeoxyglucose (FDG) is used. F-18-FDG competes with glucose for transport as well as phosphorylation by hexokinase. Once it is in the cytosol and phosphorylated it cannot be further processes by glycogen synthesis and is therefore trapped in the cell (45, 48). Its half-life of 110 min makes it easy to handle. To assess myocardial viability of a perfusion defect in stress and rest or in rest only (preferably from PET scans) an additional PET scan with F-18-FDG according to a special protocol can be performed. For non-diabetic and diabetic patients fasting for at least 6 h is required. After measurement of the serum glucose a protocol for glucose loading and insulin is required before F-18-FDG is administered intravenously (glucose $<$ 100 mg/dl 25–100 g oral load or dextrose infusion, later insulin is administered according to the glucose level, glucose $<$ 250 mg/dl only insulin is administered without an additional glucose load). In a viability study areas with highly reduced or absent perfusion but preserved or even enhanced metabolic activity Perfusion/metabolism mismatch, are hibernating but viable and have a high probability of regaining function after revascularization. Areas that show no perfusion during rest but do have preserved glucose metabolism are viable whereas the absence of glucose metabolism indicates non-viable myocardium. There are three different patterns which can be seen combining myocardial perfusion imaging at rest with F-18-FDG: (1) hibernating myocardium showing reduced perfusion with preserved FDG-uptake, (2) transmural scar without perfusion and without FDG-uptake, and (3) non-transmural scar with partially reduced perfusion of the myocardium with concordant FDG-uptake.

In CAD patients in general, an ischemia-driven revascularization approach guided by PET could result in a reduction in angina severity and a slight improvement in the left ventricular ejection fraction (49). Stulijfzand et al. who examined 69 CTO patients with O-15 water PET, found no correlation between the degree of ischemia and volumetric or functional improvements after CTO PCI but observed a significant ischemic burden reduction (13). In another study, this improvement in myocardial blood flow correlated to the defect size in a baseline PET examination (50). To summarize, PET imaging is a useful tool for evaluating ischemia and viability, with excellent spatial and temporal resolutions.

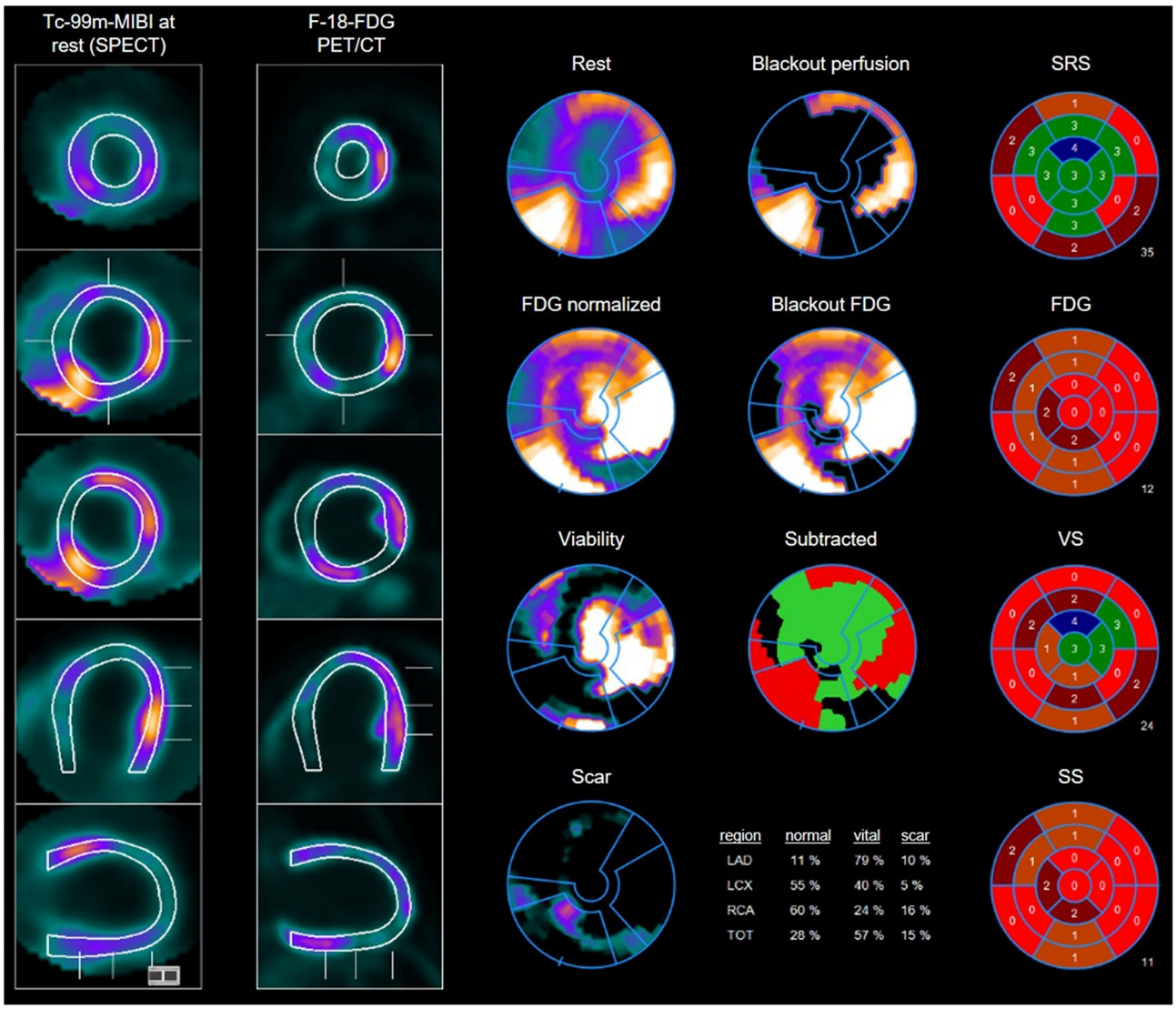

FIGURE 2 | Example of multiple perfusion defect with hibernating myocardium as well as areas of scars: 45 years old male with perfusion defects in the anteroseptal wall as well as on the anterolateral and posterolateral wall in the Tc-99m-MIBI rest scan. FDG uptake in the viability F-18-FDG-PET/CT scan shows some uptake in the areas with perfusion defects resulting in the diagnosis of hibernating myocardium but also some areas with no FDG uptake especially septal and posterior resulting in the diagnosis of scars. Overview and polar maps with SRS, summed rest score; VS, vitality score; SS, scar score.

COMPUTER TOMOGRAPHY

Computed tomography (CT) angiography has traditionally been used for anatomical evaluations of the coronary tree. With the advent of new-generation scanners with dual-source imaging, 64-row scanners, and modern software techniques, plaque morphology and regional calcium burden evaluations and functional assessments have also become possible (51, 52).

Since CTOs are found in many patients with known or suspected CAD, CT examinations can also contribute to their diagnosis. However, the distinction between a "true" CTO and subtotal stenosis constitutes a diagnostic difficulty. The distal lumen is often contrasted via collaterals, and the spatial resolution of CT is relatively low in comparison to classical angiography. Diagnostic markers such as a lesion length over 9 mm and the so-called reverse attenuation gradient sign have proven to be helpful, enabling a clear diagnosis in most cases (53–55). Apart from pure diagnostics, CT angiography is increasingly used for prognostic assessments and pre-procedural planning of coronary interventions and offers the possibility of follow-up restenosis assessments (56). Blooming artifacts are a limitation caused by severe calcification or stent struts, leading to a potential overestimation of lumen narrowing. This affects diagnosis of CTO as well as follow-up evaluation of the stent patency. Novel techniques and algorithms sought to overcome this limitation (57).

A key task of the pre-interventional examination of CTO patients is the abovementioned viability test. While cardiac CT was previously used for purely anatomical assessments of the coronary tree, it can also be used for hibernation assessments. These are based on classic measures, such as global and regional function, wall thickness, and wall thickening in systole, while assessment methods derived from CMR have not yet found their way into clinical routine. Reduced perfusion can be indicated by reduced contrast during the arterial phase. Similar to the flooding behavior of gadolinium-containing magnetic resonance imaging (MRI) contrast agents, delayed (late) enhancement with iodine-containing contrast media indicates myocardial scarring. A mismatch between underperfusion (arterial phase) and late enhancement indicates a potential intervention target (58). An additional late CT examination (5–15 min after the administration of the contrast medium) is associated with considerable radiation exposure. Currently, only data from experimental and animal studies showing good agreement with CMR scans are available (23, 52, 59, 60).

For the prediction of interventional recanalization success, the Computed Tomography Registry of Chronic Total Occlusion Revascularization (CT-RECTOR) score was established by analogy with angiography-based scores, such as the Japanese Multicenter CTO Registry (J-CTO) and Prospective Global Registry for the Study of Chronic Total Occlusion Intervention (PROGRESS-CTO) scores (61). It is calculated based on the presence of multiple occlusions, a blunt stump, severe calcification in the cross-sectional area of the occluded vessel, tortuosity, anamnestic information from a second attempt, and the presumed duration of the CTO. However, the J-CTO score has also shown applicability to CT angiographies (62).

The actual procedure can also be planned using CT angiography. Depending on factors such as good collateralization or the presence of an intensively calcified proximal cap, the access route (antegrade or retrograde) can be determined, or in the case of severe calcifications over short distances, an early switch to a stiffer wire can be decided. The anticipation of a need for rotablation or debulking devices is a potentially time-saving and patient-friendly factor (63). In a single-center study involving one interventionalist and 73 patients with CTOs, the use of pre-procedural CT angiography for planning significantly increased the recanalization rate in the matched analysis from 64 to 88% (64). In another study with 15 patients with pre-procedural CT planning and 59 patients in a purely classical angiographically controlled group, a stiff wire was chosen significantly more often as the initial wire, and there was less contrast exposure (65). An option after a CT scan that should not be neglected is referral to another center if there is no experience in the use of retrograde maneuvers or foreseeably necessary material is not available.

CT angiography can also be used to detect in-stent restenosis in follow-up investigations. However, as it has shown a high negative predictive value but a low positive predictive value (66–68), its clinical benefit in the case of frequent inconclusive findings, and thus the necessity of an invasive examination with double exposure to radiation and contrast media, must be further investigated in clinical trials. A combination with CT perfusion imaging or fractional flow reserve CT could further increase its value (69, 70).

In summary, pre-interventional multi-slice CT is a useful additional pre-interventional diagnostic tool. If necessary, it should be combined with other examination modalities to detect hibernation. Among all diagnostic modalities, CT is the closest to integrating diagnosis, risk calculation, intervention planning, and follow-up care in one modality.

CARDIOVASCULAR MAGNETIC RESONANCE

Cardiovascular magnetic resonance (CMR) is the gold standard for the evaluation of the left and right ventricular volumes and function, as well as ischemia and viability. A major advantage of CMR over nuclear and CT imaging is the lack of a need for ionizing radiation and the better tolerance of gadolinium-containing contrast media compared to iodine-containing contrast media. Its spatial and temporal resolutions are good thanks to modern sequences, such as balanced steady-state free precision imaging, ECG-gating, and breath holding techniques (71). Image quality is getting worse only in patients with severe arrhythmia or non-compliant patients. Real-time imaging without the need for breath holding is evolving to overcome these disadvantages (72).

Ischemia can be visualized using adenosine perfusion CMR. Less contrasted myocardial areas under vasodilator stress indicate a myocardium at risk (73). In CAD patients in general, adenosine perfusion imaging has shown potential for diagnosis and risk prediction (74, 75). Dobutamine stress can be used as an alternative to vasodilatory stress for risk assessment with comparable results (76, 77). However, the role of stress imaging in evaluating CTOs is controversial, as a study found a perfusion deficit in every CTO patient (78). Nevertheless, it can be argued that it may have its place in myocardium risk assessment. Perhaps the ongoing CARISMA_CTO study will provide more clarity on the matter (79).

Two modalities have been developed for viability assessment: low-dose dobutamine CMR (LDD-CMR) and LGE. LDD-CMR is the older method, but it has shown excellent results in predicting functional recovery after revascularization, even in direct comparison with other imaging techniques (80, 81). In low doses, dobutamine increases the regional function of an ischemic or hibernating myocardium ("contractile reserve"). Therefore, an increase in systolic wall thickness with low dobutamine doses is a predictor of functional recovery after revascularization in CAD patients in general. Conversely, in higher doses, the systolic function of an ischemic myocardium deteriorates. A combination with strain imaging is a promising method for improving diagnostic accuracy (82). To date, no studies have evaluated the utility of LDD-CMR prior to CTO revascularization.

LGE imaging is a valuable tool for distinguishing a hibernating myocardium from post-infarction scarring. Five to 15 min after the administration of a gadolinium-based contrast agent, focal deposits of gadolinium in the myocardium show a widening

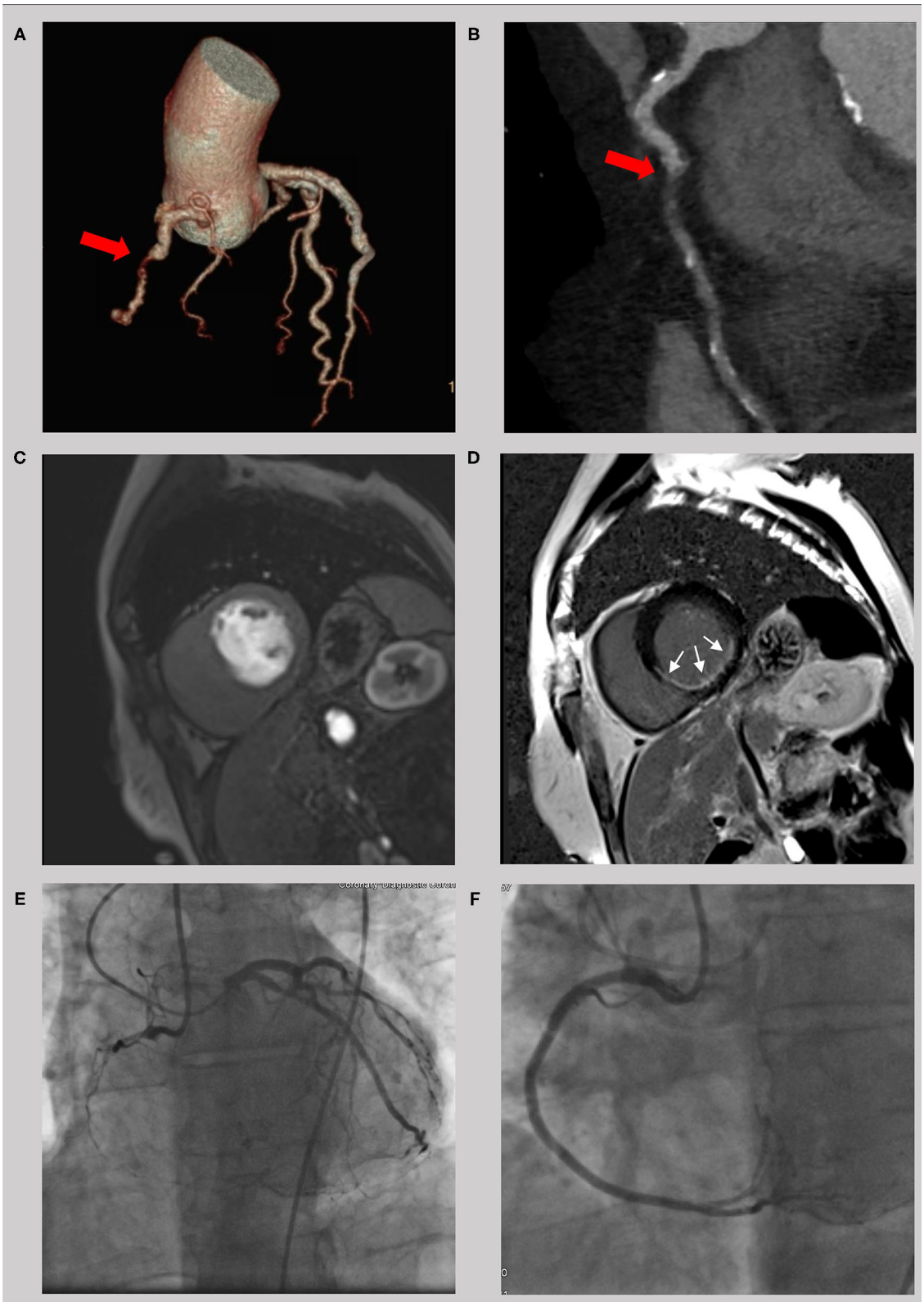

FIGURE 3 | Example of a 56 year old male with a chronic total occlusion of the right coronary artery. The occlusion is seen in the computer tomography coronary angiogram (**A** and **B**, red cross) with a short occlusion length and a small amount of calcification. Because of an impaired regional function with thinning of the left ventricular wall, imaging of ischemia (**C**, first-pass perfusion) and scarring (**D**, late gadolinium enhancement) was done using cardiac magnetic resonance. With a LGE of <50% transmurality (white crosses) and a high symptom burden, interventional revascularization was successfully performed **(E,F)** with significant clinical improvement.

of the extracellular volume, indicating fibrosis and scarring, because of a delayed washout. LGE has shown a good correlation with PET examinations and excellent inter- and intra-observer agreement (83). In stable CAD, the combination of adenosine perfusion imaging and LGE has been shown to improve risk stratification and to help identify patients who will benefit from revascularization (74, 75, 84).

In a trial involving 59 patients with successful CTO PCIs, a pre-interventional LGE extent of <50% was associated with functional recovery of the related segment (85). In another study, CTO PCI was associated with an improvement of myocardial blood flow assessed using CMR and a reduction in the ischemic symptom burden (86). In that study, patients with a transmural LGE extent of more than 75% in most segments in the CTO territory were excluded. Although this approach seems obvious, it should not be seen as absolute, as the perfusion areas of the individual coronaries show significant variations between patients (87). Nevertheless, the two aforementioned studies suggest that a CMR-guided approach to CTO revascularization significantly improves regional blood flow and systolic function and sufficiently reduces patient symptoms. Accordingly, CMR imaging offers great benefits in the pre-interventional diagnostics of CTO patients, with a high prognostic value. An example of the combined use of CT and CMR in a patient with CTO is seen in **Figure 3**.

For even better workups, new techniques, such as parametric mapping, are currently under investigation. In a first study, the extracellular volume was found to be superior to LGE for functional recovery assessments (88).

Using CMR, patients have already been examined after complex PCI in order to investigate the extent and clinical impact of a peri-interventional infarction. This revealed a relevant proportion of patients with new LGE after PCI, which in turn had a negative impact on the clinical outcome (89). Techniques that are particularly prone to infarction, such as rotablation, could therefore have a negative impact on endpoints in CTO studies (90). Here CMR offers the potential for further investigations.

OUTLOOK

A central point of future developments, besides a further increase in diagnostic accuracy, will be a reduction in patient exposure to contrast media or radiation. Since CMR typically works without radiation, a further improvement of CMR coronary angiography would be an obvious direction in the quest to overcome the disadvantages of CT in CTO intervention planning. CMR coronary angiography is already feasible for the evaluation of plaque morphology and composition (91–93). At the same time, radiation exposure in SPECT, PET, and CT imaging is now only a fraction of the historically required doses thanks to the constant development of new detectors, collimators, techniques, and software.

Another goal for further improvement of interventional outcomes is the integration of imaging modalities into the actual intervention. Opolski et al. demonstrated the feasibility and safety of an augmented-reality glass that provides the interventional cardiologist with additional information from coronary CT angiography (65). This is yet another indication that CT is the closest to integrating diagnostics, prognostic assessment, planning, and follow-up care.

As already discussed, each modality has its own strengths and weaknesses. Therefore, fusion imaging, such as PET/CT or PET/MRI, could improve the pre-interventional workup of CTO patients. For example, a combination of morphological assessments using CT with metabolic assessments using PET could improve patient selection (94). In a first human study using PET/MRI fusion scans prior to CTO PCI in 49 patients, the combined images predicted functional improvement more accurately than PET or CMR alone (95). However, their high costs and limited access in daily care are clear limitations of these techniques.

In summary, the use of non-invasive imaging for ischemia and viability assessments before interventional recanalization of a CTO is desirable. Although some imaging techniques have clear advantages over others, the selection depends mainly on regional availability and expertise. Better patient selection and prediction of interventional success should be the target of future prospective studies.

AUTHOR CONTRIBUTIONS

JK and DB: concept and writing of the manuscript. NE and VP: writing of the SPECT and PET section, proofreading, and image examples. MK, SM, JM, NN, TS, MT, and TT: interpretation of the sources, proofreading, and image example. WR: supervision, concept, and proofreading. All authors contributed to the article and approved the submitted version.

REFERENCES

1. Suero JA, Marso SP, Jones PG, Laster SB, Huber KC, Giorgi LV, et al. Procedural outcomes and long-term survival among patients undergoing percutaneous coronary intervention of a chronic total occlusion in native coronary arteries: a 20-year experience. *J Am College Cardiol.* (2001) 38:409–14. doi: 10.1016/s0735-1097(01)01349-3
2. Teng H-I, Sung S-H, Huang S-S, Pan J-P, Lin S-J, Chan W-L, et al. The impact of successful revascularization of coronary chronic total occlusions on long-term clinical outcomes in patients with non-ST-segment elevation myocardial infarction. *J Interv Cardiol.* (2018) 31:302–9. doi: 10.1111/joic.12501
3. Khan MF, Wendel CS, Thai HM, Movahed MR. Effects of percutaneous revascularization of chronic total occlusions on clinical outcomes: a meta-analysis comparing successful versus failed percutaneous intervention for chronic total occlusion. *Catheter Cardiovasc Interv.* (2013) 82:95–107. doi: 10.1002/ccd.24863
4. Werner GS, Gitt AK, Zeymer U, Juenger C, Towae F, Wienbergen H, et al. Chronic total coronary occlusions in patients with stable angina pectoris: impact on therapy and outcome in present day clinical practice. *Clin Res Cardiol.* (2009) 98:435–41. doi: 10.1007/s00392-009-0013-5
5. Werner GS, Martin-Yuste V, Hildick-Smith D, Boudou N, Sianos G, Gelev V, et al. A randomized multicentre trial to compare revascularization

with optimal medical therapy for the treatment of chronic total coronary occlusions. *Eur Heart J.* (2018) 39:2484–93. doi: 10.1093/eurheartj/ehy220
6. Mashayekhi K, Nührenberg TG, Toma A, Gick M, Ferenc M, Hochholzer W, et al. A randomized trial to assess regional left ventricular function after stent implantation in chronic total occlusion: the REVASC Trial. *JACC Cardiovasc Interv.* (2018) 11:1982–91. doi: 10.1016/j.jcin.2018.05.041
7. Brilakis ES, Mashayekhi K, Tsuchikane E, Abi Rafeh N, Alaswad K, Araya M, et al. Guiding principles for chronic total occlusion percutaneous coronary intervention. *Circulation.* (2019) 140:420–33. doi: 10.1161/CIRCULATIONAHA.119.039797
8. Neumann F-J, Sousa-Uva M, Ahlsson A, Alfonso F, Banning AP, Benedetto U, et al. 2018 ESC/EACTS Guidelines on myocardial revascularization. *Eur Heart J.* (2019) 40:87–165. doi: 10.1093/eurheartj/ehy394
9. Patel MR, Calhoon JH, Dehmer GJ, Grantham JA, Maddox TM, Maron DJ, et al. ACC/AATS/AHA/ASE/ASNC/SCAI/SCCT/STS 2017 appropriate use criteria for coronary revascularization in patients with stable ischemic heart disease. *J Am College Cardiol.* (2017) 69:2212–41. doi: 10.1016/j.jacc.2017.02.001
10. Levine GN, Bates ER, Blankenship JC, Bailey SR, Bittl JA, Cercek B, et al. 2011 ACCF/AHA/SCAI Guideline for percutaneous coronary intervention: a report of the American College of Cardiology Foundation/American Heart Association Task Force on Practice Guidelines and the Society for Cardiovascular Angiography and Interventions. *Circulation.* (2011) 124:e574–651. doi: 10.1161/CIR.0b013e31823ba622
11. Shaw LJ, Berman DS, Maron DJ, Mancini GB, Hayes SW, Hartigan PM, et al. Optimal medical therapy with or without percutaneous coronary intervention to reduce ischemic burden: results from the clinical outcomes utilizing revascularization and aggressive drug evaluation (COURAGE) trial nuclear substudy. *Circulation.* (2008) 117:1283–91. doi: 10.1161/CIRCULATIONAHA.107.743963
12. Sachdeva R, Agrawal M, Flynn SE, Werner GS, Uretsky BF. The myocardium supplied by a chronic total occlusion is a persistently ischemic zone. *Catheter Cardiovasc Interv.* (2014) 83:9–16. doi: 10.1002/ccd.25001
13. Stuijfzand WJ, Biesbroek PS, Raijmakers PG, Driessen RS, Schumacher SP, van Diemen P, et al. Effects of successful percutaneous coronary intervention of chronic total occlusions on myocardial perfusion and left ventricular function. *EuroIntervention.* (2017) 13:345–54. doi: 10.4244/EIJ-D-16-01014
14. Maron DJ, Hochman JS, Reynolds HR, Bangalore S, O'Brien SM, Boden WE, et al. Initial invasive or conservative strategy for stable coronary disease. *N Engl J Med.* (2020) 382:1395–407. doi: 10.1056/NEJMoa1915922
15. Luca L, Uguccioni M, Meessen J, Temporelli PL, Tomai F, Rosa FM, et al. External applicability of the ISCHEMIA trial: an analysis of a prospective, nationwide registry of patients with stable coronary artery disease. *EuroIntervention.* (2020) 16:e966–73. doi: 10.4244/EIJ-D-20-00610
16. Schumacher SP, Everaars H, Stuijfzand WJ, Huynh JW, van Diemen PA, Bom MJ, et al. Coronary collaterals and myocardial viability in patients with chronic total occlusions. *EuroIntervention.* (2020) 16:e453–61. doi: 10.4244/EIJ-D-19-01006
17. Dong W, Li J, Mi H, Song X, Jiao J, Li Q. Relationship between collateral circulation and myocardial viability of 18F-FDG PET/CT subtended by chronic total occluded coronary arteries. *Ann Nucl Med.* (2018) 32:197–205. doi: 10.1007/s12149-018-1234-3
18. Al-Mohammad A, Norton MY, Mahy IR, Patel JC, Welch AE, Mikecz P, et al. Can the surface electrocardiogram be used to predict myocardial viability? *Heart.* (1999) 82:663–7. doi: 10.1136/hrt.82.6.663
19. Haft JI, Hammoudeh AJ, Conte PJ. Assessing myocardial viability: Correlation of myocardial wall motion abnormalities and pathologic Q waves with technetium 99m sestamibi single photon emission computed tomography. *Am Heart J.* (1995) 130:994–8. doi: 10.1016/0002-8703(95)90199-X
20. Schinkel AFL, Bax JJ, Elhendy A, Boersma E, Vourvouri EC, Sozzi FB, et al. Assessment of viable tissue in Q-wave regions by metabolic imaging using single-photon emission computed tomography in ischemic cardiomyopathy. *Am J Cardiol.* (2002) 89:1171–5. doi: 10.1016/S0002-9149(02)02299-3
21. Henzlova MJ, Duvall WL, Einstein AJ, Travin MI, Verberne HJ. ASNC imaging guidelines for SPECT nuclear cardiology procedures: stress, protocols, and tracers. *J Nucl Cardiol.* (2016) 23:606–39. doi: 10.1007/s12350-015-0387-x
22. Bax JJ, Wijns W, Cornel JH, Visser FC, Boersma E, Fioretti PM. Accuracy of currently available techniques for prediction of functional recovery after revascularization in patients with left ventricular dysfunction due to chronic coronary artery disease: comparison of pooled data. *J Am College Cardiol.* (1997) 30:1451–60. doi: 10.1016/s0735-1097(97)00352-5
23. Matsuda T, Kido T, Itoh T, Saeki H, Shigemi S, Watanabe K, et al. Diagnostic accuracy of late iodine enhancement on cardiac computed tomography with a denoise filter for the evaluation of myocardial infarction. *Int J Cardiovasc Imaging.* (2015) 31(Suppl. 2):177–85. doi: 10.1007/s10554-015-0716-9
24. Case JA, deKemp RA, Slomka PJ, Smith MF, Heller GV, Cerqueira MD. Status of cardiovascular PET radiation exposure and strategies for reduction: an information statement from the cardiovascular PET task force. *J Nucl Cardiol.* (2017) 24:1427–39. doi: 10.1007/s12350-017-0897-9
25. Romero J, Xue X, Gonzalez W, Garcia MJ. CMR imaging assessing viability in patients with chronic ventricular dysfunction due to coronary artery disease: a meta-analysis of prospective trials. *JACC Cardiovasc Imaging.* (2012) 5:494–508. doi: 10.1016/j.jcmg.2012.02.009
26. Schinkel AF, Bax JJ, Poldermans D, Elhendy A, Ferrari R, Rahimtoola SH. Hibernating myocardium: diagnosis and patient outcomes. *Curr Probl Cardiol.* (2007) 32:375–410. doi: 10.1016/j.cpcardiol.2007.04.001
27. Cigarroa CG, deFilippi CR, Brickner ME, Alvarez LG, Wait MA, Grayburn PA. Dobutamine stress echocardiography identifies hibernating myocardium and predicts recovery of left ventricular function after coronary revascularization. *Circulation.* (1993) 88:430–6. doi: 10.1161/01.cir.88.2.430
28. Krahwinkel W, Ketteler T, Wolfertz J, Gödke J, Krakau I, Ulbricht LJ, et al. Detection of myocardial viability using stress echocardiography. *Eur Heart J.* (1997) 18(Suppl. D):D111–6. doi: 10.1093/eurheartj/18.suppl_D.111
29. La Canna G, Alfieri O, Giubbini R, Gargano M, Ferrari R, Visioli O. Echocardiography during infusion of dobutamine for identification of reversible dyfunction in patients with chronic coronary artery disease. *J Am College Cardiol.* (1994) 23:617–26. doi: 10.1016/0735-1097(94)90745-5
30. Galatro K, Chaudhry FA. Prognostic implications of myocardial contractile reserve in patients with ischemic cardiomyopathy. *Echocardiography.* (2000) 17:61–7. doi: 10.1111/j.1540-8175.2000.tb00996.x
31. Afridi I, Grayburn PA, Panza JA, Oh JK, Zoghbi WA, Marwick TH. Myocardial viability during dobutamine echocardiography predicts survival in patients with coronary artery disease and severe left ventricular systolic dysfunction. *J Am College Cardiol.* (1998) 32:921–6. doi: 10.1016/S0735-1097(98)00321-0
32. Sicari R, Picano E, Cortigiani L, Borges AC, Varga A, Palagi C, et al. Prognostic value of myocardial viability recognized by low-dose dobutamine echocardiography in chronic ischemic left ventricular dysfunction. *Am J Cardiol.* (2003) 92:1263–6. doi: 10.1016/j.amjcard.2003.08.004
33. Mertes H, Sawada SG, Ryan T, Segar DS, Kovacs R, Foltz J, et al. Symptoms, adverse effects, and complications associated with dobutamine stress echocardiography. Experience in 1118 patients. *Circulation.* (1993) 88:15–9. doi: 10.1161/01.cir.88.1.15
34. Sicari R, Nihoyannopoulos P, Evangelista A, Kasprzak J, Lancellotti P, Poldermans D, et al. Stress echocardiography expert consensus statement–executive summary: European association of echocardiography (EAE) (a registered branch of the ESC). *Eur Heart J.* (2009) 30:278–89. doi: 10.1093/eurheartj/ehn492
35. Rösner A, Avenarius D, Malm S, Iqbal A, Bijnens B, Schirmer H. Severe regional myocardial dysfunction by stress echocardiography does not predict the presence of transmural scarring in chronic coronary artery disease. *Eur Heart J Cardiovasc Imaging.* (2015) 16:1074–81. doi: 10.1093/ehjci/jev096
36. Vitarelli A, Montesano T, Gaudio C, Conde Y, Cimino E, D'angeli I, et al. Strain rate dobutamine echocardiography for prediction of recovery after revascularization in patients with ischemic left ventricular dysfunction. *J Card Fail.* (2006) 12:268–75. doi: 10.1016/j.cardfail.2006.02.003
37. Kitsiou AN, Srinivasan G, Quyyumi AA, Summers RM, Bacharach SL, Dilsizian V. Stress-induced reversible and mild-to-moderate irreversible thallium defects: are they equally accurate for predicting recovery of regional left ventricular function after revascularization? *Circulation.* (1998) 98:501–8. doi: 10.1161/01.cir.98.6.501
38. Zimmermann R, Mall G, Rauch B, Zimmer G, Gabel M, Zehelein J, et al. Residual 201Tl activity in irreversible defects as a marker of

myocardial viability. Clinicopathological study. *Circulation.* (1995) 91:1016–21. doi: 10.1161/01.cir.91.4.1016
39. Maes AF, Borgers PM, Flameng W, Nuyts JL, van de Werf F, Ausma JJ, et al. Assessment of myocardial viability in chronic coronary artery disease using technetium-99m Sestamibi SPECT. *J Am College Cardiol.* (1997) 29:62–8. doi: 10.1016/S0735-1097(96)00442-1
40. Parker MW, Iskandar A, Limone B, Perugini A, Kim H, Jones C, et al. Diagnostic accuracy of cardiac positron emission tomography versus single photon emission computed tomography for coronary artery disease: a bivariate meta-analysis. *Circ Cardiovasc Imaging.* (2012) 5:700–7. doi: 10.1161/CIRCIMAGING.112.978270
41. Galassi AR, Werner GS, Tomasello SD, Azzarelli S, Capodanno D, Barrano G, et al. Prognostic value of exercise myocardial scintigraphy in patients with coronary chronic total occlusions. *J Interv Cardiol.* (2010) 23:139–48. doi: 10.1111/j.1540-8183.2010.00527.x
42. Sun D, Wang J, Tian Y, Narsinh K, Wang H, Li C, et al. Multimodality imaging evaluation of functional and clinical benefits of percutaneous coronary intervention in patients with chronic total occlusion lesion. *Theranostics.* (2012) 2:788–800. doi: 10.7150/thno.4717
43. Katz JS, Ruisi M, Giedd KN, Rachko M. Assessment of transient ischemic dilation (TID) ratio in gated SPECT myocardial perfusion imaging (MPI) using regadenoson, a new agent for pharmacologic stress testing. *J Nucl Cardiol.* (2012) 19:727–34. doi: 10.1007/s12350-012-9559-0
44. Dilsizian V. Interpretation and clinical management of patients with "Fixed" myocardial perfusion defects A call for quantifying endocardial-to-epicardial distribution of blood flow. *J Nucl Cardiol.* (2021) 28:723–8. doi: 10.1007/s12350-020-02492-8
45. Dilsizian V, Bacharach SL, Beanlands RS, Bergmann SR, Delbeke D, Dorbala S, et al. ASNC imaging guidelines/SNMMI procedure standard for positron emission tomography (PET) nuclear cardiology procedures. *J Nucl Cardiol.* (2016) 23:1187–226. doi: 10.1007/s12350-016-0522-3
46. Bateman TM, Heller GV, McGhie AI, Friedman JD, Case JA, Bryngelson JR, et al. Diagnostic accuracy of rest/stress ECG-gated Rb-82 myocardial perfusion PET: comparison with ECG-gated Tc-99m sestamibi SPECT. *J Nucl Cardiol.* (2006) 13:24–33. doi: 10.1016/j.nuclcard.2005.12.004
47. Maddahi J, Lazewatsky J, Udelson JE, Berman DS, Beanlands RS, Heller GV, et al. Phase-III clinical trial of fluorine-18 flurpiridaz positron emission tomography for evaluation of coronary artery disease. *J Am College Cardiol.* (2020) 76:391–401. doi: 10.1016/j.jacc.2020.05.063
48. Underwood SR, Bax JJ, vom Dahl J, Henein MY, Knuuti J, van Rossum AC, et al. Imaging techniques for the assessment of myocardial hibernation. Report of a Study Group of the European Society of Cardiology. *Eur Heart J.* (2004) 25:815–36. doi: 10.1016/j.ehj.2004.03.012
49. Eitzman D, al-Aouar Z, Kanter HL, vom Dahl J, Kirsh M, Deeb GM, et al. Clinical outcome of patients with advanced coronary artery disease after viability studies with positron emission tomography. *J Am College Cardiol.* (1992) 20:559–65. doi: 10.1016/0735-1097(92)90008-b
50. Schumacher SP, Kockx M, Stuijfzand WJ, Driessen RS, van Diemen PA, Bom MJ, et al. Ischaemic burden and changes in absolute myocardial perfusion after chronic total occlusion percutaneous coronary intervention. *EuroIntervention.* (2020) 2020:e462–71. doi: 10.4244/EIJ-D-19-00631
51. Abdelmoneim I, Sadek A, Mosaad MA, Yassin I, Radwan Y, Shokry K, et al. Diagnostic accuracy of multi-slice computed tomography in identifying lesion characteristics in coronary total occlusion. *Int J Cardiovasc Imaging.* (2018) 34:1813–8. doi: 10.1007/s10554-018-1392-3
52. Hoe J. CT coronary angiography of chronic total occlusions of the coronary arteries: how to recognize and evaluate and usefulness for planning percutaneous coronary interventions. *Int J Cardiovasc Imaging.* (2009) 25(Suppl. 1):43–54. doi: 10.1007/s10554-009-9424-7
53. Erffa J von, Ropers D, Pflederer T, Schmid M, Marwan M, Daniel WG, et al. Differentiation of total occlusion and high-grade stenosis in coronary CT angiography. *Eur Radiol.* (2008) 18:2770–5. doi: 10.1007/s00330-008-1068-9
54. Li M, Zhang J, Pan J, Lu Z. Obstructive coronary artery disease: reverse attenuation gradient sign at CT indicates distal retrograde flow–a useful sign for differentiating chronic total occlusion from subtotal occlusion. *Radiology.* (2013) 266:766–72. doi: 10.1148/radiol.12121294
55. Choi J-H, Kim E-K, Kim SM, Kim H, Song YB, Hahn J-Y, et al. Noninvasive discrimination of coronary chronic total occlusion and subtotal occlusion by coronary computed tomography angiography. *JACC Cardiovasc Interv.* (2015) 8:1143–53. doi: 10.1016/j.jcin.2015.03.042
56. Opolski MP, Achenbach S. CT angiography for revascularization of CTO: crossing the borders of diagnosis and treatment. *JACC Cardiovasc Imaging.* (2015) 8:846–58. doi: 10.1016/j.jcmg.2015.05.001
57. Li P, Xu L, Yang L, Wang R, Hsieh J, Sun Z, et al. Blooming artifact reduction in coronary artery calcification by a new de-blooming algorithm: initial study. *Sci Rep.* (2018) 8:6945. doi: 10.1038/s41598-018-25352-5
58. Mahnken AH, Mühlenbruch G, Günther RW, Wildberger JE. CT imaging of myocardial viability: experimental and clinical evidence. *Cardiovasc J Afr.* (2007) 18:169–74.
59. Mahnken AH, Bruners P, Kinzel S, Katoh M, Mühlenbruch G, Günther RW, et al. Late-phase MSCT in the different stages of myocardial infarction: animal experiments. *Eur Radiol.* (2007) 17:2310–7. doi: 10.1007/s00330-006-0569-7
60. Buecker A, Katoh M, Krombach GA, Spuentrup E, Bruners P, Günther RW, et al. A feasibility study of contrast enhancement of acute myocardial infarction in multislice computed tomography: comparison with magnetic resonance imaging and gross morphology in pigs. *Invest Radiol.* (2005) 40:700–4. doi: 10.1097/01.rli.0000179524.58411.a2
61. Opolski MP, Achenbach S, Schuhbäck A, Rolf A, Möllmann H, Nef H, et al. Coronary computed tomographic prediction rule for time-efficient guidewire crossing through chronic total occlusion: insights from the CT-RECTOR multicenter registry (Computed Tomography Registry of Chronic Total Occlusion Revascularization). *JACC Cardiovasc Interv.* (2015) 8:257–67. doi: 10.1016/j.jcin.2014.07.031
62. Fujino A, Otsuji S, Hasegawa K, Arita T, Takiuchi S, Fujii K, et al. Accuracy of J-CTO score derived from computed tomography versus angiography to predict successful percutaneous coronary intervention. *JACC Cardiovasc Imaging.* (2018) 11:209–17. doi: 10.1016/j.jcmg.2017.01.028
63. Magro M, Schultz C, Simsek C, Garcia-Garcia HM, Regar E, Nieman K, et al. Computed tomography as a tool for percutaneous coronary intervention of chronic total occlusions. *EuroIntervention.* (2010) 6(Suppl. G):G123–31.
64. Rolf A, Werner GS, Schuhbäck A, Rixe J, Möllmann H, Nef HM, et al. Preprocedural coronary CT angiography significantly improves success rates of PCI for chronic total occlusion. *Int J Cardiovasc Imaging.* (2013) 29:1819–27. doi: 10.1007/s10554-013-0258-y
65. Opolski MP, Debski A, Borucki BA, Staruch AD, Kepka C, Rokicki JK, et al. Feasibility and safety of augmented-reality glass for computed tomography-assisted percutaneous revascularization of coronary chronic total occlusion: A single center prospective pilot study. *J Cardiovasc Comput Tomogr.* (2017) 11:489–96. doi: 10.1016/j.jcct.2017.09.013
66. Kumbhani DJ, Ingelmo CP, Schoenhagen P, Curtin RJ, Flamm SD, Desai MY. Meta-analysis of diagnostic efficacy of 64-slice computed tomography in the evaluation of coronary in-stent restenosis. *Am J Cardiol.* (2009) 103:1675–81. doi: 10.1016/j.amjcard.2009.02.024
67. Wan Y-L, Tsay P-K, Chen C-C, Juan Y-H, Huang Y-C, Chan W-H, et al. Coronary in-stent restenosis: predisposing clinical and stent-related factors, diagnostic performance and analyses of inaccuracies in 320-row computed tomography angiography. *Int J Cardiovasc Imaging.* (2016) 32(Suppl. 1):105–15. doi: 10.1007/s10554-016-0872-6
68. Eckert J, Renczes-Janetzko P, Schmidt M, Magedanz A, Voigtländer T, Schmermund A. Coronary CT angiography (CCTA) using third-generation dual-source CT for ruling out in-stent restenosis. *Clin Res Cardiol.* (2019) 108:402–10. doi: 10.1007/s00392-018-1369-1
69. Andreini D, Mushtaq S, Pontone G, Conte E, Collet C, Sonck J, et al. CT perfusion versus coronary CT angiography in patients with suspected in-stent restenosis or CAD progression. *JACC Cardiovasc Imaging.* (2020) 13:732–42. doi: 10.1016/j.jcmg.2019.05.031
70. Andreini D, Mushtaq S, Pontone G, Rogers C, Pepi M, Bartorelli AL. Severe in-stent restenosis missed by coronary CT angiography and accurately detected with FFRCT. *Int J Cardiovasc Imaging.* (2017) 33:119–20. doi: 10.1007/s10554-016-0971-4
71. Attili AK, Schuster A, Nagel E, Reiber JH, van der Geest RJ. Quantification in cardiac MRI: advances in image acquisition and processing. *Int J Cardiovasc Imaging.* (2010) 26(Suppl. 1):27–40. doi: 10.1007/s10554-009-9571-x

72. Li H, Metze P, Abaei A, Rottbauer W, Just S, Lu Q, et al. Feasibility of real-time cardiac MRI in mice using tiny golden angle radial sparse. *NMR Biomed.* (2020) 33:e4300. doi: 10.1002/nbm.4300
73. Nagel E, Klein C, Paetsch I, Hettwer S, Schnackenburg B, Wegscheider K, et al. Magnetic resonance perfusion measurements for the noninvasive detection of coronary artery disease. *Circulation.* (2003) 108:432–7. doi: 10.1161/01.CIR.0000080915.35024.A9
74. Buckert D, Dewes P, Walcher T, Rottbauer W, Bernhardt P. Intermediate-term prognostic value of reversible perfusion deficit diagnosed by adenosine CMR: a prospective follow-up study in a consecutive patient population. *JACC Cardiovasc Imaging.* (2013) 6:56–63. doi: 10.1016/j.jcmg.2012.08.011
75. Buckert D, Witzel S, Steinacker JM, Rottbauer W, Bernhardt P. Comparing cardiac magnetic resonance-guided versus angiography-guided treatment of patients with stable coronary artery disease: results from a prospective randomized controlled trial. *JACC Cardiovasc Imaging.* (2018) 11:987–96. doi: 10.1016/j.jcmg.2018.05.007
76. Jahnke C, Nagel E, Gebker R, Kokocinski T, Kelle S, Manka R, et al. Prognostic value of cardiac magnetic resonance stress tests: adenosine stress perfusion and dobutamine stress wall motion imaging. *Circulation.* (2007) 115:1769–76. doi: 10.1161/CIRCULATIONAHA.106.652016
77. Stacey RB, Vera T, Morgan TM, Jordan JH, Whitlock MC, Hall ME, et al. Asymptomatic myocardial ischemia forecasts adverse events in cardiovascular magnetic resonance dobutamine stress testing of high-risk middle-aged and elderly individuals. *J Cardiovasc Magn Reson.* (2018) 20:75. doi: 10.1186/s12968-018-0492-5
78. Monti L, Di Giovine G, Scardino C, Nardi B, Balzarini L, Gasparini G. Role of adenosine stress CMR before chronic total occlusion reopening. *J Cardiovasc Magn Reson.* (2016) 18:80. doi: 10.1186/1532-429X-18-S1-P80
79. Pica S, Di Giovine G, Bollati M, Testa L, Bedogni F, Camporeale A, et al. Cardiac magnetic resonance for ischaemia and viability detection. Guiding patient selection to revascularization in coronary chronic total occlusions: The CARISMA_CTO study design. *Int J Cardiol.* (2018) 272:356–62. doi: 10.1016/j.ijcard.2018.08.061
80. Baer FM, Voth E, LaRosée K, Schneider CA, Theissen P, Deutsch HJ, et al. Comparison of dobutamine transesophageal echocardiography and dobutamine magnetic resonance imaging for detection of residual myocardial viability. *Am J Cardiol.* (1996) 78:415–9. doi: 10.1016/s0002-9149(96)00329-3
81. Baer FM, Theissen P, Schneider CA, Voth E, Sechtem U, Schicha H, et al. Dobutamine magnetic resonance imaging predicts contractile recovery of chronically dysfunctional myocardium after successful revascularization. *J Am College Cardiol.* (1998) 31:1040–8. doi: 10.1016/s0735-1097(98)00032-1
82. Schuster A, Kutty S, Padiyath A, Parish V, Gribben P, Danford DA, et al. Cardiovascular magnetic resonance myocardial feature tracking detects quantitative wall motion during dobutamine stress. *J Cardiovasc Magn Reson.* (2011) 13:58. doi: 10.1186/1532-429X-13-58
83. Zhang LJ, Dong W, Li JN, Mi HZ, Jiao J, Dou RY, et al. Quantification of late gadolinium enhancement cardiovascular MRI in patients with coronary artery chronic total occlusion. *Clin Radiol.* (2020) 75:643.e19-643.e26. doi: 10.1016/j.crad.2020.03.032
84. Bernhardt P, Spiess J, Levenson B, Pilz G, Höfling B, Hombach V, et al. Combined assessment of myocardial perfusion and late gadolinium enhancement in patients after percutaneous coronary intervention or bypass grafts: a multicenter study of an integrated cardiovascular magnetic resonance protocol. *JACC Cardiovasc Imaging.* (2009) 2:1292–300. doi: 10.1016/j.jcmg.2009.05.011
85. Nakachi T, Kato S, Kirigaya H, Iinuma N, Fukui K, Saito N, et al. Prediction of functional recovery after percutaneous coronary revascularization for chronic total occlusion using late gadolinium enhanced magnetic resonance imaging. *J Cardiol.* (2017) 69:836–42. doi: 10.1016/j.jjcc.2017.01.002
86. Bucciarelli-Ducci C, Auger D, Di Mario C, Locca D, Petryka J, O'Hanlon R, et al. CMR guidance for recanalization of coronary chronic total occlusion. *JACC Cardiovasc Imaging.* (2016) 9:547–56. doi: 10.1016/j.jcmg.2015.10.025
87. Ortiz-Pérez JT, Rodríguez J, Meyers SN, Lee DC, Davidson C, Wu E. Correspondence between the 17-segment model and coronary arterial anatomy using contrast-enhanced cardiac magnetic resonance imaging. *JACC Cardiovasc Imaging.* (2008) 1:282–93. doi: 10.1016/j.jcmg.2008.01.014
88. Chen Y, Zheng X, Jin H, Deng S, Ren D, Greiser A, et al. Role of myocardial extracellular volume fraction measured with magnetic resonance imaging in the prediction of left ventricular functional outcome after revascularization of chronic total occlusion of coronary arteries. *Korean J Radiol.* (2019) 20:83–93. doi: 10.3348/kjr.2018.0069
89. Rahimi K, Banning AP, Cheng AS, Pegg TJ, Karamitsos TD, Channon KM, et al. Prognostic value of coronary revascularisation-related myocardial injury: a cardiac magnetic resonance imaging study. *Heart.* (2009) 95:1937–43. doi: 10.1136/hrt.2009.173302
90. McEntegart M, Corcoran D, Carrick D, Clerfond G, Sidik N, Collison D, et al. Incidence of procedural myocardial infarction and cardiac magnetic resonance imaging-detected myocardial injury following percutaneous coronary intervention with rotational atherectomy. *EuroIntervention.* (2018) 14:819–23. doi: 10.4244/EIJ-D-17-01077
91. Kato S, Kitagawa K, Ishida N, Ishida M, Nagata M, Ichikawa Y, et al. Assessment of coronary artery disease using magnetic resonance coronary angiography: a national multicenter trial. *J Am College Cardiol.* (2010) 56:983–91. doi: 10.1016/j.jacc.2010.01.071
92. Schuetz GM, Zacharopoulou NM, Schlattmann P, Dewey M. Meta-analysis: noninvasive coronary angiography using computed tomography versus magnetic resonance imaging. *Ann Intern Med.* (2010) 152:167–77. doi: 10.7326/0003-4819-152-3-201002020-00008
93. Hosoda H, Asaumi Y, Noguchi T, Morita Y, Kataoka Y, Otsuka F, et al. Correction to: Three-dimensional assessment of coronary high-intensity plaques with T1-weighted cardiovascular magnetic resonance imaging to predict periprocedural myocardial injury after elective percutaneous coronary intervention. *J Cardiovasc Magn Reson.* (2020) 22:27. doi: 10.1186/s12968-020-00620-4
94. Stuijfzand WJ, Raijmakers PG, Driessen RS, van Royen N, Nap A, van Rossum AC, et al. Value of hybrid imaging with PET/CT to guide percutaneous revascularization of chronic total coronary occlusion. *Curr Cardiovasc Imaging Rep.* (2015) 8:26. doi: 10.1007/s12410-015-9340-2
95. Vitadello T, Kunze KP, Nekolla SG, Langwieser N, Bradaric C, Weis F, et al. Hybrid PET/MR imaging for the prediction of left ventricular recovery after percutaneous revascularisation of coronary chronic total occlusions. *Eur J Nucl Med Mol Imaging.* (2020) 47:3074–83. doi: 10.1007/s00259-020-04877-w

Conflict of Interest: The authors declare that the research was conducted in the absence of any commercial or financial relationships that could be construed as a potential conflict of interest.

frontiers in Cardiovascular Medicine

REVIEW
published: 22 September 2021
doi: 10.3389/fcvm.2021.736223

Artificial Intelligence Based Multimodality Imaging: A New Frontier in Coronary Artery Disease Management

*Riccardo Maragna[1], Carlo Maria Giacari[1], Marco Guglielmo[1], Andrea Baggiano[1,2], Laura Fusini[1], Andrea Igoren Guaricci[3], Alexia Rossi[4,5], Mark Rabbat[6,7] and Gianluca Pontone[1]**

[1] Centro Cardiologico Monzino, Istituto di Ricovero e Cura a Carattere Scientifico (IRCCS), Milan, Italy, [2] Department of Clinical Sciences and Community Health, Cardiovascular Section, University of Milan, Milan, Italy, [3] Department of Emergency and Organ Transplantation, Institute of Cardiovascular Disease, University Hospital Policlinico of Bari, Bari, Italy, [4] Department of Nuclear Medicine, University Hospital Zurich, Zurich, Switzerland, [5] Center for Molecular Cardiology, University Hospital Zurich, Zurich, Switzerland, [6] Department of Medicine and Radiology, Division of Cardiology, Loyola University of Chicago, Chicago, IL, United States, [7] Department of Medicine, Division of Cardiology, Edward Hines Jr. VA Hospital, Hines, IL, United States

Coronary artery disease (CAD) represents one of the most important causes of death around the world. Multimodality imaging plays a fundamental role in both diagnosis and risk stratification of acute and chronic CAD. For example, the role of Coronary Computed Tomography Angiography (CCTA) has become increasingly important to rule out CAD according to the latest guidelines. These changes and others will likely increase the request for appropriate imaging tests in the future. In this setting, artificial intelligence (AI) will play a pivotal role in echocardiography, CCTA, cardiac magnetic resonance and nuclear imaging, making multimodality imaging more efficient and reliable for clinicians, as well as more sustainable for healthcare systems. Furthermore, AI can assist clinicians in identifying early predictors of adverse outcome that human eyes cannot see in the fog of "big data." AI algorithms applied to multimodality imaging will play a fundamental role in the management of patients with suspected or established CAD. This study aims to provide a comprehensive overview of current and future AI applications to the field of multimodality imaging of ischemic heart disease.

Keywords: artificial intelligence, coronary artery disease, multimodality imaging, machine learning, deep learning, radiomics

OPEN ACCESS

Edited by:
Grigorios Korosoglou, GRN Klinik Weinheim, Germany

Reviewed by:
Alexandros Kallifatidis, St. Luke's Hospital, Greece
Anastasios Panagopoulos, University of Nebraska Medical Center, United States

***Correspondence:**
Gianluca Pontone
gianluca.pontone@ccfm.it

Specialty section:
This article was submitted to Cardiovascular Imaging, a section of the journal Frontiers in Cardiovascular Medicine

Received: *04 July 2021*
Accepted: *25 August 2021*
Published: *22 September 2021*

Citation:
Maragna R, Giacari CM, Guglielmo M, Baggiano A, Fusini L, Guaricci AI, Rossi A, Rabbat M and Pontone G (2021) Artificial Intelligence Based Multimodality Imaging: A New Frontier in Coronary Artery Disease Management. Front. Cardiovasc. Med. 8:736223. doi: 10.3389/fcvm.2021.736223

INTRODUCTION

Cardiovascular disease represents one of the leading causes of morbidity and mortality in the world (1). In 2017, coronary artery disease (CAD) affected 1.72% of the global population and was recognized as the leading cause of death (1).

This highlights the need of an effective and efficient diagnostic-therapeutic path for the diagnosis and risk stratification of CAD patients.

CAD management has dramatically changed over the past few decades. Currently, invasive coronary angiography remains the gold standard for patients with a high risk of CAD allowing for both the diagnosis and potential for therapeutic intervention. However, this strategy is time consuming and prone to intra- or periprocedural risks (e.g., bleeding risk, puncture site bleeding,

coronary artery dissection, radiation exposure, and contrast induced nephrotoxicity) and thus is typically not recommended as a first line strategy for patients at low-to-intermediate risk for CAD.

In this category of patients, multimodality imaging is assuming an increasingly important role, as outlined in the latest ESC guidelines on the management of chronic coronary syndromes (CCS) (2), with the aim of both improving the early detection of significant asymptomatic CAD and making the diagnostic workflow more efficient; for example, by avoiding a large number of negative invasive coronary angiograms.

With the increasing availability of powerful computers and large datasets, the implementation of artificial intelligence (AI) in the current workflow of multimodality imaging for CAD diagnosis appears a promising tool in aiding cardiologists and radiologists in the growing demand of cardiovascular imaging examinations.

In this review, we will explore the current AI applications of multimodality imaging applied to CAD management, highlighting the great potential and possible pitfalls of this new frontier in CAD management.

BASIC CONCEPTS OF ARTIFICIAL INTELLIGENCE

The term AI outlines the ambitious attempt to replicate with a machine the most distinctive feature of the human being, its ability to think. In order to simulate the characteristics of human thought, an AI algorithm must be able to perform tasks considered distinctive of a human being: to understand a language, to recognize images, to identify known objects, to solve problems, and to learn from its own mistakes.

The concept of AI was first mentioned in 1956 (3). At that time its implementation in real life appeared to most people as a distant futuristic utopia. However, AI applications are rapidly entering everyday life (4–6) and the medical field, possibly representing a new frontier for the evolution of our society.

AI algorithms can be developed with the increasing availability of large amounts of data ("big-data") and powerful computational machines.

AI applications are based on two main methods: machine learning (ML) and deep learning (DL).

ML is a technique that provides AI algorithms the ability to learn when exposed to large datasets of correctly classified features. Beyond the quality of the algorithm itself, the quality of the characterization of the data and their heterogeneity are crucial factors for the real-world application of the algorithm. For this reason, ML applications are first developed on training and validation datasets and then tested in an independent dataset to verify their adaptability for use outside the domain in which they were developed.

Two main models of ML have been developed to date: supervised and unsupervised learning. The main difference between these two methods resides in the presence or absence of a prefixed outcome. In supervised learning the AI model navigates the dataset to find the best combination of features that fits with the prefixed outcome; while in unsupervised learning the algorithm simply tries to discover any potential consistent pattern concealed in the dataset (6).

Examples of ML supervised learning methods are regression analysis, support vector machines (SVM) and random forests (RF); while unsupervised learning is funded on principal component and cluster analysis approaches. A more detailed explanation of these concepts goes beyond the scope of this review (6).

DL can be considered a particular subset of ML that uses multiple artificial neural networks to directly interrogate datasets to make predictions. In the medical imaging context, the most widely DL network is represented by Convoluted Neural Network (CNN), a network of multiple interconnected layers that roughly mimics the functioning of the visual human cortex (6). In the context of cardiovascular imaging both ML and DL have been applied. The former has mainly been used to predict diagnostic or prognostic outcomes and bases the analysis on datasets of manually labeled image features; while the latter have directly been applied to images in order to automatically obtain diagnoses (6, 7).

Early-stage AI applications were deployed to automate time-consuming medical tasks to reduce workload (e.g., to shorten image acquisition, image analysis and reporting time); more recently their development has been focused to more complex duties, such as to perform autonomous diagnoses and risk-stratification (8).

In this context, in recent years a new technique called radiomics has emerged as a new tool to combine with traditional AI applications to dig deep into the images to identify possible risk predictors or unearth features that can lead to early diagnoses. Radiomics is able to convert every voxel of a digital medical image in a high amount of quantitative mathematical imaging data that can be later analyzed by high-performance computers and AI algorithms (9, 10). This analysis can aid the human operator to see beyond the limit of its eye, revealing textures concealed behind medical images; when combined together, this information can be automatically quantified and analyzed by AI with a process called "texture analysis" that can lead to new diagnostic tools or prognostic models.

AI APPLICATIONS IN THE CLINICAL WORKFLOW OF CAD PATIENTS

The most recent ESC guidelines on CCS base the choice of the diagnostic tool for CAD detection on the pre-test individual clinical likelihood of disease, in order to select the most appropriate invasive or non-invasive diagnostic test to perform, according to individual patient characteristics (2).

Figure 1 highlights AI applications deployed in all the steps of the diagnostic definition of CAD, from pre-test risk definition to their implementation in individual imaging methods used in clinical practice for CAD assessment.

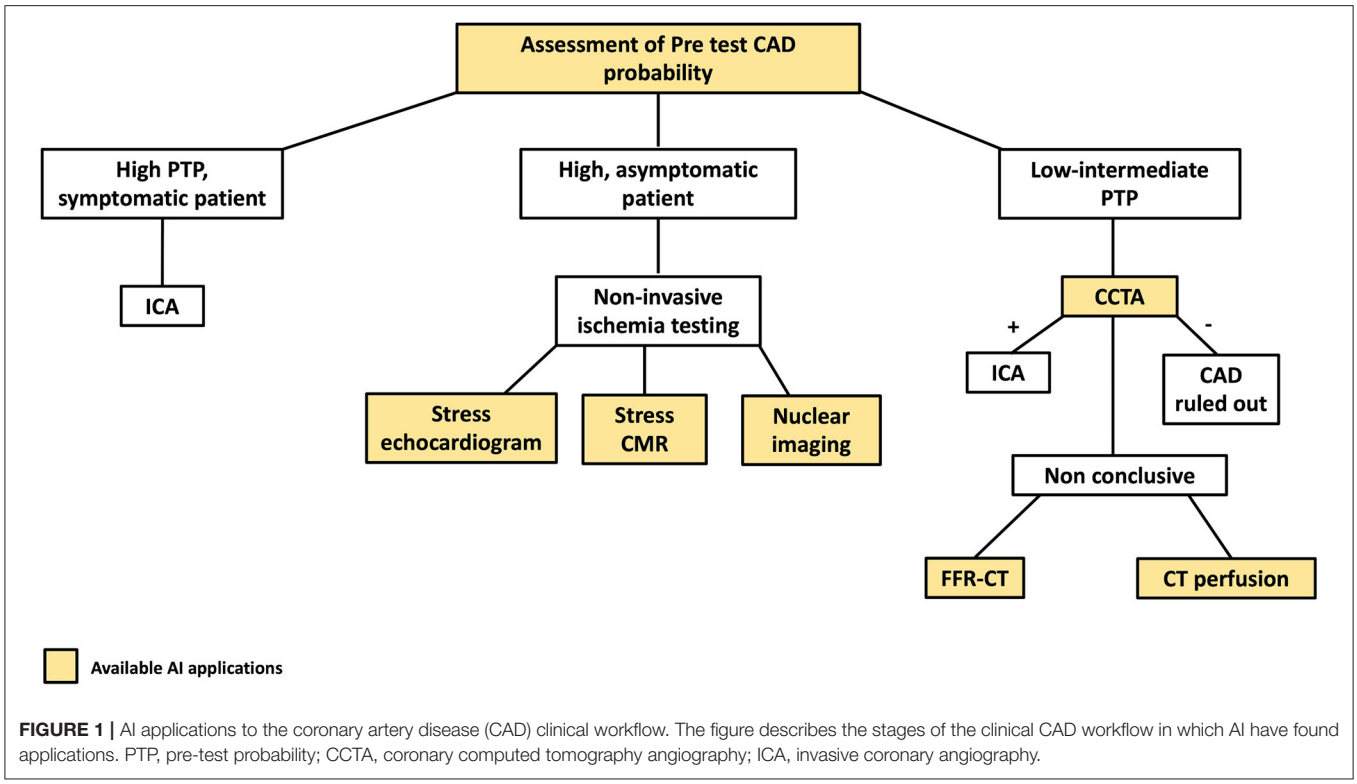

FIGURE 1 | AI applications to the coronary artery disease (CAD) clinical workflow. The figure describes the stages of the clinical CAD workflow in which AI have found applications. PTP, pre-test probability; CCTA, coronary computed tomography angiography; ICA, invasive coronary angiography.

AI APPLICATIONS IN CAD PRE-TEST LIKELIHOOD DEFINITION

The last ESC Guidelines base the definition of the pre-test individual likelihood of CAD from a pooled analysis of clinical and demographic characteristics (i.e., age, sex, and the nature of symptoms) of 15,815 patients symptomatic for chest pain (2). Many clinical models that incorporate information on clinical risk factors for CVD, resting ECG changes, or coronary artery calcification have improved the identification of patients with obstructive CAD and the Guidelines recognize these factors as an integrated part of cardiovascular risk evaluation, to better identify a personalized clinical likelihood of CAD.

In addition, imaging parameters such as coronary artery calcium (CAC) score and epicardial adipose tissue (EAT) quantification are assuming a role of increasing importance in the quantification of cardiovascular risk.

In this paragraph, we will summarize the principal AI applications developed for the automatic quantification of CAC and EAT (**Table 1**).

AI Applications for Coronary Artery CAC Scoring

CAC score is a well-established predictor of obstructive CAD, particularly useful in identifying patients with high CV risk, independent of clinical risk assessment scores.

CAC scoring requires dedicated software for semi-automatic image segmentation and time demanding manual measurement by trained experts on a dedicated ECG-gated cardiac CT. This time-consuming approach is not feasible for everyday clinical practice and hinders the application of CAC score on non-targeted routine chest CT, despite the demonstration of its good reliability on non-targeted CT exams (20), thus limiting the large-scale application of CAC score as a screening method for CAD.

The application of AI algorithm for CAC scoring in dedicated non-contrast-enhanced, ECG-gated CT scans is feasible, as demonstrated by Sandstedt et al. (14), who demonstrated an excellent comparability of a fully automated CAC score AI application vs. a traditional semi-automated measurement in 315 CAC-scoring dedicated CT scans ($r = 0.935$ for Agatston score assessment between the two methods). Similarly, Wolterink et al. (12), developed a ML approach that automatically quantified total patient and per coronary artery calcifications and selected the most complex cases to be reviewed by experts. This system led to an excellent intra-class correlation coefficient between the manual and the AI determined coronary artery CAC volume of 0.95. Similar results were obtained for CAC volume for each epicardial coronary artery.

CAC score analysis can express its full potential as a screening tool if applied on a large scale, even in examinations not aimed at cardiac analysis, as in the case of patients undergoing low-dose chest CT for cancer screening or follow-up.

In this context, the application of ML and DL algorithms has proven their efficacy in ensuring automatic measurement of CAC score values in large datasets of low-dose, non-ECG gated CT scans (>1,500 CT scans) performed for lung cancer screening (11, 13).

TABLE 1 | Main AI powered imaging methods for the definition of the pre-test likelihood of CAD.

References	Summary	Performance
CAC scoring		
Takx et al. (11)	Automated CAC scoring on non-contrast-enhanced, non-gated chest CT recorded for lung cancer screening	$k = 0.85$ for Agatston risk categories between the automated and reference scores
Wolterink et al. (12)	Automated per patient and per coronary artery CAC scoring	High ICCs (0.98 for LAD; 0.69 for LCx and 0.95 for RCA) for CAC volume scoring compared with manual scoring
Lessmann et al. (13)	Automated CAC scoring on low-dose chest CT recorded for lung cancer screening	*k* coefficient = 0.9 for risk category assignment based on per subject coronary artery calcium
Sandstedt et al. (14)	Automated CAC scoring on non-contrast CT images	High correlation ($\rho = 0.935$) between AI and traditional Agatston score determination
van Velzen et al. (15)	Automated CAC scoring automatically adapting to non-contrast CT scans performed with multiple acquisition protocols	ICCs of 0.79–0.97 for CAC scoring among different scan types and $k = 0.9$ in patients' risk stratification according to Agatston score
Zeleznik et al. (16)	Automated CAC scoring on CT scans performed with multiple acquisition protocols and in different clinical scenarios	High correlation ($\rho = 0.92$) with manually measured CAC scores; accurate risk stratification for CVE across CT scans acquired with different protocols, in patients with different clinical presentations*
EAT analysis		
Commandeur et al. (17)	Automated EAT quantification	High correlation ($\rho = 0.97$) with manual quantification
Commandeur et al. (18)	Prediction of hard CVE though a ML algorithm	Higher AUC for the AI application compared to clinical risk scores (0.82) and CAC score (0.77)
Eisenberg et al. (19)	MACE prediction through a fully automated EFV and attenuation quantification	Increased EAT volume and decreased EAT attenuation were both independently associated with MACE (HR 1.35 and 0.83, respectively)

AUC, area under the curve; CAC, Coronary artery calcium; CVE, cardiovascular events; EAT, epicardial adipose tissue; EFV, epicardial fat volume; HR, hazard ratio; k, correlation coefficient; ICCs, intra class correlations; MACE, major cardiovascular events; ρ, Spearman correlation coefficient.
**In the context of both primary and secondary CAD prevention and both in patients with acute and chronic chest pain.*

Based on the demonstration that AI applications were reliable in quantifying CAC on CT scans not targeted for that scope, Van Velzen et al. (15) demonstrated how a DL method can adapt to different types of CT examinations and acquisition protocols, if trained to do so. In this study, the authors elaborated a DL algorithm composed of two consecutive CNN. The algorithm was then trained on large datasets of more than 7,000 CT acquired with different CT protocols. The DL application showed a remarkable correlation with manual CAC scoring, both in correctly identifying CAC among different scan types (internal class correlation comprised between 0.79 and 0.97) and in correctly risk stratifying patients according to their Agatston score (*k* correlation for all test= 0.9).

Recently, a study by Zeleznik et al. (16) confirmed the possibility to broadly use AI applications to use CTs acquired in different clinical scenarios to screen for CAD using CAC score. The authors first developed a DL application trained to identify and quantify CAC based on manual segmentations performed by expert CT readers on 1,636 cardiac CT scans. Two CNN were trained for the correct localization and segmentation of the heart and then tested among CT scans acquired with different protocols. The DL application not only demonstrated high correlation with manually measured CAC scores (rho = 0.92) in a cohort of 5,521 patients, but accurately stratified the risk for cardiovascular events across a large test cohort of 19,421 patients with different clinical presentations (from primary to secondary CAD prevention and acute to chronic chest pain settings) and different CT scan acquisition protocols (predicted AUC for automated and manual CAC score event prediction were 0.74 and 0.75, respectively, $p = 0.544$).

AI powered CAC score has the potential to become a fundamental tool for risk stratification of patients with suspected acute or chronic CAD, helping the clinician in correctly defining the cardiovascular risk profile of each individual patient.

AI Applications for Epicardial and Pericoronary Adipose Tissue Characterization

Interest has grown toward the correct quantification and analysis of the epicardial adipose tissue (EAT), namely the fat layer located between the myocardium and the visceral pericardium (**Figure 2**), due to the emerging evidence that identified its role in atherosclerosis development and consequently in obstructive CAD (21). An even more important role in atherosclerosis seems to be played by the pericoronary adipose tissue (PCAT), the EAT layer directly surrounding the coronary arteries.

In physiological conditions it is fundamental in maintaining the homeostasis of the vascular wall; while when dysfunctional (e.g., in inflammatory conditions) it plays a key role in atherogenesis by the production of pro-inflammatory cytokines.

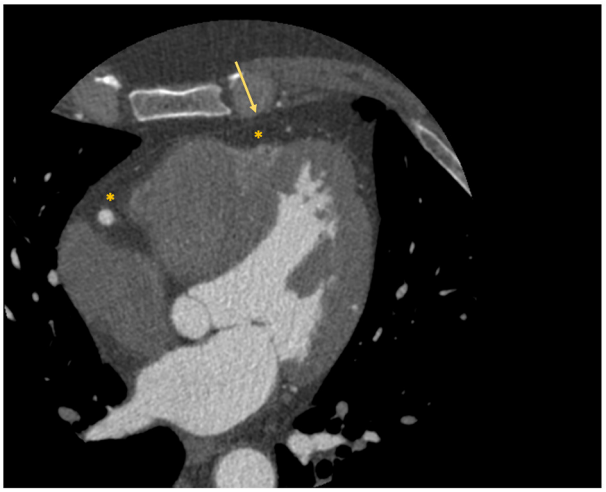

FIGURE 2 | Localization of epicardial adipose tissue at cardiac CT scan. The figure depicts an example of visualization of the epicardial adipose tissue with a cardiac CT scan. The asterisk identifies the hypodense area of adipose tissue; while the arrow identifies the visceral pericardium.

Various cardiac imaging modalities are capable of quantifying EAT, ranging from traditional echocardiography to CMR and cardiac computed tomography. The latter has recently become the key modality in this field due to its ability not only to visualize and precisely quantify EAT, but also to assess the coronary arteries and the PCAT simultaneously.

A paper by Antonopoulos et al. (22) demonstrated the possibility to identify this inflammatory process with CCTA *via* an imaging biomarker called "fat attenuation index (FAI)." The authors showed that PCAT signal attenuation was a biomarker of adipose tissue inflammation and also demonstrated that FAI correlated with the presence of CAD and was associated with stenosis >50%.

AI applications have been developed to automate the processes of EAT and PCAT quantification and characterization.

Since conventional EAT measurement by semi-automated software can be time-consuming, several AI applications have been developed to shorten this process (17, 23, 24), proving their ability to correctly quantify EAT from non-contrast cardiac CT scans.

In 2020, two studies demonstrated the ability of AI powered solutions to improve patients cardiovascular risk stratification with the implementation of information regarding EAT in the analysis of non-contrast cardiac CT.

Commandeur et al. (18) created a ML algorithm that integrated clinical variables, CAC score and EAT quantification to predict hard cardiovascular events (i.e., MI or CV death) during a mean follow-up of 14.5 years in a large population of 1,912 asymptomatic subjects from the EISNER trial. The AI algorithm clearly outperformed both well-established clinical risk scores and CAC score in CV event prediction.

Similarly, Eisenberg et al. (19) confirmed the predictive value of the DL assessment of EAT volume as an independent cardiovascular risk factor; additionally, they found that the detection of EAT attenuation by their DL algorithm demonstrated a significant inverse correlation with the occurrence of cardiovascular events at follow-up.

Finally, two other studies used a combined AI powered radiomics approach to demonstrate the incremental value of assessing PCAT attenuation over traditional CCTA based cardiovascular risk prediction tools (25, 26).

AI-powered detection of imaging biomarkers shows the potential to impact individual cardiovascular risk stratification, a fundamental process to guide the selection of the most appropriate invasive or non-invasive diagnostic testing for CAD patients.

AI APPLICATIONS FOR CAD DIAGNOSIS AND RISK STRATIFICATION

Functional non-invasive ischemia testing is recommended in patients with high PTP (i.e., >15%) or known CAD; according to the last ESC Guidelines, non-invasive functional imaging should be primarily used to detect ischemia (2).

Myocardial ischemia can be detected through rest or stress induced wall motion abnormalities (RWMA) with stress echocardiograph and areas of reduced myocardial perfusion with stress cardiac magnetic resonance (S-CMR) and with nuclear radiology techniques.

In this section, we will summarize the principal AI applications developed for functional imaging.

AI APPLICATIONS TO REST AND STRESS ECHOCARDIOGRAPHY

Echocardiography is the most available imaging tool for the management of CAD patients. As aforementioned, stress echocardiography is recommended as one of the functional non-invasive imaging tests of choice for the detection of new onset coronary artery disease in the follow-up of CCS patients (2).

The impact of AI applications in echocardiography has been steadily growing: first applications served to improve image quality; gradually, the focus shifted to automatic diagnostic echocardiographic window classification and measures assessment (27).

AI solutions have mainly focused in reducing the high inter-observer variability in the evaluation of regional wall motion abnormalities (RWMA) with rest and stress echocardiography (**Table 2**).

The detection of RWMA on rest echocardiograms was initially attempted using ML methods, which demonstrated high levels of accuracy in distinguishing between normal and infarcted echocardiographic images by correctly identifying the presence of RWMAs (28, 33).

Kusunose et al. (29) demonstrated the application of DL in assessing RWMAs. The authors applied five different DL models to the rest echocardiograms of 300 known CAD patients and 100 age-matched controls. Known CAD patients had an equal distribution of scar myocardium in the territory of left

TABLE 2 | Main AI applications to rest and stress echocardiography.

References	Summary	Performance
Rest echocardiography		
Raghavendra et al. (28)	Automated detection of RWMAs on rest echocardiograms to identify CAD	96% sensibility and specificity in detecting RWMAs
Kusunose et al. (29)	Automated detection of RWMAs on rest echocardiograms to identify CAD	The DL algorithm performed similar to expert cardiologists in RWMAs detection (AUC 0.99 vs. 0.98; $p = 0.15$) and significantly outperformed the ability of resident physicians (AUC 0.99 vs. 0.9; $p = 0.002$
Stress echocardiography		
Mansor et al. (30)	Automated detection of RWMAs on rest and stress echocardiograms to identify CAD	80–85% accuracy in classifying RWMAs
Chykeyuk et al. (31)	Automated detection of RWMAs on rest and stress echocardiograms to identify CAD	93% accuracy in classifying RWMAs
Omar et al. (32)	Comparison of ML and DL algorithms for the automated detection of RWMAs on rest and stress echocardiograms to identify CAD	DL application demonstrated the best accuracy in detecting RWMAs (75% accuracy), followed by the RF (72%) and SVM (71%).

CAD, coronary artery disease; ML, machine learning; DL, deep learning; RF, random forest; RWMAs, regional wall motion abnormalities; SVM, support vector machine.

anterior descending, left circumflex and right coronary artery. The five DL models performed similarly to expert cardiologists in detecting RWMAs (AUC 0.99 vs. 0.98; $p = 0.15$) and significantly outperformed the ability of resident physicians (AUC 0.99 vs. 0.9; $p = 0.002$).

Initial attempts to apply AI to stress echocardiography were made using techniques of supervised ML. The first examples date back to 2008 and 2011, when Mansor et al. (30) used a Hidden Markov Model (HMM) to develop a cardiac wall segment model for a normal and an abnormal heart and tested it on rest, stress and combined rest and stress sequences in a relatively small dataset of 44 dobutamine stress echocardiograms (DSE), reaching an accuracy in classifying RWMA of 80–85% with the analysis of combined rest and stress sequences. Few years later, Chykeyuk et al. (31) improved this result using a Relevance Vector Model in a dataset of 173 DSE reaching an accuracy of 93%.

Omar et al. (32) compared different ML and DL algorithms in detecting RWMAs at stress echocardiography. A DL application using a CNN demonstrated the best accuracy by achieving a 75% accuracy, followed by the RF (72%) and SVM (71%).

AI applications (both with ML and DL) to rest and stress echocardiography have shown good results in detecting RWMAs for CAD diagnosis. In particular, they demonstrated high accuracy both with rest and stress images, improving on the high inter-observer variability experienced in human evaluation. Further developments and test cohorts are required for the wide-spread clinical implementation of AI in real-life echocardiographic workflow for CAD diagnosis.

AI APPLICATIONS TO STRESS CARDIAC MAGNETIC RESONANCE

S-CMR is a powerful diagnostic tool that allows a comprehensive evaluation of known or suspected CAD patients.

Different from other techniques, S-CMR combines the evaluation of global cardiac function with an accurate and reproducible definition of regional myocardial viability by combining information on cardiac muscle function, tissue characterization, persistent and inducible ischemia (34).

Below, we will summarize AI applications to S-CMR for the assessment of cardiac function, tissue characterization and rest and stress myocardial perfusion (**Table 3**).

Cardiac Function

The first AI applications to S-CMR were focused on semi-automated myocardial segmentation on cine CMR images, in order to speed-up the manual time-consuming process of endo- and epicardial border definition. Many applications have sought to automate the analysis of cine CMR images (36, 48).

Although highly accurate, the majority of these applications were tested on small training datasets, thus limiting their real-life applicability. Bai et al. (35) overcame this limitation by applying a DL algorithm for myocardial segmentation in the UK Biobank, thus training the CNN on the cine CMR images of more than 4,500 patients. When applied on a test set of 600 patients, the DL application showed excellent correlation with manual measurements, with a mean absolute difference of ∼6 mL for left ventricular end-diastolic volume (LVEDV), 5 mL for left ventricular end-systolic volume (LVESV) and 7 g for left ventricular mass.

Tissue Characterization

The correct identification and quantification of the areas of late gadolinium enhancement (LGE) on CMR images portends a well-established prognostic role in CAD patients (49).

Some authors have successfully applied DL algorithms to perform automated LGE quantification (**Figure 3**).

Xu et al. (38) proposed an end-to-end DL algorithm composed of three function layers capable of detecting the MI area at the pixel level, thus automatically obtaining the extension, position,

TABLE 3 | Main AI applications to stress cardiac magnetic resonance (S-CMR).

References	Summary	Performance
Assessment of cardiac function		
Bai et al. (35)	Automated myocardial segmentation using a DL algorithm trained in a huge dataset (>4,500 subjects)	Excellent correlation with manual measurement (Dice's coefficient 0.94 for the LV cavity, 0.88 for the LV myocardium and 0.90 for the RV cavity)
Curiale et al. (36)	Automated LV quantification using DL	Good accuracy for myocardial segmentation (Dice's coefficient 0.9); high correlation index for LVEDV and LVESV (0.99), LV EF (0.95), and for SV and CO (0.93).
Tissue characterization		
Kotu et al. (37)	Arrhythmic risk stratification of CAD patients through the radiomic analysis of the scar tissue	Highly accurate (94%) classification of CAD patients in high- and low arrhythmic risk groups
Xu et al. (38)	Automated detection of MI	94% overall accuracy in detecting the MI area extension, position and shape
Larroza et al. (39)	Distinction of acute and chronic MI on CMR-LGE and non-enhanced CMR through an ML model combined with radiomics	High AUC, sensitivity and specificity in the distinction between acute and chronic MI both on CMR-LGE (0.86, 0.81, and 0.84, respectively) and on non-enhanced CMR (0.82, 0.79, and 0.80, respectively)
Larroza et al. (40)	Automated identification of myocardial transmural scar on non-enhanced CMR	Sensitivity of 92% for transmural scar identification
Baessler et al. (41)	Automated scar detection on non-enhanced CMR images with a combined ML and radiomics algorithm	Identification of five independent texture features, which allowed scar identification. The best features combination allowed an AUC of 0.93 and 0.92 for diagnosing large and small MI, respectively
Moccia et al. (42)	Comparison of two DL scar segmentation protocols for automated scar detection on CMR-LGE images	88% median sensitivity and 71% DICE similarity coefficient by the protocol that limited the analysis to the myocardial region.
Zabihollahy et al. (43)	Semiautomated DL method for LV myocardial scar segmentation from 3D CMR-LGE images.	94% DICE similarity coefficient for LV myocardial scar segmentation
Zhang et al. (44)	Automated detection, localization and quantification of myocardial fibrosis on non-enhanced CMR	No difference between non-enhanced cardiac cine and CMR-LGE analyses: number of scar segments ($p = 0.38$), mean per-patient scar area ($p = 0.27$) percentage of damaged myocardial tissue ($p = 0.17$)
Ma et al. (45)	Combination of radiomics and T1 mapping for the automated identification of MVO	Radiomics combined with T1 values compared to T1 values alone better identified MVO (AUC 0.86) and showed higher predictive value for LV longitudinal systolic myocardial contractility recovery (AUC 0.77).
Perfusion S-CMR		
Scannell et al. (46)	Automated processing and segmentation myocardial perfusion data on S-CMR	High accuracy compared to manual processing and segmentation (Dice similarity coefficient for myocardial segmentation 0.8)
Xue et al. (47)	Automated assessment of MBF on S-CMR	High accuracy compared to manual analysis in myocardial segmentation (Dice similarity coefficient 0.93). No difference in the per-sector MBF identification ($p = 0.92$)

CAD, coronary artery disease; CO, cardiac output; EF, ejection fraction; LGE, late-gadolinium enhancement; LV, left ventricle; LVEDV, left ventricle end diastolic volume; LVESV, left ventricle end systolic volume; MBF, myocardial blood flow; MI, myocardial infarction; MVO, microvascular obstruction; SV, stroke volume; SVM, support vector machine.

and shape of the MI area for each of the 114 patients analyzed, with a classification accuracy of 94%.

Two other authors developed different DL algorithms, both obtaining high DICE similarity coefficients in LGE quantification when compared to manual segmentation. In the first case, Moccia et al. (42) successfully modified and trained an existing DL application based on two CNN (ENet) to segment scar tissue on enhanced CMR images of 30 patients with known CAD. In the second case, Zabihollahy et al. (43), demonstrated an accurate three-dimensional segmentation of myocardial fibrotic tissue by using a semiautomated method using a 3D CNN.

Albeit promising, these studies are still based on small cohorts, thus limiting the applicability in the routine S-CMR workflow.

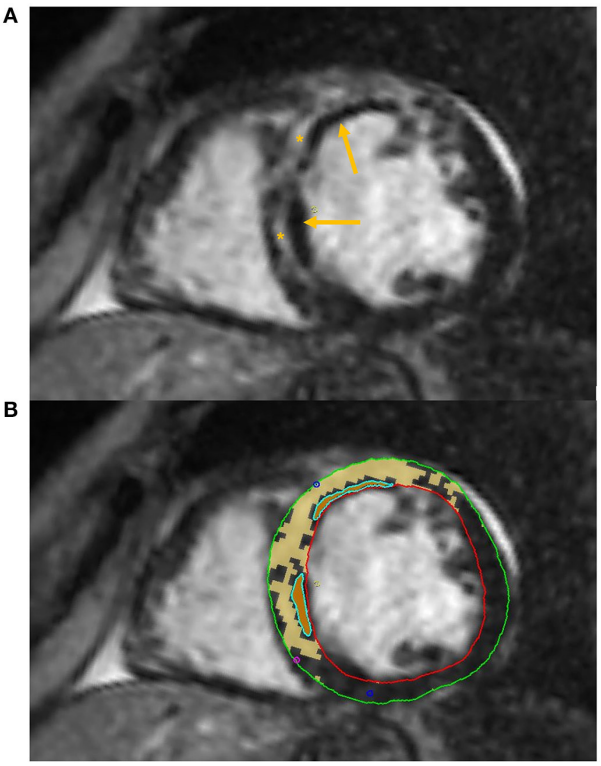

FIGURE 3 | Tissue characterization with Cardiac Magnetic Resonance (CMR). The figure shows an example of tissue characterization in a patient with a history of antero-septal myocardial infarction. **(A)** Depicts a transmural myocardial scar (asterisks) in the antero-septal region with concomitant evidence of subendocardial areas of microvascular obstruction (MVO, arrows). **(B)** Shows the automatic identification and quantification of late gadolinium enhancement and the semi-automatic identification of MVO areas on CMR images.

Zhang et al. (44) successfully developed a DL model capable to detect, localize and quantify myocardial areas of fibrosis in non-enhanced cine CMR of 212 CAD patients and 87 healthy controls. Notably, the authors did not find any difference between non-enhanced cardiac cine and LGE CMR analyses in the number of scar segments ($p = 0.38$), in the mean per-patient scar area ($p = 0.27$), and in the percentage of damaged myocardial tissue ($p = 0.17$). If confirmed on larger sample sizes, the ability of an AI model to correctly quantify myocardial LGE on unenhanced cine CMR images paves the way to the possibility to perform tissue characterization in patients with end stage renal disease on dialysis, which represents a contraindication to perform contrast enhanced CMR.

Other authors developed AI applications capable of assessing myocardial viability and scar area without the use of LGE with the combination of traditional AI models and radiomics. In two consecutive studies Larroza et al. (39) demonstrated the possibility to use a support vector machine (SVM) combined with radiomics texture analysis to distinguish between acute and chronic MI with similar sensitivity and specificity between analyses conducted on enhanced and non-enhanced cine CMR images and to identify non-viable myocardial segments (i.e., segments with LGE $\geq$ 50% transmural extension) in non-enhanced cine MRI sequences with a sensitivity of 92% (40).

Similarly, Baessler et al. (41) used a ML algorithm to select five independent texture analysis features to differentiate between ischemic scar and normal myocardium on non-enhanced cine MR images of 120 patients with chronic or subacute MI.

A recent study by Ma et al. (45) has also proven the ability of texture analysis combined with native T1 mapping values to better identify microvascular obstruction (MVO, **Figure 3**) compared to T1 mapping alone in a small group of patients with recent ST-segment-elevation MI. Combined radiomics features and native T1 values also provided a higher predictive value for LV longitudinal systolic myocardial contractility recovery compared to T1 values in a subset of patients that underwent 6-months follow up CMR.

Finally, Kotu et al. (37) provided an interesting proof of concept of how radiomics can help in CAD risk stratification. The authors successfully created a radiomic algorithm able to perform a correct risk-stratification for the occurrence of life-threatening arrhythmias in 34 known CAD patients on the basis of the radiomic analysis of the scar tissue.

Albeit deeply interesting, radiomics studies applied to CMR are still based on small datasets and currently does not appear feasible for large-scale routine use. Further investigations on larger CMR datasets are needed to broaden the spectrum of use.

Perfusion S-CMR

S-CMR can detect hemodynamically significant CAD through the assessment of myocardial ischemia through the evaluation of perfusion defects. In routine clinical practice, the analysis of S-CMR images is performed qualitatively, through the visual assessment of S-CMR images by an expert reporting physician.

First pass gadolinium enhanced CMR perfusion imaging has shown the potential to delineate a fully quantitative assessment of myocardial blood flow (MBF). Fully automatic MBF maps have been validated against gold standard perfusion techniques, such as positron emission tomography (50).

Albeit highly accurate in CAD diagnosis (51), quantitative S-CMR perfusion is time consuming and therefore restricted to research purposes (52).

In recent years, innovative AI applications have been developed to allow fully automated perfusion mapping approaches to enter clinical practice.

Preliminary work by Scannell et al. (46) successfully developed a DL algorithm to fully automatize image processing for myocardial perfusion assessment.

More recently, Xue et al. (47) validated a CNN model on more than 1,800 CMR rest and stress scans from 1,034 patients. The DL model showed excellent mean Dice similarity coefficient ratio of automatic and manual myocardial segmentation (0.93 ± 0.04) and did not differ significantly from per-sector MBF manual assessment ($p = 0.92$). The same group of authors demonstrated (53) that MBF and myocardial perfusion reserve (MPR, i.e., ratio of stress to rest MBF) automatically assessed using their DL model were independently associated with death and MACE in a cohort of >1,000 patients.

TABLE 4 | Main AI applications to nuclear imaging for the detection of ischemia.

References	Summary	Performance
Identification of patients with obstructive CAD		
Arsanjani et al. (56)	Comparison of automated quantification of myocardial perfusion SPECT to expert visual analysis	AUC for TPD was significantly better compared to visual evaluation of two expert analysis (0.91 vs. 0.87 and 0.89, $P < 0.01$).
Arsanjani et al. (57)	Comparison of automated quantification of myocardial perfusion SPECT integrated with clinical information to expert visual analysis and traditional TPD quantification	ML diagnostic accuracy (87%) was similar to Expert 1 (86%), but superior to TPD quantification (83%) and Expert 2 (82%) ($P < 0.01$).
Betancur et al. (58)	Automated prediction of obstructive CAD by DL algorithm on SPECT as compared with total perfusion deficit (TPD)	DL AUC for disease prediction was higher than for TPD (per patient analysis: 0.80 vs. 0.78; per vessel analysis: 0.76 vs. 0.73: $p < 0.01$)
Otaki et al. (59)	Automated prediction of obstructive CAD by externally validated DL algorithm on SPECT as compared to expert visual analysis and with total perfusion deficit (TPD)	DL AUC for obstructive CAD detection was higher than for TPD and visual assessment (0.80 vs. 0.73 and 0.65, respectively). The algorithm was self-explainable and externally validated
Prognostic evaluation		
Arsanjani et al. (60)	Application of ML algorithm to SPECT analysis to predict early revascularization in patients with suspected CAD	The ML algorithm showed similar sensitivity for prediction of revascularization to expert visual assessment (74% for both) with a better specificity he specificity of ML (75 vs. 67%, $P < 0.05$)
Betancur et al. (61)	MACE risk prediction with a ML application integrated with clinical and SPECT imaging features	3-years MACE prediction by ML application combined with clinical data outperformed ML with imaging data alone (AUC: 0.81 vs. 0.78) and showed also higher predictive accuracy compared with expert evaluation and automated TPD (AUC: 0.81 vs. 0.65 vs. 0.73, respectively)
Hu et al. (62)	Efficacy of per-vessel prediction of early revascularization compared among ML application, expert evaluation and standard TPD quantification	The per-vessel and per-patient AUC of early revascularization prediction (0.79 and 0.81, respectively) was higher than by TPD ($p < 0.001$) and outperformed qualitative experts' interpretation

AUC, area under the curve; CAD, coronary artery disease; SPECT, single positron emission tomography; TPD, total perfusion deficit.

This large, multicenter study paves the way for automatic assessment of MBF and MPR from quantitative CMR perfusion mapping to enter the routine diagnostic workflow of patients undergoing S-CMR.

AI APPLICATIONS TO NUCLEAR IMAGING FOR THE DETECTION OF ISCHEMIA

Nuclear radiology has been one of the first imaging methods applied to ischemia assessment in CAD patients and still represents the most widely used test to detect myocardial ischemia.

Single-photon emission computed tomography (SPECT) and positron emission tomography (PET) represent the two main tools of nuclear imaging applied to cardiology.

Despite its relative low cost and discrete accuracy in detecting CAD, the detection of ischemia by SPECT analysis mostly relies on qualitative methods and appears prone to possible CAD underestimation, especially in patients with non-obstructive multivessel coronary artery disease. PET is able to provide robust quantitative analysis of myocardial blood flow and can detect microvascular ischemia. However, the utilization of PET analysis is limited by its high technical complexity and high costs (54).

Apart from those aimed at image pre-processing and segmentation (55), the major AI applications to myocardial perfusion SPECT focused on boosting the power of cardiac nuclear imaging in two principal tasks: to identify patients with obstructive CAD and to define their prognosis (**Table 4**).

In 2013, Arsanjani et al. published two different studies on relatively large populations. The first one (56) demonstrating that a fully automated quantification of myocardial perfusion SPECT was equivalent on a per-patient level and superior on a per-vessel level, in detecting significant coronary artery stenosis (i.e., $\geq$ 70%) when compared with expert visual analysis. The second paper (57) analyzed the application of a ML LogitBoost model which integrated quantitative perfusion and clinical data to a dataset of 1,181 myocardial perfusion SPECTs. The AI application significantly outperformed the visual qualitative analysis of two expert readers who were provided with the same imaging, quantitative, and clinical data.

More recently, Betancur et al. (58) introduced the possibility to use a DL algorithm for the analysis of myocardial perfusion SPECT. The authors trained their application on a large

dataset of more than 1,500 myocardial perfusion SPECT polar maps. As previously demonstrated for the ML applications proposed by Arsanjani et al., the DL algorithm improved the identification of patients with obstructive CAD, compared to standard clinical evaluation.

Finally, Otaki et al. (59) recently introduced a novel DL algorithm for the detection of obstructive CAD following SPECT myocardial perfusion imaging. The AI application was first developed in a dataset of more than 2,000 patients and then externally tested in 555 patients with excellent AUC compared to traditional TPD quantification and expert visual assessment (AUC 0.80, 0.73, and 0.65, respectively). External validation of AI applications represents a fundamental step to obtain the fast implementation of AI algorithms in clinical practice and will soon be required for every newly developed AI algorithm.

ML and DL models have also been applied to myocardial perfusion SPECT to improve its prognostic value.

Arsanjani et al. (60) demonstrated how a ML application could improve the prediction of early revascularization in patients with suspected CAD undergoing perfusion SPECT. The authors developed a ML LogitBoost model that integrated clinical data and quantitative features derived from perfusion SPECT. When tested on 713 rest perfusion SPECT scans, the ML application showed comparable or better performance with respect to expert readers in predicting early revascularization.

Recently, Hu et al. (62) provided a more robust example of a ML algorithm able to perform a per-vessel prediction of early coronary revascularization (i.e., within 90 days) after SPECT myocardial perfusion imaging. To do so, the authors developed and tested ∼2,000 patients using a ML algorithm that integrated multiple clinical, stress test and SPECT imaging variables and compared its performance with standard quantitative SPECT analysis (i.e., total perfusion deficit, TPD) and expert evaluation. The LogitBoost application outperformed automatic myocardial perfusion quantitation by TPD and expert's interpretation.

Finally, Betancur et al. (61) developed a robust ML application integrated with clinical and imaging features. This model demonstrated high predictive accuracy to determine the risk of major cardiovascular adverse events (MACE) in a large population of 2,619 patients followed for ∼3 years. The algorithm demonstrated its superiority over all existing visual or automated perfusion assessments.

AI APPLICATIONS FOR CORONARY COMPUTED TOMOGRAPHY ANGIOGRAPHY

Initial applications of CCTA in CAD management were on the anatomical detection or exclusion of obstructive CAD, with CCTA progressively assuming the role of gatekeeper to unnecessary ICAs. Due to its high negative predictive power, CCTA has been indicated as the preferred test to rule out CAD in low to intermediate clinical PTP patients by the most recent ESC Guidelines on the management of CCS (2).

However, CCTA has rapidly advanced beyond the qualitative anatomical assessment of the presence of obstructive CAD and is now capable of offering a complete anatomical and functional characterization of CAD, thus providing important diagnostic and prognostic (63) information for patients' management.

In this section, we will review the principal AI applications developed for the anatomical and functional assessment of CAD with CCTA (**Table 5**).

Coronary Stenoses Grading

The degree of luminal stenosis and the localization of CAD with CCTA has a defined prognostic role (63). AI applications are trying to automate and standardize the process of coronary image reconstruction, segmentation and stenosis degree quantification, which currently relies on visual assessment and is troubled by high inter operator variability (79). Recently AI applications have also focused to significantly shorten reporting time (80), also with non-optimal images, i.e., in the presence of heavy calcifications or in the case of scarce image quality (81).

In 2011, Kelm et al. (64) developed one of the first examples of an AI algorithm capable of correctly analyzing CCTA images to detect, grade and classify as significant coronary stenoses caused by all types of plaques. The ML algorithm was composed of a multistep approach that included automatic centerline verification and lumen cross section estimation and showed good values of sensitivity and specificity (i.e., 95 and 67%, respectively) when compared with expert qualitative evaluation. Importantly, the time required for the ML algorithm to analyze each case was only 1.8 s.

Later, Kang et al. (65) used a different ML algorithm, which showed an even improved accuracy in CAD detection, despite a further reduction in the time required for analysis (only 1 s per case).

In 2019, Hong et al. (67), validated a DL algorithm with CNN across a dataset of 156 CCTAs. The application automatically performed coronary lumen and plaque segmentation and computed minimal luminal area (MLA), percent diameter stenosis (DS) and percent contrast density difference (CDD) with excellent correlation to expert readers ($r = 0.984$ for MLA; $r = 0.957$ for DS; and $r = 0.975$ for CDD, $p < 0.001$ for all).

Recently, Muscogiuri, et al. (68) demonstrated good results of a DL CNN in classifying CCTAs examinations in the correct category of an existing reporting system (namely the Coronary Artery Disease Reporting and Data System, CAD-RADS) (**Figure 4**). If confirmed on larger datasets, this study paves the way to the use of a CNN algorithm in clinical practice to rule out the presence of CAD in a relatively short time, reducing referring physicians' workload and helping them in focusing only on pathological CCTAs.

An alternative approach for assessing the presence of hemodynamically significant coronary artery stenosis is the one proposed by Zreik et al. (66), who demonstrated that a DL algorithm could perform an automatic analysis of the LV myocardium in a single CCTA scan acquired at rest, without assessment of the anatomy of the coronary arteries, to identify patients with functionally significant coronary artery

TABLE 5 | Main AI applications to Coronary Computed Tomography Angiography (CCTA).

References	Summary	Performance
Coronary stenoses grading		
Kelm et al. (64)	Automated ML detection, grading and stenoses grading on CCTA images	Good sensitivity and specificity (95 and 67%) compared to expert evaluation to correctly detect significant coronary artery stenoses
Kang et al. (65)	Automated ML detection of coronary artery stenoses on CCTA images	High sensitivity (93%), specificity (95%), and accuracy (94%), with AUC (0.94) for coronary artery stenoses detection compared to experts' visual assessment
Zreik et al. (66)	Automated LV myocardium analysis to identify patients with significant coronary artery stenoses	The DL application correctly performed LV segmentation (Dice similarity coefficient 0.91) and identified patients with significant coronary artery stenosis with an AUC value of 0.74
Hong et al. (67)	Automated DL coronary artery stenoses grading (plaque segmentation, MLA and percent DS quantification) on CCTA images	Excellent correlation of ML performance to expert readers ($\rho = 0.984$ for MLA; $\rho = 0.957$ for DS $p < 0.001$ for all)
Muscogiuri et al. (68)	Automated DL classification of coronary artery stenoses according to CAD-RADS	The DL algorithm showed its best performance in differentiating between CADRADS 0 (i.e., no coronary atherosclerosis) vs. CADRADS > 0 (i.e., detectable coronary atherosclerosis) with a sensitivity of 66% and a specificity of 91%, compared to experts' analysis
Plaque phenotype characterization		
Dey et al. (69)	Automated distinction between calcified and non-calcified plaques	Strong correlation between automated plaque analysis and expert readers ($\rho = 0.94$, for NCP volume; $\rho = 0.88$, for CP volume; $\rho = 0.90$ for NCP and CP composition)
Kolossváry et al. (70)	Identification of radiomic features associated to the presence of NRS in coronary artery plaques	Identification of NRS through radiomic analysis with an AUC > 0.92. One radiomic feature reached a remarkable AUC of 0.92 for NRS identification
Masuda et al. (71)	Automated ML algorithm for the detection of fibrous or fibro-fatty coronary artery plaques	The ML algorithm identified high risk coronary plaques better than intravascular ultrasound evaluation (AUC 0.92 vs. 0.83)
Zreik et al. (72)	DL application to perform a complete anatomical coronary artery assessment (stenosis grading associated to plaque features analysis)	Good accuracy in plaque phenotype characterization (AUC 0.77) and in determining its anatomical significance (i.e., stenosis degree above or below 50%, AUC 0.80)
Han et al. (73)	Automated ML algorithm to identify RPP	The ML model that included clinical variables, qualitative and most importantly quantitative plaque features showed the highest performance in identifying patients at risk of RPP (AUC 0.83)
Choi et al. (74)	DL application to perform a complete anatomical coronary artery assessment (stenosis grading associated to plaque features analysis) and CAD-RADS classification	Accuracy compared to three expert readers' analysis for stenoses >70%: 99.7%; accuracy for stenoses>50%: 94.8%. Excellent concordance in CAD-RADS classification with expert readers: agreement within one CAD-RADS category: 98% exams per-patient; 99.9% vessels on a per-vessel basis.
AI powered CT-FFR		
Coenen et al. (75)	Definition of the diagnostic accuracy of a ML application to CT-FFR	In the per-vessel analysis, ML-CT-FFR improved diagnostic accuracy by 20% compared to CTA (from 58 to 78%). The per-patient accuracy improved by 14% compared to CTA (from 71 to 85%). Seventy-three percent false-positive CTA results were correctly reclassified by ML-CT-FFR
Nous et al. (76)	Feasibility of ML-CT-FFR application in patients with DM	Overall diagnostic accuracy of ML-CT-FFR in diabetic patients was higher (83%) than in non-diabetic patients (75%); AUC 0.88 and 0.82 for diabetic and non-diabetic patients, respectively
Baumann et al. (77)	Differences in ML-CT-FFR application between patients of different genders	ML-FFR-CT equally performed in both genders, not showing significative difference in the AUC between males (0.83) and females (0.83)
Tesche et al. (78)	Feasibility of ML-CT-FFR application in the presence of heavy calcifications	No statistically significant differences in the diagnostic accuracy, sensitivity, or specificity of ML-CT-FFR were observed across CT scans of patients attributed to different Agatston score categories

CAD-RADS, Coronary Artery Disease Reporting and Data System; DM, diabetes mellitus; CP, calcified plaque; DS, diameter stenosis; FFR, fractional flow reserve; MLA, minimal luminal area; NCP, non-calcified plaque; NRS, Napkin ring sign; RPP, rapid plaque progression.

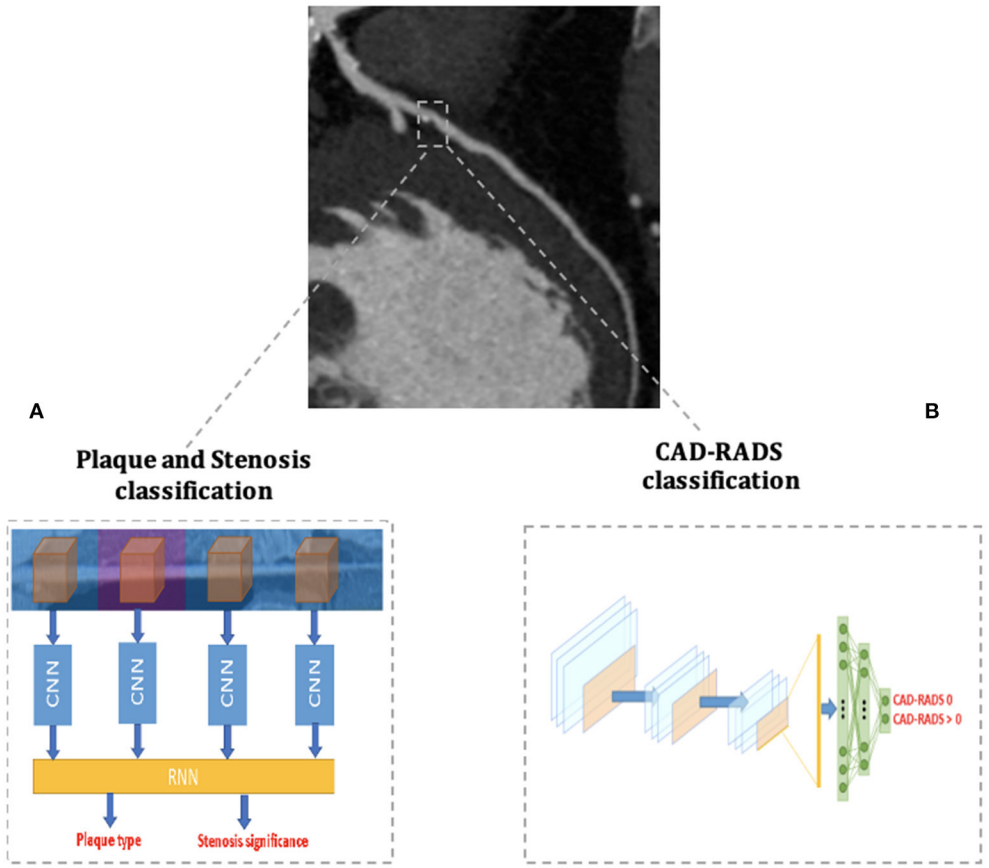

FIGURE 4 | AI applications to cardiac CT. The figure depicts two examples of AI workflow applied to the automatic analysis of coronary artery stenoses by Coronary Computed Tomography Angiography (CCTA). **(A)** Schematizes the algorithm proposed by Zreik et al. (72) and composed of a 3D convolutional neural network (CNN) used for coronary artery features extraction and a subsequent recurrent neural network for a two-task classification of plaque phenotype and stenosis degree. **(B)** Schematizes the algorithm applied by Muscogiuri et al. (68) for the fully automatic CAD-RADS classification of CCTA scans with a CNN.

stenosis with an AUC value of 0.74. When applied to a dataset of 100 CCTAs with intermediate grade coronary artery stenosis (82), the implementation of this DL application to the quantification of stenosis degree outperformed the traditional method of anatomical stenosis evaluation alone (AUC 0.76 and 0.68, respectively).

Plaque Phenotype Characterization

One of the key advantages of CCTA for the assessment of CAD is the ability to fully characterize coronary plaque phenotype.

Not all coronary lesions imply the same cardiovascular risk. In particular, the detection of prevalent fibrotic composition and other specific plaque features at CCTA (**Figure 5**) have been associated with an increased risk of cardiovascular events (83). These high-risk features are represented by spotty calcifications, positive remodeling, low attenuation, and the napkin-ring sign (NRS) (83).

AI applications have been developed to automate this process, in order to provide the clinician a full set of information to guide patient management.

One of the first AI approaches demonstrated the ability of an automated algorithm to correctly classify calcified and non-calcified lesions compared to expert manual quantification (69).

Masuda et al. (71) applied a ML histogram algorithm for the automatic detection of fibrous or fibro-fatty coronary plaques with CCTA. The ML method significantly outperformed the conventional CT parameters in the identification of high-risk plaques, when compared to intravascular ultrasound (IVUS) evaluation (AUC 0.92 vs. 0.83, respectively; $p = 0.001$).

Another feature correlated with high risk of cardiovascular events is rapid plaque progression (RPP), defined as an annual progression of percentage atheroma volume $\geq$1.0%. The study by Han et al. (73) provided an interesting demonstration of how a ML framework that incorporated clinical information together with qualitative and quantitative CCTA plaque parameters could better discriminate at risk patients compared to traditional risk scores and also ML models that incorporated only clinical or clinical and qualitative variables together.

This and other ML integrated clinical and CCTA parameter risk scores have shown the potential

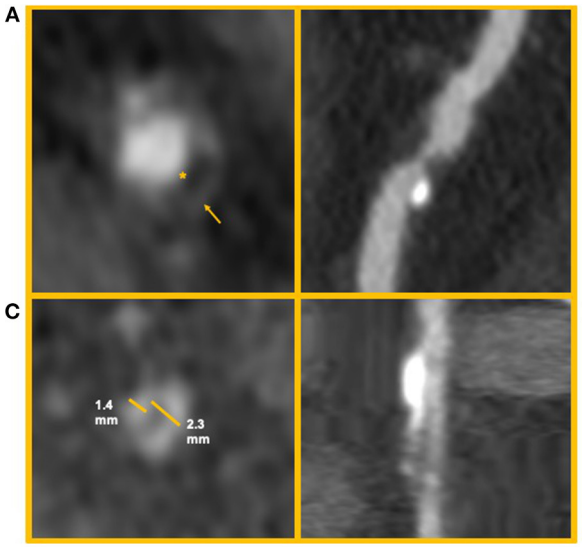

FIGURE 5 | High risk features of coronary artery plaques. The figure shows clinical examples of high-risk plaque feature. **(A)** Depicts an example of a Napkin-ring sign. The asterisk identifies the hypodense necrotic core; the arrow identifies the hyperdense ring-like thin cap. **(B)** Depicts a high-risk coronary plaque with spotty calcifications and low attenuation (i.e., attenuation <30 HU). **(C,D)** Depict a coronary artery plaque with positive remodeling (i.e., a positive ratio between diameter of the vessel outside the plaque and its internal diameter) in short and long axis, respectively.

to clearly outperform traditional CCTA risk score evaluations (73, 84) when applied in large cohorts with long follow-up.

In the future, the application of these AI empowered risk scores will enhance risk prediction in CAD patients, ultimately boosting the power of CCTA and other imaging exams.

Zreik et al. (72) developed a comprehensive anatomical DL application trained to analyze both the presence of significant CAD (i.e., the presence of stenoses with ≥50% of luminal narrowing) and to classify the phenotype of coronary artery plaques. To do so, the DL application was structured with a 3D CNN used to extract features of each coronary artery and with a recurrent neural network used to perform the two simultaneous classification tasks (**Figure 4**). The algorithm was validated on CCTA scans of 163 patients and reached good levels of accuracy in plaque phenotype characterization (0.77) and in determining its anatomical significance (0.80). If validated on larger cohorts, this comprehensive approach allows the clinician to maximize the anatomical evaluation of coronary artery plaques with CCTA.

Recently also Choi et al. (74) (CIT) proposed a new AI application capable of performing a comprehensive anatomical plaque quantification with impressive value of accuracy when compared to the analysis of three expert readers (accuracy for stenoses >70%: 99.7%; accuracy for stenoses>50%: 94.8%). Notably, the algorithm was also able to classify patients according to the CAD-RADS score with an excellent concordance with expert readers agreement within one CAD-RADS category in 98% exams per-patient and 99.9% vessels on a per-vessel basis.

Another innovative approach to coronary plaque characterization has been represented by the combination of radiomics with AI applications, which has shown the potential to provide useful information on high-risk coronary plaque features.

Kolossvary et al. (70) detected more than 400 radiomic features that significantly differed between plaques with and without napkin-ring sign, reaching an AUC > 0.8. Among these, one parameter called "short run low gray-level emphasis" reached an impressive AUC of 0.92 in NRS plaque identification.

The same authors expanded the previous observation by demonstrating that CCTA radiomics could identify invasive and radionuclide imaging markers of plaque vulnerability significantly better than traditional quantitative and qualitative CT parameters (85).

AI FOR FUNCTIONAL ISCHEMIA ASSESSMENT BY CARDIAC CT

AI Powered CT-FFR

Traditional CCTA techniques only provide anatomical assessment of CAD. In cases of coronary atherosclerosis of uncertain hemodynamic significance, current guidelines support the use of an ischemia test to assess the need for revascularization (2).

In recent years, the development of a non-invasive method to calculate CT-derived fractional flow reserve has permitted the evaluation of the anatomical and functional hemodynamic significance of coronary artery lesions (86–90). This approach has been validated in numerous studies (86, 91) against gold standard invasive FFR and resulted in high diagnostic accuracy in detecting hemodynamically significant stenosis and in determining their prognostic impact (92), especially when combined with information regarding coronary plaque phenotypes (54, 93).

Importantly, Rabbat et al. (94) studied 431 patients who underwent a CCTA alone vs. CCTA + FFRCT diagnostic pathway and demonstrated the safe deferral of ICA in patient with stable CAD who underwent the CCTA + FFRCT strategy. FFR_{CT} was feasible with a conclusive result in >90% of patients. Among those who deferred ICA, there were no major adverse cardiac events. A high proportion of those who underwent ICA were revascularized, resulting in higher diagnostic ICA yield and more efficient utilization of catheterization lab resources.

Multiple AI applications have been developed in recent years to automate the assessment of CT-FFR (75, 95).

Notably, the application of ML to CT-FFR has been clinically validated in a retrospective trial called MACHINE Registry that involved five different centers in Europe, USA and Asia. The ML based computation of CT-FFR outperformed CCTA in terms of diagnostic accuracy; when compared to invasive FFR, ML CT-FFR showed 78% accuracy in comparison to the 58% accuracy of visual CTA alone and the AUC for the detection of hemodynamically significant coronary artery stenosis favored the

ML CT-FFR approach (AUC 0.84 vs. 0.69 for CCTA alone). ML CT-FFR was capable of correctly reclassifying 73% false-positive CTA results.

The ML application to CT-FFR in the MACHINE registry were later confirmed in multiple sub-studies that investigated their reproducibility in different clinical scenarios: in particular, ML CT-FFR proved its feasibility in the presence of heavy coronary calcifications (78); in patients with diabetes mellitus (76) and between genders (77).

Poor image quality and high heart rate represent potential limitations to CT-FFR (96).

CT Perfusion Analysis

The study of myocardial perfusion through cardiac CT is a powerful and promising tool, since it can provide combined anatomical and functional information for every coronary territory with a single test. CT perfusion (CTP) is able to detect obstructive CAD better than CCTA alone (97) and is non-inferior to CMR in the functional evaluation of hemodynamically significant coronary artery stenosis (98).

Despite the great potential of this technique, to date only a few examples of AI applications to CTP exist in the literature and are based on the ML algorithm's ability to assess defects of myocardial perfusion from CTA images acquired at rest (99, 100).

In the future, AI applications have the potential to dramatically impact the field of CTP with applications focused on automatic myocardium segmentation and perfusion defect identification. A particular advantage of this algorithm will be the possibility to directly correlate the presence of anatomically detectable obstructive CAD with the functional evaluation of specific lesions with CTP sequences.

This approach has particular potential in complex CCTAs analysis, for example in the presence of previously revascularized vessels.

DISCUSSION

The implementation of AI applications to the multimodality imaging applied for the diagnosis and risk stratification of CAD patients represents a new frontier in cardiology. The implementation of AI in the clinical workflow will impact different aspects of the routine clinical workflow.

First, it will offer the possibility to shorten reporting time and to provide pre-reading evaluation of normal exams, to save radiologists and cardiologists time only pathological examinations.

Secondly, it will reduce inter-observer variability in the evaluation of exams. Moreover, it will provide more accurate models of prognostication (7), giving the clinician the possibility to tailor the treatment to the single patient. In this context, unsupervised learning will probably allow to enable the so-called "precision cardiology" by allowing the precision phenotypization of patients, allowing the cardiologist to go beyond the traditional monolithic disease concepts and tailor prognostication and therapy on the single patient features (101).

To spread the application of AI models in real-world clinical practice, however, some potential limitations, pitfalls and ethical considerations need to be considered (102).

As a first limitation, we must acknowledge the vast majority of AI applications have been validated in single-center studies with a limited number of cases and is therefore still restricted to research settings. As aforementioned, in fact, a fundamental principle of AI models is represented by the availability of huge sets of high-quality data for the algorithms to be developed, trained and tested.

In the field of cardiovascular imaging, the availability of large datasets from different centers is particularly crucial to overcome the biases currently present in the development of AI applications.

A first bias is represented by the great variability in terms of exams quality and interpretation (for example in the field of echocardiography) and in the lack in homogeneity in acquisition protocols and machine vendors (for example in the field of cardiac MRI). Therefore, a crucial step to assure AI algorithms generalizability is to perform their development on datasets containing information from machines from multiple vendors and obtained with different acquisition protocols, as in the case of cardiac MRI.

Secondly, in view of the great interobserver variability in some methods such as echocardiography, it is particularly important that the implementation of the training datasets and the quality control process, although time-consuming and costly, is not carried out by a single operator, but by teams of experienced cardiologists, if possible, from different centers. In fact, the risk is that the implementation of quality control by a single operator may lead to the unconscious introduction of new biases into the algorithm, making it usable only within the research group in which it was developed.

Future collaboration among different research groups and hardware vendors will constitute the basis for the development of more generalizable algorithms.

A further possible bias that can limit the general application of AI algorithms is the prevalence of certain ethnic or gender groups within the datasets on which AI applications are developed.

Thinking of a future world in which the use of AI should become routine, it is certainly necessary to ensure that this technology is equally available for all people, independent of gender, social class and ethnic origin. In order to make this possible, several obstacles must be overcome.

First, for AI algorithms to work homogeneously on people of different genders and ethnicities, they would have to be trained on heterogeneous datasets, including different ethnic groups and an equal number of people of both genders. At present, however, women and people from ethnic minorities have been consistently underrepresented in large trial databases (103).

This must be avoided, as it could lead to the exclusion of entire sections of the population from access to the most advanced medical care, thus exacerbating the inequalities already present today. In fact, even though AI applications are in most cases still at an early stage of development, examples have already been reported in the literature of discrimination between different ethnic or economic groups by some AI applications (104).

In order to overcome this possible bias, it is necessary for regulatory agencies to enforce fair inclusion in AI application development databases of patients of different gender and ethnic origin.

Secondly, given the high development costs and the great need of medical records, AI applications will mainly be implemented in high-income countries, based on the organizational needs of their national health systems. This could lead to a substantial inapplicability of AI algorithms in poorer countries, making advanced care even more inaccessible to their citizens.

This could be avoided by devoting some of the public resources allocated to the development of AI algorithms in richer countries to the implementation of applications that improve the quality of care in low-income countries.

Once obtained, robust AI applications will also require validation in large clinical trials to prove benefits in patient care, the economic sustainability and safety of their implementation in routine clinical workflow.

AI application validation in clinical trials will in fact help in overcoming a further issue, which is represented by the medical-legal aspect. In the future doctors will probably base their decisions on risk score algorithms and diagnostic tools powered by AI applications. In this scenario, who will be considered responsible, in the case of a wrong decision made on the basis of incorrect information?

This issue seems even more important if we consider that the majority of AI applications are characterized by a lack of transparency of their intermedium processes: the human operator knows the input data and the result of the elaboration, but can hardly understand the internal algorithm processes.

To overcome this possible pitfall there will be a need to act on two fronts.

On one side, national and transnational medical regulatory authorities will need to further regulate laws and protocols in perspective of a large-scale use of AI algorithms in everyday clinical workflow.

The European Commission on medical AI (105) published a white paper that sought to establish founding principles (such as safety, privacy, data governance transparency, diversity and non-discrimination) for the development of future AI applications, opening up the possibility of supplementing legislation already in place to better protect the health and safety of its citizens.

On the other side, AI developers will need to work on algorithms' self-explicability and internal transparency, to produce so-called explainable AI applications, namely AI software able to provide justification for every stage of their choices, in order to provide the physician all the information needed for thoughtful clinical decision making.

CONCLUSIONS

The medical management of patients with coronary artery disease, one of the most prevalent diseases in the world, is rapidly progressing with the implementation of multimodality imaging in diagnostic and prognostic routine workflows.

AI applications have proven the ability to significantly improve the detection of coronary artery disease with both an anatomical and a functional imaging approach.

Thus, the application of AI to multimodality imaging will continue to play a prominent role in every stage of the diagnostic, risk-stratification and follow-up of patients affected by coronary artery disease. Larger clinical validation and research on safety need to be implemented before large-scale adoption in routine clinical practice.

AUTHOR CONTRIBUTIONS

All authors made a substantial contribution to the conception, design of this review paper, including drafting and revisions, and granted their approval for all aspects of the manuscript and its submission.

REFERENCES

1. Khan MA, Hashim MJ, Mustafa H, Baniyas MY, Al Suwaidi SKBM, AlKatheeri R, et al. Global epidemiology of ischemic heart disease: results from the global burden of disease study. *Cureus.* (2020) 12:e9349. doi: 10.7759/cureus.9349
2. Knuuti J, Wijns W, Saraste A, Capodanno D, Barbato E, Funck-Brentano C, et al. 2019 ESC guidelines for the diagnosis and management of chronic coronary syndromes. *Eur Heart J.* (2020) 41:407–77. doi: 10.1093/eurheartj/ehz425
3. Haenlein MKA. A brief history of artificial intelligence: on the past, present, and future of artificial intelligence. *California Manag Rev*. (2019) 61:8125619864925. doi: 10.1177/0008125619864925
4. Deo RC. Machine learning in medicine. *Circulation.* (2015) 132:1920–30. doi: 10.1161/CIRCULATIONAHA.115.001593
5. Obermeyer Z, Emanuel EJ. Predicting the future - big data, machine learning, and clinical medicine. *N Engl J Med.* (2016) 375:1216–9. doi: 10.1056/NEJMp1606181
6. Dey D, Slomka PJ, Leeson P, Comaniciu D, Shrestha S, Sengupta PP, et al. Artificial intelligence in cardiovascular imaging: JACC state-of-the-art review. *J Am Coll Cardiol.* (2019) 73:1317–35. doi: 10.1016/j.jacc.2018.12.054
7. van Assen M, Muscogiuri G, Caruso D, Lee SJ, Laghi A, De Cecco CN. Artificial intelligence in cardiac radiology. *Radiol Med.* (2020) 125:1186–99. doi: 10.1007/s11547-020-01277-w
8. Muscogiuri G, Van Assen M, Tesche C, De Cecco CN, Chiesa M, Scafuri S, et al. Artificial intelligence in coronary computed tomography angiography: from anatomy to prognosis. *Biomed Res Int.* (2020) 2020:6649410. doi: 10.1155/2020/6649410
9. Gillies RJ, Kinahan PE, Hricak H. Radiomics: images are more than pictures, they are data. *Radiology.* (2016) 278:563–77. doi: 10.1148/radiol.2015151169
10. Leiner T, Rueckert D, Suinesiaputra A, Baeßler B, Nezafat R, Išgum I, et al. Machine learning in cardiovascular magnetic resonance: basic concepts and applications. *J Cardiovasc Magn Reson.* (2019) 21:61. doi: 10.1186/s12968-019-0575-y
11. Takx RA, de Jong PA, Leiner T, Oudkerk M, de Koning HJ, Mol CP, et al. Automated coronary artery calcification scoring in non-gated chest CT: agreement and reliability. *PLoS ONE.* (2014) 9:e91239. doi: 10.1371/journal.pone.0091239
12. Wolterink JM, Leiner T, Takx RA, Viergever MA, Isgum I. Automatic coronary calcium scoring in non-contrast-enhanced ECG-triggered cardiac CT with ambiguity detection. *IEEE Trans Med Imaging.* (2015) 34:1867–78. doi: 10.1109/TMI.2015.2412651

13. Lessmann N, van Ginneken B, Zreik M, de Jong PA, de Vos BD, Viergever MA, et al. Automatic Calcium Scoring in Low-Dose Chest CT Using Deep Neural Networks With Dilated Convolutions. IEEE Trans Med Imaging. (2018) 37:615–25. doi: 10.1109/TMI.2017.2769839
14. Sandstedt M, Henriksson L, Janzon M, Nyberg G, Engvall J, De Geer J, et al. Evaluation of an AI-based, automatic coronary artery calcium scoring software. *Eur Radiol.* (2020) 30:1671–8. doi: 10.1007/s00330-019-06489-x
15. van Velzen SGM, Lessmann N, Velthuis BK, Bank IEM, van den Bongard D, Leiner T, et al. Deep learning for automatic calcium scoring in CT: validation using multiple cardiac CT and chest CT protocols. *Radiology.* (2020) 295:66–79. doi: 10.1148/radiol.2020191621
16. Zeleznik R, Foldyna B, Eslami P, Weiss J, Alexander I, Taron J, et al. Deep convolutional neural networks to predict cardiovascular risk from computed tomography. *Nat Commun.* (2021) 12:715. doi: 10.1038/s41467-021-20966-2
17. Commandeur F, Goeller M, Razipour A, Cadet S, Hell MM, Kwiecinski J, et al. Fully automated CT quantification of epicardial adipose tissue by deep learning: a multicenter study. *Radiol Artif Intell.* (2019) 1:e190045. doi: 10.1148/ryai.2019190045
18. Commandeur F, Slomka PJ, Goeller M, Chen X, Cadet S, Razipour A, et al. Machine learning to predict the long-term risk of myocardial infarction and cardiac death based on clinical risk, coronary calcium, and epicardial adipose tissue: a prospective study. *Cardiovasc Res.* (2020) 116:2216–25. doi: 10.1093/cvr/cvz321
19. Eisenberg E, McElhinney PA, Commandeur F, Chen X, Cadet S, Goeller M, et al. Deep learning-based quantification of epicardial adipose tissue volume and attenuation predicts major adverse cardiovascular events in asymptomatic subjects. *Circ Cardiovasc Imaging.* (2020) 13:e009829. doi: 10.1161/CIRCIMAGING.119.009829
20. Huang YL, Wu FZ, Wang YC, Ju YJ, Mar GY, Chuo CC, et al. Reliable categorisation of visual scoring of coronary artery calcification on low-dose CT for lung cancer screening: validation with the standard Agatston score. *Eur Radiol.* (2013) 23:1226–33. doi: 10.1007/s00330-012-2726-5
21. Guglielmo M, Lin A, Dey D, Baggiano A, Fusini L, Muscogiuri G, et al. Epicardial fat and coronary artery disease: role of cardiac imaging. *Atherosclerosis.* (2021) 321:30–8. doi: 10.1016/j.atherosclerosis.2021.02.008
22. Antonopoulos AS, Sanna F, Sabharwal N, Thomas S, Oikonomou EK, Herdman L, et al. Detecting human coronary inflammation by imaging perivascular fat. *Sci Transl Med.* (2017) 9:aal2658. doi: 10.1126/scitranslmed.aal2658
23. Ding X, Terzopoulos D, Diaz-Zamudio M, Berman DS, Slomka PJ, Dey D. Automated pericardium delineation and epicardial fat volume quantification from noncontrast CT. *Med Phys.* (2015) 42:5015–26. doi: 10.1118/1.4927375
24. Militello C, Rundo L, Toia P, Conti V, Russo G, Filorizzo C, et al. A semi-automatic approach for epicardial adipose tissue segmentation and quantification on cardiac CT scans. *Comput Biol Med.* (2019) 114:103424. doi: 10.1016/j.compbiomed.2019.103424
25. Oikonomou EK, Williams MC, Kotanidis CP, Desai MY, Marwan M, Antonopoulos AS, et al. A novel machine learning-derived radiotranscriptomic signature of perivascular fat improves cardiac risk prediction using coronary CT angiography. *Eur Heart J.* (2019) 40:3529–43. doi: 10.1093/eurheartj/ehz592
26. Lin A, Kolossváry M, Yuvaraj J, Cadet S, McElhinney PA, Jiang C, et al. Myocardial infarction associates with a distinct pericoronary adipose tissue radiomic phenotype: a prospective case-control study. *JACC Cardiovasc Imaging.* (2020) 13:2371–83. doi: 10.1016/j.jcmg.2020.06.033
27. Kusunose K. Steps to use artificial intelligence in echocardiography. *J Echocardiogr.* (2021) 19:21–7. doi: 10.1007/s12574-020-00496-4
28. Raghavendra U, Anjan Gudigar HF, Ranjan S, Krishnananda N, Umesh P, Jyothi Samanth U, et al. Automated technique for coronary artery disease characterization and classification using DD-DTDWT in ultrasound images. *Biomed Sign Proces Contr.* (2018) 40:324–34. doi: 10.1016/j.bspc.2017.09.030
29. Kusunose K, Abe T, Haga A, Fukuda D, Yamada H, Harada M, et al. A deep learning approach for assessment of regional wall motion abnormality from echocardiographic images. *JACC Cardiovasc Imag.* (2020) 13:374–81. doi: 10.1016/j.jcmg.2019.02.024
30. Mansor S, Hughes NP, Noble JA. Wall motion classification of stress echocardiography based on combined rest-and-stress data. *Med Image Comput Comput Assist Interv.* (2008) 11:139–46. doi: 10.1007/978-3-540-85990-1_17
31. Chykeyuk K, Clifton DA, Noble JA. Feature extraction and wall motion classification of 2D stress echocardiography with relevance vector machines. In: *2011 IEEE International Symposium on Biomedical Imaging: From Nano to Macro.* (2011). p. 677–80. doi: 10.1109/ISBI.2011.5872497
32. Omar HA, Patra A, Domingos JS, Leeson P, Noblel AJ. Automated myocardial wall motion classification using handcrafted features vs a deep CNN-based mapping. *Annu Int Conf IEEE Eng Med Biol Soc.* (2018) 2018:3140–3. doi: 10.1109/EMBC.2018.8513063
33. Vidya KS, Ng EY, Acharya UR, Chou SM, Tan RS, Ghista DN. Computer-aided diagnosis of Myocardial Infarction using ultrasound images with DWT, GLCM and HOS methods: a comparative study. *Comput Biol Med.* (2015) 62:86–93. doi: 10.1016/j.compbiomed.2015.03.033
34. Baessato F, Guglielmo M, Muscogiuri G, Baggiano A, Fusini L, Scafuri S, et al. Stress CMR in known or suspected CAD: diagnostic and prognostic role. *Biomed Res Int.* (2021) 2021:6678029. doi: 10.1155/2021/6678029
35. Bai W, Sinclair M, Tarroni G, Oktay O, Rajchl M, Vaillant G, et al. Automated cardiovascular magnetic resonance image analysis with fully convolutional networks. *J Cardiovasc Magn Reson.* (2018) 20:65. doi: 10.1186/s12968-018-0471-x
36. Curiale AH, Colavecchia FD, Mato G. Automatic quantification of the LV function and mass: a deep learning approach for cardiovascular MRI. *Comput Methods Programs Biomed.* (2019) 169:37–50. doi: 10.1016/j.cmpb.2018.12.002
37. Kotu LP, Engan K, Borhani R, Katsaggelos AK, Ørn S, Woie L, et al. Cardiac magnetic resonance image-based classification of the risk of arrhythmias in post-myocardial infarction patients. *Artif Intell Med.* (2015) 64:205–15. doi: 10.1016/j.artmed.2015.06.001
38. Xu C, Xu L, Gao Z, Zhao S, Zhang H, Zhang Y, et al. Direct detection of pixel-level myocardial infarction areas *via* a deep-learning algorithm. In: Descoteaux M, Maier-Hein L, Franz A, Jannin P, Collins DL, Duchesne S, editors, *Medical Image Computing and Computer Assisted Intervention – MICCAI 2017*. Basel: Springer International Publishing. (2017). p. 240–9. doi: 10.1007/978-3-319-66179-7_28
39. Larroza A, Materka A, López-Lereu MP, Monmeneu JV, Bodí V, Moratal D. Differentiation between acute and chronic myocardial infarction by means of texture analysis of late gadolinium enhancement and cine cardiac magnetic resonance imaging. *Eur J Radiol.* (2017) 92:78–83. doi: 10.1016/j.ejrad.2017.04.024
40. Larroza A, López-Lereu MP, Monmeneu JV, Gavara J, Chorro FJ, Bodí V, et al. Texture analysis of cardiac cine magnetic resonance imaging to detect nonviable segments in patients with chronic myocardial infarction. *Med Phys.* (2018) 45:1471–80. doi: 10.1002/mp.12783
41. Baessler B, Mannil M, Oebel S, Maintz D, Alkadhi H, Manka R. Subacute and chronic left ventricular myocardial scar: accuracy of texture analysis on nonenhanced cine MR images. *Radiology.* (2018) 286:103–12. doi: 10.1148/radiol.2017170213
42. Moccia S, Banali R, Martini C, Muscogiuri G, Pontone G, Pepi M, et al. Development and testing of a deep learning-based strategy for scar segmentation on CMR-LGE images. *Magma.* (2019) 32:187–95. doi: 10.1007/s10334-018-0718-4
43. Zabihollahy F, White JA, Ukwatta E. Convolutional neural network-based approach for segmentation of left ventricle myocardial scar from 3D late gadolinium enhancement MR images. *Med Phys.* (2019) 46:1740–51. doi: 10.1002/mp.13436
44. Zhang N, Yang G, Gao Z, Xu C, Zhang Y, Shi R, et al. Deep learning for diagnosis of chronic myocardial infarction on nonenhanced cardiac cine MRI. *Radiology.* (2019) 291:606–17. doi: 10.1148/radiol.2019182304
45. Ma Q, Ma Y, Yu T, Sun Z, Hou Y. Radiomics of non-contrast-enhanced T1 mapping: diagnostic and predictive performance for myocardial injury in acute ST-segment-elevation myocardial infarction. *Korean J Radiol.* (2021) 22:535–46. doi: 10.3348/kjr.2019.0969
46. Scannell CM, Veta M, Villa ADM, Sammut EC, Lee J, Breeuwer M, et al. Deep-learning-based preprocessing for quantitative myocardial perfusion MRI. *J Magn Reson Imaging.* (2020) 51:1689–96. doi: 10.1002/jmri.26983

47. Xue H, Davies RH, Brown LAE, Knott KD, Kotecha T, Fontana M, et al. Automated inline analysis of myocardial perfusion MRI with deep learning. *Radiol Artif Intell.* (2020) 2:e200009. doi: 10.1148/ryai.2020200009
48. Tan LK, Liew YM, Lim E, McLaughlin RA. Convolutional neural network regression for short-axis left ventricle segmentation in cardiac cine MR sequences. *Med Image Anal.* (2017) 39:78–86. doi: 10.1016/j.media.2017.04.002
49. Kim RJ, Wu E, Rafael A, Chen EL, Parker MA, Simonetti O, et al. The use of contrast-enhanced magnetic resonance imaging to identify reversible myocardial dysfunction. *N Engl J Med.* (2000) 343:1445–53. doi: 10.1056/NEJM200011163432003
50. Engblom H, Xue H, Akil S, Carlsson M, Hindorf C, Oddstig J, et al. Fully quantitative cardiovascular magnetic resonance myocardial perfusion ready for clinical use: a comparison between cardiovascular magnetic resonance imaging and positron emission tomography. *J Cardiovasc Magn Reson.* (2017) 19:78. doi: 10.1186/s12968-017-0388-9
51. Hsu LY, Jacobs M, Benovoy M, Ta AD, Conn HM, Winkler S, et al. Diagnostic performance of fully automated pixel-wise quantitative myocardial perfusion imaging by cardiovascular magnetic resonance. *JACC Cardiovasc Imaging.* (2018) 11:697–707. doi: 10.1016/j.jcmg.2018.01.005
52. Schulz-Menger J, Bluemke DA, Bremerich J, Flamm SD, Fogel MA, Friedrich MG, et al. Standardized image interpretation and post-processing in cardiovascular magnetic resonance - 2020 update: Society for Cardiovascular Magnetic Resonance (SCMR): board of Trustees Task Force on Standardized Post-Processing. *J Cardiovasc Magn Reson.* (2020) 22:19. doi: 10.1186/s12968-020-00610-6
53. Knott KD, Seraphim A, Augusto JB, Xue H, Chacko L, Aung N, et al. The prognostic significance of quantitative myocardial perfusion: an artificial intelligence-based approach using perfusion mapping. *Circulation.* (2020) 141:1282–91. doi: 10.1161/CIRCULATIONAHA.119.044666
54. Daubert MA, Tailor T, James O, Shaw LJ, Douglas PS, Koweek L. Multimodality cardiac imaging in the 21st century: evolution, advances and future opportunities for innovation. *Br J Radiol.* (2021) 94:20200780. doi: 10.1259/bjr.20200780
55. Betancur J, Rubeaux M, Fuchs TA, Otaki Y, Arnson Y, Slipczuk L, et al. Automatic valve plane localization in myocardial perfusion SPECT/CT by machine learning: anatomic and clinical validation. *J Nucl Med.* (2017) 58:961–7. doi: 10.2967/jnumed.116.179911
56. Arsanjani R, Xu Y, Hayes SW, Fish M, Lemley M, Gerlach J, et al. Comparison of fully automated computer analysis and visual scoring for detection of coronary artery disease from myocardial perfusion SPECT in a large population. *J Nucl Med.* (2013) 54:221–8. doi: 10.2967/jnumed.112.108969
57. Arsanjani R, Xu Y, Dey D, Vahistha V, Shalev A, Nakanishi R, et al. Improved accuracy of myocardial perfusion SPECT for detection of coronary artery disease by machine learning in a large population. *J Nucl Cardiol.* (2013) 20:553–62. doi: 10.1007/s12350-013-9706-2
58. Betancur J, Commandeur F, Motlagh M, Sharir T, Einstein AJ, Bokhari S, et al. Deep learning for prediction of obstructive disease from fast myocardial perfusion SPECT: a multicenter study. *JACC Cardiovasc Imaging.* (2018) 11:1654–63. doi: 10.1016/j.jcmg.2018.01.020
59. Otaki Y, Singh A, Kavanagh P, Miller RJH, Parekh T, Tamarappoo BK, et al. Clinical deployment of explainable artificial intelligence of SPECT for diagnosis of coronary artery disease. *JACC Cardiovasc Imaging.* (2021) 4:30. doi: 10.1016/j.jcmg.2021.04.030
60. Arsanjani R, Dey D, Khachatryan T, Shalev A, Hayes SW, Fish M, et al. Prediction of revascularization after myocardial perfusion SPECT by machine learning in a large population. *J Nucl Cardiol.* (2015) 22:877–84. doi: 10.1007/s12350-014-0027-x
61. Betancur J, Otaki Y, Motwani M, Fish MB, Lemley M, Dey D, et al. Prognostic value of combined clinical and myocardial perfusion imaging data using machine learning. *JACC Cardiovasc Imaging.* (2018) 11:1000–9. doi: 10.1016/j.jcmg.2017.07.024
62. Hu LH, Betancur J, Sharir T, Einstein AJ, Bokhari S, Fish MB, et al. Machine learning predicts per-vessel early coronary revascularization after fast myocardial perfusion SPECT: results from multicentre REFINE SPECT registry. *Eur Heart J Cardiovasc Imaging.* (2020) 21:549–59. doi: 10.1093/ehjci/jez177
63. Min JK, Dunning A, Lin FY, Achenbach S, Al-Mallah M, Budoff MJ, et al. Age- and sex-related differences in all-cause mortality risk based on coronary computed tomography angiography findings results from the International Multicenter CONFIRM (Coronary CT Angiography Evaluation for Clinical Outcomes: An International Multicenter Registry) of 23,854 patients without known coronary artery disease. *J Am Coll Cardiol.* (2011) 58:849–60. doi: 10.1016/j.jacc.2011.02.074
64. Kelm BM, Mittal S, Zheng Y, Tsymbal A, Bernhardt D, Vega-Higuera F, et al. Detection, grading and classification of coronary stenoses in computed tomography angiography. *Med Image Comput Comput Assist Interv.* (2011) 14:25–32. doi: 10.1007/978-3-642-23626-6_4
65. Kang D, Dey D, Slomka PJ, Arsanjani R, Nakazato R, Ko H, et al. Structured learning algorithm for detection of nonobstructive and obstructive coronary plaque lesions from computed tomography angiography. *J Med Imaging.* (2015) 2:014003. doi: 10.1117/1.JMI.2.1.014003
66. Zreik M, Lessmann N, van Hamersvelt RW, Wolterink JM, Voskuil M, Viergever MA, et al. Deep learning analysis of the myocardium in coronary CT angiography for identification of patients with functionally significant coronary artery stenosis. *Med Image Anal.* (2018) 44:72–85. doi: 10.1016/j.media.2017.11.008
67. Hong Y, Commandeur F, Cadet S, Goeller M, Doris MK, Chen X, et al. Deep learning-based stenosis quantification from coronary CT. *Angiography Proc SPIE Int Soc Opt Eng.* (2019) 12:10949. doi: 10.1117/12.2512168
68. Muscogiuri G, Chiesa M, Trotta M, Gatti M, Palmisano V, Dell'Aversana S, et al. Performance of a deep learning algorithm for the evaluation of CAD-RADS classification with CCTA. *Atherosclerosis.* (2020) 294:25–32. doi: 10.1016/j.atherosclerosis.2019.12.001
69. Dey D, Cheng VY, Slomka PJ, Nakazato R, Ramesh A, Gurudevan S, et al. Automated 3-dimensional quantification of noncalcified and calcified coronary plaque from coronary CT angiography. *J Cardiovasc Comput Tomogr.* (2009) 3:372–82. doi: 10.1016/j.jcct.2009.09.004
70. Kolossváry M, Karády J, Szilveszter B, Kitslaar P, Hoffmann U, Merkely B, et al. Radiomic features are superior to conventional quantitative computed tomographic metrics to identify coronary plaques with napkin-ring sign. *Circ Cardiovasc Imaging.* (2017) 10:e006843. doi: 10.1161/CIRCIMAGING.117.006843
71. Masuda T, Nakaura T, Funama Y, Okimoto T, Sato T, Higaki T, et al. Machine-learning integration of CT histogram analysis to evaluate the composition of atherosclerotic plaques: Validation with IB-IVUS. *J Cardiovasc Comput Tomogr.* (2019) 13:163–9. doi: 10.1016/j.jcct.2018.10.018
72. Zreik M, van Hamersvelt RW, Wolterink JM, Leiner T, Viergever MA, Isgum I. A recurrent CNN for automatic detection and classification of coronary artery plaque and stenosis in coronary CT angiography. *IEEE Trans Med Imaging.* (2019) 38:1588–98. doi: 10.1109/TMI.2018.2883807
73. Han D, Kolli KK, Al'Aref SJ, Baskaran L, van Rosendael AR, Gransar H, et al. Machine learning framework to identify individuals at risk of rapid progression of coronary atherosclerosis: from the PARADIGM registry. *J Am Heart Assoc.* (2020) 9:e013958. doi: 10.1161/JAHA.119.013958
74. Choi AD, Marques H, Kumar V, Griffin WF, Rahban H, Karlsberg RP, et al. CT EvaLuation by Artificial Intelligence For Atherosclerosis, Stenosis and Vascular MorphologY (CLARIFY): a multi-center, international study. *J Cardiovasc Comput Tomogr.* (2021). 5:4. doi: 10.1016/j.jcct.2021.05.004
75. Coenen A, Kim YH, Kruk M, Tesche C, De Geer J, Kurata A, et al. Diagnostic accuracy of a machine-learning approach to coronary computed tomographic angiography-based fractional flow reserve: result from the MACHINE consortium. *Circ Cardiovasc Imaging.* (2018) 11:e007217. doi: 10.1161/CIRCIMAGING.117.007217
76. Nous FMA, Coenen A, Boersma E, Kim YH, Kruk MBP, Tesche C, et al. Comparison of the diagnostic performance of coronary computed tomography angiography-derived fractional flow reserve in patients with versus without diabetes mellitus (from the MACHINE Consortium). *Am J Cardiol.* (2019) 123:537–43. doi: 10.1016/j.amjcard.2018.11.024
77. Baumann S, Renker M, Schoepf UJ, De Cecco CN, Coenen A, De Geer J, et al. Gender differences in the diagnostic performance of machine learning coronary CT angiography-derived fractional flow reserve -results from the MACHINE registry. *Eur J Radiol.* (2019) 119:108657. doi: 10.1016/j.ejrad.2019.108657

78. Tesche C, Otani K, De Cecco CN, Coenen A, De Geer J, Kruk M, et al. Influence of coronary calcium on diagnostic performance of machine learning CT-FFR: results from MACHINE registry. *JACC Cardiovasc Imaging.* (2020) 13:760–70. doi: 10.1016/j.jcmg,.2019.06.027
79. Lin A, Kolossváry M, Motwani M, Išgum I, Maurovich-Horvat P, Slomka PJ, et al. Artificial intelligence in cardiovascular imaging for risk stratification in coronary artery disease. *Radiol Cardiothorac Imaging.* (2021) 3:e200512. doi: 10.1148/ryct.2021200512
80. Benjamin MM, Rabbat MG. Machine learning-based advances in coronary computed tomography angiography. *Quant Imaging Med Surg.* (2021) 11:2208–13. doi: 10.21037/qims-21-99
81. Liu CY, Tang CX, Zhang XL, Chen S, Xie Y, Zhang XY, et al. Deep learning powered coronary CT angiography for detecting obstructive coronary artery disease: The effect of reader experience, calcification and image quality. *Eur J Radiol.* (2021) 142:109835. doi: 10.1016/j.ejrad.2021.109835
82. van Hamersvelt RW, Zreik M, Voskuil M, Viergever MA, Išgum I, Leiner T. Deep learning analysis of left ventricular myocardium in CT angiographic intermediate-degree coronary stenosis improves the diagnostic accuracy for identification of functionally significant stenosis. *Eur Radiol.* (2019) 29:2350–9. doi: 10.1007/s00330-018-5822-3
83. Andreini D, Magnoni M, Conte E, Masson S, Mushtaq S, Berti S, et al. Coronary plaque features on CTA can identify patients at increased risk of cardiovascular events. *JACC Cardiovasc Imaging.* (2020) 13:1704–17. doi: 10.1016/j.jcmg.2019.06.019
84. van Rosendael AR, Maliakal G, Kolli KK, Beecy A, Al'Aref SJ, Dwivedi A, et al. Maximization of the usage of coronary CTA derived plaque information using a machine learning based algorithm to improve risk stratification; insights from the CONFIRM registry. *J Cardiovasc Comput Tomogr.* (2018) 12:204–9. doi: 10.1016/j.jcct.2018.04.011
85. Kolossváry M, Park J, Bang JI, Zhang J, Lee JM, Paeng JC, et al. Identification of invasive and radionuclide imaging markers of coronary plaque vulnerability using radiomic analysis of coronary computed tomography angiography. *Eur Heart J Cardiovasc Imaging.* (2019) 20:1250–8. doi: 10.1093/ehjci/jez033
86. Min JK, Leipsic J, Pencina MJ, Berman DS, Koo BK, van Mieghem C, et al. Diagnostic accuracy of fractional flow reserve from anatomic CT angiography. *J Am Med Assoc.* (2012) 308:1237–45. doi: 10.1001/2012.jama.11274
87. Nørgaard BL, Leipsic J, Gaur S, Seneviratne S, Ko BS, Ito H, et al. Diagnostic performance of noninvasive fractional flow reserve derived from coronary computed tomography angiography in suspected coronary artery disease: the NXT trial (Analysis of Coronary Blood Flow Using CT Angiography: Next Steps). *J Am Coll Cardiol.* (2014) 63:1145–55. doi: 10.1016/j.jacc.2013.11.043
88. Lu MT, Ferencik M, Roberts RS, Lee KL, Ivanov A, Adami E, et al. Noninvasive FFR derived from coronary CT angiography: management and outcomes in the PROMISE trial. *JACC Cardiovasc Imaging.* (2017) 10:1350–8. doi: 10.1016/j.jcmg.2016.11.024
89. Rabbat MG, Berman DS, Kern M, Raff G, Chinnaiyan K, Koweek L, et al. Interpreting results of coronary computed tomography angiography-derived fractional flow reserve in clinical practice. *J Cardiovasc Comput Tomogr.* (2017) 11:383–8. doi: 10.1016/j.jcct.2017.06.002
90. Kitabata H, Leipsic J, Patel MR, Nieman K, De Bruyne B, Rogers C, et al. Incidence and predictors of lesion-specific ischemia by FFR. *J Cardiovasc Comput Tomogr.* (2018) 12:95–100. doi: 10.1016/j.jcct.2018.01.008
91. Koo BK, Erglis A, Doh JH, Daniels DV, Jegere S, Kim HS, et al. Diagnosis of ischemia-causing coronary stenoses by noninvasive fractional flow reserve computed from coronary computed tomographic angiograms. Results from the prospective multicenter DISCOVER-FLOW (Diagnosis of Ischemia-Causing Stenoses Obtained Via Noninvasive Fractional Flow Reserve) study. *J Am Coll Cardiol.* (2011) 58:1989–97. doi: 10.1016/j.jacc.2011.06.066
92. Patel MR, Nørgaard BL, Fairbairn TA, Nieman K, Akasaka T, Berman DS, et al. 1-year impact on medical practice and clinical outcomes of FFR. *JACC Cardiovasc Imaging 13(1 Pt 1).* (2020) 97–105. doi: 10.1016/j.jcmg.2019.03.003
93. Tesche C, De Cecco CN, Caruso D, Baumann S, Renker M, Mangold S, et al. Coronary CT angiography derived morphological and functional quantitative plaque markers correlated with invasive fractional flow reserve for detecting hemodynamically significant stenosis. *J Cardiovasc Comput Tomogr.* (2016) 10:199–206. doi: 10.1016/j.jcct.2016.03.002
94. Rabbat M, Leipsic J, Bax J, Kauh B, Verma R, Doukas D, et al. Fractional flow reserve derived from coronary computed tomography angiography safely defers invasive coronary angiography in patients with stable coronary artery disease. *J Clin Med.* (2020) 9. doi: 10.3390/jcm9020604
95. Tesche C, De Cecco CN, Baumann S, Renker M, McLaurin TW, Duguay TM, et al. Coronary CT angiography-derived fractional flow reserve: machine learning algorithm versus computational fluid dynamics modeling. *Radiology.* (2018) 288:64–72. doi: 10.1148/radiol.2018171291
96. Xu PP, Li JH, Zhou F, Jiang MD, Zhou CS, Lu MJ, et al. The influence of image quality on diagnostic performance of a machine learning-based fractional flow reserve derived from coronary CT angiography. *Eur Radiol.* (2020) 30:2525–34. doi: 10.1007/s00330-019-06571-4
97. Celeng C, Leiner T, Maurovich-Horvat P, Merkely B, de Jong P, Dankbaar JW, et al. Anatomical and functional computed tomography for diagnosing hemodynamically significant coronary artery disease: a meta-analysis. *JACC Cardiovasc Imaging.* (2019) 12:1316–25. doi: 10.1016/j.jcmg.2018.07.022
98. Takx RA, Blomberg BA, El Aidi H, Habets J, de Jong PA, Nagel E, et al. Diagnostic accuracy of stress myocardial perfusion imaging compared to invasive coronary angiography with fractional flow reserve meta-analysis. *Circ Cardiovasc Imaging.* (2015) 8:2666. doi: 10.1161/CIRCIMAGING.114.002666
99. Xiong G, Kola D, Heo R, Elmore K, Cho I, Min JK. Myocardial perfusion analysis in cardiac computed tomography angiographic images at rest. *Med Image Anal.* (2015) 24:77–89. doi: 10.1016/j.media.2015.05.010
100. Han D, Lee JH, Rizvi A, Gransar H, Baskaran L, Schulman-Marcus J, et al. Incremental role of resting myocardial computed tomography perfusion for predicting physiologically significant coronary artery disease: a machine learning approach. *J Nucl Cardiol.* (2018) 25:223–33. doi: 10.1007/s12350-017-0834-y
101. Johnson KW, Torres Soto J, Glicksberg BS, Shameer K, Miotto R, Ali M, et al. Artificial intelligence in cardiology. *J Am Coll Cardiol.* (2018) 71:2668–79. doi: 10.1016/j.jacc.2018.03.521
102. Tat E, Bhatt DL, Rabbat MG. Addressing bias: artificial intelligence in cardiovascular medicine. *Lancet Digit Health.* (2020) 2:e635–6. doi: 10.1016/S2589-7500(20)30249-1
103. Tahhan AS, Vaduganathan M, Greene SJ, Alrohaibani A, Raad M, Gafeer M, et al. Enrollment of older patients, women, and racial/ethnic minority groups in contemporary acute coronary syndrome clinical trials: a systematic review. *J Am Med Assoc Cardiol.* (2020) 5:714–22. doi: 10.1001/jamacardio.2020.0359
104. Obermeyer Z, Powers B, Vogeli C, Mullainathan S. Dissecting racial bias in an algorithm used to manage the health of populations. *Science.* (2019) 366:447–53. doi: 10.1126/science.aax2342
105. The European Commission on medical AI. *European Commission White Paper. On Artificial Intelligence— A European Approach to Excellence and Trust*, Bruxelles (2020).

Conflict of Interest: The authors declare that the research was conducted in the absence of any commercial or financial relationships that could be construed as a potential conflict of interest.

Publisher's Note: All claims expressed in this article are solely those of the authors and do not necessarily represent those of their affiliated organizations, or those of the publisher, the editors and the reviewers. Any product that may be evaluated in this article, or claim that may be made by its manufacturer, is not guaranteed or endorsed by the publisher.

frontiers in Cardiovascular Medicine

REVIEW
published: 29 October 2021
doi: 10.3389/fcvm.2021.768563

Clinical Application of Dynamic Contrast Enhanced Perfusion Imaging by Cardiovascular Magnetic Resonance

Russell Franks[1], *Sven Plein*[1,2] *and Amedeo Chiribiri*[1]*

[1] School of Biomedical Engineering and Imaging Sciences, King's College London, London, United Kingdom, [2] Leeds Institute of Cardiovascular and Metabolic Medicine, University of Leeds, Leeds, United Kingdom

Functionally significant coronary artery disease impairs myocardial blood flow and can be detected non-invasively by myocardial perfusion imaging. While multiple myocardial perfusion imaging modalities exist, the high spatial and temporal resolution of cardiovascular magnetic resonance (CMR), combined with its freedom from ionising radiation make it an attractive option. Dynamic contrast enhanced CMR perfusion imaging has become a well-validated non-invasive tool for the assessment and risk stratification of patients with coronary artery disease and is recommended by international guidelines. This article presents an overview of CMR perfusion imaging and its clinical application, with a focus on chronic coronary syndromes, highlighting its strengths and challenges, and discusses recent advances, including the emerging role of quantitative perfusion analysis.

Keywords: myocardial perfusion imaging (MPI), cardiovascular magnetic resonance (CMR), quantitative perfusion, coronary artery disease, dynamic contrast enhance magnetic resonance, first-pass perfusion MRI

OPEN ACCESS

Edited by:
Steffen Erhard Petersen, Queen Mary University of London, United Kingdom

Reviewed by:
Michael Jerosch-Herold, Brigham and Women's Hospital and Harvard Medical School, United States
Alessia Gimelli, Gabriele Monasterio Tuscany Foundation (CNR), Italy

***Correspondence:**
Amedeo Chiribiri
amedeo.chiribiri@kcl.ac.uk

Specialty section:
This article was submitted to Cardiovascular Imaging, a section of the journal Frontiers in Cardiovascular Medicine

Received: *31 August 2021*
Accepted: *27 September 2021*
Published: *29 October 2021*

Citation:
Franks R, Plein S and Chiribiri A (2021) Clinical Application of Dynamic Contrast Enhanced Perfusion Imaging by Cardiovascular Magnetic Resonance. Front. Cardiovasc. Med. 8:768563. doi: 10.3389/fcvm.2021.768563

INTRODUCTION

Myocardial perfusion imaging (MPI) plays a central role in the diagnosis, management, and risk stratification of patients with coronary artery disease (CAD) and is recommended by international guidelines (1). Unlike angiographic imaging, which provides anatomical data on the patency of major epicardial coronary arteries, MPI offers information on the downstream effects of epicardial coronary stenoses, as well as the function of the coronary microcirculation (2). Whilst there are a several non-invasive imaging modalities capable of MPI, cardiovascular magnetic resonance (CMR) is unique in its ability to provide high-resolution myocardial perfusion data alongside global and regional biventricular function, assessment of myocardial infarction, and without need for ionising radiation. This article presents an overview of the CMR method of dynamic contrast enhanced (DCE) perfusion imaging.

DYNAMIC CONTRAST ENHANCED PERFUSION IMAGING BY CMR

DCE perfusion imaging is designed to track and display the first passage of a contrast agent (CA) bolus through the myocardium during maximal coronary vasodilation, and often during resting conditions (**Figure 1**) (3).

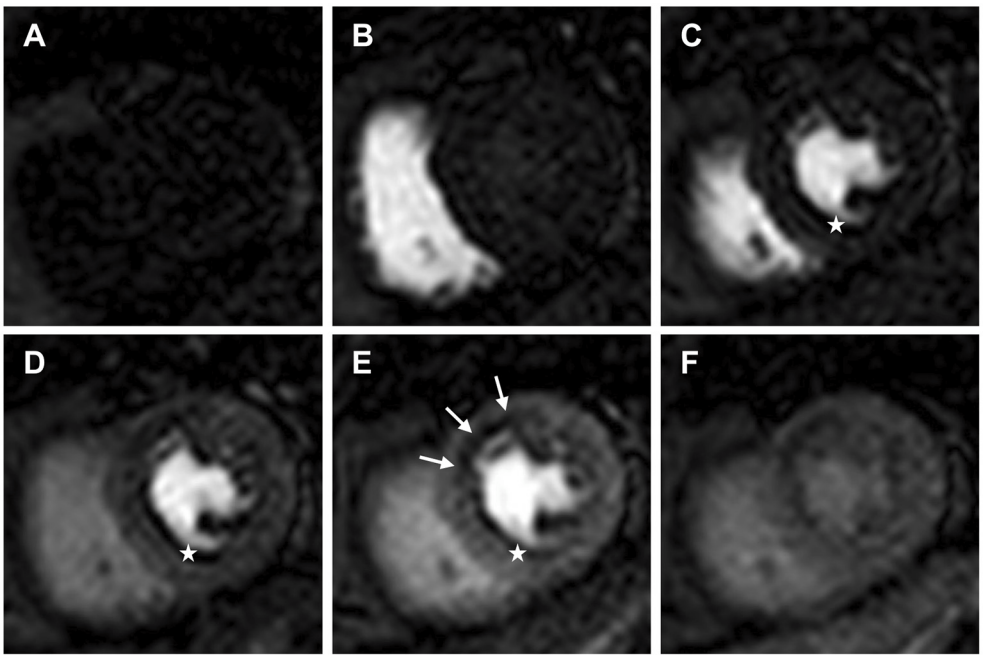

FIGURE 1 | Dynamic contrast enhanced perfusion CMR tracks and displays the first passage of an injected contrast agent bolus through the heart. Mid ventricular slice **(A)** pre-contrast arrival; **(B)** contrast arrival in the right ventricle; **(C)** contrast arrival in the left ventricle (LV); **(D)** contrast arrival in the LV myocardium; **(E)** maximal myocardial contrast between remote myocardium and the subendocardial region of relative hypoperfusion (white arrows); **(F)** second pass and redistribution of the contrast agent. White stars identify a dark rim artefact, which can be seen on arrival of contrast in the LV prior to myocardial contrast enhancement.

The technique relies upon the heterogeneity of contrast perfusion in myocardium supplied by obstructed vs. unobstructed coronary arteries. Flow limiting stenoses blunt the augmentation of myocardial perfusion during hyperaemia, manifesting as a relative perfusion defect at stress, which is not seen at rest, compared with myocardium subtended by unobstructed coronary arteries (**Figure 2**) (4). Maximal coronary vasodilation is typically achieved with an intravenous adenosine infusion or a bolus injection of the adenosine receptor agonist regadenoson. Both adenosine and regadenoson produce coronary vasodilatation by their agonistic action on the A2a receptors found in coronary smooth muscle and endothelial cells, inducing hyperpolerization of smooth muscle and release of nitric oxide (5). The phosphodiesterase enzyme inhibitor dipyridamole can also be used to induce coronary vasodilation. Dipyridamole inhibits cyclic adenosine monophosphate degradation and blocks cellular reuptake of adenosine, thereby increasing the circulating concentration of endogenous adenosine (6).

Basic Principles

The clinical feasibility of tracking the first-pass of contrast through the myocardium with CMR was first demonstrated by Atkinson et al. in 1990 who used an inversion recovery gradient echo (GRE) sequence to track the first-pass of CA through rodent and human hearts (2, 7). Following an intravenous injection of CA, multiple (typically 3 short-axis) images of the heart are acquired, each with a different anatomical location and cardiac phase, which remain constant across sequential cardiac cycles (8). On arrival of the CA to the myocardium, the paramagnetic gadolinium chelate interacts with water molecules within the extracellular space, reducing T1 relaxation times and thus increasing signal intensity on a T1 weighted image. Areas of relative hypoperfusion therefore appear hypointense in comparison to well-perfused myocardium (4). In contemporary perfusion sequences, T1-weighting of images is typically achieved by use of a 90° saturation recovery (SR) radiofrequency pulse. A 180° inversion recovery pulse can generate greater contrast between normal and hypoperfused myocardium but is limited by longer imaging times and sensitivity to heart rate variations and miss-triggers, which can result in incomplete magnetisation recovery and signal intensity variation. Thus, saturation-prepared sequences are the current standard (2, 4). Preparation pulses are typically non-selective in order to reduce myocardial sensitivity to through-plane motion as well as achieve uniform contrast enhancement in the left ventricular (LV) blood pool. Whilst use of a single shared SR preparation offers increased efficiency, typically, separate SR preparations are used for each imaging slice to ensure uniform image quality (4).

To ensure adequate coverage of the 16 standard AHA segments, guidelines recommend a minimum acquisition of 3 short-axis myocardial slices, in addition to a minimum spatial resolution of 3×3 mm (3, 9). In order to accurately display changes in signal intensity over time, imaging should ideally be acquired for consecutive R-R intervals during the first passage of the contrast bolus (3). During pharmacologically

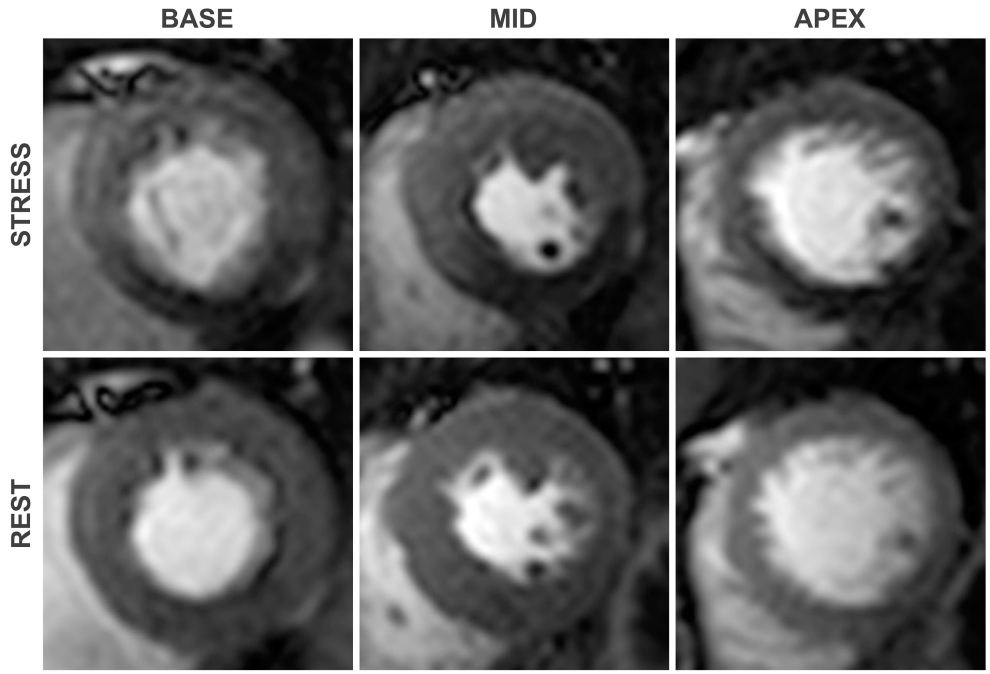

FIGURE 2 | First-pass perfusion images at pharmacologically induced stress **(top)** and at rest **(bottom)**. An inducible perfusion defect is seen in the Inferior and inferoseptal segments when compared with the remote segments, consistent with flow limiting disease in the right coronary artery. As is typical of perfusion defects secondary to obstructive coronary stenoses, contrast hypoenhancement is most pronounced in the subendocardial region.

induced stress, the R-R interval can be short and thus rapid data acquisition is needed to meet these high spatial and temporal demands. A standard spatial resolution of 2–3 mm can be achieved with a fast read-out sequence, such as fast GRE, balanced steady state free procession (bSSFP) or hybrid echo planar imaging, combined with spatial under-sampling (2). Increasing data sampling speeds further can be used to achieve even higher in-plane spatial resolution (1–2 mm) and/or greater spatial coverage. Conventional spatial-under-sampling techniques, such as parallel imaging, are limited to ∼2-fold acceleration owing to a significant signal to noise (SNR) penalty above this acceleration level. However, under-sampling in both the spatial and-temporal domain can significantly increase data acquisition speed without compromising on either SNR or temporal resolution (10). Higher in-plane spatial resolution (1–2 mm) can reduce endocardial dark-rim artefact and improve the image quality and diagnostic accuracy for the detection of CAD including in single-vessel and multivessel disease (10, 11). If the spatio-temporal acceleration is used to increase spatial coverage, additional short-axis myocardial slices or even 3-dimensional (3D) myocardial perfusion data for whole-heart coverage can be acquired. 3D perfusion CMR is highly accurate to detect CAD as defined by invasive coronary physiology, however, any clinical benefit over conventional 3 short-axis high-resolution myocardial slices remains unclear (12, 13). Use of multiband radiofrequency pulses for simultaneous multi-slice data acquisition has been proposed as a strategy to increase spatial coverage whilst maintaining in-plane spatial resolution, however, this method still awaits clinical validation in patients with CAD (14).

In the clinical setting, perfusion CMR is performed at either 1.5 Tesla (T) or 3T field strengths, with 1.5T being more widely available. A major advantage of perfusion CMR at 3T is the superior SNR that can be obtained. The higher field strength also improves contrast enhancement, and importantly, offers improved diagnostic accuracy for the detection of single vessel and multivessel CAD (15, 16). Despite the overall image quality being superior at 3T (10), the associated increased field inhomogeneities heighten the sensitivity to susceptibility artefacts (17). Use of a GRE readout as opposed to a bSSFP readout is therefore preferred at 3T to minimise this undesirable consequence (18).

Artefacts

An in-depth review of imaging artefacts is beyond the scope of this review, however, two types of artefact are of particular importance in DCE perfusion CMR imaging and warrant brief discussion. Despite high data acquisition speeds, DCE perfusion imaging is susceptible to both in-plane and through-plane motion, which can be cardiac or respiratory related, and results in image artefacts (4, 19). This can be exacerbated by a high respiratory rate during pharmacologically induced stress. In-plane motion can be reliably corrected in-line after data acquisition (20), however, through-plane motion remains problematic and highlights the importance of patient

education and focus on gentle controlled breathing during the acquisition of stress images. Another important artefact in DCE perfusion CMR imaging is the subendocardial dark-rim artefact. There are several causes of dark-rim artefacts, the most common being Gibbs ringing, cardiac motion and magnetic field inhomogeneities resulting from the strong paramagnetic properties of a gadolinium based CA arriving in the heart (19). The dark-rim artefact is of particular importance as it can mimic inducible perfusion defects and reduce diagnostic accuracy. However, dark-rim artefacts do have features which enable an experienced reader to differentiate them from true perfusion defects. Typically, unlike true inducible perfusion defects, dark-rim artefacts appear on arrival of contrast in the LV blood pool, lead to a signal reduction compared with baseline (pre-contrast), are usually only one pixel wide, and most frequently appear in the phase encoding direction (21). An example of a dark-rim artefact is shown in **Figure 1**.

QUALITATIVE STRESS PERFUSION CMR

Qualitative stress perfusion CMR is one of the most robust non-invasive methods for the detection of CAD (22). The visual assessment of myocardial contrast enhancement during the first-passage of CA enables detection of regions of relative hypoperfusion. Comparison of myocardial perfusion is made between endocardial and epicardial regions as well as between myocardial segments. Significant inducible perfusion defects are more severe at the subendocardium, appear on the arrival of CA to the myocardium, are more than 2 pixels wide, and must persist beyond the peak myocardial enhancement. Furthermore, for a perfusion defect to be significant for ischemia, it should be present during stress but not at rest (if available) and, in the context of CAD, have a distribution consistent with one or more coronary territories (21). A transmural gradient of perfusion, with more severe hypoperfusion in the subendocardial layers, is usually observed in the involved segments (21, 23). Perfusion imaging is read alongside the corresponding late gadolinium enhancement (LGE) imaging, with matching LGE-perfusion defects being considered negative for inducible ischemia (21, 24).

There are numerous single centre and multi-centre studies demonstrating the accuracy of qualitative stress perfusion CMR. In a large meta-analysis by Jaarsma et al. data was pooled from 22 studies that evaluated qualitative stress perfusion CMR against anatomical luminal stenosis on invasive coronary angiography (ICA) and found a patient level sensitivity and specificity of 90 and 74%, respectively (25). Using invasive fraction flow reserve (FFR) as the reference standard, a more recent meta-analysis by Kiaos et al. pooled 6 studies and found sensitivity and specificity of 90 and 85%, respectively (26). More important for guiding revascularisation decision making is the ability of stress perfusion CMR to accurately detect ischemia at the level of the perfusion territory. In 2013 Ebersberger et al. evaluated 116 patients with suspected or known CAD with qualitative stress perfusion CMR at 3 Tesla and found a high diagnostic accuracy for detecting diseased vessels (defined by invasive coronary angiography with FFR) with an area under the receiver operator characteristic curve (AUC) of 0.93, sensitivity of 89% and specificity of 95% (27). Similar high diagnostic accuracies have also been reported by others (23, 28, 29).

The accuracy of qualitative stress perfusion CMR has been extensively compared with other non-invasive MPI modalities. In 2008, the MR-IMPACT study was the first multicentre multivendor study to demonstrate non-inferiority of stress perfusion CMR to the then clinical standard single-photon emission computerised tomography (SPECT) for the detection of CAD in 42 patients against coronary angiography (lumen stenosis > 50%) with AUCs of 0.86 and 0.75 for CMR and SPECT, respectively (30). The subsequent larger MR-IMPACT II study with 515 patients across 33 centres found superior sensitivity of perfusion CMR over SPECT (0.67 vs. 0.59) but inferior specificity (0.61 vs. 0.72) (31). In 2011 the single centre CE-MARC trial was the first large scale prospective comparison of CMR vs. SPECT for the detection of CAD on ICA (>70% stenosis) and found superior sensitivities (87 vs. 67%) and similar specificities (83 vs. 83%) for CMR vs. SPECT (32, 33). In 2015, a meta-analysis by Takx et al. compared the diagnostic accuracy of perfusion CMR with other non-invasive MPI techniques and found perfusion CMR had a similarly high diagnostic performance to positron emission tomography (PET) and computerised tomography (CT) perfusion and superior performance to SPECT and myocardial contrast echocardiography. This analysis, which included 15 perfusion CMR studies with 798 patients, found a pooled sensitivity and specificity for perfusion CMR of 0.89 and 0.87, respectively, at the patient level and 0.87 and 0.91 at the vessel level (22). It is noteworthy that this meta-analysis included CMR studies analysed qualitatively as well as quantitatively.

Multiple retrospective and prospective trials have demonstrated the prognostic value of qualitative stress perfusion CMR for risk stratification of patients with known or suspected CAD (34, 35). A large meta-analysis of 15 pooled studies evaluating 7,606 patients with known or suspected CAD undergoing stress perfusion CMR found a positive stress perfusion CMR was associated with an annualised event rate of 4.9% compared with only 0.9% in those with a negative study (35). Consistent with this, and its high diagnostic performance, stress perfusion CMR is an effective gatekeeper to invasive evaluation and management of patients with angina. In 2016, the CE-MARC II trial in patients with suspected angina found initial investigation by CMR resulted in a lower probability of unnecessary invasive coronary angiography than the since updated UK National Institute for Health and Care Excellence (NICE) guidelines–directed care, with no increase in adverse events (36). More recently, the multi-centre MR-INFORM trial demonstrated stress perfusion CMR can be used with the same efficacy and safety as invasive FFR in the initial management of patients with stable angina and risk factors for CAD (37). The study randomly assigned 918 patients to either a perfusion CMR scan or invasive coronary angiography with FFR, and found non-inferiority of the CMR strategy for the composite primary outcome of death, non-fatal myocardial infarction, or target-vessel revascularization within 1 year. In addition, the CMR based strategy was associated with a lower incidence of coronary revascularisation. Using stress perfusion CMR as a

gate-keeper prior to ICA is also a cost effective approach in patients at intermediate risk of obstructive CAD (38).

Challenges of Qualitative Stress Perfusion CMR

In addition to its strengths, qualitative stress perfusion CMR also has its challenges:

(1) Operator training - Perfusion data interpretation is subjective and as such is dependent on operator training and experience. The high diagnostic accuracies reported in the literature mostly come from experienced academic CMR centres with expert readers. A study from Villa et al. demonstrated that the level of reader training is the main determinant of diagnostic accuracy in the identification of CAD. They found Level 3 readers to have an 83.6% diagnostic accuracy compared with 65.7 and 55.7% for level 2 and level 1 readers, respectively (39).

(2) Balanced ischemia, multi-vessel disease and ischemic burden - Evidence of inducible myocardial ischemia is associated with adverse prognosis (35). Furthermore, prognosis worsens as the ischemic burden increases, and only revascularisation of flow-limiting coronary stenoses is associated with improved outcomes (40, 41). Therefore, accurate detection and quantification of the myocardial ischemic burden is of paramount importance when stratifying patient risk and considering coronary revascularisation. As aforementioned, qualitative stress perfusion CMR relies upon the heterogeneity of myocardial contrast perfusion associated with the presence or absence of flow-limiting coronary stenoses. In situations of global ischemia, such as three vessel disease (3VD) or microvascular dysfunction (MVD), there is often an absence of normally perfused reference myocardium and hence qualitative assessment can be challenging. The detrimental impact of "balanced ischemia" on diagnostic accuracy is well-documented in SPECT with up to 20% of patients with 3VD being incorrectly reported as normal (42), and as few as 29% of patients having perfusion defects reported in all coronary territories despite angiographically proven 3VD (43). Perfusion CMR has superior spatial resolution to SPECT (typically 1.5–3 vs. 12–15 mm) and is able to overcome this limitation to some extent, however, the diagnostic accuracy of qualitative assessment remains lower in patients with multivessel CAD and MVD (44–47). Kotecha et al. reported a diagnostic accuracy for qualitative stress perfusion CMR at 1.5 Tesla of 40 and 48% for correct classification of 3-vessel and 2-vessel CAD, respectively, as proven with invasive coronary angiography and FFR (48). Using a high-resolution perfusion CMR sequence, Motwani et al. demonstrated a diagnostic accuracy of 57% for detecting perfusion defects in all coronary territories in patients with angiographically proven 3VD (49). Rahman et al. recently reported a qualitative stress perfusion CMR sensitivity of 41% and specificity of 83% with an AUC of 0.60 to detect MVD defined by invasive physiology (44).

(3) Prior coronary artery bypass grafting (CABG) - Evaluation of myocardial perfusion in patients with prior CABG is challenging. These patients frequently have complex multivessel disease, established myocardial infarction, and extensive collateralisation (50, 51). Increased contrast dispersion, delayed contrast arrival at the myocardium (52), and the variability of flow dynamics associated with bypass grafts (53) add to the complexity and likely contribute to the reduced diagnostic accuracy of qualitative perfusion CMR compared with patients without prior CABG (24, 50). In the largest study to date of 110 patients with prior CABG (and 236 with previous percutaneous coronary intervention (PCI)), Bernhardt et al. reported a sensitivity and specificity of 73 and 77%, respectively, for detecting obstructive angiographic disease in patients with prior CABG, while in patients with previous PCI, a sensitivity and specificity of 88 and 90% were reported (24).

QUANTITATIVE PERFUSION CMR

Analysis of myocardial and LV signal intensity (SI)-time curves from DCE perfusion CMR enables quantitative and semi-quantitative analysis of myocardial perfusion, which has been proposed to offer a solution to some of the challenges of qualitative assessment (54).

Semi-Quantitative Myocardial Perfusion CMR

Whilst the field is moving toward absolute perfusion quantification, prior to the recent technical developments that made full quantification of myocardial perfusion possible, various semi-quantitative measures of myocardial perfusion were proposed. These methods describe the characteristics of the myocardial SI-time curves without attempting to estimate absolute myocardial blood flow (MBF). The most commonly used of these is the maximal myocardial "upslope" parameter, but others including "upslope integral ratio," "contrast enhancement ratio (CER)," and the "time to peak" have also been evaluated (**Figure 3**) (21, 54, 55). Since myocardial perfusion is driven by systemic arterial perfusion, semi-quantitative parameters are dependent upon the underlying haemodynamic conditions and can be normalised to enable comparison of rest and stress values, as well as a comparison between individuals (54).

Underlying haemodynamic conditions are partially reflected by the shape of the arterial input, which can be measured from the LV blood pool. Division of the myocardial parameter by the equivalent arterial input function (AIF) parameter serves to normalise perfusion parameters and defines a perfusion index (PI). The ratio of the normalised stress and rest perfusion indices defines a myocardial perfusion reserve index (MPRI), a non-invasive surrogate for coronary flow reserve (CFR) and an index of the functional severity of a coronary lesion (54, 56, 57). It is noteworthy that this method of PI normalisation represents a

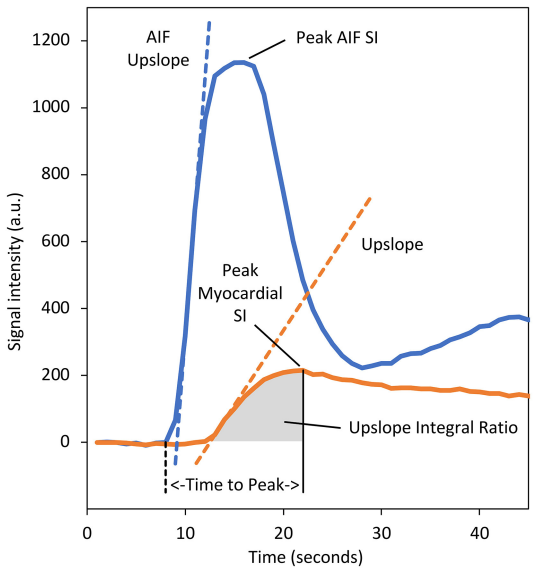

FIGURE 3 | Baseline corrected signal intensity (SI)–time curves for myocardial tissue (orange) and the arterial input function (AIF) (blue) sampled from the left ventricular (LV) blood-pool. Various semi-quantitative perfusion parameters are demonstrated. The dashed orange line represents the "upslope" parameter and denotes the maximal rate of myocardial contrast enhancement. Division of the myocardial upslope by the equivalent AIF upslope (dashed blue line) defines the "upslope index," which normalises for the haemodynamic conditions and enables comparison between stress and rest, and calculation of a myocardial perfusion reserve index. The area under the myocardial tissue curve from the arrival of contrast at the myocardium to the time of peak enhancement defines the "upslope integral ratio." The area under the myocardial curve from contrast arrival to the time of peak AIF enhancement has also been used to define this parameter. The "time to peak" myocardial enhancement is measured from the arrival of contrast in the LV blood pool (dashed black line) to the time of peak myocardial enhancement. The "contrast enhancement ratio" parameter is not displayed as this requires an uncalibrated baseline (defined as $SI_{peak} - SI_{baseline})/SI_{baseline}$ (55). a.u., arbitrary units.

heuristic approach, and one which has been shown to underestimate perfusion reserve when compared against microspheres. A more accurate MPRI requires the PI to be normalised by the analogous AIF parameter as well as the time delay between the foot of the tissue curve and peak tissue enhancement (58).

Perfusion dyssynchrony has previously been proposed for the identification of hemodynamically significant CAD, as defined by FFR, and is based on the analysis of the variance of the time to peak across the LV myocardium (59).

Semi-quantitative parameters have been validated against microspheres and coronary angiography for detection of CAD with a high diagnostic accuracy (60–62). A recent meta-analysis of 6 studies using semi-quantitative analyses of myocardial perfusion at the territory level found pooled sensitivity of 77% and specificity of 84% (63). However, there are a number of drawbacks to semi-quantitative perfusion reserve indices:

(1) The only modest gains over qualitative assessment come at the expense of a significant time penalty necessary for processing the perfusion data (64).
(2) When validated against microspheres, semi-quantitative parameters underestimate MBF at flow rates above 1.5 ml/g/min. This can cause underestimation of PIs and MPRI in healthy myocardium where typical stress MBF rates exceed 2 ml/g/min (55).
(3) MPRI from different semi-quantitative perfusion parameters tend to have different thresholds to identify myocardial ischemia and their magnitude cannot be directly compared to that of an invasively measured coronary flow reserve (54).
(4) MPRI requires the acquisition of DCE perfusion imaging during stress and rest, partially conflicting with current international imaging guidelines, which are moving away from the routine acquisition of rest imaging in a quest to reduce CMR scan duration (3).
(5) MPRI is unable to distinguish between a state of globally reduced stress MBF with normal resting MBF (for example multivessel epicardial coronary disease), and a state of globally preserved stress MBF but increased resting MBF (for example hypertension or aortic stenosis). Both clinical scenarios result in a diminished global MPRI. Only by quantifying absolute MBF in millilitres per gramme of myocardium per minute (ml/g/min) during rest and maximal hyperaemia can we differentiate these two very different clinical scenarios (54).

Quantitative Myocardial Perfusion CMR

Measurement of absolute MBF in ml/g/min is possible through the application of tracer-kinetic models to the perfusion data. Myocardial perfusion reserve (MPR), a useful indicator of the significance of coronary artery stenoses, is defined as the ratio of MBF at stress and rest (57).

Several different methodologies for perfusion quantification have been developed. The technical aspects of the various approaches are beyond the scope of our review, however, in brief the methods can be broadly divided into two distinct groups; "tracer-kinetic model dependent" and "tracer-kinetic model independent" (54). Model-dependent methods, of which there are numerous, make the assumption that the tissue structures can be divided into distinct compartments, typically an intravascular and interstitial compartment, and use complex mathematical equations to describe the contrast exchange occurring between these compartments. Tracer-kinetic models are applied to perfusion data beyond the first pass of contrast and can infer knowledge on the permeability surface area product and intravascular volumes in addition to MBF (54). The accuracy of the measurements is dependent on assumptions made with respect to parameters such as signal saturation, relaxivity of contrast agent, baseline T1 and T2 values in the myocardium and blood, homogeneity of the magnetic and RF excitation fields, blood heamatocrit and others (65).

Tracer-kinetic model-independent approaches are centred around the central volume principle, which dictates that MBF can be measured from knowledge of the contrast transit times through the vascular system (66). This value can be estimated from the transfer function, obtained by normalising the myocardial SI curves by the AIF curve using a deconvolution

operation. The initial amplitude of the transfer function is proportional to MBF (67). The transfer function is, in practise, obtained using a forward modelling approach that involves the use of different mathematical models and data fitting procedures (67). One of the most widely used and validated deconvolution technique employs the use of a Fermi function to constrain the transfer function to fit the likely behaviour of an intravascular tracer (54, 67).

Quantitative perfusion (QP) measurements require the existence of a linear relationship between CA concentration and measured SI. However, the relationship between these parameters becomes non-linear at higher contrast concentrations due to saturation of the T1-weighted contrast enhancement and T2* effects (68, 69). This phenomenon is more frequently observed in the AIF where CA concentration is highest. Any underestimation of the AIF will result in an overestimation of MBF with a magnitude relative to the magnitude of the saturation effect (54). Signal saturation must therefore be avoided or corrected for accurate MBF measurements. Use of a lower CA dose can avoid signal saturation in the blood pool but would provide inadequate contrast-to-noise for myocardial assessment. Proposed solutions include; (1) a dual-bolus acquisition; (2) a dual-sequence acquisition; and (3) retrospective correction using calibration curves (54). Whilst calibration curves can be generated from knowledge of the sequence parameters and the pre-contrast T1 measurements, this is a somewhat cumbersome approach to correct blood-pool signal saturation, and minor changes in the perfusion sequence parameters can necessitate the need for re-calibration (70). The dual bolus approach measures the AIF from a dilute CA pre-bolus, which maintains the linearity of SI to CA concentration in the blood pool. The pre-bolus is followed by a neat CA bolus for myocardial assessment (71, 72). As the dilution ratio is known, the AIF SI-time curve can be rescaled (and time shifted) prior to perfusion quantification (54). This technique has been validated against microspheres for measurement of MBF (55, 73) and has clinical validation against PET and invasive FFR for the detection of flow limiting CAD (23, 74, 75). However, clinical implementation of the dual bolus technique is onerous owing to the need for multiple injections and longer sequence acquisition times (72).

A dual sequence acquisition uses a single bolus of neat contrast but acquires an addition imaging slice with a short saturation delay, low resolution and reduced T1-weighting (69). This low resolution slice enables measurement of the AIF without blood pool signal saturation. Higher resolution perfusion slices are acquired following the low-resolution image and during the same R-R interval, permitting myocardial and AIF assessment within the same cardiac cycle (69, 76, 77). When a dual sequence approach is employed, and prior to quantification of MBF, SI-time curves must be converted to correspond to CA concentrations (69). A comparison of MBF estimates in pigs found a good correlation between dual-bolus and dual-sequence methods (77). The dual sequence method has been validated against invasive coronary physiology and PET, and is becoming the method of choice for quantitative CMR perfusion owing to its easier integration within the clinical workflow (78, 79).

Another important consideration prior to perfusion quantification is the intrinsic spatial variations in receive-coil sensitivity, which can produce SI variation across the myocardium and lead to inaccuracies when quantifying MBF. This can be corrected for by acquisition of proton-density weighted maps. Alternatively, coil sensitivity can be estimated from pre-contrast images and corrected for by dividing the myocardial signal by its pre-contrast value (54).

Automation of Perfusion Quantification by CMR

The quantification process is complex and requires multiple data processing steps (**Figure 4**). Perfusion images must first be reconstructed from the raw data. The dynamic image series require correction for respiratory motion in addition to correction for coil sensitivity bias (80, 81). Segmentation of the left ventricle and myocardium is required to enable extraction of the AIF and myocardial tissue curves. A point of reference, typically the superior RV insertion point, must be identified to enable standardised AHA cardiac segmentation (9). If a dual sequence approach has been employed, SI data requires conversion to CA concentration. Only at this stage are quantification models applied to the perfusion data to calculate MBF (81). Until recently, these multiple processing steps required time-consuming and laborious manual input, which restricted the application of quantitative perfusion CMR from mainstream clinical practise. However, recent developments in quantification pipelines now enables full automation of the quantification process and generation of pixel-wise perfusion maps either offline, or in-line and within minutes of data acquisition (79).

In 2017, Kellman et al. presented a fully automated quantification pipeline, utilising a dual-sequence approach for derivation of the AIF and a blood tissue exchange model for quantification of MBF. All reconstruction and processing steps were implemented in-line within the opensource Gadgetron software framework and pixel-wise perfusion maps were output within minutes of data acquisition (69, 82). In the same year this approach was validated against PET with good agreement between perfusion values (78), and later demonstrated good repeatability in a study of healthy volunteers, with within subject coefficient of variations between 8 and 12% for both rest and stress MBF measurements (20). In 2019, Kotecha et al. validated the same automated perfusion quantification pipeline against invasive coronary physiology and found high diagnostic accuracy with an AUC of 0.90 for detecting of functionally significant epicardial coronary disease (79). Knott et al. recently demonstrated a strong prognostic value of the same automated pipeline (83). Other fully automated perfusion quantification pipelines have since been developed. Using a two-compartment exchange model for perfusion quantification, Scannell et al. demonstrated highly accurate MBF values from an automated deep-learning based pre-processing pipeline when compared with manual pre-processing (84). Using model-constrained deconvolution, Hsu et al. demonstrated excellent correlation between perfusion values from fully automated and manual

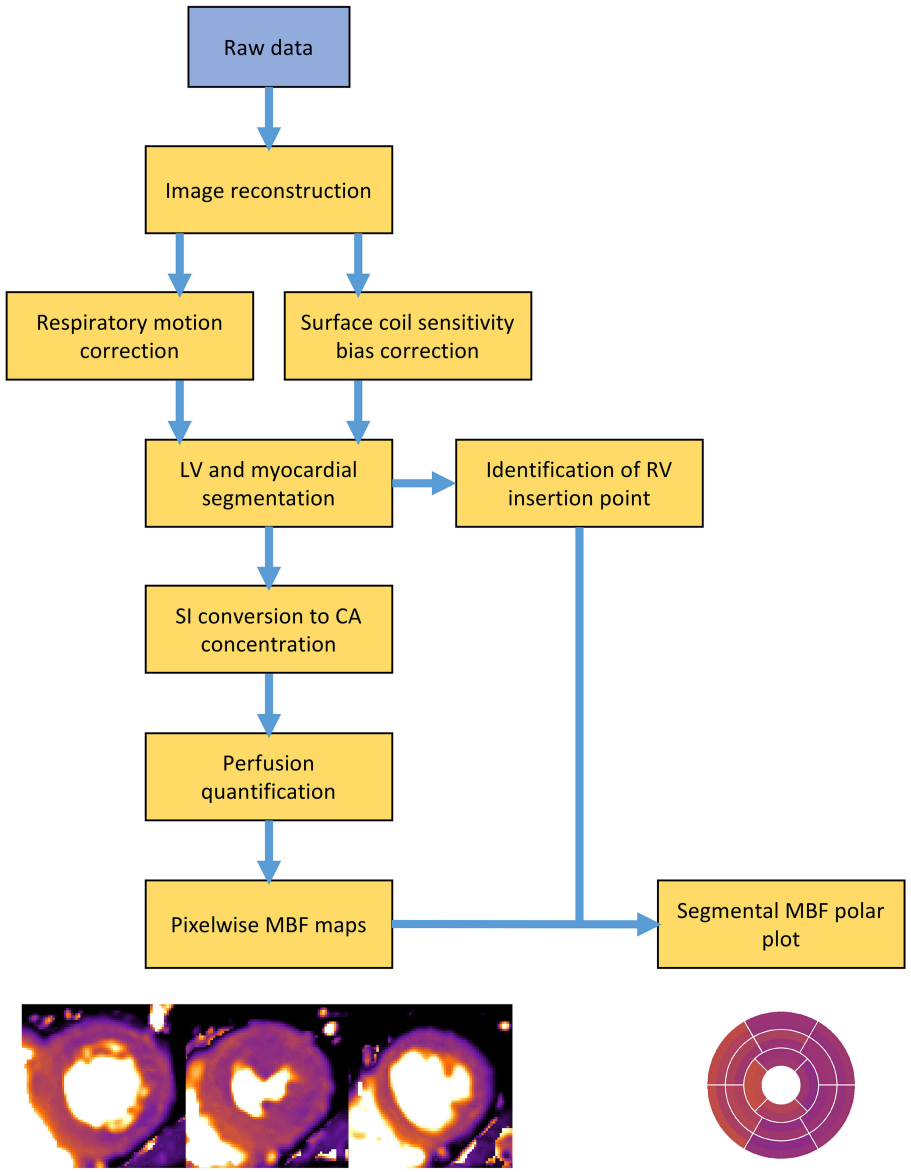

FIGURE 4 | Overview schematic outlining the processing steps involved in a typical perfusion quantification pipeline. LV, left ventricle; RV, right ventricle; SI, signal intensity; CA, contrast agent; MBF, myocardial blood flow.

processing pipelines, as well as high diagnostic accuracy for the detection of CAD with AUCs between 0.86 and 0.93 for automated quantitative perfusion metrics (85).

Clinical Value of Quantitative Perfusion CMR

Several clinical advantages of QP CMR have been demonstrated over qualitative assessment:

(1) The diagnostic accuracy of QP CMR for the detection of CAD is at least equivalent to a level 3 experienced reader, thus offering an observer independent solution to smaller centres that may lack the experience and volume of the larger academic CMR laboratories. A study from Villa et al. found the diagnostic accuracy of QP CMR at the patient level was similar to the qualitative report of a level 3 trained reader and superior to a level 2 trained reader (QP: 86.3%, qualitative level 3: 83.6%, qualitative level 2: 65.7%) (39). This is consistent with a sub-study of the CE-MARC trial that compared stress MBF, MPR, and qualitative assessment (by expert readers in academic centres) and found no difference in diagnostic accuracies (86).

(2) In multivessel coronary disease QP CMR has superior diagnostic accuracy for the detection of CAD at the vessel level (**Figure 5**). A study by Kotecha et al. with a

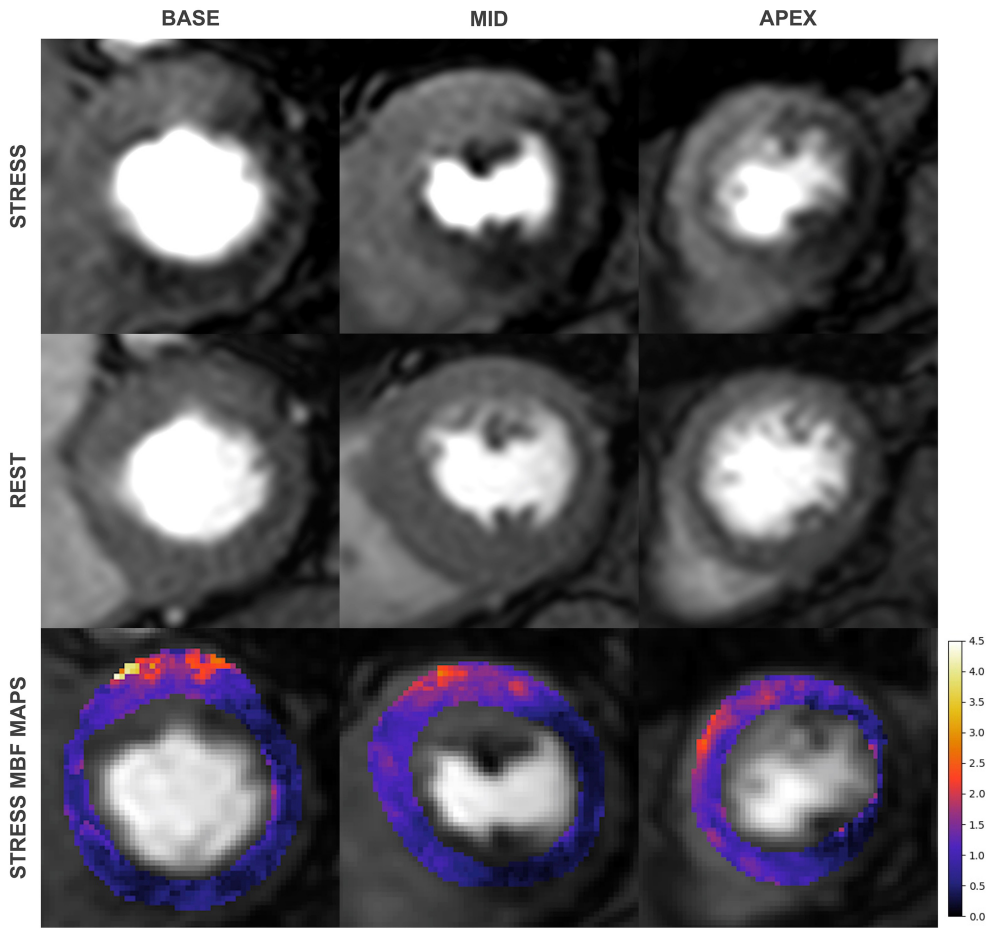

FIGURE 5 | First-pass perfusion images during adenosine induced stress **(top)** and at rest **(middle)** with corresponding pixel-wise myocardial blood flow (MBF) maps **(bottom)** from a 79-year old man with significant 3 vessel disease on invasive coronary angiography. Qualitative assessment identifies inducible perfusion defects in the left circumflex and right coronary artery territories but only perfusion mapping identifies 3 vessel disease.

cohort of 151 patients (95 patients with multivessel disease defined by invasive angiography with FFR), found stress MBF to have superior diagnostic accuracy than qualitative perfusion CMR to identify 3-vessel (87 vs. 40%) and 2-vessel disease (71 vs. 48%) but similar accuracy for the detection of single vessel disease (71 vs. 71%) (48). In line with these findings, QP CMR also enables a more accurate estimation of the myocardial ischemic burden in cases of multivessel disease. In a study of 41 patients, Patel et al. found qualitative assessment was unable to differentiate the ischemic burdens of single-vessel and three-vessel CAD (21 vs. 31%, $p = 0.26$) unlike myocardial perfusion reserve (MPR), which found a significant difference (25 vs. 60%, $p = 0.02$) (45). A similar advantage of QP CMR is also seen in patients with MVD, in whom global ischemia is often present without a region of reference myocardium. A recent study by Rahman et al. of 75 patients with non-obstructed coronary disease, found MPR had a diagnostic accuracy of 79% for the detection of MVD (defined by invasive physiology), significantly superior to qualitative assessment, which had a diagnostic accuracy of 58% (44). Similar findings were reported by Kotecha et al. who found stress MBF had 71% sensitivity, 70% specificity and an AUC of 0.73 for detecting MVD. This study went on to demonstrate that global stress MBF thresholds could be used to non-invasively differentiate 3-vessel coronary disease form MVD (79).

(3) Another potential advantage of QP CMR is its ability to correct for scarred myocardium. The pixel-wise nature of perfusion quantification enables pixel-wise exclusion of LGE from the analysis. This was demonstrated in a study by Villa et al. who fused myocardial perfusion reserve maps with LGE maps to quantify microvascular ischemia in patients with hypertrophic cardiomyopathy. They demonstrated that not accounting for LGE leads to a significant overestimation of the ischemic burden (87). This combined QP and LGE analysis has also been demonstrated feasible in patients with ischemic cardiomyopathy in whom high scar burdens are often present and revascularisation decision making is

complex (88). The prognostic value of such an approach to predict myocardial recovery post revascularisation remains unclear.

(4) There is emerging data that QP CMR enables improved patient risk stratification. In 395 patients with suspected CAD and a median follow up of 460 days, Sammut et al. found that the ischemic burden as measured by MPR provided incremental prognostic value to qualitative assessment (89). In another study of 1,049 patients with suspected or known CAD and a median follow up of 605 days, Knott et al. found stress MBF and MPR were both independently associated with death and major adverse cardiovascular events (83).

(5) Unlike semi-quantitative analysis, fully quantitative analysis has the potential to improve clinical workflow by automated post processing, and potential to reduce scan time by acquiring only stress data. There is some evidence that the accuracy of stress MBF is not enhanced by measurements of MBF at rest (79, 90), however, this remains a contentious issue as evidence to the contrary also exists, particularly in patients with MVD (44, 74, 91).

Quantitative Perfusion CMR and PET

Cardiac PET enables highly accurate measurements of myocardial perfusion, particularly when tracers with linear or near linear extraction are used, and is currently the clinical standard for the non-invasive quantification of myocardial perfusion (78, 92). Recently, perfusion quantification by CMR has been validated against PET with good agreement between perfusion measures (78). As compared to cardiac PET, CMR offers the advantage of higher spatial resolution, wider availability, lower costs, and freedom from ionising radiation. However, where-as the volumetric acquisition of cardiac PET allows for full heart coverage, 3D whole-heart perfusion imaging by CMR remains confined to a research tool and clinical CMR perfusion imaging is typically planned to sample the 16 standard AHA myocardial segments using 3 short-axis slices (3, 13).

FUTURE DIRECTIONS

DCE stress perfusion CMR has made significant strides over the past 2 decades to become an accurate, well-validated, and safe non-invasive method for assessing the functional significance of CAD (26). Advances in data acquisition methods appear promising and high-resolution full LV coverage is likely to be achieved in the coming years (14). The development and validation of QP CMR offers incremental diagnostic and prognostic value, particularly in patients with advanced CAD (48, 89). Advances in artificial intelligence technology are likely to play an increasingly important role in the clinical interpretation of perfusion maps (83). However, for the widespread use of QP CMR outside of the academic institutions, cross vendor standardisation and regulatory approval for the use of in-line myocardial perfusion quantification is required.

CONCLUSION

Stress perfusion CMR is a well-validated and guideline-backed non-invasive tool for the assessment and risk stratification of patients with CAD. Qualitative analysis has high diagnostic accuracy and prognostic value when performed by experienced readers. Contemporary, fully automated perfusion quantification pipelines can provide an accessible, reliable, observer independent analysis with superior diagnostic and prognostic performance, particularly in patients with complex multivessel CAD and MVD.

AUTHOR CONTRIBUTIONS

RF: writing—original draught, review and editing. SP and AC: writing—review and editing. All authors contributed to the article and approved the submitted version.

FUNDING

The authors acknowledge financial support from: The British Heart Foundation [PG/18/71/34009 and TG/18/2/33768]; The Department of Health via the National Institute for Health Research (NIHR) comprehensive Biomedical Research Centre award to Guy's & St Thomas' NHS Foundation Trust in partnership with King's College London and King's College Hospital NHS Foundation Trust; The NIHR Cardiovascular MedTech Co-operative; Wellcome/EPSRC Centre for Medical Engineering [WT 203148/Z/16/Z].

ACKNOWLEDGMENTS

The authors would like to acknowledge Drs. Xenios Milidonis and Cian Scannell of King's College London, School of Biomedical Engineering and Imaging Sciences for providing the perfusion maps displayed in **Figures 4**, **5**, respectively.

REFERENCES

1. Knuuti J, Wijns W, Saraste A, Capodanno D, Barbato E, Funck-Brentano C, et al. 2019 ESC Guidelines for the diagnosis and management of chronic coronary syndromes: the task force for the diagnosis and management of chronic coronary syndromes of the European Society of Cardiology (ESC). *Eur Heart J*. (2020) 41:407–77. doi: 10.1093/eurheartj/ehz425
2. Gerber BL, Raman SV, Nayak K, Epstein FH, Ferreira P, Axel L, et al. Myocardial first-pass perfusion cardiovascular magnetic resonance: history, theory, and current state of the art. *J Cardiovasc Magn Reson*. (2008) 10:18. doi: 10.1186/1532-429X-10-18
3. Kramer CM, Barkhausen J, Bucciarelli-Ducci C, Flamm SD, Kim RJ, Nagel E. Standardized cardiovascular magnetic resonance imaging (CMR) protocols: 2020 update. *J Cardiovasc Magn Reson*. (2020) 22:17. doi: 10.1186/s12968-020-00607-1

4. Kellman P, Arai AE. Imaging sequences for first pass perfusion – a review. *J Cardiovasc.* (2007) 9:525–37. doi: 10.1080/10976640601187604
5. Mustafa SJ, Morrison RR, Teng B, Pelleg A. Adenosine receptors and the heart: role in regulation of coronary blood flow and cardiac electrophysiology. *Handb Exp Pharmacol.* (2009) 193:161–88. doi: 10.1007/978-3-540-89615-9_6
6. Gupta A, Samarany S. *Dipyridamole Nuclear Stress Test*. Treasure Island, FL (2021).
7. Atkinson DJ, Burstein D, Edelman RR. First-pass cardiac perfusion: evaluation with ultrafast MR imaging. *Radiology*. (1990) 174:757–62. doi: 10.1148/radiology.174.3.2305058
8. Biglands JD, Radjenovic A, Ridgway JP. Cardiovascular magnetic resonance physics for clinicians: part II. *J Cardiovasc Magn Reson.* (2012) 14:66. doi: 10.1186/1532-429X-14-66
9. Cerqueira MD, Weissman NJ, Dilsizian V, Jacobs AK, Kaul S, Laskey WK, et al. Standardized myocardial segmentation and nomenclature for tomographic imaging of the heart. A statement for healthcare professionals from the Cardiac Imaging Committee of the Council on Clinical Cardiology of the American Heart Association. *Circulation.* (2002) 105:539–42. doi: 10.1161/hc0402.102975
10. Plein S, Schwitter J, Suerder D, Greenwood JP, Boesiger P, Kozerke S. k-Space and time sensitivity encoding-accelerated myocardial perfusion MR imaging at 3.0 T: comparison with 1.5 T. *Radiology*. (2008) 249:493–500. doi: 10.1148/radiol.2492080017
11. Motwani M, Maredia N, Fairbairn TA, Kozerke S, Radjenovic A, Greenwood JP, et al. High-resolution versus standard-resolution cardiovascular MR myocardial perfusion imaging for the detection of coronary artery disease. *Circ Cardiovasc Imaging.* (2012) 5:306–13. doi: 10.1161/CIRCIMAGING.111.971796
12. Motwani M, Jogiya R, Kozerke S, Greenwood JP, Plein S. Advanced cardiovascular magnetic resonance myocardial perfusion imaging: high-spatial resolution versus 3-dimensional whole-heart coverage. *Circ Cardiovasc Imaging*. (2013) 6:339–48. doi: 10.1161/CIRCIMAGING.112.000193
13. Manka R, Wissmann L, Gebker R, Jogiya R, Motwani M, Frick M, et al. Multicenter evaluation of dynamic three-dimensional magnetic resonance myocardial perfusion imaging for the detection of coronary artery disease defined by fractional flow reserve. *Circ Cardiovasc Imaging*. (2015) 8:e003061. doi: 10.1161/CIRCIMAGING.114.003061
14. Nazir MS, Neji R, Speier P, Reid F, Stäb D, Schmidt M, et al. Simultaneous multi slice (SMS) balanced steady state free precession first-pass myocardial perfusion cardiovascular magnetic resonance with iterative reconstruction at 1.5 T. *J Cardiovasc Magn Reson*. (2018) 20:84. doi: 10.1186/s12968-018-0502-7
15. Cheng ASH, Pegg TJ, Karamitsos TD, Searle N, Jerosch-Herold M, Choudhury RP, et al. Cardiovascular magnetic resonance perfusion imaging at 3-tesla for the detection of coronary artery disease: a comparison with 1.5-tesla. *J Am Coll Cardiol.* (2007) 49:2440–9. doi: 10.1016/j.jacc.2007.03.028
16. Araoz PA, Glockner JF, McGee KP, Potter DDJ, Valeti VU, Stanley DW, et al. 3 Tesla MR imaging provides improved contrast in first-pass myocardial perfusion imaging over a range of gadolinium doses. *J Cardiovasc Magn Reson.* (2005) 7:559–64. doi: 10.1081/JCMR-200060622
17. Holtackers RJ, Wildberger JE, Wintersperger BJ, Chiribiri A. Impact of field strength in clinical cardiac magnetic resonance imaging. *Invest Radiol.* (2021). 56:764–72. doi: 10.1097/RLI.0000000000000809
18. Oshinski JN, Delfino JG, Sharma P, Gharib AM, Pettigrew RI. Cardiovascular magnetic resonance at 3.0T: current state of the art. *J Cardiovasc Magn Reson*. (2010) 12:55. doi: 10.1186/1532-429X-12-55
19. Ferreira PF, Gatehouse PD, Mohiaddin RH, Firmin DN. Cardiovascular magnetic resonance artefacts. *J Cardiovasc Magn Reson*. (2013) 15:41. doi: 10.1186/1532-429X-15-41
20. Brown LAE, Onciul SC, Broadbent DA, Johnson K, Fent GJ, Foley JRJ, et al. Fully automated, inline quantification of myocardial blood flow with cardiovascular magnetic resonance: repeatability of measurements in healthy subjects. *J Cardiovasc Magn Reson.* (2018) 20:48. doi: 10.1186/s12968-018-0462-y
21. Schulz-Menger J, Bluemke DA, Bremerich J, Flamm SD, Fogel MA, Friedrich MG, et al. Standardized image interpretation and post-processing in cardiovascular magnetic resonance - 2020 update : society for Cardiovascular Magnetic Resonance (SCMR): board of trustees task force on standardized post-processing. *J Cardiovasc Magn Reson*. (2020) 22:19. doi: 10.1186/s12968-020-00610-6
22. Takx RAP, Blomberg BA, El Aidi H, Habets J, de Jong PA, Nagel E, et al. Diagnostic accuracy of stress myocardial perfusion imaging compared to invasive coronary angiography with fractional flow reserve meta-analysis. *Circ Cardiovasc Imaging.* (2015) 8:e002666. doi: 10.1161/CIRCIMAGING.114.002666
23. Chiribiri A, Hautvast GL, Lockie T, Schuster A, Bigalke B, Olivotti L, et al. Assessment of coronary artery stenosis severity and location: quantitative analysis of transmural perfusion gradients by high-resolution MRI versus FFR. *JACC Cardiovasc Imaging.* (2013) 6:600–9. doi: 10.1016/j.jcmg.2012.09.019
24. Bernhardt P, Spiess J, Levenson B, Pilz G, Höfling B, Hombach V, et al. Combined Assessment of myocardial perfusion and late gadolinium enhancement in patients after percutaneous coronary intervention or bypass grafts. A multicenter study of an integrated cardiovascular magnetic resonance protocol. *JACC Cardiovasc Imaging.* (2009) 2:1292–300. doi: 10.1016/j.jcmg.2009.05.011
25. Jaarsma C, Leiner T, Bekkers SC, Crijns HJ, Wildberger JE, Nagel E, et al. Diagnostic performance of noninvasive myocardial perfusion imaging using single-photon emission computed tomography, cardiac magnetic resonance, and positron emission tomography imaging for the detection of obstructive coronary artery disease: a meta-anal. *J Am Coll Cardiol*. (2012) 59:1719–28. doi: 10.1016/j.jacc.2011.12.040
26. Kiaos A, Tziatzios I, Hadjimiltiades S, Karvounis C, Karamitsos TD. Diagnostic performance of stress perfusion cardiac magnetic resonance for the detection of coronary artery disease: a systematic review and meta-analysis. *Int J Cardiol*. (2018) 252:229–33. doi: 10.1016/j.ijcard.2017.11.066
27. Ebersberger U, Makowski MR, Schoepf UJ, Platz U, Schmidtler F, Rose J, et al. Magnetic resonance myocardial perfusion imaging at 3.0 Tesla for the identification of myocardial ischaemia: comparison with coronary catheter angiography and fractional flow reserve measurements. *Eur Heart J Cardiovasc Imaging*. (2013) 14:1174–80. doi: 10.1093/ehjci/jet074
28. Lockie T, Ishida M, Perera D, Chiribiri A, De Silva K, Kozerke S, et al. High-resolution magnetic resonance myocardial perfusion imaging at 3.0-tesla to detect hemodynamically significant coronary stenoses as determined by fractional flow reserve. *J Am Coll Cardiol.* (2010) 57:70–5. doi: 10.1016/j.jacc.2010.09.019
29. Bettencourt N, Chiribiri A, Schuster A, Ferreira N, Sampaio F, Duarte R, et al. Cardiac magnetic resonance myocardial perfusion imaging for detection of functionally significant obstructive coronary artery disease: a prospective study. *Int J Cardiol.* (2013) 168:765–73. doi: 10.1016/j.ijcard.2012.09.231
30. Schwitter J, Wacker CM, van Rossum AC, Lombardi M, Al-Saadi N, Ahlstrom H, et al. MR-IMPACT: comparison of perfusion-cardiac magnetic resonance with single-photon emission computed tomography for the detection of coronary artery disease in a multicentre, multivendor, randomized trial. *Eur Heart J.* (2008) 29:480–9. doi: 10.1093/eurheartj/ehm617
31. Schwitter J, Wacker CM, Wilke N, Al-Saadi N, Sauer E, Huettle K, et al. MR-IMPACT II: magnetic resonance imaging for myocardial perfusion assessment in coronary artery disease trial: perfusion-cardiac magnetic resonance vs. single-photon emission computed tomography for the detection of coronary artery disease: a comparative. *Eur Heart J.* (2013) 34:775–81. doi: 10.1093/eurheartj/ehs022
32. Greenwood JP, Motwani M, Maredia N, Brown JM, Everett CC, Nixon J, et al. Comparison of cardiovascular magnetic resonance and single-photon emission computed tomography in women with suspected coronary artery disease from the Clinical Evaluation of Magnetic Resonance Imaging in Coronary Heart Disease (CE-MARC) trial. *Circulation.* (2014) 129:1129–38. doi: 10.1161/CIRCULATIONAHA.112.000071
33. Schuster A. *Validation of Quantitative Myocardial Perfusion Magnetic Resonance Imaging*. Ph.D. thesis, King's College London, London, United Kingdom (2012).
34. Kwong RY, Ge Y, Steel K, Bingham S, Abdullah S, Fujikura K, et al. Cardiac magnetic resonance stress perfusion imaging for

evaluation of patients with chest pain. *J Am Coll Cardiol*. (2019) 74:1741–55. doi: 10.1016/j.jacc.2019.07.074
35. Lipinski MJ, McVey CM, Berger JS, Kramer CM, Salerno M. Prognostic value of stress cardiac magnetic resonance imaging in patients with known or suspected coronary artery disease: a systematic review and meta-analysis. *J Am Coll Cardiol*. (2013) 62:826–38. doi: 10.1016/j.jacc.2013.03.080
36. Greenwood JP, Ripley DP, Berry C, McCann GP, Plein S, Bucciarelli-Ducci C, et al. Effect of care guided by cardiovascular magnetic resonance, myocardial perfusion scintigraphy, or NICE guidelines on subsequent unnecessary angiography rates: the CE-MARC 2 randomized clinical trial. *JAMA*. (2016) 316:1051–60. doi: 10.1001/jama.2016.12680
37. Nagel E, Greenwood JP, McCann GP, Bettencourt N, Shah AM, Hussain ST, et al. Magnetic resonance perfusion or fractional flow reserve in coronary disease. *N Engl J Med*. (2019) 380:2418–28. doi: 10.1056/NEJMoa1716734
38. Ge Y, Pandya A, Steel K, Bingham S, Jerosch-Herold M, Chen Y-Y, et al. Cost-effectiveness analysis of stress cardiovascular magnetic resonance imaging for stable chest pain syndromes. *JACC Cardiovasc Imaging*. (2020) 13:1505–17. doi: 10.1016/j.jcmg.2020.02.029
39. Villa ADM, Corsinovi L, Ntalas I, Milidonis X, Scannell C, Di Giovine G, et al. Importance of operator training and rest perfusion on the diagnostic accuracy of stress perfusion cardiovascular magnetic resonance. *J Cardiovasc Magn Reson*. (2018) 20:74. doi: 10.1186/s12968-018-0493-4
40. Shaw LJ, Berman DS, Picard MH, Friedrich MG, Kwong RY, Stone GW, et al. Comparative definitions for moderate-severe ischemia in stress nuclear, echocardiography, and magnetic resonance imaging. *JACC Cardiovasc Imaging*. (2014) 7:593–604. doi: 10.1016/j.jcmg.2013.10.021
41. Shaw LJ, Berman DS, Maron DJ, Mancini GBJ, Hayes SW, Hartigan PM, et al. Optimal medical therapy with or without percutaneous coronary intervention to reduce ischemic burden: results from the Clinical Outcomes Utilizing Revascularization and Aggressive Drug Evaluation (COURAGE) trial nuclear substudy. *Circulation*. (2008) 117:1283–91. doi: 10.1161/CIRCULATIONAHA.107.743963
42. Martin W, Tweddel AC, Hutton I. Balanced triple-vessel disease: enhanced detection by estimated myocardial thallium uptake. *Nucl Med Commun*. (1992) 13:149–53. doi: 10.1097/00006231-199203000-00005
43. Christian TF, Miller TD, Bailey KR, Gibbons RJ. Noninvasive identification of severe coronary artery disease using exercise tomographic thallium-201 imaging. *Am J Cardiol*. (1992) 70:14–20. doi: 10.1016/0002-9149(92)91382-E
44. Rahman H, Scannell CM, Demir OM, Ryan M, McConkey H, Ellis H, et al. High-resolution cardiac magnetic resonance imaging techniques for the identification of coronary microvascular dysfunction. *JACC Cardiovasc Imaging*. (2021) 14:978–86. doi: 10.1016/j.jcmg.2020.10.015
45. Patel AR, Antkowiak PF, Nandalur KR, West AM, Salerno M, Arora V, et al. Assessment of advanced coronary artery disease: advantages of quantitative cardiac magnetic resonance perfusion analysis. *J Am Coll Cardiol*. (2010) 56:561–9. doi: 10.1016/j.jacc.2010.02.061
46. Chung S-Y, Lee K-Y, Chun EJ, Lee W-W, Park EK, Chang H-J, et al. Comparison of stress perfusion MRI and SPECT for detection of myocardial ischemia in patients with angiographically proven three-vessel coronary artery disease. *AJR Am J Roentgenol*. (2010) 195:356–62. doi: 10.2214/AJR.08.1839
47. Driessen RS, Raijmakers PG, Stuijfzand WJ, Knaapen P. Myocardial perfusion imaging with PET. *Int J Cardiovasc Imaging*. (2017) 33:1021–31. doi: 10.1007/s10554-017-1084-4
48. Kotecha T, Chacko L, Chehab O, O'Reilly N, Martinez-Naharro A, Lazari J, et al. Assessment of multivessel coronary artery disease using cardiovascular magnetic resonance pixelwise quantitative perfusion mapping. *JACC Cardiovasc Imaging*. (2020) 13:2546–57. doi: 10.1016/j.jcmg.2020.06.041
49. Motwani M, Maredia N, Fairbairn TA, Kozerke S, Greenwood JP, Plein S. Assessment of ischaemic burden in angiographic three-vessel coronary artery disease with high-resolution myocardial perfusion cardiovascular magnetic resonance imaging. *Eur Heart J Cardiovasc Imaging*. (2014) 15:701–8. doi: 10.1093/ehjci/jet286
50. Klein C, Nagel E, Gebker R, Kelle S, Schnackenburg B, Graf K, et al. Magnetic resonance adenosine perfusion imaging in patients after coronary artery bypass graft surgery. *JACC Cardiovasc Imaging*. (2009) 2:437–45. doi: 10.1016/j.jcmg.2008.12.016
51. Seraphim A, Knott KD, Beirne AM, Augusto JB, Menacho K, Artico J, et al. Use of quantitative cardiovascular magnetic resonance myocardial perfusion mapping for characterization of ischemia in patients with left internal mammary coronary artery bypass grafts. *J Cardiovasc Magn Reson*. (2021) 23:82. doi: 10.1186/s12968-021-00763-y
52. Kelle S, Graf K, Dreysse S, Schnackenburg B, Fleck E, Klein C. Evaluation of contrast wash-in and peak enhancement in adenosine first pass perfusion CMR in patients post bypass surgery. *J Cardiovasc Magn Reson*. (2010) 12:28. doi: 10.1186/1532-429X-12-28
53. Chong WCF, Collins P, Webb CM, De Souza AC, Pepper JR, Hayward CS, et al. Comparison of flow characteristics and vascular reactivity of radial artery and long saphenous vein grafts [NCT00139399]. *J Cardiothorac Surg*. (2006) 1:4. doi: 10.1186/1749-8090-1-4
54. Jerosch-Herold M. Quantification of myocardial perfusion by cardiovascular magnetic resonance. *J Cardiovasc Magn Reson*. (2010) 12:57. doi: 10.1186/1532-429X-12-57
55. Christian TF, Rettmann DW, Aletras AH, Liao SL, Taylor JL, Balaban RS, et al. Absolute myocardial perfusion in canines measured by using dual-bolus first-pass MR imaging. *Radiology*. (2004) 232:677–84. doi: 10.1148/radiol.2323030573
56. Cullen JHS, Horsfield MA, Reek CR, Cherryman GR, Barnett DB, Samani NJ. A myocardial perfusion reserve index in humans using first-pass contrast-enhanced magnetic resonance imaging. *J Am Coll Cardiol*. (1999) 33:1386–94. doi: 10.1016/S0735-1097(99)00004-2
57. Gould KL, Lipscomb K. Effects of coronary stenoses on coronary flow reserve and resistance. *Am J Cardiol*. (1974) 34:48–55. doi: 10.1016/0002-9149(74)90092-7
58. Jerosch-Herold M, Hu X, Murthy NS, Rickers C, Stillman AE. Magnetic resonance imaging of myocardial contrast enhancement with MS-325 and its relation to myocardial blood flow and the perfusion reserve. *J Magn Reson Imaging*. (2003) 18:544–54. doi: 10.1002/jmri.10384
59. Chiribiri A, Villa ADM, Sammut E, Breeuwer M, Nagel E. Perfusion dyssynchrony analysis. *Eur Heart J Cardiovasc Imaging*. (2016) 17:1414–23. doi: 10.1093/ehjci/jev326
60. Klocke FJ, Simonetti OP, Judd RM, Kim RJ, Harris KR, Hedjbeli S, et al. Limits of detection of regional differences in vasodilated flow in viable myocardium by first-pass magnetic resonance perfusion imaging. *Circulation*. (2001) 104:2412–6. doi: 10.1161/hc4501.099306
61. Nagel E, Klein C, Paetsch I, Hettwer S, Schnackenburg B, Wegscheider K, et al. Magnetic resonance perfusion measurements for the noninvasive detection of coronary artery disease. *Circulation*. (2003) 108:432–7. doi: 10.1161/01.CIR.0000080915.35024.A9
62. Al-Saadi N, Nagel E, Gross M, Bornstedt A, Schnackenburg B, Klein C, et al. Noninvasive detection of myocardial ischemia from perfusion reserve based on cardiovascular magnetic resonance. *Circulation*. (2000) 101:1379–83. doi: 10.1161/01.CIR.101.12.1379
63. van Dijk R, van Assen M, Vliegenthart R, de Bock GH, van der Harst P, Oudkerk M. Diagnostic performance of semi-quantitative and quantitative stress CMR perfusion analysis: a meta-analysis. *J Cardiovasc Magn Reson*. (2017) 19:92. doi: 10.1186/s12968-017-0393-z
64. Knott KD, Fernandes JL, Moon JC. Automated quantitative stress perfusion in a clinical routine. *Magn Reson Imaging Clin N Am*. (2019) 27:507–20. doi: 10.1016/j.mric.2019.04.003
65. Sourbron SP, Buckley DL. Tracer kinetic modelling in MRI: estimating perfusion and capillary permeability. *Phys Med Biol*. (2012) 57:R1–33. doi: 10.1088/0031-9155/57/2/R1
66. Zierler KL. Theoretical basis of indicator-dilution methods for measuring flow and volume. *Circ Res*. (1962) 10:393–407. doi: 10.1161/01.RES.10.3.393
67. Robinson AA, Salerno M, Kramer CM. Contemporary issues in quantitative myocardial perfusion CMR imaging. *Curr Cardiovasc Imaging Rep*. (2019) 12:9. doi: 10.1007/s12410-019-9484-6
68. Ichihara T, Ishida M, Kitagawa K, Ichikawa Y, Natsume T, Yamaki N, et al. Quantitative analysis of first-pass contrast-enhanced myocardial perfusion MRI using a Patlak plot method and blood saturation correction. *Magn Reson Med*. (2009) 62:373–83. doi: 10.1002/mrm.22018
69. Kellman P, Hansen MS, Nielles-Vallespin S, Nickander J, Themudo R, Ugander M, et al. Myocardial perfusion cardiovascular magnetic resonance: optimized

dual sequence and reconstruction for quantification. *J Cardiovasc Magn Reson*. (2017) 19:43. doi: 10.1186/s12968-017-0355-5
70. Cernicanu A, Axel L. Theory-based signal calibration with single-point T1 measurements for first-pass quantitative perfusion MRI studies. *Acad Radiol*. (2006) 13:686–93. doi: 10.1016/j.acra.2006.02.040
71. Hsu L-Y, Rhoads KL, Holly JE, Kellman P, Aletras AH, Arai AE. Quantitative myocardial perfusion analysis with a dual-bolus contrast-enhanced first-pass MRI technique in humans. *J Magn Reson Imaging*. (2006) 23:315–22. doi: 10.1002/jmri.20502
72. Ishida M, Schuster A, Morton G, Chiribiri A, Hussain S, Paul M, et al. Development of a universal dual-bolus injection scheme for the quantitative assessment of myocardial perfusion cardiovascular magnetic resonance. *J Cardiovasc Magn Reson*. (2011) 13:28. doi: 10.1186/1532-429X-13-28
73. Hsu LY, Groves DW, Aletras AH, Kellman P, Arai AE. A quantitative pixel-wise measurement of myocardial blood flow by contrast-enhanced first-pass CMR perfusion imaging: microsphere validation in dogs and feasibility study in humans. *JACC Cardiovasc Imaging*. (2012) 5:154–66. doi: 10.1016/j.jcmg.2011.07.013
74. Morton G, Chiribiri A, Ishida M, Hussain ST, Schuster A, Indermuehle A, et al. Quantification of absolute myocardial perfusion in patients with coronary artery disease: comparison between cardiovascular magnetic resonance and positron emission tomography *J Am Coll Cardiol*. (2012) 60:1546–55. doi: 10.1016/j.jacc.2012.05.052
75. Schuster A, Morton G, Chiribiri A, Perera D, Vanoverschelde JL, Nagel E. Imaging in the management of ischemic cardiomyopathy: special focus on magnetic resonance. *J Am Coll Cardiol*. (2012) 59:359–70. doi: 10.1016/j.jacc.2011.08.076
76. Kim D, Axel L. Multislice, dual-imaging sequence for increasing the dynamic range of the contrast-enhanced blood signal and CNR of myocardial enhancement at 3T. *J Magn Reson Imaging*. (2006) 23:81–6. doi: 10.1002/jmri.20471
77. Sánchez-González J, Fernandez-jiménez R, Nothnagel ND, López-martín G, Fuster V, Ibañez B. Optimization of dual-saturation single bolus acquisition for quantitative cardiac perfusion and myocardial blood flow maps. *J Cardiovasc Magn Reson*. (2015) 17:21. doi: 10.1186/s12968-015-0116-2
78. Engblom H, Xue H, Akil S, Carlsson M, Hindorf C, Oddstig J, et al. Fully quantitative cardiovascular magnetic resonance myocardial perfusion ready for clinical use: a comparison between cardiovascular magnetic resonance imaging and positron emission tomography. *J Cardiovasc Magn Reson*. (2017) 19:78. doi: 10.1186/s12968-017-0388-9
79. Kotecha T, Martinez-Naharro A, Boldrini M, Knight D, Hawkins P, Kalra S, et al. Automated pixel-wise quantitative myocardial perfusion mapping by CMR to detect obstructive coronary artery disease and coronary microvascular dysfunction: validation against invasive coronary physiology. *JACC Cardiovasc Imaging*. (2019) 12:1958–69. doi: 10.1016/j.jcmg.2018.12.022
80. Scannell CM, Villa ADM, Lee J, Breeuwer M, Chiribiri A. Robust non-rigid motion compensation of free-breathing myocardial perfusion MRI data. *IEEE Trans Med Imaging*. (2019) 38:1812–20. doi: 10.1109/TMI.2019.2897044
81. Jacobs M, Benovoy M, Chang L-C, Corcoran D, Berry C, Arai AE, et al. Automated segmental analysis of fully quantitative myocardial blood flow maps by first-pass perfusion cardiovascular magnetic resonance. *IEEE Access Pract Innov Open Solut*. (2021) 9:52796–811. doi: 10.1109/ACCESS.2021.3070320
82. Hansen MS, Sørensen TS. Gadgetron: an open source framework for medical image reconstruction. *Magn Reson Med*. (2013) 69:1768–76. doi: 10.1002/mrm.24389
83. Knott KD, Seraphim A, Augusto JB, Xue H, Chacko L, Aung N, et al. The prognostic significance of quantitative myocardial perfusion: an artificial intelligence based approach using perfusion mapping. *Circulation*. (2020) 141:1282–91. doi: 10.1161/CIRCULATIONAHA.119.044666
84. Scannell CM, Veta M, Villa ADM, Sammut EC, Lee J, Breeuwer M, et al. Deep-learning-based preprocessing for quantitative myocardial perfusion MRI. *J Magn Reson Imaging*. (2020) 51:1689–96. doi: 10.1002/jmri.26983
85. Hsu LY, Jacobs M, Benovoy M, Ta AD, Conn HM, Winkler S, et al. Diagnostic performance of fully automated pixel-wise quantitative myocardial perfusion imaging by cardiovascular magnetic resonance. *JACC Cardiovasc Imaging*. (2018) 11:697–707. doi: 10.1016/j.jcmg.2018.01.005
86. Biglands JD, Ibraheem M, Magee DR, Radjenovic A, Plein S, Greenwood JP. Quantitative myocardial perfusion imaging versus visual analysis in diagnosing myocardial ischemia a CE-MARC substudy. *JACC Cardiovasc Imaging*. (2018) 11:711–8. doi: 10.1016/j.jcmg.2018.02.019
87. Villa ADM, Sammut E, Zarinabad N, Carr-White G, Lee J, Bettencourt N, et al. Microvascular ischemia in hypertrophic cardiomyopathy: New insights from high-resolution combined quantification of perfusion and late gadolinium enhancement. *J Cardiovasc Magn Reson*. (2016) 18:4. doi: 10.1186/s12968-016-0223-8
88. Villa AD, Sammut E, Shome JS, Razavi R, Plein S, Chiribiri A. Combined high-resolution assessment of quantitative perfusion and late enhancement. Towards accurate estimation of the ischaemic burden in patients with coronary artery disease. *J Cardiovasc Magn Reson*. (2016) 18:Q15. doi: 10.1186/1532-429X-18-S1-Q15
89. Sammut EC, Villa ADM, Di Giovine G, Dancy L, Bosio F, Gibbs T, et al. Prognostic value of quantitative stress perfusion cardiac magnetic resonance. *JACC Cardiovasc Imaging*. (2018) 11:686–94. doi: 10.1016/j.jcmg.2017.07.022
90. Huber A, Sourbron S, Klauss V, Schaefer J, Bauner KU, Schweyer M, et al. Magnetic resonance perfusion of the myocardium: semiquantitative and quantitative evaluation in comparison with coronary angiography and fractional flow reserve. *Invest Radiol*. (2012) 47:332–8. doi: 10.1097/RLI.0b013e31824f54cb
91. Schwab F, Ingrisch M, Marcus R, Bamberg F, Hildebrandt K, Adrion C, et al. Tracer kinetic modeling in myocardial perfusion quantification using MRI. *Magn Reson Med*. (2015) 73:1206–15. doi: 10.1002/mrm.25212
92. Murthy VL, Bateman TM, Beanlands RS, Berman DS, Borges-Neto S, Chareonthaitawee P, et al. Clinical quantification of myocardial blood flow using PET: joint position paper of the SNMMI cardiovascular council and the ASNC. *J Nucl Med*. (2018) 59:273–93. doi: 10.2967/jnumed.117.201368

Author Disclaimer: The views expressed are those of the authors and not necessarily those of the NHS or funding bodies. The funding bodies did not have a role in the writing of this manuscript.

Conflict of Interest: The authors declare that the research was conducted in the absence of any commercial or financial relationships that could be construed as a potential conflict of interest.

The handling editor declared a shared research group with one of the author AC at time of review.

Publisher's Note: All claims expressed in this article are solely those of the authors and do not necessarily represent those of their affiliated organizations, or those of the publisher, the editors and the reviewers. Any product that may be evaluated in this article, or claim that may be made by its manufacturer, is not guaranteed or endorsed by the publisher.

frontiers in Cardiovascular Medicine

REVIEW
published: 23 December 2021
doi: 10.3389/fcvm.2021.795195

Non-invasive Ischaemia Testing in Patients With Prior Coronary Artery Bypass Graft Surgery: Technical Challenges, Limitations, and Future Directions

Andreas Seraphim[1,2], *Kristopher D. Knott*[1,2], *Joao B. Augusto*[1,2], *Katia Menacho*[1,2], *Sara Tyebally*[1], *Benjamin Dowsing*[1,2], *Sanjeev Bhattacharyya*[1], *Leon J. Menezes*[1], *Daniel A. Jones*[1,3], *Rakesh Uppal*[1,3], *James C. Moon*[1,2] *and Charlotte Manisty*[1,2]*

[1] Department of Cardiac Imaging, Barts Health National Health System Trust, London, United Kingdom, [2] Institute of Cardiovascular Science, University College London, London, United Kingdom, [3] William Harvey Research Institute, Queen Mary University of London, London, United Kingdom

OPEN ACCESS

Edited by:
Carla Sousa,
São João University Hospital Center, Portugal

Reviewed by:
Kevin Domingues,
District Hospital of Santarém, Portugal
Alvise Guariento,
Hospital for Sick Children, Canada

***Correspondence:**
Charlotte Manisty
c.manisty@ucl.ac.uk

Specialty section:
This article was submitted to Cardiovascular Imaging, a section of the journal Frontiers in Cardiovascular Medicine

Received: 14 October 2021
Accepted: 25 November 2021
Published: 23 December 2021

Citation:
Seraphim A, Knott KD, Augusto JB, Menacho K, Tyebally S, Dowsing B, Bhattacharyya S, Menezes LJ, Jones DA, Uppal R, Moon JC and Manisty C (2021) Non-invasive Ischaemia Testing in Patients With Prior Coronary Artery Bypass Graft Surgery: Technical Challenges, Limitations, and Future Directions. Front. Cardiovasc. Med. 8:795195. doi: 10.3389/fcvm.2021.795195

Coronary artery bypass graft (CABG) surgery effectively relieves symptoms and improves outcomes. However, patients undergoing CABG surgery typically have advanced coronary atherosclerotic disease and remain at high risk for symptom recurrence and adverse events. Functional non-invasive testing for ischaemia is commonly used as a gatekeeper for invasive coronary and graft angiography, and for guiding subsequent revascularisation decisions. However, performing and interpreting non-invasive ischaemia testing in patients post CABG is challenging, irrespective of the imaging modality used. Multiple factors including advanced multi-vessel native vessel disease, variability in coronary hemodynamics post-surgery, differences in graft lengths and vasomotor properties, and complex myocardial scar morphology are only some of the pathophysiological mechanisms that complicate ischaemia evaluation in this patient population. Systematic assessment of the impact of these challenges in relation to each imaging modality may help optimize diagnostic test selection by incorporating clinical information and individual patient characteristics. At the same time, recent technological advances in cardiac imaging including improvements in image quality, wider availability of quantitative techniques for measuring myocardial blood flow and the introduction of artificial intelligence-based approaches for image analysis offer the opportunity to re-evaluate the value of ischaemia testing, providing new insights into the pathophysiological processes that determine outcomes in this patient population.

Keywords: CABG, ischaemia detection, surgical revascularisation, stress imaging, myocardial perfusion

INTRODUCTION

Coronary artery bypass surgery is the most frequently performed cardiac surgical procedure, with ∼200,000 patients undergoing isolated coronary artery bypass surgery each year in the US (1). Despite improved post-operative survival (2) particularly among high risk groups (3, 4), patients undergoing surgical revascularisation represent the severe end of coronary artery disease spectrum and comprise a high risk group. With long term survival of patients undergoing CABG approaching that of the general population (5–7), a significant number of patients with prior CABG surgery are expected to experience symptom recurrence requiring re-intervention (8). Studies have reported considerable rates of myocardial infarction and ischaemia-driven revascularisation even within the first 5-years post CABG (9). Data from the European Heart Survey suggests that 14% of patients undergoing coronary revascularisation between 2001 and 2002 had had a history of CABG (10), with similar rates seen in more contemporary data from the UK (11). Importantly, outcomes following repeat revascularisation are significantly worse compared to patients with no history of CABG, both in the context of stable coronary artery disease (11) and acute coronary syndromes (12). It is therefore not surprising that there is a clinically-driven, high demand for detailed functional non-invasive investigations for myocardial ischaemia in this patient group.

CORONARY AND GRAFT DISEASE POST CORONARY ARTERY BYPASS GRAFT SURGERY

The two key pathophysiological processes thought to be driving symptom recurrence are vein graft failure and progression of native vessel coronary disease. Graft failure after coronary artery bypass graft surgery is thought to follow a bimodal distribution, often defined as early (<6 months) or late (13), and is known to be higher for venous compared to arterial grafts (5, 14). Vein graft failure (VGF) rates of up to 25% during the first 12–18 months post CABG are reported even in contemporary studies (15, 16), with VGF rates of 40–50% seen at 10 years (17). In contrast, internal mammary grafts have a reported 10-year patency rate over 90% (18). At the same time, native disease progression appears to accelerate particularly in bypassed vessels, with up to 46% new total occlusions seen within 5 years post CABG (19). Although data on the prognostic impact of graft failure is conflicting (20–22), both graft failure and native disease progression are associated with symptom recurrence, and are often the suspected processes prompting evaluation of ischaemia.

Abbreviations: ACC, American College of Cardiology; AHA, American Heart Association; CABG, Coronary Artery Bypass Graft; CMR, Cardiovascular Magnetic Resonance; CNR, Contrast to Noise Ratio; CTCA, Computed Tomography Coronary Angiography; FFR, Fractional Flow Reserve; LAD, Left Anterior Descending (artery); LIMA, Left Internal Mammary Artery; LGE, Late Gadolinium Enhancement; LV, Left Ventricle; MACE, Major adverse cardiovascular events; MBF, Myocardial Blood Flow; MPR, Myocardial Perfusion Reserve; PCI, Percutaneous Coronary Intervention; PET, Positron Emission Tomography; SPECT, Single-Photon Emission Computed.

Invasive coronary and graft angiography remains the definitive anatomical test for evaluating the extent of coronary disease, but may not provide sufficient information to guide complex management decisions post CABG due to the lack of functional correlation. Physiological lesion assessment using fractional flow reserve (FFR) is more challenging in the context of grafts, due to the severity and complexity of native coronary artery disease (calcification, tortuosity, and chronic total occlusions) and the differing flow relationships between native and graft circulations. Therefore, clinical decision-making based on FFR warrants caution (23), as although technically feasible there is limited data to support its use. Importantly, given the different physiological profile of vein grafts compared to native coronary vessels with regards to the rate of disease progression, extrapolating findings of major clinical trials (24) demonstrating the clinical utility of FFR assessment in native vessels which tended to exclude post CABG patients may be inappropriate. Furthermore, alterations in native coronary anatomy and the interplay between extensive diffuse disease and development of collateral systems result in unique and complex haemodynamic circuits that are difficult to evaluate (25). Detection of ischaemia in the context of chronic coronary artery disease is therefore often performed using a range of non-invasive imaging tests, and represents a large proportion of cardiac investigations, resulting in significant healthcare costs (26). Both the United Kingdom National Institute of Clinical Excellence (NICE) (27) and European Society of Cardiology guidelines (28) advocate the use of a non-invasive functional testing for evaluation of patients with known coronary artery disease, including those with previous revascularisation.

CURRENT GUIDELINE RECOMMENDATIONS AND CHALLENGES FOR IMAGING POST CABG

All non-invasive imaging modalities have technical limitations in terms of image acquisition and interpretation, affecting their diagnostic performance. The challenges associated with the use of non-invasive ischaemia evaluation of patients with prior CABG are indeed reflected by a degree of discrepancy among societal guidelines. For example, according to American College of Cardiology (ACC) Task force recommendations, the use of stress echocardiography in asymptomatic patients solely for the purpose of risk stratification is not recommended within 5 years from CABG surgery (29). In contrast, the more recent European Society of Cardiology (ESC) guidelines are more liberal in the use of non-invasive testing post revascularisation, even supporting the use of early ischaemia testing for setting a reference, or periodically every 3–5 years (28). In terms of symptomatic patients with prior CABG, the American College of Cardiology/American Heart Association (ACC/AHA) guidelines recommend evaluation using non-invasive stress imaging tests, with a preference toward exercise as a method of stress (30). Similarly, the European guidelines recommend the use of stress imaging over exercise stress ECG if practically possible (28). Beyond this, international guidelines offer little guidance on

the choice of functional testing after CABG, resulting in wide variations in practice patterns. Indeed, large multicentre registry data confirm that the choice of stress testing after CABG is primarily defined by the clinical center rather than patient clinical characteristics (31).

Both detection and interpretation of ischaemia testing in patients with CABG remains a challenge, and despite the availability of a wide array of diagnostic imaging tools no test has demonstrated superiority in these patients. Difficulties associated with ischaemia testing in patients following surgical revascularisation are primarily due to the complex anatomical, haemodynamic and myocardial alterations that result from surgery. Surgery results in variable degrees of electro-mechanical myocardial abnormalities (32, 33) and changes in coronary anatomy and flow (34), often limiting the diagnostic performance of all non-invasive tests. Consequently, questions remain as to whether any functional imaging test is sensitive and specific enough to identify subtle differences in regional myocardial blood flow or contractility and provide reliable data to inform revascularisation strategies and appropriately risk stratify patients. As any form of revascularisation post coronary artery bypass is associated with increased risk of complications (35, 36) and suboptimal outcomes (37, 38), accurate detection and consistent interpretation of ischaemia becomes important. Furthermore, accepting the notion that the extent of myocardial ischaemia translates to a higher risk of future ischaemic events, and considering the poor outcomes after myocardial infarction in this patient group (39), accurate detection of ischaemia in these patients may enable risk stratification and potentially guide clinical management.

CHALLENGES IN NON-INVASIVE STRESS TESTING POST-SURGICAL REVASCULARISATION

Patients referred for CABG surgery typically have advanced epicardial disease, which is often a combination of both focal and diffuse atherosclerosis involving multiple coronary territories. This is also a reflection of a higher risk population that suffers with significant comorbidity, which further complicates ischaemia testing. For example, left ventricular (LV) dysfunction is not uncommon in patients post-surgical revascularisation, and this poses additional challenges in the evaluation of ischaemia beyond the complexity of the underlying coronary artery disease. The degree of LV impairment is thought to impact the stress response to pharmacological vasodilators such as adenosine, with prior studies suggesting that increased dosing may be needed in these patients (40). Similarly, the presence of LV dysfunction increases arrhythmic complications in those undergoing dobutamine stress testing (41), whereas pharmacological therapy such as beta-blockers may blunt heart rate augmentation during exercise. Beyond the haemodynamic effects of LV dysfunction, the presence of implantable electronic devices can be detrimental to image quality and the ability to elicit adequate heart rate response during stress. The high prevalence of cardiovascular factors that contribute to the development of coronary artery disease also increase the risk of chronic kidney and lung disease (42), introducing additional limitations in the use of each imaging modality. Furthermore, additional challenges related to the complexity of post-CABG coronary and myocardial blood flow physiology, as well as technicalities in image acquisition further complicate ischaemia assessment.

Challenges in Evaluating Myocardial Blood Flow Post Coronary Artery Bypass Graft Surgery

Coronary Anatomy and Myocardial Ischaemia Correlation

Coronary artery bypass graft surgery results in significant alterations in coronary physiology, with significant variations in post-operative anatomy among individual patients. Variations in anastomosis position and complex grafting approaches based on the distribution and severity of native vessel disease mean that correlation of ischaemia and coronary anatomy is often difficult in patients following surgery (**Figure 1**).

Integration of anatomical and perfusion data may therefore facilitate re-assignment of ischaemia to culprit vessel, and may provide additional insights into the mechanism of ischaemia (43). It is therefore unsurprising that hybrid imaging techniques that combine anatomical and functional testing in patients post CABG provide incremental information on the localization of atherosclerotic lesions (43) as well as prognosis (44) (**Figure 2**).

However, the extent of coronary artery disease encountered in these patients often promotes the development of extensive collateral systems (45) and these can often complicate correlation of ischaemia to a corresponding epicardial vessel. Similarly, CABG surgery often results in unique haemodynamic conditions such as retrograde and competitive blood flow (46) that cannot be easily characterized by non-invasive tests. A number of studies evaluating stress myocardial perfusion post CABG reported a high prevalence of perfusion defects in territories supplied by patent grafts (43, 47–50), however the underlying mechanism of this remains unclear (**Figure 3**). Discrepancy between graft and native vessel size (47), persistent microvascular dysfunction (52), technical limitations associated with delayed contrast arrival (53) and native coronary artery disease progression either proximal or distal to the anastomosis (48, 51) have all been proposed as potential contributing mechanisms. Data from the SWEDEHEART registry suggested that a substantial amount of invasive coronary angiography performed due to symptom recurrence identified no graft failure, highlighting the possibility that symptom recurrence post CABG may be largely attributed to native disease progression (54). However, despite the frequency of such perfusion defects in patients post CABG, interpretation and subsequent management varies considerably between clinicians.

Myocardial Infarction and Evaluation of Peri-Infarct Ischaemia

Patients with prior surgical revascularisation often have complex patterns of previous myocardial infarction with a number of studies demonstrating a wide range of scar pattern and

FIGURE 1 | Panel of nine cases of coronary anatomy post coronary artery bypass graft surgery. All cases show a left internal mammary artery anastomosed to the to the left anterior descending artery (LAD), demonstrating significant variations in anastomosis position along the length of the vessel, as well as significant variations in the post-operative anatomy of the remaining vessels.

distribution post procedure (55, 56). This indeed reflects the multi-factorial etiology of ischaemic injury sustained by these patients, including the impact of surgery itself. The presence of complex myocardial scar makes evaluation of ischaemia challenging, particularly when this is super-imposed or adjacent to areas of scar. Bernhardt et al., combined CMR perfusion and tissue characterization with late gadolinium enhancement (LGE) assessment and reported improved prediction of clinically relevant bypass graft stenosis, supporting the idea that ischaemia interpretation in patients post CABG requires some knowledge of scar distribution (57) (**Figure 4**).

Evidently, imaging modalities that can provide simultaneous evaluation of ischaemia and tissue characterization can be advantageous in these circumstances, more so in cases of extensive or complex anatomical scar. Similarly, imaging modalities capable of providing complete LV coverage such as PET and SPECT enable a more comprehensive assessment of the relation between ischaemia and scar in this context,

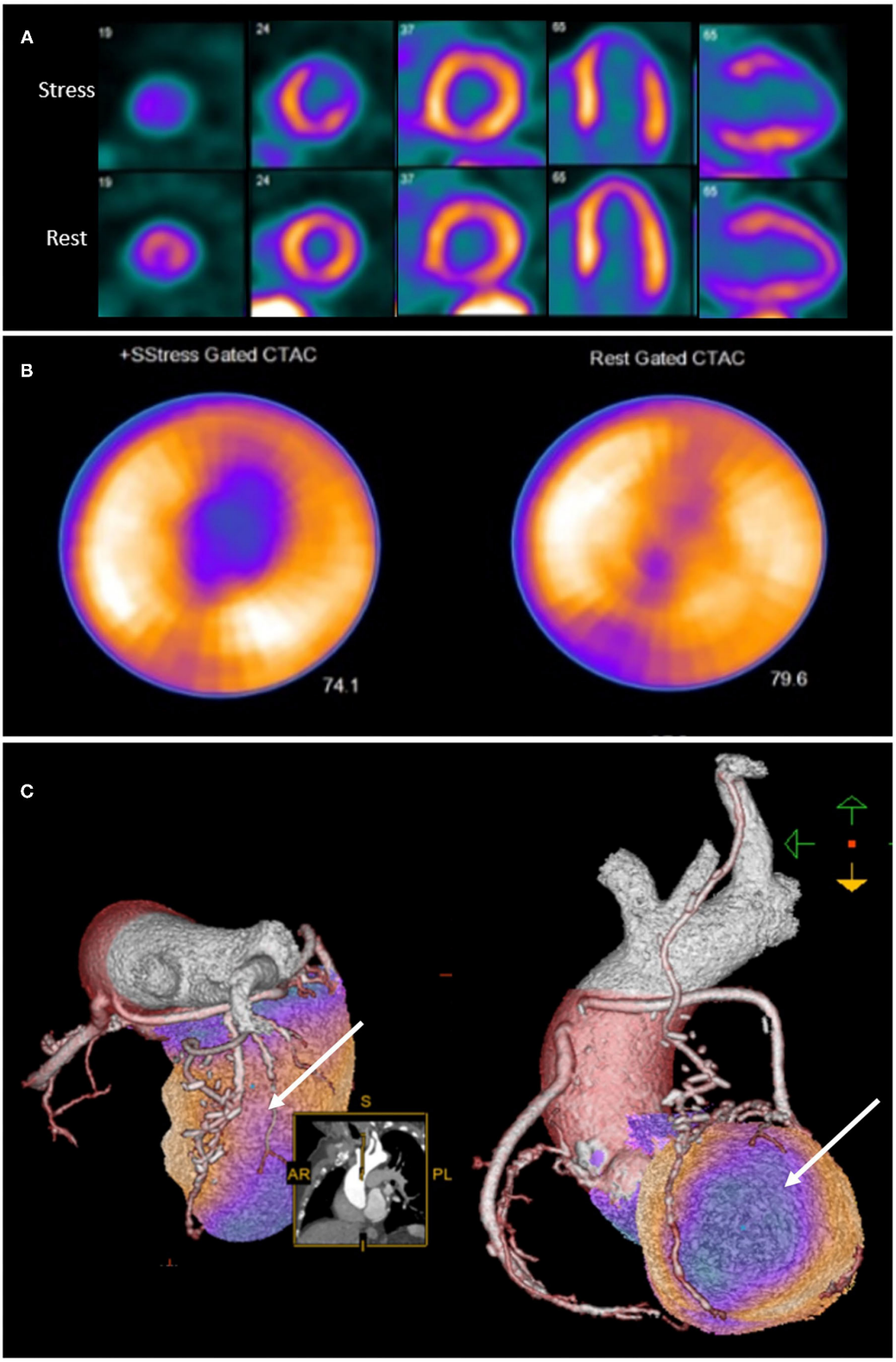

FIGURE 2 | Rubidium-82 PET-CT with adenosine stress in an 86-year-old male with previous coronary artery bypass grafting. PET-CT images **(A,B)** obtained at stress and rest demonstrate a reversible perfusion defect in the mid to apical anterior segments extending into the apex. Cardiac hybrid imaging with three-dimensional fusion of PET-CT with CT coronary angiography enables localization of ischaemia to a coronary artery territory **(C)**. CT coronary angiography reveals a patent LIMA to LAD graft with good distal opacification, and obstructive plaques in the proximal and mid segments of an intermediate artery (white arrow), responsible for the reversible perfusion defect demonstrated.

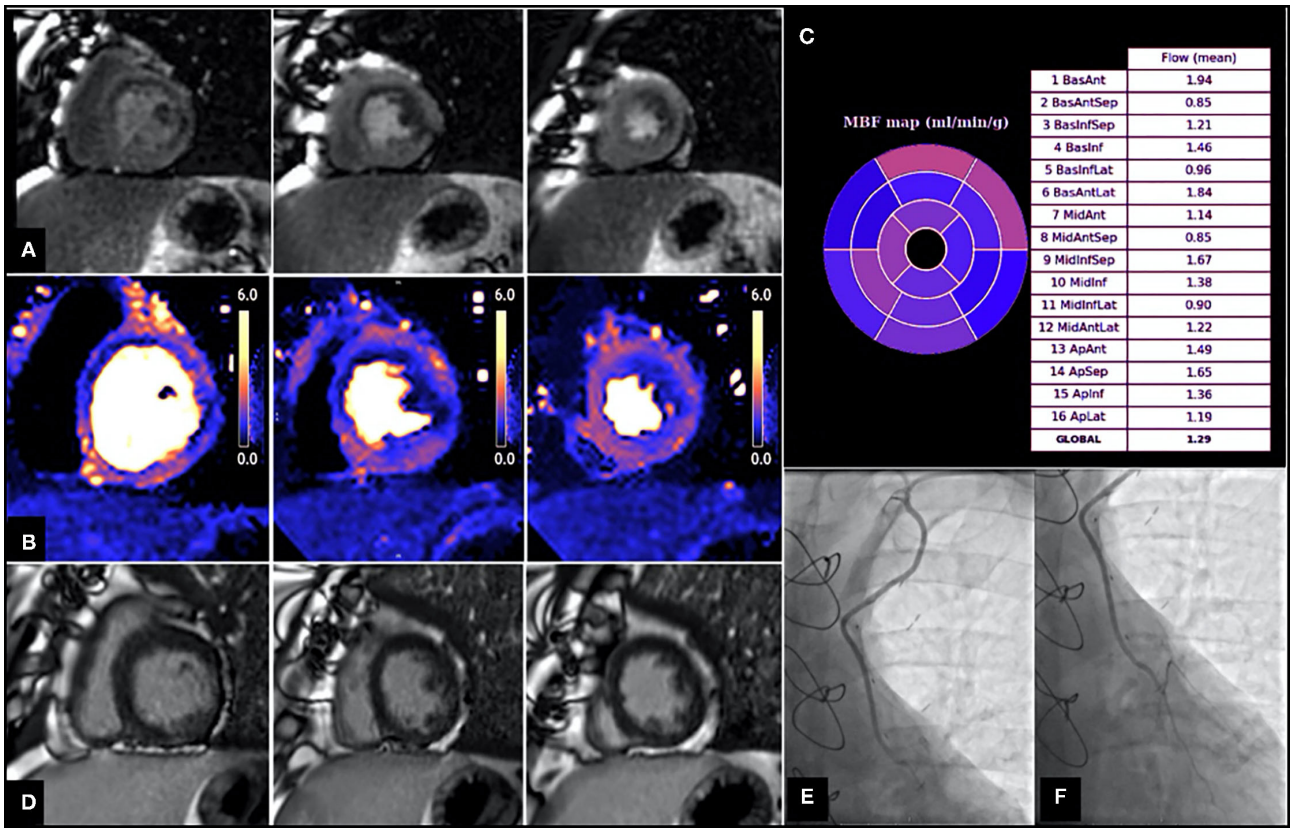

FIGURE 3 | Patient with angiographically confirmed patent LIMA to LAD and evidence of inducible perfusion defect in LIMA—native LAD subtended territories. Images shown are short axis views from base to apex (left to right). **(A)** First pass perfusion imaging with adenosine stress, demonstrating a perfusion defect in the basal to mid antero-septum, basal to mid anterolateral and inferolateral and apical lateral walls. **(B)** Stress myocardial blood flow (MBF) evaluation using perfusion CMR showing reduced MBF in multiple territories, including those supplied by the LIMA—native LAD (e.g., MBF in mid antero-septum is 0.85 ml/g/min, MBF in apical septum is 1.65 ml/g/min). **(C)** Bullseye plot demonstrating stress MBF in each myocardial territory based on American Heart Association (AHA) segmentation. **(D)** Late gadolinium images showing no evidence of previous infarction in the LIMA—native LAD territories. **(E,F)** Coronary angiography demonstrating patent LIMA graft **(E)** and anastomosis site **(F)** with good distal run off. From Seraphim et al. (51). Reproduced under the Creative Commons Attribution 4.0 International License.

particularly when paired with anatomical data (**Figure 2**). Despite this, echocardiography remains the most widely used modality for evaluation of relative differences in wall motion, and often enables accurate evaluation of the extent of regional viability and ischaemia, particularly when facilitated by contrast echocardiography (**Figure 5**) (58). It is worth noting that a recent expert consensus statement on the use of multimodality of myocardial viability, makes no recommendations on a preferred imaging modality in this population (59), further highlighting the complexities in the evaluation of patients with prior CABG.

Incomplete Revascularisation at the Time of Surgery

One of the key aims of coronary artery bypass graft surgery is to minimize myocardial ischaemia through complete revascularisation if this is technically attainable (60). However, native vessel characteristics such as heavy calcification and small vessel size, often result in modification of the revascularisation strategy intra-operatively, with a number of myocardial territories remaining un-grafted (61). In a meta-analysis of 25,938 patients undergoing CABG surgery, Garcia and colleagues (62) reported that incomplete revascularisation was detected in 25% of patients. Beyond this, even if complete anatomical bypassing of significant epicardial coronary lesions is performed, restoration of coronary flow using grafts is unlikely to accurately replicate native coronary disease flow and haemodynamic conditions. Indeed, studies evaluating myocardial blood flow shortly after CABG surgery, reported that myocardial blood flow remains lower than commonly reported values in patients with native vessel disease (**Table 1**). Although arguably a reflection of more advanced coronary artery disease, it is conceivable that in a significant proportion of patients post CABG, some degree of ischaemia is often encountered despite successful surgical revascularisation.

Differentiating graft failure or progression of native coronary disease from incompletely revascularised myocardium is challenging, especially without some form of early post-operative evaluation as a baseline. Indeed, the latest ESC guidelines on chronic coronary syndromes (28) recommend the use of non-invasive ischaemia evaluation for documentation of residual ischaemia as a reference for subsequent assessment.

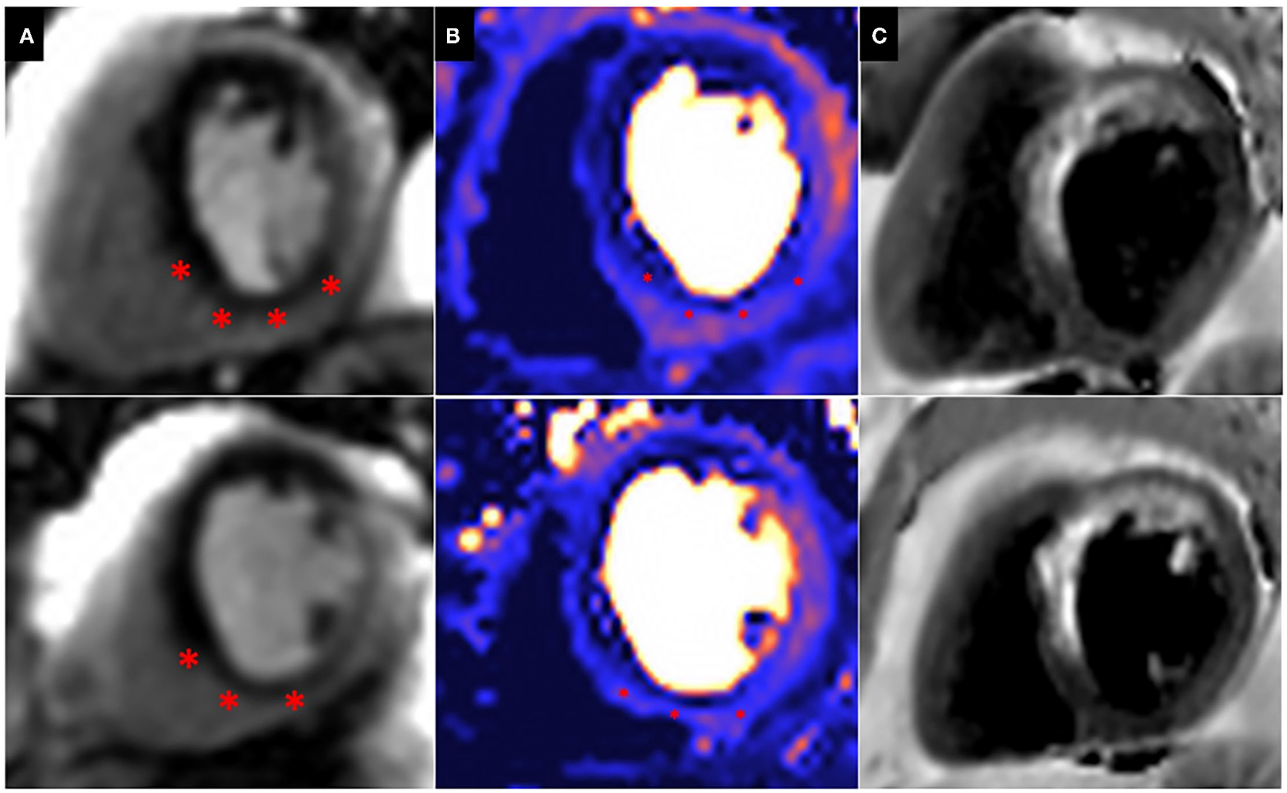

FIGURE 4 | Peri-infarct ischaemia and scar. Basal (top) and Mid (Bottom) short axis views of a CMR perfusion in patient scheduled to undergo coronary artery bypass graft surgery, demonstrating a previous infarct within the left anterior descending (LAD) territory and a large superimposed perfusion defect extending beyond the area of previous infarction (*). **(A)** First pass perfusion CMR during adenosine stress; **(B)** Perfusion mapping of the same myocardial segment as shown in **(A)**. **(C)** Dark blood LGE demonstrating a previous infarction within the LAD territory.

Microvascular Ischaemia

Myocardial blood flow following surgical revascularisation is not solely governed by native epicardial coronary disease. Microvascular disease, is almost universal in patients post CABG, and is also associated with a reduction in stress MBF and perfusion reserve (MPR) (68). Itself an independent predictor of outcomes in patients with native vessel disease (69), the clinical consequences of microvascular disease in patients with prior CABG are poorly understood. Our understanding of the physiological impact of surgery itself, particularly the effect of cardioplegic arrest and cardiopulmonary bypass (70) on microvascular function is limited, with both invasive and non-invasive studies reporting an early post-operative impairment of flow that appears to recover over time (52, 71). Importantly, the impact of surgery may differ among subgroups, with some evidence suggesting that patients with diabetes experience worse microvascular dysfunction post-operatively (72). Advances in image quality across all modalities has meant that non-invasive tests are becoming increasingly capable of detecting microvascular disease, thereby providing additional insights into the pathophysiological mechanisms of reduced myocardial blood flow. Quantitative perfusion indices such as stress MBF and MPR have been used to help differentiate epicardial coronary disease and microvascular dysfunction in the context of native vessel disease (73), but whether a similar assessment can be performed in patients with prior surgical revascularisation is unclear.

Technical Challenges in Non-invasive Stress Imaging in Patients With Prior CABG

The Effect of Prolonged Contrast Transit Time in Graft Subtended Myocardial Territories

All tracer-based methods of ischaemia evaluation, rely on the peripheral injection of an intravenous contrast or tracer and the subsequent acquisition of a dynamic series of myocardial images. Subsequent use of tracer-specific kinetic models allows quantification of myocardial blood flow (MBF) (74). In patients with prior CABG, the increased length of graft conduits results in a prolonged tracer transit time, potentially distorting the first pass kinetics of the contrast bolus complicating both the visual interpretation of relative perfusion defects and the subsequent estimation of myocardial blood flow in graft-subtended territories (75). Such delay in contrast arrival, although small, is thought to particularly affect longer conduits, such as internal mammary (LIMA) grafts (53). Very few studies evaluated the effects of delayed transit of contrast in grafts, with conflicting results in terms of its absolute impact on quantitative indices of myocardial perfusion (51, 53). Data

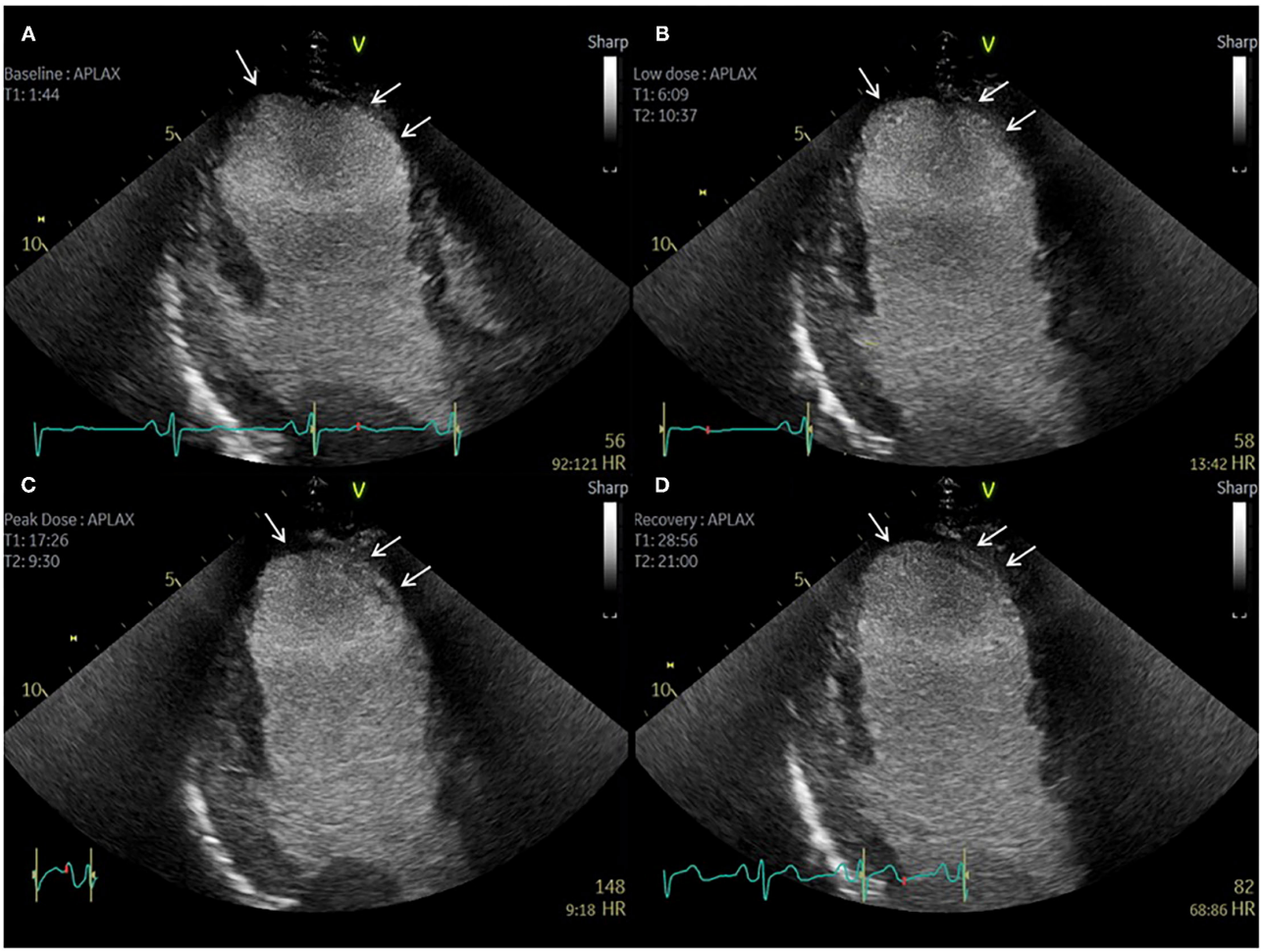

FIGURE 5 | Contrast echocardiography post coronary artery bypass graft surgery. Sixty-three-year-old patient with previous CABG and atypical chest pain. **(A–D)** Apical 3 Chamber view. Baseline, low dose, peak dose, and recovery stages, respectively. Contrast Enhanced Images. Akinetic mid and apical antero-septal wall segments (arrow). No improvement in contractility of these segments during low dose stage confirms non-viable segments. Improvement in contractility of all other segments during low dose and peak dose suggests the presence of viable myocardium and no inducible ischaemia.

using computational fluid dynamics modeling reveals a close relationship between local coronary hemodynamics and contrast dispersion that potentially impacts any bolus-based perfusion measurement (76, 77). It is therefore possible, that all tracer kinetic modeling methods used to estimate MBF would need to consider the effects of differential contrast arrival, presence of collateral flow and blood mixing from competitive flow as possible sources of systematic error of quantitative blood flow measurements.

Differential Response to Pharmacological Stress Between Vein vs. Arterial Grafts

Most non-invasive tests for ischaemia rely on the detection of relative perfusion imbalances caused by a differential hyperaemic response to some form of pharmacological challenge. The effect of a number of vasoactive agents such as adenosine, dipyridamole and regadenoson (78), on the native coronary circulation is to a certain degree predictable and reproducible (66), and this simplifies their use as pharmacological stressors. However, the possibility of a differential vasoactive effect on grafts, particularly a disparity between arterial and venous grafts raises concerns with regards to the use of these agents in patients post CABG.

Previous studies using invasive haemodynamic data showed a reduced, or indeed absent, vasodilatory response of venous compared to arterial grafts following intra-graft injection of adenosine (79, 80). Similar findings were obtained with other pharmacological vasodilators (81). Indeed, these differences in vasomotor properties between graft conduits have been proposed as a possible explanation for the variability in long-term patency between arterial and venous grafts (82). Whether this differential response to pharmacological stress limits the diagnostic accuracy of perfusion detects remains unclear. Arnold et al. demonstrated that the hyperaemic MBF in response to

TABLE 1 | Non-invasive myocardial blood flow assessment post-surgical revascularisation.

References	Modality	Number of patients	Indication for perfusion assessment	Time from CABG	Stress MBF*	MPR*
Myocardial blood flow post CABG						
Aikawa et al. (63)	^{15}O-water PET	47	Protocol-driven assessment	6 months	1.45 (1.27–1.88)	1.93 (1.64–2.56)
Driessen et al. (64)	^{15}O-water PET	18	Protocol-driven assessment	62 days	2.05 ± 0.65	2.63 ± 0.87
Seraphim et al. (51)	Adenosine stress CMR	38	Clinical indication for scan; patent LIMA grafts	5 years	1.54 ± 0.47	1.94 ± 0.63
Spyrou et al. (52)	^{15}O-water PET	8	Protocol-driven assessment	6 months	2.45 ± 0.64	2.57 ± 0.49
Healthy controls						
Gould et al. (65)	PET (different tracers)	3,482	Healthy controls	n/a	2.86 ± 1.29	3.55 ± 1.36
Brown et al. (66)	Adenosine stress CMR	42	Healthy controls	n/a	2.71 ± 0.61	4.24 ± 0.69
Zorach et al. (67)	Regadenoson stress CMR	20	Healthy controls	n/a	3.17 ± 0.49	2.93 (2.76–3.19)

MBF, myocardial blood flow; MRP, myocardial perfusion reserve; LIMA, left internal mammary artery.
**Results presented as median (inter-quartile range) or mean ± standard deviation.*

adenosine was higher in segments supplied by arterial compared to venous grafts as assessed by quantitative CMR (83), further highlighting that quantitative ranges and cut offs for defining normal myocardial blood flow and myocardial perfusion reserve may differ from those seen in native coronaries. Whether the use of alternative pharmacological stress agents such as dobutamine would overcome this potential limitation is unclear. Dobutamine increases myocardial blood flow predominantly through an increase in myocardial oxygen demand, resulting from the increase in heart rate and myocardial contractility (84), although it is also thought to exert a relative weaker direct vasodilatation effect (85). Limited data exist on head to head comparison of different stress agents in patients post CABG (86, 87), but superiority of dobutamine over commonly used stressors has not been confirmed. Data from patients without previous surgical revascularisation would suggest that coronary flow augmentation is significantly higher with vasodilator agents such as adenosine and regadenoson compared to dobutamine or exercise, but whether this translates to an improved diagnostic performance is unclear. Furthermore, comparison between exercise and pharmacological stressors has not been widely studied in the context of previous CABG (88).

Arrhythmia and Electro-Mechanical Changes Post CABG

Surgical revascularisation results in both electrical and myocardial structural changes (89), thought to be secondary to procedural-related factors such as shifts in myocardial position (90), pericardial release (91), and peri-operative ischaemic injury (92). Atrial arrhythmias, particularly atrial fibrillation, are also common after surgery (93) and these are known to impact on the diagnostic performance of essentially all non-invasive ischaemia tests. Abnormal septal motion is common after cardiac surgery (94), making the interpretation of wall motion evaluation at both rest and peak stress challenging. Similarly, the electro-mechanical response to pharmacological agents such as dobutamine is thought to be altered in patients following CABG (95).

DIAGNOSTIC PERFORMANCE OF NON-INVASIVE ISCHAEMIA TESTING FOR THE DETECTION OF GRAFT FAILURE AND NATIVE DISEASE PROGRESSION

Ischaemia testing post-surgical revascularisation is broadly performed to evaluate distinct pathophysiological processes, which if identified can potentially alter clinical management. These include the presence of graft failure, native disease progression and in some cases the presence of residual ischaemia when incomplete revascularisation is suspected.

Each imaging modality suffers from its own limitations (**Table 2**) when it comes to surgically treated patients and in most studies the reported performance is inferior to that seen in patients without prior CABG (57, 96). Echocardiography is the most widely used technique for ischaemia evaluation and its diagnostic accuracy has been reported in a number of studies, using both pharmacological and exercise testing (97–102). In the context of CABG, limited LV coverage, and challenges in visualizing viable myocardium, peri-infarct ischaemia, and detecting multi-vessel disease are the main limitations. Although myocardial contrast echocardiography can overcome some of these limitations by offering quantitative perfusion assessment (103), it has not gained wider acceptance clinically, mainly due to lack of automation that hinders its adoption into the clinical workflow. CMR is being increasingly described as a reproducible and accurate method of ischaemia assessment, with an expanding body of evidence confirming its prognostic value and cost-effectiveness in the context of native coronary artery disease (104, 105). However, all major studies evaluating the diagnostic and prognostic performance of stress perfusion CMR have excluded patients with prior CABG, reflecting the complexity of ischaemia assessment in this patient population. Limited LV coverage with CMR poses challenges, particularly in terms of co-registering coronary anatomy and perfusion assessment and as in all modalities depending on first pass perfusion, there are questions regarding the impact of arterial delay of contrast through long grafts (51, 75). Despite increasing evidence on the safety of CMR

TABLE 2 | Comparison of non-invasive imaging tests for the assessment of myocardial ischaemia in patients with previous coronary artery bypass grafts—features, strengths, and limitations.

Imaging modality	Stressor	Accessibility/risks	Ischaemia / perfusion	Viability and function	Coronary anatomy	Quantitative perfusion
Stress echo	• Exercise, dobutamine, vasodilator	• Widely available • Often requires use of contrast for image quality • No radiation • Risk associated with dobutamine in the context of LV dysfunction	• Limited LV coverage • Less sensitive to identify subtle RWMA • Arrhythmia and abnormal septal motion limit performance • Spatial resolution: 1×1–3×3–6 mm^3	• Viability assessment suboptimal compared to CMR and PET	• N/A	• Requires use of microbubbles and associated with technical challenges • Linear relationship between blood flow and tracer
CMR	• Mainly vasodilator • Dobutamine and exercise possible but limited	• Not widely available • Vendor, field strength, sequence differences • No radiation • Devices affect image quality	• Limited LV coverage (conventionally 3x short axis slices used) • Arrhythmia can be detrimental • Can identify peri-infarct ischaemia • Spatial resolution: $1\times2\times6$–8 mm^3	• Gold standard modality for volume assessment • Peri-infarct ischaemia assessment • Additional tissue characterization	• Not performed routinely • Limited LV coverage	• Altered contrast kinetics associated with complex graft-native vessel flow • Non-linearity between blood flow, contrast and signal intensity
SPECT	• Exercise or vasodilator	• Widely available • Radiation (significantly reduced with modern scanners)	• Isotropic left ventricle coverage • Limited spatial resolution: $10\times10\times10$ mm^3	• Viability and function assessment possible • Limited temporal resolution	• Hybrid imaging with CT possible	• Limited temporal resolution • New generation scanners offer quantitative analysis
PET	• Exercise or vasodilator	• Not widely available • Radiation	• Isotropic left ventricle coverage • Endocardial-epicardial flow estimation possible • Spatial resolution 4 $\times$ 4 $\times$ 4 mm^3	• Viability assessment possible • Lower spatial resolution than CMR	• Hybrid imaging with CT possible	• Linear relationship between blood flow and ^{15}O-water • Linear relationship between tracer and image signal
CT perfusion/ angiography	• Vasodilator	• Perfusion not widely available • Radiation	• Spatial resolution (image analysis): $0.5\times0.5\times6$–8 mm^3 • Isotropic left ventricle coverage • Low CNR • Coronary and graft anatomy available	• Viability and function assessment possible, but increased radiation dose	• Data on anatomy • Difficulties with anastomosis sites and natives. • CT-FFR not validated for patients post CABG	• Non-linear relationship between blood flow and contrast

SPECT, Single-Photon Emission Computed Tomography; CMR, Cardiac Magnetic Resonance; PET, Positron Emission Tomography; CNR, contrast to noise ratio; FFR, fractional flow reserve.

imaging in patients with implantable electronic devices (106), artifact can affect image quality and perfusion interpretation. Furthermore, cost and limited availability continue to impede its clinical adoption as a mainstream test for ischaemia evaluation. Despite this, due to its high spatial resolution CMR is well-suited for evaluation of peri-infarct ischaemia and viability assessment in the same setting. Nuclear techniques (both PET and SPECT), have historically been crucial non-invasive modalities for ischaemia testing, and their performance and prognostic use is supported by a large body of evidence (22, 88, 107–112). As for native disease assessment, exposure to ionizing radiation continues to be considered a limitation, although with novel cameras and tracer technology the dose of this is decreasing. Furthermore, the possibility of hybrid imaging with computed tomography (CT) offers a great potential, with the advantage of paired anatomical and perfusion analysis being particularly relevant in the context of prior surgical revascularisation. Computed tomography coronary angiography itself offers an excellent tool for anatomical evaluation of graft patency (113), with high diagnostic accuracy for detection of graft occlusion or stenosis, but heavy calcification and native vessel disease especially in anastomotic sites and small-caliber distal runoff vessels, reduce its overall diagnostic performance without the benefit of paired perfusion assessment. Beyond this, mathematically modeled fractional flow reserve using CT (FFR_{CT}) has not been validated among patients with prior CABG

TABLE 3 | Diagnostic performance of non-invasive stress tests to identify graft failure and native disease progression post coronary artery bypass graft surgery.

References	Modality	Type of stress	Time from CABG (years)	Number of patients	Study population symptom status	Sensitivity (%)	Specificity (%)
Pittella et al. (97)	Echocardiography	Dobutamine	0.32	25	Asymptomatic patients	83	69
Hoffman et al. (98)	Echocardiography	Dobutamine	6.4	60	Symptomatic [45] and asymptomatic [15] patients	78	86
Sawada et al. (99)	Echocardiography	Exercise	6.3	41	Symptomatic [23] and asymptomatic [18] patients	88	86
Chirillo et al. (100)	Echocardiography	Dipyridamole	2.2	106	Patients scheduled to undergo coronary angiography	67	91
Elhendy et al. (101)	Echocardiography	Dobutamine	5.1	60	Both symptomatic [38] and asymptomatic [12] patients	78	89
Kafka et al. (102)	Echocardiography	Exercise	3.6	182	Mostly asymptomatic patients [148]	77	96
Crouse et al. (116)	Echocardiography	Exercise	7	125	Mainly symptomatic patients [96]	98	92
Al Aloul et al. (88)	SPECT	Exercise	1	79	Unselected cohort prospectively assessed 1 year post CABG	77	69
Pfisterer et al. (107)	SPECT	Exercise	12	55	Symptomatic [26] and asymptomatic [29] patients	80	88
Khoury et al. (108)	SPECT	Adenosine	6.7	109	Wide range of indications for cohort selection, including "periodic check-up" in 31 patients	96	61
Lakkis et al. (109)	SPECT	Exercise	4.2	50	30 patients with typical and 20 patients with atypical chest pain	80	87
Klein et al. (96)	Perfusion CMR	Adenosine	8	78	Suspicion of progression of stable angina	77	90
Bernhardt et al. (57)	Perfusion CMR	Adenosine	1.2	110	Clinical indication for invasive angiography	73	77
Klein et al. (86)*	Perfusion CMR Dobutamine	Dobutamine (wall motion analysis)	9.5	109	Data not available	88	96

SPECT, Single-Photon Emission Computed Tomography; CMR, Cardiac Magnetic Resonance; PET, Positron Emission Tomography.
**Abstract only.*

(114) and its use in this patient population is not currently recommended (115).

No single technique appears to have a clear diagnostic advantage over other, and selection is primarily based on patient-specific criteria, local expertise, and technique availability. A number of studies examined the diagnostic performance of non-invasive stress tests for the detection of graft failure or indeed the progression of native coronary artery disease post CABG (**Table 3**). These reported variable diagnostic accuracy against invasive coronary angiography and the majority made no distinction between ischaemia secondary to graft failure or ischaemia secondary to non-grafted native vessel disease. Furthermore, the lack of baseline studies immediately or soon after surgery makes it difficult to draw conclusions about ischaemia caused by incomplete revascularisation at the time of surgery vs. ischaemia caused by a new pathophysiological process. Finally, most studies used a combination of symptomatic and asymptomatic patients, making comparisons between modalities challenging.

Comparison of the diagnostic accuracy of each test is hindered by the lack of systematic evaluation of their limitations in this patient group, but also the absence of contemporary studies using the latest state of the art tools. Indeed, most studies were historically performed using SPECT and stress echocardiography and were significantly limited by the existing technology, which warrants caution in extrapolating these results to current practice. Certainly, the true potential of modern tools of advanced echocardiography such as strain and myocardial contrast echocardiography (117), the use of solid-state detector technology in SPECT imaging (118) as well as artificial intelligence-based approaches in quantitative myocardial perfusion in the evaluation of patients with prior CABG remains unknown.

PROGNOSTIC ROLE OF ISCHAEMIA TESTING FOLLOWING SURGICAL REVASCULARISATION

Despite the technical challenges associated with ischaemia testing in patients with prior CABG surgery, a number of studies across the entire spectrum of imaging modalities suggested that detection of ischaemia post CABG predicts adverse clinical outcomes (**Table 3**). As such, evaluation of ischaemia in this group of patients becomes important for both risk stratification and for potentially guiding treatment decisions.

TABLE 4 | Prognostic role of non-invasive ischaemia testing in patients with prior coronary artery bypass graft surgery.

References*	Study design	Imaging modality	Stressor	Number of patients	Male (%)	Follow up (months)	Study result
Cortigiani et al. (121)	Observational, multicenter	Stress echo	Dipyridamole	349	77	22	Ischemia associated with prognosis. CFVR of LAD ≤2 associated with HR 2.28
Harb et al. (122)	Observational, single center	Stress echo	Exercise	962	88	69	Ischaemia predicted mortality (HR 2.10)
Cortigiani et al. (123)	Observational, single center	Stress echo	Dobutamine Exercise Dipyridamole	500	80	25	Peak wall motion score index predicted mortality and MI (HR 3.07)
Arruda et al. (124)	Observational, single center	Stress echo	Exercise	718	82	35	18% reduction in hazard for every 10% incremental increase in exercise LVEF
Ortiz et al. (22)	Observational, single center	SPECT	Exercise Adenosine	84	100	119	Defect size 1 year following CABG, predicted death and CHF
Acampa et al. (110)	Observational, single center	SPECT	Dipyridamole Exercise	362	90	26	SPECT performed 5 years after CABG predicted death and MI (HR 3.7).
Sarda et al. (111)	Observational, single center	SPECT	Dipyridamole Exercise	115	90	35	Extent of stress defect predicted cardiac death and MI
Shapira et al. (112)*	Observational, single center	SPECT	-	170	-	48	SPECT performed soon after CABG has prognostic value
Palmas et al. (125)	Observational, single center	SPECT	Exercise	294	86	31	Incremental prognostic information provided by SPECT
Miller et al. (126)	Observational, single center	SPECT	Exercise	411	80	70	Exercise Tl-201 imaging performed within 2 years of CABG predicts outcomes
Lauer et al. (127)	Observational, single center	SPECT	Exercise	873	91	36	Exercise capacity and perfusion defects predict death (HR 2.78) in asymptomatic patients
Zellweger et al. (128)	Observational, single center	SPECT	Adenosine Exercise	1,765	80	23	MPS is strongly predictive of subsequent adverse events
Pen et al. (129)	Observational, multi-center	PET	Site-specific	953	70.8	29	Summed stress score predicted mortality (HR1.6) and cardiac death (HR1.8)
Kinnel et al. (130)	Observational, single center	CMR	Dipyridamole	852	89	50.4	Ischaemia predicted CV death (HR 2.15)

SPECT, Single-Photon Emission Computed Tomography; CMR, Cardiac Magnetic Resonance; PET, Positron Emission Tomography; HR, hazard ratio; MI, myocardial infarction; CHF, Congestive heart failure.
**Abstract available only.*

Historical data using exercise testing suggested that the presence of residual ischaemia post CABG is associated with increased risk of mortality, even among asymptomatic patients (119). Given the limitations of treadmill exercise ECG testing in patients with prior CABG (120), a number of studies subsequently evaluated the prognostic effect of ischaemia testing using non-invasive imaging, with the majority demonstrating a prognostic role for these tests (**Table 4**).

Most evidence on the prognostic impact of ischaemia detection comes from stress echocardiography (121, 123, 124, 131) and SPECT imaging (22, 31, 110–112, 127, 128), reflecting the dominant role of these modalities, particularly in previous decades. Despite including a large number of patients and long follow up times, collective interpretation of these studies is made difficult by significant study design heterogeneity (131), including differences in stress agents, use of optimal medical therapy, abnormal test definitions and primary end points. Very few studies have used advanced imaging techniques (121), including newly developed methods of quantitative myocardial perfusion evaluation which have already demonstrated incremental prognostic utility in patients without prior CABG (118, 132–134). Furthermore, in view of their retrospective design most studies did not provide data on the mechanism of ischaemia, complicating the translation of this finding into a form of clinical therapy.

There is a wide range of pathophysiological processes that can contribute to myocardial ischaemia in patients post CABG, and each may have a different impact on prognosis. Graft failure, native disease progression and microvascular dysfunction may all affect patient outcomes, but their respective contribution is unclear. Similarly, outcomes following any form of revascularisation are generally thought to be superior

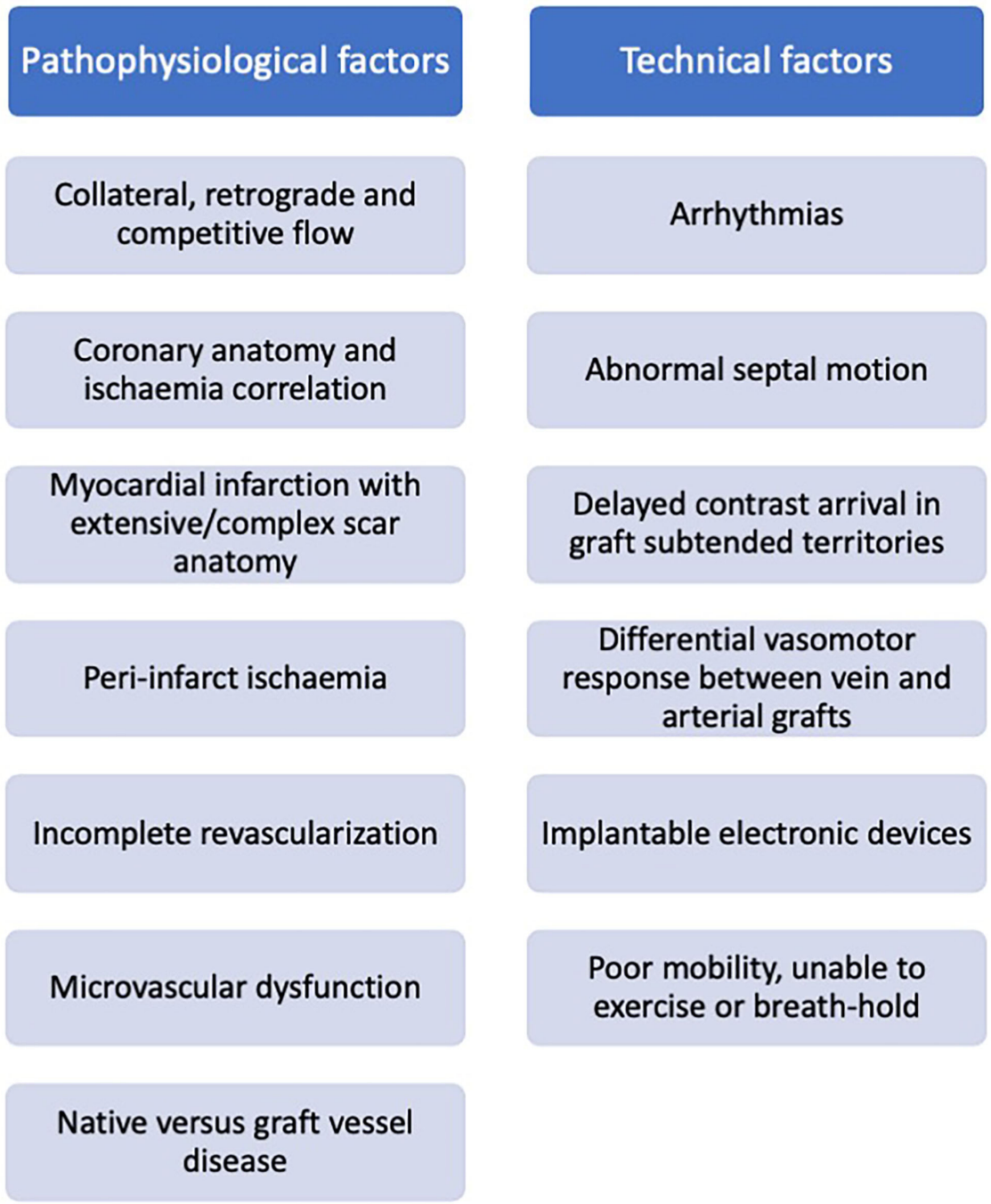

FIGURE 6 | Factors impacting non-invasive ischaemia assessment in patients with prior surgical revascularization.

if "complete revascularisation" is achieved, with a reduction in adverse events including subsequent myocardial infarction, repeat revascularisation and mortality (135). The mechanisms by which the completeness of revascularisation affects outcomes are also not well-defined, and may not be entirely associated with restoration of myocardial blood flow. One of the challenges in unraveling this, is that the vast majorities of studies have used relative crude anatomical definitions of completeness of revascularisation (136) with very few studies deploying a functional assessment for evaluating the effect of completeness of revascularisation on prognosis (137, 138).

However, evidence supporting the notion that detection of ischaemia in this patient group improves clinical outcomes is lacking, particularly in asymptomatic patients. Harb et al.

(122), evaluated the impact of routine stress testing post CABG, and found that although ischaemia detection was associated with adverse clinical events, repeat revascularisation did not alter outcomes. Similarly, in the large, multi-centered ROSETTA-CABG registry, patients undergoing routine post-CABG perfusion assessment with SPECT were compared with patients undergoing selective testing, and no difference in adverse clinical outcomes between the two groups was found (139).

FUTURE DIRECTIONS

The field of cardiac imaging has undergone dramatic developments in recent years, not only enabling enhanced diagnostic accuracy but providing tools for re-evaluating physiology and pathophysiological processes. Indeed, basic concepts in clinical cardiology, including that of myocardial ischaemia, continue to be centered on knowledge derived several decades ago and commonly remain uncontested. Recent studies, such as the ORBITA (140) and ISCHEMIA (141) trials have challenged our traditional ideas of myocardial ischaemia and its impact on patients symptoms and outcomes.

Advances in scanner performance, image reconstruction and wider availability of machine learning methods for data analysis have made it feasible to introduce quantitative methods of myocardial perfusion into routine clinical workflow. Such quantitative measures can be acquired in a highly automated fashion and offer incremental diagnostic value for ischaemia assessment particularly in complex models of coronary artery disease (142). Despite this, validation of such non-invasive myocardial perfusion indices against invasive coronary physiology in patients with prior CABG is lacking. Future prospective studies with paired information on coronary anatomy and quantitative perfusion imaging could provide new insights into the pathophysiological mechanisms of ischaemia in this patient population, potentially offering improved patient risk stratification and identification of novel therapeutic targets.

CONCLUSION

Patients commonly re-present for clinical assessment post coronary artery bypass grafting, and often pose a diagnostic challenge. Ischaemia evaluation in these patients is complex and subsequent clinical decision-making in response to the imaging results may be inconsistent. Challenges relate to both cardiovascular disease complexity (native coronary disease and collateralisation, graft variation, and infarction), and technical difficulties (arrhythmia, contrast transit time, and devices) (**Figure 6**), with no single imaging technique demonstrating clear superiority. Acknowledging the technical limitations of each modality may facilitate our decision making in selecting the most appropriate test based on the clinical scenario, personalized to the individual patient. Advances in imaging technology combined with the enhanced computational support of machine learning may help our understanding of these mechanisms, offering insights into the effects of revascularisation and potentially identifying novel therapeutic targets.

AUTHOR CONTRIBUTIONS

All authors listed have made a substantial, direct, and intellectual contribution to the work and approved it for publication.

FUNDING

This work was supported by a Clinical Research Training Fellowship (A Seraphim) from the British Heart Foundation (FS/18/83/34025) and directly and indirectly from the NIHR Biomedical Research Centers at University College London Hospitals and Barts Health NHS Trusts. This work forms part of the research areas contributing to the translational research portfolio of the Biomedical Research Center at Barts which was supported and funded by the National Institute for Health Research.

REFERENCES

1. Weiss AJ, Elixhauser A. Trends in operating room procedures in U.S. Hospitals, 2001–2011: statistical brief #171. In: *Healthcare Cost and Utilization Project (HCUP) Statistical Briefs*. Rockville: MD: Agency for Healthcare Research and Quality (US) (2006). Available online at: http://www.ncbi.nlm.nih.gov/books/NBK201926/ (accessed May 17, 2021).
2. Yusuf S, Zucker D, Peduzzi P, Fisher LD, Takaro T, Kennedy JW, et al. Effect of coronary artery bypass graft surgery on survival: overview of 10-year results from randomised trials by the Coronary Artery Bypass Graft Surgery Trialists Collaboration. *Lancet Lond Engl.* (1994) 344:563–70. doi: 10.1016/S0140-6736(94)91963-1
3. The BARI 2D Study Group. A randomized trial of therapies for type 2 diabetes and coronary artery disease. *N Engl J Med*. (2009) 360:2503–15. doi: 10.1056/NEJMoa0805796
4. Velazquez EJ, Lee KL, Jones RH, Al-Khalidi HR, Hill JA, Panza JA, et al. Coronary-artery bypass surgery in patients with ischemic cardiomyopathy. *N Engl J Med.* (2016) 374:1511–20. doi: 10.1056/NEJMoa1602001
5. Fitzgibbon GM, Kafka HP, Leach AJ, Keon WJ, Hooper GD, Burton JR. Coronary bypass graft fate and patient outcome: angiographic follow-up of 5,065 grafts related to survival and reoperation in 1,388 patients during 25 years. *J Am Coll Cardiol.* (1996) 28:616–26. doi: 10.1016/0735-1097(96)00206-9
6. Engebretsen KVT, Friis C, Sandvik L, Tønnessen T. Survival after CABG–better than predicted by EuroSCORE and equal to the general population. *Scand Cardiovasc J SCJ.* (2009) 43:123–8. doi: 10.1080/14017430802354085
7. Adelborg K, Horváth-Puhó E, Schmidt M, Munch T, Pedersen L, Nielsen PH, et al. Thirty-year mortality after coronary artery bypass graft surgery: a Danish Nationwide Population-Based Cohort Study. *Circ Cardiovasc Qual Outcomes.* (2017) 10:e002708. doi: 10.1161/CIRCOUTCOMES.116.002708
8. Sergeant P, Blackstone E, Meyns B, Stockman B, Jashari R. First cardiological or cardiosurgical reintervention for ischemic heart disease after primary coronary artery bypass grafting. *Eur J Cardio-Thorac Surg Off J Eur Assoc Cardio-Thorac Surg.* (1998) 14:480–7. doi: 10.1016/S1010-7940(98)00214-0
9. Stone GW, Kappetein AP, Sabik JF, Pocock SJ, Morice M-C, Puskas J, et al. Five-year outcomes after PCI or CABG for left main coronary disease. *N Engl J Med.* (2019) 381:1820–30. doi: 10.1056/NEJMoa1909406
10. Lenzen MJ, Boersma E, Bertrand ME, Maier W, Moris C, Piscione F, et al. Management and outcome of patients with established coronary artery disease: the Euro Heart Survey on coronary revascularization. *Eur Heart J.* (2005) 26:1169–79. doi: 10.1093/eurheartj/ehi238

11. Rathod KS, Beirne A-M, Bogle R, Firoozi S, Lim P, Hill J, et al. Prior coronary artery bypass graft surgery and outcome after percutaneous coronary intervention: an observational study from the Pan-London Percutaneous Coronary Intervention Registry. *J Am Heart Assoc.* (2020) 9:e014409. doi: 10.1161/JAHA.119.014409
12. Nikolsky E, McLaurin BT, Cox DA, Manoukian SV, Xu K, Mehran R, et al. Outcomes of patients with prior coronary artery bypass grafting and acute coronary syndromes: analysis from the ACUITY (Acute Catheterization and Urgent Intervention Triage Strategy) trial. *JACC Cardiovasc Interv.* (2012) 5:919–26. doi: 10.1016/j.jcin.2012.06.009
13. Björk VO, Ekeström S, Henze A, Ivert T, Landou C. Early and late patency of aortocoronary vein grafts. *Scand J Thorac Cardiovasc Surg.* (1981) 15:11–21. doi: 10.3109/14017438109101020
14. Lytle BW, Loop FD, Cosgrove DM, Ratliff NB, Easley K, Taylor PC. Long-term (5 to 12 years) serial studies of internal mammary artery and saphenous vein coronary bypass grafts. *J Thorac Cardiovasc Surg.* (1985) 89:248–58. doi: 10.1016/S0022-5223(19)38820-8
15. Hess CN, Lopes RD, Gibson CM, Hager R, Wojdyla DM, Englum BR, et al. Saphenous vein graft failure after coronary artery bypass surgery: insights from PREVENT IV. *Circulation.* (2014) 130:1445–51. doi: 10.1161/CIRCULATIONAHA.113.008193
16. Zhao Q, Zhu Y, Xu Z, Cheng Z, Mei J, Chen X, et al. Effect of ticagrelor plus aspirin, ticagrelor alone, or aspirin alone on saphenous vein graft patency 1 year after coronary artery bypass grafting: a randomized clinical trial. *J Am Med Assoc.* (2018) 319:1677–86. doi: 10.1001/jama.2018.3197
17. Goldman S, Zadina K, Moritz T, Ovitt T, Sethi G, Copeland JG, et al. Long-term patency of saphenous vein and left internal mammary artery grafts after coronary artery bypass surgery: results from a Department of Veterans Affairs Cooperative Study. *J Am Coll Cardiol.* (2004) 44:2149–56. doi: 10.1016/j.jacc.2004.08.064
18. Sabik JF, Lytle BW, Blackstone EH, Houghtaling PL, Cosgrove DM. Comparison of saphenous vein and internal thoracic artery graft patency by coronary system. *Ann Thorac Surg.* (2005) 79:544–51. doi: 10.1016/j.athoracsur.2004.07.047
19. Pond KK, Martin GV, Every N, Lehmann KG, Anderson R, Caldwell JH, et al. Predictors of progression of native coronary narrowing to total occlusion after coronary artery bypass grafting. *Am J Cardiol.* (2003) 91:971–4. doi: 10.1016/S0002-9149(03)00115-2
20. Lopes RD, Mehta RH, Hafley GE, Williams JB, Mack MJ, Peterson ED, et al. Relationship between vein graft failure and subsequent clinical outcomes after coronary artery bypass surgery. *Circulation.* (2012) 125:749–56. doi: 10.1161/CIRCULATIONAHA.111.040311
21. Loop FD, Lytle BW, Cosgrove DM, Stewart RW, Goormastic M, Williams GW, et al. Influence of the internal-mammary-artery graft on 10-year survival and other cardiac events. *N Engl J Med.* (1986) 314:1–6. doi: 10.1056/NEJM198601023140101
22. Ortiz F, Mbai M, Adabag S, Garcia S, Nguyen J, Goldman S, et al. Utility of nuclear stress imaging in predicting long-term outcomes one-year post CABG surgery. *J Nucl Cardiol Off Publ Am Soc Nucl Cardiol.* (2018) 2018:1469. doi: 10.1007/s12350-018-01469-y
23. Pellicano M, De Bruyne B, Toth GG, Casselman F, Wijns W, Barbato E. Fractional flow reserve to guide and to assess coronary artery bypass grafting. *Eur Heart J.* (2017) 38:1959–68. doi: 10.1093/eurheartj/ehw505
24. Zimmermann FM, Ferrara A, Johnson NP, van Nunen LX, Escaned J, Albertsson P, et al. Deferral vs. performance of percutaneous coronary intervention of functionally non-significant coronary stenosis: 15-year follow-up of the DEFER trial. *Eur Heart J.* (2015) 36:3182–8. doi: 10.1093/eurheartj/ehv452
25. Escaned J. Secondary revascularization after CABG surgery. *Nat Rev Cardiol.* (2012) 9:540–9. doi: 10.1038/nrcardio.2012.100
26. Trägårdh E, Tan SS, Bucerius J, Gimelli A, Gaemperli O, Lindner O, et al. Systematic review of cost-effectiveness of myocardial perfusion scintigraphy in patients with ischaemic heart disease: a report from the cardiovascular committee of the European Association of Nuclear Medicine. Endorsed by the European Association of Cardiovascular Imaging. *Eur Heart J Cardiovasc Imaging.* (2017) 18:825–32. doi: 10.1093/ehjci/jex095
27. National Institute of Clinical Excellence. *Recent-Onset Chest Pain of Suspected Cardiac Origin: Assessment and Diagnosis*. (2016). p. 30. Available online at: https://www.nice.org.uk/guidance/cg95 (accessed December 4, 2021).
28. Knuuti J, Wijns W, Saraste A, Capodanno D, Barbato E, Funck-Brentano C, et al. 2019 ESC Guidelines for the diagnosis and management of chronic coronary syndromes. *Eur Heart J.* (2020) 41:407–77. doi: 10.1093/eurheartj/ehz425
29. American College of Cardiology Foundation Appropriate Use Criteria Task Force, American Society of Echocardiography, American Heart Association, American Society of Nuclear Cardiology, Heart Failure Society of America, Heart Rhythm Society, et al. ACCF/ASE/AHA/ASNC/HFSA/HRS/SCAI/SCCM/SCCT/SCMR 2011 appropriate use criteria for echocardiography. a report of the American College of Cardiology Foundation Appropriate Use Criteria Task Force, American Society of Echocardiography, American Heart Association, American Society of Nuclear Cardiology, Heart Failure Society of America, Heart Rhythm Society, Society for Cardiovascular Angiography and Interventions, Society of Critical Care Medicine, Society of Cardiovascular Computed Tomography, Society for Cardiovascular Magnetic Resonance American College of Chest Physicians. *J Am Soc Echocardiogr Off Publ Am Soc Echocardiogr.* (2011) 24:229–67. doi: 10.1016/j.echo.2010.12.008
30. Fihn SD, Gardin JM, Abrams J, Berra K, Blankenship JC, Dallas AP, et al. 2012 ACCF/AHA/ACP/AATS/PCNA/SCAI/STS guideline for the diagnosis and management of patients with stable ischemic heart disease. *J Am Coll Cardiol.* (2012) 60:e44–164. doi: 10.1016/j.jacc.2012.07.012
31. Eisenberg MJ, Wou K, Nguyen H, Duerr R, Del Core M, Fourchy D, et al. Use of stress testing early after coronary artery bypass graft surgery. *Am J Cardiol.* (2006) 97:810–6. doi: 10.1016/j.amjcard.2005.09.130
32. Ellenberger C, Sologashvili T, Cikirikcioglu M, Verdon G, Diaper J, Cassina T, et al. Risk factors of postcardiotomy ventricular dysfunction in moderate-to-high risk patients undergoing open-heart surgery. *Ann Card Anaesth.* (2017) 20:287–96. doi: 10.4103/aca.ACA_60_17
33. Ding W, Ji Q, Shi Y, Ma R. Predictors of low cardiac output syndrome after isolated coronary artery bypass grafting. *Int Heart J.* (2015) 56:144–9. doi: 10.1536/ihj.14-231
34. Wilson RF, Marcus ML, White CW. Effects of coronary bypass surgery and angioplasty on coronary blood flow and flow reserve. *Prog Cardiovasc Dis.* (1988) 31:95–114. doi: 10.1016/0033-0620(88)90013-8
35. Coolong A, Baim DS, Kuntz RE, O'Malley AJ, Marulkar S, Cutlip DE, et al. Saphenous vein graft stenting and major adverse cardiac events: a predictive model derived from a pooled analysis of 3958 patients. *Circulation.* (2008) 117:790–7. doi: 10.1161/CIRCULATIONAHA.106.651232
36. Pucelikova T, Mehran R, Kirtane AJ, Kim Y-H, Fahy M, Weisz G, et al. Short- and long-term outcomes after stent-assisted percutaneous treatment of saphenous vein grafts in the drug-eluting stent era. *Am J Cardiol.* (2008) 101:63–8. doi: 10.1016/j.amjcard.2007.07.048
37. Morrison DA, Sethi G, Sacks J, Henderson WG, Grover F, Sedlis S, et al. Percutaneous coronary intervention versus repeat bypass surgery for patients with medically refractory myocardial ischemia: AWESOME randomized trial and registry experience with post-CABG patients. *J Am Coll Cardiol.* (2002) 40:1951–4. doi: 10.1016/S0735-1097(02)02560-3
38. Harskamp RE, Beijk MA, Damman P, Kuijt WJ, Woudstra P, Grundeken MJ, et al. Clinical outcome after surgical or percutaneous revascularization in coronary bypass graft failure. *J Cardiovasc Med Hagerstown Md.* (2013) 14:438–45. doi: 10.2459/JCM.0b013e328356a4fc
39. Berry C, Pieper KS, White HD, Solomon SD, Van de Werf F, Velazquez EJ, et al. Patients with prior coronary artery bypass grafting have a poor outcome after myocardial infarction: an analysis of the VALsartan in acute myocardial iNfarcTion trial (VALIANT). *Eur Heart J.* (2009) 30:1450–6. doi: 10.1093/eurheartj/ehp102
40. Brown LAE, Saunderson CED, Das A, Craven T, Levelt E, Knott KD, et al. A comparison of standard and high dose adenosine protocols in routine vasodilator stress cardiovascular magnetic resonance: dosage affects hyperaemic myocardial blood flow in patients with severe left ventricular systolic impairment. *J Cardiovasc Magn Reson.* (2021) 23:37. doi: 10.1186/s12968-021-00714-7

41. Geleijnse ML, Krenning BJ, Nemes A, van Dalen BM, Soliman O, ten Cate FJ, et al. Incidence, pathophysiology, and treatment of complications during dobutamine-atropine stress echocardiography. *Circulation.* (2010) 121:1756–67. doi: 10.1161/CIRCULATIONAHA.109.859264
42. Lim CC, Tan CS, Chia CML, Tan AK, Choo JCJ, Kaushik M, et al. Long-term risk of progressive chronic kidney disease in patients with severe acute kidney injury requiring dialysis after coronary artery bypass surgery. *Cardiorenal Med.* (2015) 5:157–63. doi: 10.1159/000381068
43. Maaniitty T, Jaakkola S, Saraste A, Knuuti J. Hybrid coronary computed tomography angiography and positron emission tomography myocardial perfusion imaging in evaluation of recurrent symptoms after coronary artery bypass grafting. *Eur Heart J - Cardiovasc Imaging.* (2019) 20:1298–304. doi: 10.1093/ehjci/jey160
44. Kawai H, Sarai M, Motoyama S, Ito H, Takada K, Harigaya H, et al. A combination of anatomical and functional evaluations improves the prediction of cardiac event in patients with coronary artery bypass. *BMJ Open.* (2013) 3:e003474. doi: 10.1136/bmjopen-2013-003474
45. Nathoe Hendrik M, Erik B, Jansen Erik WL, Suyker Willem JL, Stella Pieter R, Lahpor Jaap R, et al. Role of coronary collaterals in off-pump and on-pump coronary bypass surgery. *Circulation.* (2004) 110:1738–42. doi: 10.1161/01.CIR.0000143105.42988.FD
46. Guo L, Steinman DA, Moon BC, Wan W-K, Millsap RJ. Effect of distal graft anastomosis site on retrograde perfusion and flow patterns of native coronary vasculature. *Ann Thorac Surg.* (2001) 72:782–7. doi: 10.1016/S0003-4975(01)02801-6
47. Zafrir N, Madduri J, Mats I, Ben-Gal T, Solodky A, Assali A, et al. Discrepancy between myocardial ischemia and luminal stenosis in patients with left internal mammary artery grafting to left anterior descending coronary artery. *J Nucl Cardiol Off Publ Am Soc Nucl Cardiol.* (2003) 10:663–8. doi: 10.1016/j.nuclcard.2003.09.003
48. Henzlova MJ, Bittner V, Dubovsky E, Nath H, Pohost GM. Frequency of stress-induced thallium-201 defects in patients with patent internal mammary artery to the left anterior descending coronary artery graft. *Am J Cardiol.* (1992) 70:399–400. doi: 10.1016/0002-9149(92)90631-8
49. Hirzel HO, Nuesch K, Sialer G, Horst W, Krayenbuehl HP. Thallium-201 exercise myocardial imaging to evaluate myocardial perfusion after coronary artery bypass surgery. *Br Heart J.* (1980) 43:426–35. doi: 10.1136/hrt.43.4.426
50. Wainwright RJ, Brennand-Roper DA, Maisey MN, Sowton E. Exercise thallium-201 myocardial scintigraphy in the follow-up of aortocoronary bypass graft surgery. *Br Heart J.* (1980) 43:56–66. doi: 10.1136/hrt.43.1.56
51. Seraphim A, Knott KD, Beirne A-M, Augusto JB, Menacho K, Artico J, et al. Use of quantitative cardiovascular magnetic resonance myocardial perfusion mapping for characterization of ischemia in patients with left internal mammary coronary artery bypass grafts. *J Cardiovasc Magn Reson.* (2021) 23:82. doi: 10.1186/s12968-021-00763-y
52. Spyrou N, Khan MA, Rosen SD, Foale R, Davies DW, Sogliani F, et al. Persistent but reversible coronary microvascular dysfunction after bypass grafting. *Am J Physiol Heart Circ Physiol.* (2000) 279:H2634–40. doi: 10.1152/ajpheart.2000.279.6.H2634
53. Kelle S, Graf K, Dreysse S, Schnackenburg B, Fleck E, Klein C. Evaluation of contrast wash-in and peak enhancement in adenosine first pass perfusion CMR in patients post bypass surgery. *J Cardiovasc Magn Reson Off J Soc Cardiovasc Magn Reson.* (2010) 12:28. doi: 10.1186/1532-429X-12-28
54. Janiec M, Nazari Shafti TZ, Dimberg A, Lagerqvist B, Lindblom RPF. Graft failure and recurrence of symptoms after coronary artery bypass grafting. *Scand Cardiovasc J SCJ.* (2018) 52:113–9. doi: 10.1080/14017431.2018.1442930
55. Pegg TJ, Selvanayagam JB, Francis JM, Karamitsos TD, Maunsell Z, Yu L-M, et al. A randomized trial of on-pump beating heart and conventional cardioplegic arrest in coronary artery bypass surgery patients with impaired left ventricular function using cardiac magnetic resonance imaging and biochemical markers. *Circulation.* (2008) 118:2130–8. doi: 10.1161/CIRCULATIONAHA.108.785105
56. Steuer J, Bjerner T, Duvernoy O, Jidéus L, Johansson L, Ahlström H, et al. Visualisation and quantification of peri-operative myocardial infarction after coronary artery bypass surgery with contrast-enhanced magnetic resonance imaging. *Eur Heart J.* (2004) 25:1293–9. doi: 10.1016/j.ehj.2004.05.015
57. Bernhardt P, Spiess J, Levenson B, Pilz G, Höfling B, Hombach V, et al. Combined assessment of myocardial perfusion and late gadolinium enhancement in patients after percutaneous coronary intervention or bypass grafts: a multicenter study of an integrated cardiovascular magnetic resonance protocol. *JACC Cardiovasc Imaging.* (2009) 2:1292–300. doi: 10.1016/j.jcmg.2009.05.011
58. Schnell F, Donal E, Bernard A, Thebault C, Lelong B, Kervio G, et al. Improved diagnosis of post-operative myocardial infarction by contrast echocardiography after coronary artery bypass graft surgery. *Eur J Echocardiogr.* (2011) 12:612–8. doi: 10.1093/ejechocard/jer087
59. Almeida AG, Carpenter J-P, Cameli M, Donal E, Dweck MR, Flachskampf FA, et al. Multimodality imaging of myocardial viability: an expert consensus document from the European Association of Cardiovascular Imaging (EACVI). *Eur Heart J - Cardiovasc Imaging.* (2021) 22:e97–125. doi: 10.1093/ehjci/jeab053
60. Neumann F-J, Sousa-Uva M, Ahlsson A, Alfonso F, Banning AP, Benedetto U, et al. 2018 ESC/EACTS Guidelines on myocardial revascularization. *Eur Heart J.* (2019) 40:87–165. doi: 10.1093/eurheartj/ehy855
61. Brown JM, Poston RS, Gammie JS, Cardarelli MG, Schwartz K, Sikora JAH, et al. Off-pump versus on-pump coronary artery bypass grafting in consecutive patients: decision-making algorithm and outcomes. *Ann Thorac Surg.* (2006) 81:555–61. doi: 10.1016/j.athoracsur.2005.06.081
62. Garcia S, Sandoval Y, Roukoz H, Adabag S, Canoniero M, Yannopoulos D, et al. Outcomes after complete versus incomplete revascularization of patients with multivessel coronary artery disease: a meta-analysis of 89,883 patients enrolled in randomized clinical trials and observational studies. *J Am Coll Cardiol.* (2013) 62:1421–31. doi: 10.1016/j.jacc.2013.05.033
63. Aikawa T, Naya M, Koyanagawa K, Manabe O, Obara M, Magota K, et al. Improved regional myocardial blood flow and flow reserve after coronary revascularization as assessed by serial 15O-water positron emission tomography/computed tomography. *Eur Heart J Cardiovasc Imaging.* (2020) 21:36–46. doi: 10.1093/ehjci/jez220
64. Driessen RS, Danad I, Stuijfzand WJ, Schumacher SP, Knuuti J, Mäki M, et al. Impact of revascularization on absolute myocardial blood flow as assessed by serial [15O]H_2O positron emission tomography imaging: a comparison with fractional flow reserve. *Circ Cardiovasc Imaging.* (2018) 11:e007417. doi: 10.1161/CIRCIMAGING.117.007417
65. Gould KL, Johnson NP, Bateman TM, Beanlands RS, Bengel FM, Bober R, et al. Anatomic versus physiologic assessment of coronary artery disease. Role of coronary flow reserve, fractional flow reserve, and positron emission tomography imaging in revascularization decision-making. *J Am Coll Cardiol.* (2013) 62:1639–53. doi: 10.1016/j.jacc.2013.07.076
66. Brown LAE, Onciul SC, Broadbent DA, Johnson K, Fent GJ, Foley JRJ, et al. Fully automated, inline quantification of myocardial blood flow with cardiovascular magnetic resonance: repeatability of measurements in healthy subjects. *J Cardiovasc Magn Reson.* (2018) 20:48. doi: 10.1186/s12968-018-0462-y
67. Zorach B, Shaw PW, Bourque J, Kuruvilla S, Balfour PC, Yang Y, et al. Quantitative cardiovascular magnetic resonance perfusion imaging identifies reduced flow reserve in microvascular coronary artery disease. *J Cardiovasc Magn Reson.* (2018) 20:14. doi: 10.1186/s12968-018-0435-1
68. Rahman H, Scannell CM, Demir OM, Ryan M, McConkey H, Ellis H, et al. High-resolution cardiac magnetic resonance imaging techniques for the identification of coronary microvascular dysfunction. *JACC Cardiovasc Imaging.* (2020) 10:15. doi: 10.1016/j.jcmg.2020.10.015
69. Nishi T, Murai T, Ciccarelli G, Shah SV, Kobayashi Y, Derimay F, et al. Prognostic value of coronary microvascular function measured immediately after percutaneous coronary intervention in stable coronary artery disease. *Circ Cardiovasc Interv.* (2019) 12:e007889. doi: 10.1161/CIRCINTERVENTIONS.119.007889
70. Sellke FW, Friedman M, Dai HB, Shafique T, Schoen FJ, Weintraub RM, et al. Mechanisms causing coronary microvascular dysfunction following crystalloid cardioplegia and reperfusion. *Cardiovasc Res.* (1993) 27:1925–32. doi: 10.1093/cvr/27.11.1925
71. Akasaka T, Yoshikawa J, Yoshida K, Maeda K, Hozumi T, Nasu M, et al. Flow capacity of internal mammary artery grafts: early restriction and later improvement assessed by Doppler guide wire.

Comparison with saphenous vein grafts. *J Am Coll Cardiol.* (1995) 25:640–7. doi: 10.1016/0735-1097(94)00448-Y
72. Feng J, Liu Y, Chu LM, Singh AK, Dobrilovic N, Fingleton JG, et al. Changes in microvascular reactivity after cardiopulmonary bypass in patients with poorly controlled versus controlled diabetes. *Circulation.* (2012) 126(11Suppl.1):S73–80. doi: 10.1161/CIRCULATIONAHA.111.084590
73. Kotecha T, Martinez-Naharro A, Boldrini M, Knight D, Hawkins P, Kalra S, et al. Automated pixel-wise quantitative myocardial perfusion mapping by CMR to detect obstructive coronary artery disease and coronary microvascular dysfunction: validation against invasive coronary physiology. *JACC Cardiovasc Imaging.* (2019) 12:1958–69. doi: 10.1016/j.jcmg.2018.12.022
74. Kellman P, Hansen MS, Nielles-Vallespin S, Nickander J, Themudo R, Ugander M, et al. Myocardial perfusion cardiovascular magnetic resonance: optimized dual sequence and reconstruction for quantification. *J Cardiovasc Magn Reson.* (2017) 19:43. doi: 10.1186/s12968-017-0355-5
75. Arnold JR, Francis JM, Karamitsos TD, Lim CC, van Gaal WJ, Testa L, et al. Myocardial perfusion imaging after coronary artery bypass surgery using cardiovascular magnetic resonance: a validation study. *Circ Cardiovasc Imaging.* (2011) 4:312–8. doi: 10.1161/CIRCIMAGING.110.959742
76. Sommer K, Bernat D, Schmidt R, Breit H-C, Schreiber LM. Resting myocardial blood flow quantification using contrast-enhanced magnetic resonance imaging in the presence of stenosis: a computational fluid dynamics study. *Med Phys.* (2015) 42:4375–84. doi: 10.1118/1.4922708
77. Martens J, Panzer S, van den Wijngaard JPHM, Siebes M, Schreiber LM. Analysis of coronary contrast agent transport in bolus-based quantitative myocardial perfusion MRI measurements with computational fluid dynamics simulations. In: Pop M, Wright GA, editors, *Functional Imaging and Modelling of the Heart*. Cham: Springer International Publishing (2017). p. 369–80. doi: 10.1007/978-3-319-59448-4_35
78. Layland J, Carrick D, Lee M, Oldroyd K, Berry C. Adenosine: physiology, pharmacology, and clinical applications. *JACC Cardiovasc Interv.* (2014) 7:581–91. doi: 10.1016/j.jcin.2014.02.009
79. Chong WC, Collins P, Webb CM, De Souza AC, Pepper JR, Hayward CS, et al. Comparison of flow characteristics and vascular reactivity of radial artery and long saphenous vein grafts [NCT00139399]. *J Cardiothorac Surg.* (2006) 1:4. doi: 10.1186/1749-8090-1-4
80. Glineur D, Poncelet A, El Khoury G, D'hoore W, Astarci P, Zech F, et al. Fractional flow reserve of pedicled internal thoracic artery and saphenous vein grafts 6 months after bypass surgery. *Eur J Cardio-Thorac Surg Off J Eur Assoc Cardio-Thorac Surg.* (2007) 31:376–81. doi: 10.1016/j.ejcts.2006.11.023
81. Hanet C, Robert A, Wijns W. Vasomotor response to ergometrine and nitrates of saphenous vein grafts, internal mammary artery grafts, and grafted coronary arteries late after bypass surgery. *Circulation.* (1992) 86(5Suppl.):II210–6. doi: 10.1016/0735-1097(91)91805-O
82. Ochiai M, Ohno M, Taguchi J, Hara K, Suma H, Isshiki T, et al. Responses of human gastroepiploic arteries to vasoactive substances: comparison with responses of internal mammary arteries and saphenous veins. *J Thorac Cardiovasc Surg.* (1992) 104:453–8. doi: 10.1016/S0022-5223(19)34803-2
83. Arnold JR, Karamitsos TD, van Gaal WJ, Testa L, Francis JM, Bhamra-Ariza P, et al. Residual ischemia after revascularization in multivessel coronary artery disease: insights from measurement of absolute myocardial blood flow using magnetic resonance imaging compared with angiographic assessment. *Circ Cardiovasc Interv.* (2013) 6:237–45. doi: 10.1161/CIRCINTERVENTIONS.112.000064
84. Fung AY, Gallagher KP, Buda AJ. The physiologic basis of dobutamine as compared with dipyridamole stress interventions in the assessment of critical coronary stenosis. *Circulation.* (1987) 76:943–51. doi: 10.1161/01.CIR.76.4.943
85. Geleijnse ML, Elhendy A, Fioretti PM, Roelandt JRTC. Dobutamine stress myocardial perfusion imaging. *J Am Coll Cardiol.* (2000) 36:2017–27. doi: 10.1016/S0735-1097(00)01012-3
86. Klein C, Gebker R, Kelle S, Graf K, Dreysse S, Schnackenburg B, et al. Direct comparison of CMR dobutamine stress wall motion and perfusion analysis with adenosine perfusion in patients after bypass surgery. *J Cardiovasc Magn Reson.* (2011) 13:P100. doi: 10.1186/1532-429X-13-S1-P100
87. Manka R, Jahnke C, Gebker R, Schnackenburg B, Paetsch I. Head-to-head comparison of first-pass MR perfusion imaging during adenosine and high-dose dobutamine/atropine stress. *Int J Cardiovasc Imaging.* (2011) 27:995–1002. doi: 10.1007/s10554-010-9748-3
88. Al Aloul B, Mbai M, Adabag S, Garcia S, Thai H, Goldman S, et al. Utility of nuclear stress imaging for detecting coronary artery bypass graft disease. *BMC Cardiovasc Disord.* (2012) 12:62. doi: 10.1186/1471-2261-12-62
89. Hatam N, Aljalloud A, Mischke K, Karfis EA, Autschbach R, Hoffmann R, et al. Interatrial conduction disturbance in postoperative atrial fibrillation: a comparative study of P-wave dispersion and Doppler myocardial imaging in cardiac surgery. *J Cardiothorac Surg.* (2014) 9:114. doi: 10.1186/1749-8090-9-114
90. Reynolds HR, Tunick PA, Grossi EA, Dilmanian H, Colvin SB, Kronzon I. Paradoxical septal motion after cardiac surgery: a review of 3,292 cases. *Clin Cardiol.* (2007) 30:621–3. doi: 10.1002/clc.20201
91. Eslami B, Roitman D, Karp RB, Sheffield LT. The echocardiogram after pericardiectomy. *Jpn Heart J.* (1979) 20:1–5. doi: 10.1536/ihj.20.1
92. Thielmann M, Sharma V, Al-Attar N, Bulluck H, Bisleri G, Bunge JJ, et al. ESC Joint Working Groups on Cardiovascular Surgery and the Cellular Biology of the Heart Position Paper: peri-operative myocardial injury and infarction in patients undergoing coronary artery bypass graft surgery. *Eur Heart J.* (2017) 38:2392–411. doi: 10.1093/eurheartj/ehx383
93. D'Agostino RS, Jacobs JP, Badhwar V, Fernandez FG, Paone G, Wormuth DW, et al. The society of thoracic surgeons adult cardiac surgery database: 2018 update on outcomes and quality. *Ann Thorac Surg.* (2018) 105:15–23. doi: 10.1016/j.athoracsur.2017.10.035
94. Lehmann KG, Lee FA, McKenzie WB, Barash PG, Prokop EK, Durkin MA, et al. Onset of altered interventricular septal motion during cardiac surgery. Assessment by continuous intraoperative transesophageal echocardiography. *Circulation.* (1990) 82:1325–34. doi: 10.1161/01.CIR.82.4.1325
95. Duncan A, Francis D, Gibson D, Pepper J, Henein M. Electromechanical left ventricular resynchronisation by coronary artery bypass surgery. *Eur J Cardio-Thorac Surg Off J Eur Assoc Cardio-Thorac Surg.* (2004) 26:711–9. doi: 10.1016/j.ejcts.2004.05.020
96. Klein C, Nagel E, Gebker R, Kelle S, Schnackenburg B, Graf K, et al. Magnetic resonance adenosine perfusion imaging in patients after coronary artery bypass graft surgery. *JACC Cardiovasc Imaging.* (2009) 2:437–45. doi: 10.1016/j.jcmg.2008.12.016
97. Pittella FJM, Cunha AB da, Romeu Filho LJM, Labrunie MM, Weitzel LH, Melhado JC, et al. Functional assessment of coronary grafts on dobutamine pharmacological stress echocardiogram. *Arq Bras Cardiol.* (2006) 87:451–5. doi: 10.1590/S0066-782X2006001700009
98. Hoffmann R, Lethen H, Falter F, Flachskampf FA, Hanrath P. Dobutamine stress echocardiography after coronary artery bypass grafting. Transthoracic vs. biplane transoesophageal imaging. *Eur Heart J.* (1996) 17:222–9. doi: 10.1093/oxfordjournals.eurheartj.a014838
99. Sawada SG, Judson WE, Ryan T, Armstrong WF, Feigenbaum H. Upright bicycle exercise echocardiography after coronary artery bypass grafting. *Am J Cardiol.* (1989) 64:1123–9. doi: 10.1016/0002-9149(89)90864-3
100. Chirillo F, Bruni A, De Leo A, Olivari Z, Franceschini-Grisolia E, Totis O, et al. Usefulness of dipyridamole stress echocardiography for predicting graft patency after coronary artery bypass grafting. *Am J Cardiol.* (2004) 93:24–30. doi: 10.1016/j.amjcard.2003.09.007
101. Elhendy A, Geleijnse ML, Roelandt JR, Cornel JH, van Domburg RT, El-Refaee M, et al. Assessment of patients after coronary artery bypass grafting by dobutamine stress echocardiography. *Am J Cardiol.* (1996) 77:1234–6. doi: 10.1016/S0002-9149(96)00171-3
102. Kafka H, Leach AJ, FitzGibbon GM. Exercise echocardiography after coronary artery bypass surgery: correlation with coronary angiography. *J Am Coll Cardiol.* (1995) 25:1019–23. doi: 10.1016/0735-1097(94)00532-U
103. Senior R, Lepper W, Pasquet A, Chung G, Hoffman R, Vanoverschelde J-L, et al. Myocardial perfusion assessment in patients with medium probability of coronary artery disease and no prior myocardial infarction: comparison of myocardial contrast echocardiography with 99mTc single-photon emission computed tomography. *Am Heart J.* (2004) 147:1100–5. doi: 10.1016/j.ahj.2003.12.030

104. Nagel E, Greenwood JP, McCann GP, Bettencourt N, Shah AM, Hussain ST, et al. Magnetic resonance perfusion or fractional flow reserve in coronary disease. *N Engl J Med.* (2019) 380:2418–28. doi: 10.1056/NEJMoa1716734
105. Kwong RY, Ge Y, Steel K, Bingham S, Abdullah S, Fujikura K, et al. Cardiac magnetic resonance stress perfusion imaging for evaluation of patients with chest pain. *J Am Coll Cardiol.* (2019) 74:1741–55. doi: 10.1016/j.jacc.2019.07.074
106. Bhuva AN, Moralee R, Brunker T, Lascelles K, Cash L, Patel KP, et al. Evidence to support magnetic resonance conditional labelling of all pacemaker and defibrillator leads in patients with cardiac implantable electronic devices. *Eur Heart J.* (2021) 2021:ehab350. doi: 10.1093/eurheartj/ehab350
107. Pfisterer M, Emmenegger H, Schmitt HE, Müller-Brand J, Hasse J, Grädel E, et al. Accuracy of serial myocardial perfusion scintigraphy with thallium-201 for prediction of graft patency early and late after coronary artery bypass surgery. A controlled prospective study. *Circulation.* (1982) 66:1017–24. doi: 10.1161/01.CIR.66.5.1017
108. Khoury AF, Rivera JM, Mahmarian JJ, Verani MS. Adenosine thallium-201 tomography in evaluation of graft patency late after coronary artery bypass graft surgery. *J Am Coll Cardiol.* (1997) 29:1290–5. doi: 10.1016/S0735-1097(97)00045-4
109. Lakkis NM, Mahmarian JJ, Verani MS. Exercise thallium-201 single photon emission computed tomography for evaluation of coronary artery bypass graft patency. *Am J Cardiol.* (1995) 76:107–11. doi: 10.1016/S0002-9149(99)80039-3
110. Acampa W, Petretta M, Evangelista L, Nappi G, Luongo L, Petretta MP, et al. Stress cardiac single-photon emission computed tomographic imaging late after coronary artery bypass surgery for risk stratification and estimation of time to cardiac events. *J Thorac Cardiovasc Surg.* (2008) 136:46–51. doi: 10.1016/j.jtcvs.2007.10.011
111. Sarda L, Fuchs L, Lebtahi R, Faraggi M, Delahaye N, Hvass U, et al. Prognostic value of 201Tl myocardial scintigraphy after coronary artery bypass grafting. *Nucl Med Commun.* (2001) 22:189–96. doi: 10.1097/00006231-200102000-00011
112. Shapira I, Heller I, Kornizky Y, Topilsky M, Isakov A. The value of stress thallium-201 single photon emission CT imaging as a predictor of outcome and long-term prognosis after CABG. *J Med.* (2001) 32:271–82.
113. Weustink AC, Nieman K, Pugliese F, Mollet NR, Meijboom WB, Meijboom BW, et al. Diagnostic accuracy of computed tomography angiography in patients after bypass grafting: comparison with invasive coronary angiography. *JACC Cardiovasc Imaging.* (2009) 2:816–24. doi: 10.1016/j.jcmg.2009.02.010
114. Eisenberg C, Hulten E, Bittencourt MS, Blankstein R. Use of CT angiography among patients with prior coronary artery bypass grafting surgery. *Cardiovasc Diagn Ther.* (2017) 7:102–5. doi: 10.21037/cdt.2016.11.08
115. Nørgaard BL, Fairbairn TA, Safian RD, Rabbat MG, Ko B, Jensen JM, et al. Coronary CT angiography-derived fractional flow reserve testing in patients with stable coronary artery disease: recommendations on interpretation and reporting. *Radiol Cardiothorac Imaging.* (2019) 1:e190050. doi: 10.1148/ryct.2019190050
116. Crouse LJ, Vacek JL, Beauchamp GD, Porter CB, Rosamond TL, Kramer PH. Exercise echocardiography after coronary artery bypass grafting. *Am J Cardiol.* (1992) 70:572–6. doi: 10.1016/0002-9149(92)90193-3
117. Toulemonde MEG, Corbett R, Papadopoulou V, Chahal N, Li Y, Leow CH, et al. High frame-rate contrast echocardiography: in-human demonstration. *JACC Cardiovasc Imaging.* (2018) 11:923–4. doi: 10.1016/j.jcmg.2017.09.011
118. Otaki Y, Betancur J, Sharir T, Hu L-H, Gransar H, Liang JX, et al. 5-year prognostic value of quantitative versus visual MPI in subtle perfusion defects: results from REFINE SPECT. *JACC Cardiovasc Imaging.* (2020) 13:774–85. doi: 10.1016/j.jcmg.2019.02.028
119. Weiner DA, Ryan TJ, Parsons L, Fisher LD, Chaitman BR, Sheffield LT, et al. Prevalence and prognostic significance of silent and symptomatic ischemia after coronary bypass surgery: a report from the Coronary Artery Surgery Study (CASS) randomized population. *J Am Coll Cardiol.* (1991) 18:343–8. doi: 10.1016/0735-1097(91)90584-V
120. Krone RJ, Hardison RM, Chaitman BR, Gibbons RJ, Sopko G, Bach R, et al. Risk stratification after successful coronary revascularization: the lack of a role for routine exercise testing. *J Am Coll Cardiol.* (2001) 38:136–42. doi: 10.1016/S0735-1097(01)01312-2
121. Cortigiani L, Ciampi Q, Rigo F, Bovenzi F, Picano E, Sicari R. Prognostic value of dual imaging stress echocardiography following coronary bypass surgery. *Int J Cardiol.* (2019) 277:266–71. doi: 10.1016/j.ijcard.2018.09.105
122. Harb SC, Cook T, Jaber WA, Marwick TH. Exercise testing in asymptomatic patients after revascularization: are outcomes altered? *Arch Intern Med.* (2012) 172:854–61. doi: 10.1001/archinternmed.2012.1355
123. Cortigiani L, Bigi R, Sicari R, Landi P, Bovenzi F, Picano E. Stress echocardiography for the risk stratification of patients following coronary bypass surgery. *Int J Cardiol.* (2010) 143:337–42. doi: 10.1016/j.ijcard.2009.03.063
124. Arruda AM, McCully RB, Oh JK, Mahoney DW, Seward JB, Pellikka PA. Prognostic value of exercise echocardiography in patients after coronary artery bypass surgery. *Am J Cardiol.* (2001) 87:1069–73. doi: 10.1016/S0002-9149(01)01463-1
125. Palmas W, Bingham S, Diamond GA, Denton TA, Kiat H, Friedman JD, et al. Incremental prognostic value of exercise thallium-201 myocardial single-photon emission computed tomography late after coronary artery bypass surgery. *J Am Coll Cardiol.* (1995) 25:403–9. doi: 10.1016/0735-1097(94)00380-9
126. Miller TD, Christian TF, Hodge DO, Mullan BP, Gibbons RJ. Prognostic value of exercise thallium-201 imaging performed within 2 years of coronary artery bypass graft surgery. *J Am Coll Cardiol.* (1998) 31:848–54. doi: 10.1016/S0735-1097(98)00011-4
127. Lauer MS, Lytle B, Pashkow F, Snader CE, Marwick TH. Prediction of death and myocardial infarction by screening with exercise-thallium testing after coronary-artery-bypass grafting. *Lancet Lond Engl.* (1998) 351:615–22. doi: 10.1016/S0140-6736(97)07062-1
128. Zellweger MJ, Lewin HC, Lai S, Dubois EA, Friedman JD, Germano G, et al. When to stress patients after coronary artery bypass surgery? Risk stratification in patients early and late post-CABG using stress myocardial perfusion SPECT: implications of appropriate clinical strategies. *J Am Coll Cardiol.* (2001) 37:144–52. doi: 10.1016/S0735-1097(00)01104-9
129. Pen A, Yam Y, Chen L, Dorbala S, Di Carli MF, Merhige ME, et al. Prognostic value of Rb-82 positron emission tomography myocardial perfusion imaging in coronary artery bypass patients. *Eur Heart J Cardiovasc Imaging.* (2014) 15:787–92. doi: 10.1093/ehjci/jet259
130. Kinnel M, Sanguineti F, Pezel T, Unterseeh T, Hovasse T, Toupin S, et al. Prognostic value of vasodilator stress perfusion CMR in patients with previous coronary artery bypass graft. *Eur Heart J Cardiovasc Imaging.* (2020) 2020:jeaa316. doi: 10.1016/j.acvdsp.2020.10.056
131. Harb SC, Marwick TH. Prognostic value of stress imaging after revascularization: a systematic review of stress echocardiography and stress nuclear imaging. *Am Heart J.* (2014) 167:77–85. doi: 10.1016/j.ahj.2013.07.035
132. Knott KD, Seraphim A, Augusto JB, Xue H, Chacko L, Aung N, et al. The prognostic significance of quantitative myocardial perfusion: an artificial intelligence based approach using perfusion mapping. *Circulation.* (2020) 119:44666. doi: 10.1161/CIRCULATIONAHA.119.044666
133. Juárez-Orozco LE, Tio RA, Alexanderson E, Dweck M, Vliegenthart R, El Moumni M, et al. Quantitative myocardial perfusion evaluation with positron emission tomography and the risk of cardiovascular events in patients with coronary artery disease: a systematic review of prognostic studies. *Eur Heart J Cardiovasc Imaging.* (2018) 19:1179–87. doi: 10.1093/ehjci/jex331
134. Patel KK, Spertus JA, Chan PS, Sperry BW, Al Badarin F, Kennedy KF, et al. Myocardial blood flow reserve assessed by positron emission tomography myocardial perfusion imaging identifies patients with a survival benefit from early revascularization. *Eur Heart J.* (2020) 41:759–68. doi: 10.1093/eurheartj/ehz389
135. Gaba P, Gersh BJ, Ali ZA, Moses JW, Stone GW. Complete versus incomplete coronary revascularization: definitions, assessment and outcomes. *Nat Rev Cardiol.* (2021) 18:155–68. doi: 10.1038/s41569-020-00457-5
136. Vander Salm TJ, Kip KE, Jones RH, Schaff HV, Shemin RJ, Aldea GS, et al. What constitutes optimal surgical revascularization? Answers from the bypass angioplasty revascularization investigation (BARI). *J Am Coll Cardiol.* (2002) 39:565–72. doi: 10.1016/S0735-1097(01)01806-X

137. Thuesen AL, Riber LP, Veien KT, Christiansen EH, Jensen SE, Modrau I, et al. Fractional flow reserve versus angiographically-guided coronary artery bypass grafting. *J Am Coll Cardiol.* (2018) 72:2732–43. doi: 10.1016/j.jacc.2018.09.043
138. Fournier S, Toth GG, De Bruyne B, Johnson NP, Ciccarelli G, Xaplanteris P, et al. Six-year follow-up of fractional flow reserve-guided versus angiography-guided coronary artery bypass graft surgery. *Circ Cardiovasc Interv.* (2018) 11:e006368. doi: 10.1161/CIRCINTERVENTIONS.117.006368
139. ROSETTA-CABG Registry, Eisenberg MJ, Wou K, Nguyen H, Duerr R, Del Core M, et al. Lack of benefit for routine functional testing early after coronary artery bypass graft surgery: results from the ROSETTA-CABG Registry. *J Invasive Cardiol.* (2006) 18:147–52.
140. Al-Lamee R, Thompson D, Dehbi H-M, Sen S, Tang K, Davies J, et al. Percutaneous coronary intervention in stable angina (ORBITA): a double-blind, randomised controlled trial. *Lancet Lond Engl.* (2018) 391:31–40. doi: 10.1016/j.jvs.2017.11.046
141. Maron DJ, Hochman JS, Reynolds HR, Bangalore S, O'Brien SM, Boden WE, et al. Initial invasive or conservative strategy for stable coronary disease. *N Engl J Med.* (2020) 382:1395–407. doi: 10.1056/NEJMoa1915922
142. Kotecha T, Chacko L, Chehab O, O'Reilly N, Martinez-Naharro A, Lazari J, et al. Assessment of multivessel coronary artery disease using cardiovascular magnetic resonance pixelwise quantitative perfusion mapping. *JACC Cardiovasc Imaging.* (2020) 13:2546–57. doi: 10.1016/j.jcmg.2020.06.041

Conflict of Interest: The authors declare that the research was conducted in the absence of any commercial or financial relationships that could be construed as a potential conflict of interest.

Publisher's Note: All claims expressed in this article are solely those of the authors and do not necessarily represent those of their affiliated organizations, or those of the publisher, the editors and the reviewers. Any product that may be evaluated in this article, or claim that may be made by its manufacturer, is not guaranteed or endorsed by the publisher.

frontiers in Cardiovascular Medicine

MINI REVIEW
published: 24 February 2022
doi: 10.3389/fcvm.2022.836473

Non-invasive Multimodality Imaging of Coronary Vulnerable Patient

*Marjorie Canu[1], Alexis Broisat[2], Laurent Riou[2], Gerald Vanzetto[1,2,3], Daniel Fagret[2,4], Catherine Ghezzi[2], Loic Djaileb[2,4] and Gilles Barone-Rochette[1,2,3]**

[1] Department of Cardiology, University Hospital, Grenoble Alpes, Grenoble, France, [2] Univ. Grenoble Alpes, INSERM, CHU Grenoble Alpes, LRB, Grenoble, France, [3] French Alliance Clinical Trial, French Clinical Research Infrastructure Network, Paris, France, [4] Department of Nuclear Medicine, University Hospital, Grenoble Alpes, Grenoble, France

Atherosclerotic plaque rupture or erosion remain the primary mechanism responsible for myocardial infarction and the major challenge of cardiovascular researchers is to develop non-invasive methods of accurate risk prediction to identify vulnerable plaques before the event occurs. Multimodal imaging, by CT-TEP or CT-SPECT, provides both morphological and activity information about the plaque and cumulates the advantages of anatomic and molecular imaging to identify vulnerability features among coronary plaques. However, the rate of acute coronary syndromes remains low and the mechanisms leading to adverse events are clearly more complex than initially assumed. Indeed, recent studies suggest that the detection of a state of vulnerability in a patient is more important than the detection of individual sites of vulnerability as a target of focal treatment. Despite this evolution of concepts, multimodal imaging offers a strong potential to assess patient's vulnerability. Here we review the current state of multimodal imaging to identify vulnerable patients, and then focus on emerging imaging techniques and precision medicine.

Keywords: vulnerable plaque, vulnerable patient, coronary artery disease, multimodal imaging, chronic coronary syndrome, risk stratification

OPEN ACCESS

Edited by:
Bernhard L. Gerber, Cliniques Universitaires Saint-Luc, Belgium

Reviewed by:
Paul Schoenhagen, Case Western Reserve University, United States
Johan Reiber, Leiden University, Netherlands

***Correspondence:**
Gilles Barone-Rochette
gbarone@chu-grenoble.fr

Specialty section:
This article was submitted to Cardiovascular Imaging, a section of the journal Frontiers in Cardiovascular Medicine

Received: *15 December 2021*
Accepted: *01 February 2022*
Published: *24 February 2022*

Citation:
Canu M, Broisat A, Riou L, Vanzetto G, Fagret D, Ghezzi C, Djaileb L and Barone-Rochette G (2022) Non-invasive Multimodality Imaging of Coronary Vulnerable Patient. Front. Cardiovasc. Med. 9:836473. doi: 10.3389/fcvm.2022.836473

INTRODUCTION

Coronary artery diseases (CAD) remain the largest single cause of death in the World. Traditionally, atherosclerosis management consists in detecting obstructive CAD and ischemia. However, this paradigm is being challenged as revascularization of obstructive CAD failed to reduce acute coronary events in recent studies (1, 2) and most of these events occur on non-obstructive plaques (3). Novel imaging techniques have emerged in this setting, targeting vulnerable coronary plaques that are more likely to lead to a plaque thrombosis and an acute coronary syndrome (ACS). However, the prospective follow-up of vulnerable plaques is deceiving in predicting future coronary events (4) and the mechanism of plaque thrombosis seems to be more complex, where not only plaque progression, but also systemic parameters such as inflammation, thrombogenic and dynamic change processes are intricated, so that the concept of vulnerable patients was introduced. Moreover, while rupture of thin-cap fibro atheroma (TCFA) remains the main cause of acute coronary events (55–65%), plaque erosion (30–35%) an, to a lower extend microcalcifications (2–7%), are also known to be responsible for such events through distinct pathobiological mechanisms (5). Importantly, most plaque with thrombosis are clinically silent and lead to plaque progression and luminal stenosis (6). Vulnerable patients, in whom the thrombosis of a vulnerable plaque is likely to result in a clinical event in the future, are not only characterized

by vulnerable plaques, but also vulnerable blood and vulnerable myocardium (7). We review here current and in-development non-invasive techniques, based on multimodal imaging on this field.

ANATOMIC FEATURES

Identifying high-risk plaques before ACS occurs has been a major research goal. Retrospective studies analyzed progression of CAD among patients presenting with ACS, by comparing plaque features on previous coronary angiography exams. Most coronary acute events occurred on unobstructed lesion at baseline (8). The histological study of culprit plaques, responsible for ACS, helped identifying common underlying features in high-risk plaques. Some of these features can be identified with invasive imaging techniques (9) but cannot be translated to routine clinical practice because of costs, and due to the fact that invasive techniques such as optical coherence tomography (OCT) or intravascular ultrasound (IVUS) cannot be employed in large populations and are restricted to patient previously identified at high risk. Improvement of multimodal imaging techniques of the plaque allow non-invasive visualization of such features.

Vulnerable Coronary Plaque

Computed tomography coronary angiography (CTCA) that permits precise visualization of the plaque became a first-line diagnostic test in the assessment of suspected CAD. At the simplest level, the segment involvement score (SIS) sums the number of diseased coronary segments, whilst the stenosis severity score (SSS) also incorporates a weighting factor for stenotic severity (10). CTCA, with high spatial resolution scanners, can provide precise structural information of the coronary artery wall and can assess for the presence and constituents of atherosclerotic plaque even in the absence of flow limiting disease. Based on histological analysis, TCFA are mainly characterized by a large necrotic core, thin fibrous cap (<65 mm), inflammation (predominantly in the form of macrophage infiltration), angiogenesis, plaque hemorrhage, positive remodeling and microcalcification (11). Not all of these features can be evaluated using non-invasive imaging. However, a number of morphologic criteria that can be assessed using CTCA have been employed to identify such lesions. In a SCOT-Heart *post-hoc* analysis, the presence of vulnerable plaque features such as positive remodeling, low attenuation plaque, spotty calcification, and the "napkin ring" sign were validated against intravascular invasive imaging (12). The results of PROMISE (13) and SCOTHEART studies (12) confirmed the association between adverse plaque characteristics and outcomes. Obstructive coronary disease is also a major risk predictor, and the combination of adverse plaque features with obstructive disease appears to confer the greatest risk (13). Moreover, CT-Leaman score, which combines stenotic severity, myocardium at risk, and high-risk plaque features, allows an improved risk stratification of the plaque (14). Currently, while they appear to be less competitive than CTCA for the identification a vulnerable plaque, a number of other high-resolution imaging systems can also be employed. **Table 1** describes the imaging modalities, their strengths and limitations and a comparison between the modalities in assessing the different aspects that characterize a vulnerable patient. Cardiac magnetic resonance imaging (CMR) holds the great advantage to be not only a non-invasive, but also a non-ionizing imaging technique. Black blood sequences confer a fairly good spatial resolution of the coronary wall (15) allowing detection of adverse plaque features, such as positive remodeling, plaque hemorrhage and subclinical thrombus (16). However, such approaches have largely been limited to the visualization of the main proximal vessels, because of the reduced spatial resolution, as compared to CTCA. Furthermore, CMR is a time-costly and less available imaging technique. Trans-thoracic echocardiography does not allow the precise visualization and analysis of coronary arteries. However, ultrasound enables carotid plaques characterization, such as differentiation between artery occlusions and high-grade stenosis, plaque morphology (plaque surface, flow data) and plaque neovascularization, thereby enabling to estimate its vulnerability (17).

If CTCA remains the best non-invasive imaging technique to detect coronary plaques and assess their vulnerability, the prospective follow-up of these vulnerable plaques is deceiving in predicting future coronary events (4) which remain low in this population. Indeed, while being of high negative predicting value, the positive predictive value of identifying a high-risk plaque in large cohort studies such as SCOTHEART or PROMISE was found to be low, with only ∼5% of events at 5 years. There are several explanations for this low positive prognostic value. The first being that the presence of at least one lesion with vulnerable plaque characteristics is probably not as rare as might have been assumed. In addition, the occurrence of an acute event does not only require the presence of a vulnerable plaque but also that of other parameters such as prothrombotic factors. Therefore, a plaque can rupture without being symptomatic. Moreover, atherosclerotic lesions are characterized by dynamic evolution, and it is not excluded that vulnerable plaques pacifies over time (18).

Coronary Atherosclerosis Disease Burden

Imaging techniques measuring coronary atherosclerosis disease burden, or call also "the adverse plaque burden", therefore confer a better risk stratification for future cardiovascular events at the patient level. While it has been shown that the more vulnerable coronary plaques a patient has, the greater the likelihood of major adverse cardiovascular events (MACE), it is rarely the plaques identified as vulnerable that will be responsible for acute arterial thrombosis. This highlights the fact to switch from a focus on individual lesions to atherosclerotic disease burden for coronary artery disease risk assessment (19). Coronary artery calcium (CAC) is a non-invasive, rapid computed-tomography (CT) technique that quantifies atherosclerotic calcifications, a well-described process occurring as a healing response to pathological inflammation within the plaque. CAC scoring is a direct marker of CADB for each patient and is effective in predicting the risk of future atherosclerotic cardiovascular events in asymptomatic patients (20). A large observational study involving 25,253 patients in the United States with a mean follow-up of 6.8

TABLE 1 | Non-invasive multimodal imaging assessment of vulnerable plaques and patients in chronic coronary syndrome.

Imaging modalities	Strenghts	Limitations
Morphological imaging techniques		
CTCA	High spatial resolution. Fast and good availability. Plaques: high risk features Measure of coronary artery disease burden on the whole coronary tree.	Limited by calcifications, stents. Radiation, contrast.Limited temporal resolution
CACS	Fast and good availability, low cost. No contrast, low radiation. Coronary atherosclerotic burden	Limited spatial resolution. No detection of non-calcified plaques.
CMR	Radiation free. Not limited by calcifications?	Poor spatial resolution. Costly, less available, Duration. Contraindications: Claustrophobia, metallic devices.
TTE	No radiation, fast, low cost, availability	No precise visualization of CA
Molecular imaging techniques		
PET	Molecular imaging of Inflammation, microcalcification activity, Thrombogenicity by Targeted radionucleotides.	Poor temporal and spatial resolution, radiation costly, duration, limited availability, FDG myocardial uptake.
SPECT	SPECT tracers are relatively inexpensive in comparison of PET agents. More available than PET.	Poor spatial and temporal resolution Radiation, costly, duration Less tracer available than PET in the field of CA.
CMR	Nanoparticles: Gd-DTPA, USPIO	Clinical translation to aortic and carotid atherosclerosis. Moderate diagnostic accuracy in coronary arteries
CTCA	FAI disponible by all 64 slice CTCA	indirect inflammation assessment Cost
TTE	CEUS: targeted microbubbles in preclinical studies	Technical challenges for clinical translation
Local hemodynamic forces		
CTCA	Wall shear stress: CT CFD	In development
Myocardial function and tissue characterization		
CMR	Reference for cardiac function assessment. Tissue characterization: fibrosis	Cost, availability ECG gating necessary
TTE	Cardiac systolic and diastolic function. Fast, low cost, availability.	No tissue characterization
CT	Cardiac volumes and function Tissue characterization: fibrosis	Retrospective acquisition: radiation Contrast injection ECG gating necessary Performance for tissue characterization is still average
PET/SPECT	Left ventricular systolic function	Poor temporal and spatial resolution ECG gating necessary

CTCA, Computed tomography coronary angiography; FFR, fractional flow reserve; CFD, computational flow dynamics; CACS, Coronary artery calcium score; CMR, Cardiac magnetic resonance imaging; CA, coronary arteries; PET, positron emission tomography, FDG, fluorodeoxyglucose; SPECT, single photon emission computed tomography; Gd-DTPA, gadolinium-diethylenetriaminepentaacetic acid; USPIO, ultrasmall superparamagnetic iron oxide; FAI, fat attenuation index; CEUS, Contrast enhanced ultrasound.

years showed that survival varied significantly according to the extent of CAC. Indeed, survival rates varied from 99.4 to 87.8%, respectively, for CAC scores of 0 and >1,000 ($p < 0.0001$) (21). However, while CAC enables estimating plaque burden, macrocalcification are not restricted to vulnerable lesions but also occurs in more stable lesions, so that more specific parameters are needed. The quantification of CADB by measure of the number of vulnerable plaques on the entire coronary tree has great potential. However, quantify CADB across the coronary vasculature is challenging. This is now possible in a rapid and robust fashion with semiautomatic software by certain vulnerable plaque features. Recently, low attenuation plaque burden appears as a strong predictor of fatal or non-fatal myocardial infarction irrespective coronary artery calcium score (22). The development of these software improving the reproducibility also allow to observe the evolution of coronary atherosclerosis disease burden under treatment (23). CTCA is a key tool for identifying high risk patients, by anatomic features. However, coupling anatomic data with molecular imaging may improve risk stratification for patient's vulnerability assessment.

FACTOR OF DYNAMIC PLAQUE CHANGE

Coronary atherosclerosis presents a dynamic nature and plaques with at least one vulnerable feature are in fact relatively common and appear dynamic process of formation and healing. Identifying the factors associated with an adverse dynamic plaque change is therefore a major priority. Molecular imaging has the enormous advantage of allowing the visualization, characterization and quantification of biological processes. Even though the molecular imaging potential of MRI and ultrasound is being investigated (24–26), nuclear imaging represents the most mature modality in this perspective. Several traceable physio pathological processes associated to adverse dynamic plaque change toward vulnerable patient could be use.

Inflammation

Atherosclerosis is an immuno-inflammatory illness powered by lipids. The major role of inflammation in the development of coronary artery plaques and in the pathophysiology of plaque rupture was comforted by the results of emerging studies in which colchicine, an anti-inflammatory treatment, was associated with a reduction in ischemic events after a MI (27) and in patients with chronic coronary disease (28). Nuclear molecular imaging, by tracking inflammation with specific molecular targets, allows the direct visualization of inflammation within the plaque. Imaging modalities include CT- positron emission tomography (PET), CMR-PET and CT-single photon emission computed tomography (SPECT). Known tracers include ^{18}F-fluorodeoxyglucose (^{18}F-FDG), ^{68}Gallium(^{68}Ga-DOTATATE), and ^{68}Ga-Pentixafor. In CAD, ^{18}F-FDG reflects plaque inflammation by detecting glucose uptake in regions of high metabolic activity (29). Hybrid ^{18}F-FDG PET- CT allow precise anatomic identification of coronary plaques coupled with molecular inflammatory inflammation. This hybrid imaging technique showed increased inflammatory activity of perivascular adipose tissue adjacent to coronary arteries segments

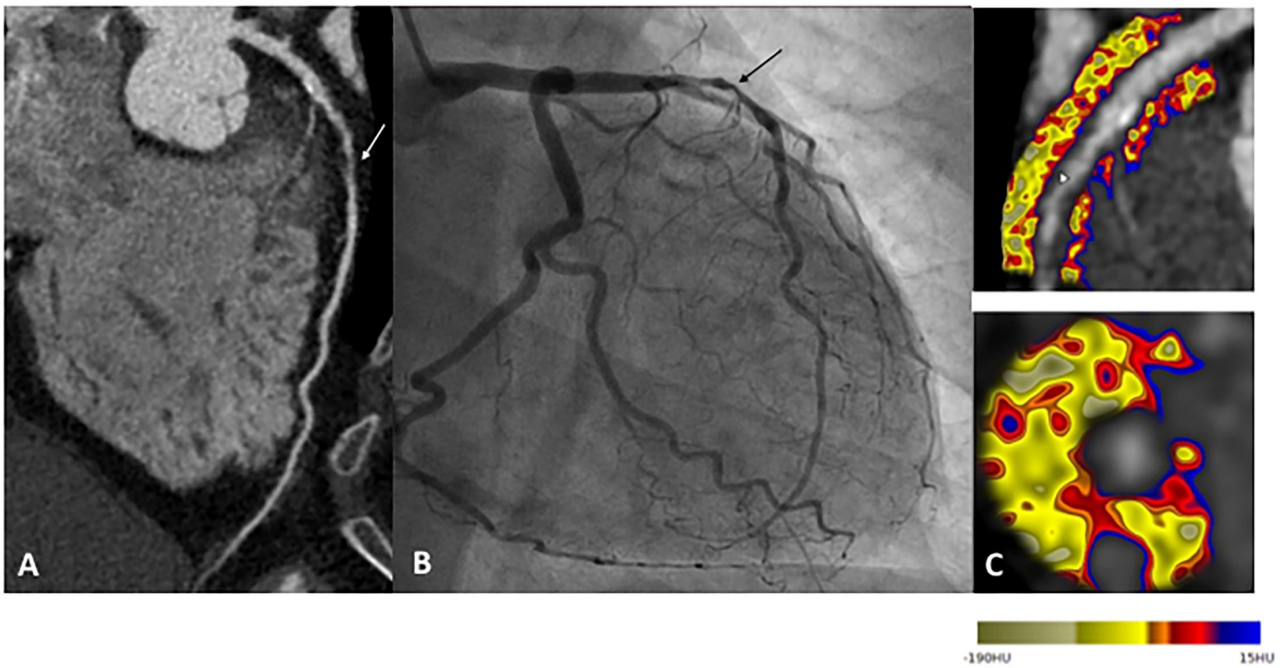

FIGURE 1 | Example of a patient reporting exertional dyspnea. In **(A)**, CTCA showed significant CAD on left anterior descending (LAD) artery (white arrow), classified CAD-RADS 4A. Coronary angiogram confirm severe stenosis of proximal LAD (black arrow), angioplasty followed by stenting was performed to relieve symptoms **(B)**. Finally, CTCA post-treatment based on the FAI-Score values **(C)** on three arteries, the coronary atherosclerotic plaque burden and the clinical risk factors showed low CaRi-Heart Risk, thereby predicting low risk of future acute coronary events and permitted treatment goals and follow-up strategies personalization.

with plaques (30) and correlation between ^{18}F-FDG PET imaging and histological macrophage uptake of carotid plaques after carotid endarterectomy (31). In ACS patients, metabolic activity detected by this radiotracer is identified not only in the culprit lesion, but also in other atherosclerotic site, such as ascending aorta or left main coronary artery, showing atherosclerotic vulnerability at the patient level (32). However, coronary ^{18}F-FDG lacks cell specificity and signal can be obscured by background myocardial uptake. In atherosclerotic plaque tissue, CXCR4 expression might be used as a surrogate marker for inflammatory atherosclerosis. *In vivo* use of ^{68}Ga-Pentixafor appear feasible to evaluation of CXCR4 expression in human carotid atherosclerotic lesions (33). ^{68}Ga-DOTATATE binds to the somatostatin receptor subtype-2 (SST2) found on the surface of pro-inflammatory M1 macrophages and targets inflammation. It was validated using PET-CT imaging in patients with carotid plaques, in carotid plaques showing high-risk CT features, and in culprit coronary plaques in the setting of ACS with superior coronary imaging and excellent macrophage specificity (34).

Off line post processing of CTA datasets proved to be very useful for the analysis of the complex interactions between coronary arteries and perivascular adipose tissue are complex. Adverse perivascular adipocyte profile, associated with some metabolic conditions, is known to trigger pro-inflammatory changes within coronary arteries (35). Recent fundamental studies suggest a bidirectional relationship between perivascular fat and coronary arteries. Coronary inflammation inhibits lipid accumulation in adjacent adipocytes, resulting in a gradient in the lipid content of perivascular fat. The CTCA analysis of epicardial and pericoronary fat provides information to improve plaque and patient ischemic risk stratification, with CTCA-measured epicardial fat volume being associated with CAD and cardiovascular events (36). However, the prognostic implications of epicardial fat attenuation remain controversial (37, 38). These discordant results could reflect the heterogeneity of epicardial fat composition and support the hypothesis that inflammatory changes in perivascular fat might be a local process limited to the adjacent regions of vulnerable plaques. CTCA-derived fat attenuation index (FAI), using the Cari-Heart algorithm, indirectly quantifies arteries inflammation burden, by analyzing the signal from perivascular fat (**Figure 1**). Higher FAI values correspond to adipose tissue morphologic changes associated with coronary inflammation (39). Recent *post-hoc* analyses of prospective CTCA and outcome data showed the incremental prognostic value of FAI to detect high-risk plaques (HRP), beyond traditional risk factors (40) and beyond HRP plaque features (41).

Microcalcification Activity

Preclinical and clinical evidence show that calcification is one of the body's primary responses to injury. ^{18}F-NaF is a marker of microcalcification activity, which binds with high affinity to the exposed surface of hydroxyapatite, a key mineral component of vascular calcification and detects plaque microcalcification,

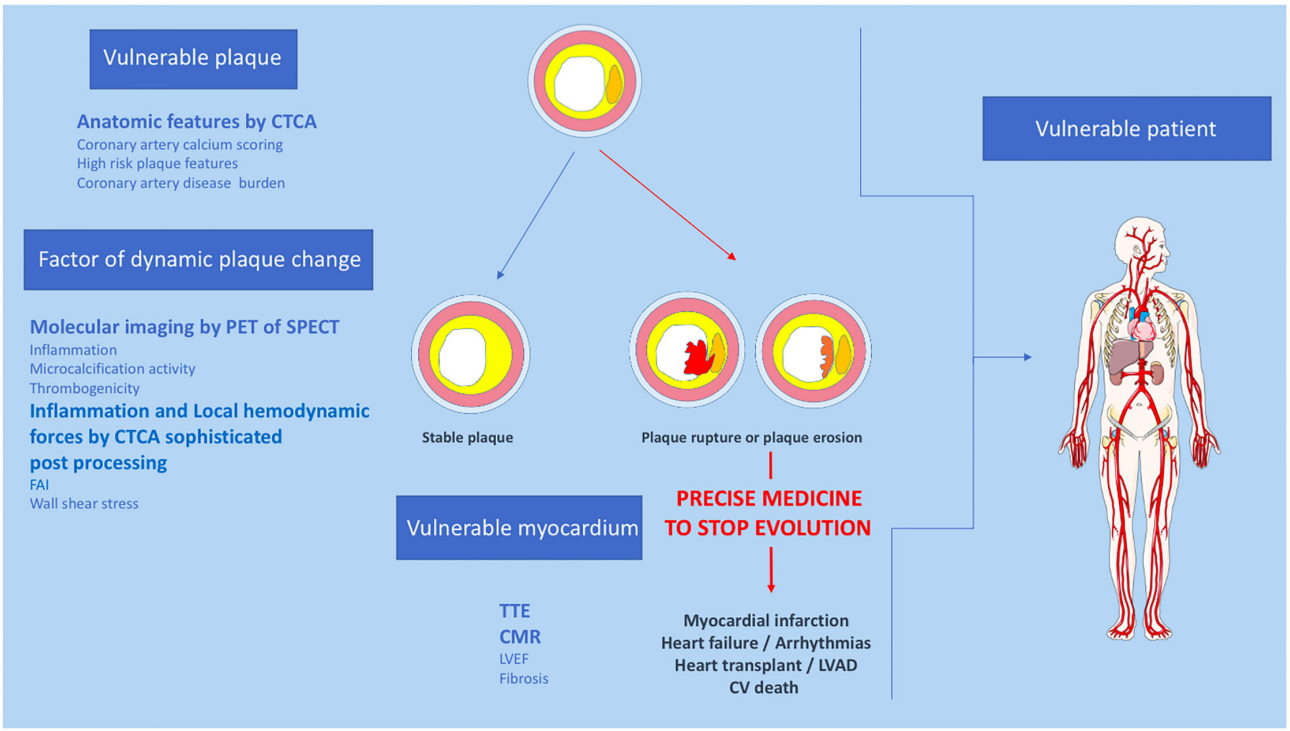

FIGURE 2 | Proposition of non-invasive multimodality imaging strategy to detect and treat coronary vulnerable patient. CTCA, Computed tomography coronary angiography; CV, cardiovascular; CMR, cardiac magnetic resonance imaging, FAI, fat attenuation index; LVEF, left ventricular ejection fraction; PET, positron emission tomography; SPECT, single photon emission computed tomography; TTE, trans thoracic echocardiography.

another feature of vulnerable plaques. Increased ^{18}F-NaF uptake is observed in coronary plaques that show multiple adverse features on CT, on virtual histology (VH)- IVUS, and on OCT (42) and could improve the risk stratification of patients with CAD.

Thrombogenicity

Several studies used radionuclide imaging approaches to analyze several thrombosis-related molecular markers (43). Factor XIIIa radiotracer and (44) ^{18}F-GP1 are safe and promising novels PET tracer for imaging acute arterial thrombosis with a favorable biodistribution and pharmacokinetic profile (45). However, none is yet available in clinical practice.

Local Hemodynamic Forces

Although the anatomic and chemical features of potentially vulnerable plaques play a significant role, additional information regarding dynamic plaque change may provide significant information. Among hemodynamic-associated biomechanical forces that increase plaque vulnerability, special attention has been paid to wall shear stress (WSS) (46). WSS may be assessed using CTCA through sophisticated post processing based on computational fluid dynamics and shows that high wall shear stress had an incremental value over luminal narrowing in discriminating high-risk plaques (47).

FUTURE DIRECTIONS

Identification of the vulnerable patient remains a challenge for cardiology today which partly depends upon progresses performed by imaging modalities. High temporal and spatial resolution of anatomical modalities is a prerequisite considering the small size and motion of coronary arteries. Cardiac hybrid imaging allows to obtain complementary morphological and molecular features information in a single setting. CT-SPECT and CT-PET are widely used, and CMR-PET may represent an alternative. However, CT-SPECT or CT-PET imaging are also controversial because of radiation dose issues. Due to technological progress, the most recent high-pitch scanning protocols using dual-source CT scanners have lowered doses into the sub-milli-Sievert range. Safety and dosimetry now represent important elements to be taken into account in the development of any radionuclide. This notion of low irradiation is essential for the repetition of the examinations during the follow-up. With regards to technological progress, SPECT detector with cadmium-zinc-telluride (CZT) improve count sensitivity, system resolution, and energy resolution, enabling significant reductions in administered activities or acquisition time, as well as facilitating dynamic SPECT. A multitude of single-photon emitters is available with half-lives longer than those of commonly used PET radionuclides, facilitating their distribution to more remote centers. In addition, SPECT tracers are relatively inexpensive in comparison of

PET agents. However, the constant evolution of PET-CT and SPECT-CT technology makes it challenging to use equipment combining the latest technological developments in SPECT, PET (48) or CT. For example, there is no hybrid machine with the latest evolution of spectral photon-counting CT (49). In this setting, the development of image fusion software may represent an alternative by obviating the need for a hybrid machine combining the latest innovations (50). This process will be supported by a shift from specializing in a particular technique that is applied to multiple organ imaging, to a cardiovascular-based approach in which the diagnostic expert is more concerned with the integration of results into clinical decision-making, and the impact of diagnostic imaging on clinical outcomes.

Images often contain more information than what is comprehensible by visual inspection. The current development of radiomics, whereby voxel-level information is extracted from digital images and used to derive multiple numerical quantifiers of shape and tissue character, may address this potential. For example, coronary CTA radiomics may provide a more accurate tool to identify vulnerable plaques compared with conventional methods (51). It is important that one keeps in mind that modalities scans are more than plain images; they are data. The analysis of such data using artificial intelligence is currently revolutionizing medical imaging (52). Big data include enormous numbers of predictors and outcomes with complex non-linear links, and conventional statistics usually fail to analysis them. Accordingly, machine-learning algorithms frequently use recently developed statistical program. Machine learning combining clinical and CCTA data was found to predict 5-year all cause of mortality significantly better than existing clinical or CCTA metrics alone (53). Machine learning can combine a large amount of data from imaging, but also from biomarkers, genomics and proteomics to derive the most accurate risk stratification models (54). The real revolution for imaging is deep learning. Deep-learning use multiple layers of convolutional neural networks (CNNs) which learn how to extract the most relevant data of the image and how best to combine them to acute event. Unlike radiomic, CNN can automatically discover such relationships at the pixel level without being defined before-hand based on human knowledge (55). Deep-learning is a promising method to develop future software incorporating further automation techniques of CADB, would therefore help facilitate more wide spread clinical adoption.

Above all, the identification of vulnerable patients should lead to precision medicine (**Figure 2**). One should not try to predict MACE but rather to develop strategies that identify patients at risk of developing MACE who require individualized drug management. Non-invasive imaging modalities aim to address this need, but such methods need to be widely available, safe, accurate, and ultimately cost-effective in order to ensure a meaningful impact on healthcare and patient outcomes. Despite its attractivity for the identification of vulnerable patients, multimodal imaging has a cost. A screening strategy must therefore be developed in parallel with imaging. It might be based upon the careful examination of clinical characteristics such as traditional risk factors and cholesterol levels and then use diagnostic test simple and available (i.e., CAC). Patients at high risk could be referred for screening by multimodality imaging techniques.

CONCLUSION

Imaging of vulnerable coronary plaque features has advanced greatly over the past decade and has improved our understanding of the highly complex and dynamic nature of coronary atherosclerosis. Despite the many advances in cardiovascular imaging, the prediction of atherosclerotic plaque rupture responsible for myocardial infarction remains difficult and is not applicable in clinical practice. However, multimodal imaging, in particular CT and nuclear molecular imaging, allow the identification of major characteristics of the vulnerable patient. Finally, randomized studies using these technological innovations will allow us to move toward precision medicine.

AUTHOR CONTRIBUTIONS

MC, LD, and GB-R contributed to conception and design of the mini review. MC wrote the first draft of the manuscript. AB, LR, and GB-R wrote sections of the manuscript. All authors contributed to manuscript revision, read, and approved the submitted version.

REFERENCES

1. Boden WE, O'Rourke RA, Teo KK, Hartigan PM, Maron DJ, Kostuk WJ, et al. Optimal medical therapy with or without PCI for stable coronary disease. *N Engl J Med.* (2007) 356:1503–16. doi: 10.1056/NEJMoa070829
2. Rutter MK, Nesto RW. The BARI 2D study: a randomised trial of therapies for type 2 diabetes and coronary artery disease. *Diab Vasc Dis Res.* (2010) 7:69–72. doi: 10.1177/1479164109354145
3. Libby P, Theroux P. Pathophysiology of coronary artery disease. *Circulation.* (2005) 111:3481–8. doi: 10.1161/CIRCULATIONAHA.105.537878
4. Stone GW, Maehara A, Lansky AJ, de Bruyne B, Cristea E, Mintz GS, et al. A prospective natural-history study of coronary atherosclerosis. *N Engl J Med.* (2011) 364:226–35. doi: 10.1056/NEJMoa1002358
5. Virmani R, Kolodgie FD, Burke AP, Farb A, Schwartz SM. Lessons from sudden coronary death: a comprehensive morphological classification scheme for atherosclerotic lesions. *Arterioscler Thromb Vasc Biol.* (2000) 20:1262–7. doi: 10.1161/01.ATV.20.5.1262
6. Arbustini E, Grasso M, Diegoli M, Pucci A, Bramerio M, Ardissino D, et al. Coronary atherosclerotic plaques with and without thrombus in ischemic heart syndromes: a morphologic, immunohistochemical, and biochemical study. *Am J Cardiol.* (1991) 68:36B−50B. doi: 10.1016/0002-9149(91)90383-V
7. Naghavi M, Libby P, Falk E, Casscells SW, Litovsky S, Rumberger J, et al. From vulnerable plaque to vulnerable patient: a call for new definitions and risk assessment strategies: Part I. *Circulation.* (2003) 108:1664–72. doi: 10.1161/01.CIR.0000087480.94275.97

8. Pasterkamp G, den Ruijter HM, Libby P. Temporal shifts in clinical presentation and underlying mechanisms of atherosclerotic disease. *Nat Rev Cardiol.* (2017) 14:21–9. doi: 10.1038/nrcardio.2016.166
9. Tearney GJ, Jang IK, Bouma BE. Optical coherence tomography for imaging the vulnerable plaque. *J Biomed Opt.* (2006) 11:021002. doi: 10.1117/1.2192697
10. Min JK, Shaw LJ, Devereux RB, Okin PM, Weinsaft JW, Russo DJ, et al. Prognostic value of multidetector coronary computed tomographic angiography for prediction of all-cause mortality. *J Am Coll Cardiol.* (2007) 50:1161–70. doi: 10.1016/j.jacc.2007.03.067
11. Virmani R, Burke AP, Farb A, Kolodgie FD. Pathology of the vulnerable plaque. *J Am Coll Cardiol.* (2006) 47(Suppl. 8):C13–8. doi: 10.1016/j.jacc.2005.10.065
12. Williams MC, Moss AJ, Dweck M, Adamson PD, Alam S, Hunter A, et al. Coronary artery plaque characteristics associated with adverse outcomes in the SCOT-HEART Study. *J Am Coll Cardiol.* (2019) 73:291–301. doi: 10.1016/j.jacc.2018.10.066
13. Ferencik M, Mayrhofer T, Bittner DO, Emami H, Puchner SB, Lu MT, et al. Use of high-risk coronary atherosclerotic plaque detection for risk stratification of patients with stable chest pain: a secondary analysis of the PROMISE randomized clinical trial. *JAMA Cardiol.* (2018) 3:144–52. doi: 10.1001/jamacardio.2017.4973
14. Mushtaq S, De Araujo Gonçalves P, Garcia-Garcia HM, Pontone G, Bartorelli AL, Bertella E, et al. Long-term prognostic effect of coronary atherosclerotic burden: validation of the computed tomography-Leaman score. *Circ Cardiovasc Imaging.* (2015) 8:e002332. doi: 10.1161/CIRCIMAGING.114.002332
15. Fayad ZA, Fuster V, Fallon JT, Jayasundera T, Worthley SG, Helft G, et al. Noninvasive *in vivo* human coronary artery lumen and wall imaging using black-blood magnetic resonance imaging. *Circulation.* (2000) 102:506–10. doi: 10.1161/01.CIR.102.5.506
16. Miao C, Chen S, Macedo R, Lai S, Liu K, Li D, et al. Positive remodeling of the coronary arteries detected by magnetic resonance imaging in an asymptomatic population: MESA (Multi-Ethnic Study of Atherosclerosis). *J Am Coll Cardiol.* (2009) 53:1708–15. doi: 10.1016/j.jacc.2008.12.063
17. Rix A, Curaj A, Liehn E, Kiessling F. Ultrasound microbubbles for diagnosis and treatment of cardiovascular diseases. *Semin Thromb Hemost.* (2020) 46:545–52. doi: 10.1055/s-0039-1688492
18. Kubo T, Maehara A, Mintz GS, Doi H, Tsujita K, Choi SY, et al. The dynamic nature of coronary artery lesion morphology assessed by serial virtual histology intravascular ultrasound tissue characterization. *J Am Coll Cardiol.* (2010) 55:1590–7. doi: 10.1016/j.jacc.2009.07.078
19. Arbab-Zadeh A, Fuster V. The myth of the "vulnerable plaque": transitioning from a focus on individual lesions to atherosclerotic disease burden for coronary artery disease risk assessment. *J Am Coll Cardiol.* (2015) 65:846–55. doi: 10.1016/j.jacc.2014.11.041
20. Hecht H, Blaha MJ, Berman DS, Nasir K, Budoff M, Leipsic J, et al. Clinical indications for coronary artery calcium scoring in asymptomatic patients: expert consensus statement from the Society of Cardiovascular Computed Tomography. *J Cardiovasc Comput Tomogr.* (2017) 11:157–68. doi: 10.1016/j.jcct.2017.02.010
21. Budoff MJ, Shaw LJ, Liu ST, Weinstein SR, Mosler TP, Tseng PH, et al. Long-term prognosis associated with coronary calcification: observations from a registry of 25,253 patients. *J Am Coll Cardiol.* (2007) 49:1860–70. doi: 10.1016/j.jacc.2006.10.079
22. Williams MC, Kwiecinski J, Doris M, McElhinney P, D'Souza MS, Cadet S, et al. Low-attenuation noncalcified plaque on coronary computed tomography angiography predicts myocardial infarction: results from the multicenter SCOT-HEART Trial (Scottish Computed Tomography of the HEART). *Circulation.* (2020) 141:1452–62. doi: 10.1161/CIRCULATIONAHA.120.049840
23. Lee SE, Chang HJ, Sung JM, Park HB, Heo R, Rizvi A, et al. Effects of statins on coronary atherosclerotic plaques: the PARADIGM Study. *JACC Cardiovasc Imaging.* (2018) 11:1475–84. doi: 10.1016/j.jcmg.2018.04.015
24. Lipinski MJ, Frias JC, Amirbekian V, Briley-Saebo KC, Mani V, Samber D, et al. Macrophage-specific lipid-based nanoparticles improve cardiac magnetic resonance detection and characterization of human atherosclerosis. *JACC Cardiovasc Imaging.* (2009) 2:637–47. doi: 10.1016/j.jcmg.2008.08.009
25. Tang TY, Howarth SP, Miller SR, Graves MJ, Patterson AJ, U-King-Im JM, et al. The ATHEROMA (Atorvastatin Therapy: Effects on Reduction of Macrophage Activity) Study Evaluation using ultrasmall superparamagnetic iron oxide-enhanced magnetic resonance imaging in carotid disease. *J Am Coll Cardiol.* (2009) 53:2039–50. doi: 10.1016/j.jacc.2009.03.018
26. Lindner JR. Molecular imaging of cardiovascular disease with contrast-enhanced ultrasonography. *Nat Rev Cardiol.* (2009) 6:475–81. doi: 10.1038/nrcardio.2009.77
27. Tardif JC, Kouz S, Waters DD, Bertrand OF, Diaz R, Maggioni AP, et al. Efficacy and safety of low-dose colchicine after myocardial infarction. *N Engl J Med.* (2019) 381:2497–505. doi: 10.1056/NEJMoa1912388
28. Nidorf SM, Fiolet ATL, Mosterd A, Eikelboom JW, Schut A, Opstal TSJ, et al. Colchicine in patients with chronic coronary disease. *N Engl J Med.* (2020) 383:1838–47. doi: 10.1056/NEJMoa2021372
29. Hara M, Goodman PC, Leder RA, FDG-PET. finding in early-phase Takayasu arteritis. *J Comput Assist Tomogr.* (1999) 23:16–8. doi: 10.1097/00004728-199901000-00004
30. Mazurek T, Kobylecka M, Zielenkiewicz M, Kurek A, Kochman J, Filipiak KJ, et al. PET/CT evaluation of (18)F-FDG uptake in pericoronary adipose tissue in patients with stable coronary artery disease: independent predictor of atherosclerotic lesions' formation? *J Nucl Cardiol.* (2017) 24:1075–84. doi: 10.1007/s12350-015-0370-6
31. Tawakol A, Migrino RQ, Bashian GG, Bedri S, Vermylen D, Cury RC, et al. *In vivo* 18F-fluorodeoxyglucose positron emission tomography imaging provides a noninvasive measure of carotid plaque inflammation in patients. *J Am Coll Cardiol.* (2006) 48:1818–24. doi: 10.1016/j.jacc.2006.05.076
32. Rogers IS, Nasir K, Figueroa AL, Cury RC, Hoffmann U, Vermylen DA, et al. Feasibility of FDG imaging of the coronary arteries: comparison between acute coronary syndrome and stable angina. *JACC Cardiovasc Imaging.* (2010) 3:388–97. doi: 10.1016/j.jcmg.2010.01.004
33. Li X, Yu W, Wollenweber T, Lu X, Wei Y, Beitzke D, et al. [^{68}Ga]Pentixafor PET/MR imaging of chemokine receptor 4 expression in the human carotid artery. *Eur J Nucl Med Mol Imaging.* (2019) 46:1616–25. doi: 10.1007/s00259-019-04322-7
34. Tarkin JM, Joshi FR, Evans NR, Chowdhury MM, Figg NL, Shah AV, et al. Detection of atherosclerotic inflammation by 68Ga-DOTATATE PET compared to [18F]FDG PET imaging. *J Am Coll Cardiol.* (2017) 69:1774–91. doi: 10.1016/j.jacc.2017.01.060
35. Skurk T, Alberti-Huber C, Herder C, Hauner H. Relationship between adipocyte size and adipokine expression and secretion. *J Clin Endocrinol Metab.* (2007) 92:1023–33. doi: 10.1210/jc.2006-1055
36. Nerlekar N, Brown AJ, Muthalaly RG, Talman A, Hettige T, Cameron JD, et al. Association of epicardial adipose tissue and high-risk plaque characteristics: a systematic review and meta-analysis. *J Am Heart Assoc.* (2017) 6:e006379. doi: 10.1161/JAHA.117.006379
37. Mahabadi AA, Balcer B, Dykun I, Forsting M, Schlosser T, Heusch G, et al. Cardiac computed tomography-derived epicardial fat volume and attenuation independently distinguish patients with and without myocardial infarction. *PLoS ONE.* (2017) 12:e0183514. doi: 10.1371/journal.pone.0183514
38. Goeller M, Achenbach S, Marwan M, Doris MK, Cadet S, Commandeur F, et al. Epicardial adipose tissue density and volume are related to subclinical atherosclerosis, inflammation and major adverse cardiac events in asymptomatic subjects. *J Cardiovasc Comput Tomogr.* (2018) 12:67–73. doi: 10.1016/j.jcct.2017.11.007
39. Antonopoulos AS, Sanna F, Sabharwal N, Thomas S, Oikonomou EK, Herdman L, et al. Detecting human coronary inflammation by imaging perivascular fat. *Sci Transl Med.* (2017) 9:eaal2658. doi: 10.1126/scitranslmed.aal2658
40. Oikonomou EK, Marwan M, Desai MY, Mancio J, Alashi A, Hutt Centeno E, et al. Non-invasive detection of coronary inflammation using computed tomography and prediction of residual cardiovascular risk (the CRISP CT study): a post-hoc analysis of prospective outcome data. *Lancet.* (2018) 392:929–39. doi: 10.1016/S0140-6736(18)31114-0
41. Oikonomou EK, Desai MY, Marwan M, Kotanidis CP, Antonopoulos AS, Schottlander D, et al. Perivascular fat attenuation index stratifies cardiac risk associated with high-risk plaques in the CRISP-CT Study. *J Am Coll Cardiol.* (2020) 76:755–7. doi: 10.1016/j.jacc.2020.05.078

42. Joshi NV, Vesey AT, Williams MC, Shah AS, Calvert PA, Craighead FH, et al. 18Ffluoride positron emission tomography for identification of ruptured and high-risk coronary atherosclerotic plaques: a prospective clinical trial. *Lancet.* (2014) 383:705–13. doi: 10.1016/S0140-6736(13)61754-7
43. Guo B, Li Z, Tu P, Tang H, Tu Y. Molecular imaging and non-molecular imaging of atherosclerotic plaque thrombosis. *Front Cardiovasc Med.* (2021) 8:692915. doi: 10.3389/fcvm.2021.692915
44. Andrews JPM, Portal C, Walton T, Macaskill MG, Hadoke PWF, Alcaide Corral C, et al. Non-invasive *in vivo* imaging of acute thrombosis: development of a novel factor XIIIa radiotracer. *Eur Heart J Cardiovasc Imaging.* (2020) 21:673–82. doi: 10.1093/ehjci/jez207
45. Chae SY, Kwon TW, Jin S, Kwon SU, Sung C, Oh SJ, et al. A phase 1, first-in-human study of ^{18}F-GP1 positron emission tomography for imaging acute arterial thrombosis. *EJNMMI Res.* (2019) 9:3. doi: 10.1186/s13550-018-0471-8
46. Gijsen F, Katagiri Y, Barlis P, Bourantas C, Collet C, Coskun U, et al. Expert recommendations on the assessment of wall shear stress in human coronary arteries: existing methodologies, technical considerations, and clinical applications. *Eur Heart J.* (2019) 40:3421–33. doi: 10.1093/eurheartj/ehz551
47. Park JB, Choi G, Chun EJ, Kim HJ, Park J, Jung JH, et al. Computational fluid dynamic measures of wall shear stress are related to coronary lesion characteristics. *Heart.* (2016) 102:1655–61. doi: 10.1136/heartjnl-2016-309299
48. Aide N, Lasnon C, Desmonts C, Armstrong IS, Walker MD, McGowan DR. Advances in PET-CT technology: an update. *Semin Nucl Med.* (2021) S0001-2998:00081-7. doi: 10.1053/j.semnuclmed.2021.10.005
49. Sandfort V, Persson M, Pourmorteza A, Noël PB, Fleischmann D, Willemink MJ. Spectral photon-counting CT in cardiovascular imaging. *J Cardiovasc Comput Tomogr.* (2021) 15:218–25. doi: 10.1016/j.jcct.2020.12.005
50. Veulemans V, Hellhammer K, Polzin A, Bönner F, Zeus T, Kelm M. Current and future aspects of multimodal and fusion imaging in structural and coronary heart disease. *Clin Res Cardiol.* (2018) 107:49–54. doi: 10.1007/s00392-018-1284-5
51. Kolossváry M, Park J, Bang JI, Zhang J, Lee JM, Paeng JC, et al. Identification of invasive and radionuclide imaging markers of coronary plaque vulnerability using radiomic analysis of coronary computed tomography angiography. *Eur Heart J Cardiovasc Imaging.* (2019) 20:1250–8. doi: 10.1093/ehjci/jez033
52. Maragna R, Giacari CM, Guglielmo M, Baggiano A, Fusini L, Guaricci AI, et al. Artificial intelligence based multimodality imaging: a new frontier in coronary artery disease management. *Front Cardiovasc Med.* (2021) 8:736223. doi: 10.3389/fcvm.2021.736223
53. Motwani M, Dey D, Berman DS, Germano G, Achenbach S, Al-Mallah MH, et al. Machine learning for prediction of all-cause mortality in patients with suspected coronary artery disease: a 5-year multicentre prospective registry analysis. *Eur Heart J.* (2017) 38:500–7. doi: 10.1093/eurheartj/ehw188
54. Krittanawong C, Zhang H, Wang Z, Aydar M, Kitai T. Artificial intelligence in precision cardiovascular medicine. *J Am Coll Cardiol.* (2017) 69:2657–64. doi: 10.1016/j.jacc.2017.03.571
55. Barone-Rochette G. Will artificial intelligence change the job of the cardiac imaging specialist? *Arch Cardiovasc Dis.* (2020) 113:1–4. doi: 10.1016/j.acvd.2019.11.002

Conflict of Interest: The authors declare that the research was conducted in the absence of any commercial or financial relationships that could be construed as a potential conflict of interest.

frontiers | Frontiers in Cardiovascular Medicine

REVIEW
published: 02 May 2022
doi: 10.3389/fcvm.2022.823091

The Role of Multimodality Imaging for Percutaneous Coronary Intervention in Patients With Chronic Total Occlusions

Eleonora Melotti[1], *Marta Belmonte*[1], *Carlo Gigante*[1], *Vincenzo Mallia*[1], *Saima Mushtaq*[1], *Edoardo Conte*[1], *Danilo Neglia*[2,3], *Gianluca Pontone*[1], *Carlos Collet*[4], *Jeroen Sonck*[4,5], *Luca Grancini*[1], *Antonio L. Bartorelli*[1,6] *and Daniele Andreini*[1,6]*

[1] Centro Cardiologico Monzino, Istituto di Ricerca e Cura a Carattere Scientifico (IRCCS), Milan, Italy, [2] Fondazione Toscana G. Monasterio, Pisa, Italy, [3] Istituto di Scienze della Vita Scuola Superiore Sant'Anna, Pisa, Italy, [4] Cardiovascular Center Aalst, OLV-Clinic, Aalst, Belgium, [5] Department of Advanced Biomedical Sciences, University of Naples Federico II, Naples, Italy, [6] Department of Biomedical and Clinical Sciences "Luigi Sacco", University of Milan, Milan, Italy

OPEN ACCESS

Edited by:
Antonios Karanasos, Hippokration General Hospital, Greece

Reviewed by:
Alfredo R. Galassi, University of Palermo, Italy
Filippo Cademartiri, Gabriele Monasterio Tuscany Foundation (CNR), Italy
Weichieh Lee, Kaohsiung Chang Gung Memorial Hospital, Taiwan

***Correspondence:**
Daniele Andreini
daniele.andreini@unimi.it

Specialty section:
This article was submitted to Cardiovascular Imaging, a section of the journal Frontiers in Cardiovascular Medicine

Received: *26 November 2021*
Accepted: *13 April 2022*
Published: *02 May 2022*

Citation:
Melotti E, Belmonte M, Gigante C, Mallia V, Mushtaq S, Conte E, Neglia D, Pontone G, Collet C, Sonck J, Grancini L, Bartorelli AL and Andreini D (2022) The Role of Multimodality Imaging for Percutaneous Coronary Intervention in Patients With Chronic Total Occlusions. Front. Cardiovasc. Med. 9:823091. doi: 10.3389/fcvm.2022.823091

Background: Percutaneous coronary intervention (PCI) of Chronic total occlusions (CTOs) has been traditionally considered a challenging procedure, with a lower success rate and a higher incidence of complications compared to non-CTO-PCI. An accurate and comprehensive evaluation of potential candidates for CTO-PCI is of great importance. Indeed, assessment of myocardial viability, left ventricular function, individual risk profile and coronary lesion complexity as well as detection of inducible ischemia are key information that should be integrated for a shared treatment decision and interventional strategy planning. In this regard, multimodality imaging can provide combined data that can be very useful for the decision-making algorithm and for planning percutaneous CTO recanalization.

Aims: The purpose of this article is to appraise the value and limitations of several non-invasive imaging tools to provide relevant information about the anatomical characteristics and functional impact of CTOs that may be useful for the pre-procedural assessment and follow-up of candidates for CTO-PCI. They include echocardiography, coronary computed tomography angiography (CCTA), nuclear imaging, and cardiac magnetic resonance (CMR). As an example, CCTA can accurately delineate CTO location and length, distal coronary bed, vessel tortuosity and calcifications that can predict PCI success, whereas stress CMR, nuclear imaging and stress-CT can provide functional evaluation in terms of myocardial ischemia and viability and perfusion defect extension.

Keywords: multimodality imaging, chronic total occlusion (CTO), cardiac CT, cardiac magnetic resonance, single photon emission computed tomography (SPECT), echocardiography, percutaneous coronary intervention (PCI)

INTRODUCTION

Chronic total occlusions (CTOs) are completely occluded coronary arteries with Thrombolysis In Myocardial Infarction (TIMI) 0 flow with an estimated duration of at least 3 months (1–3) and a prevalence in patients undergoing coronary angiography ranging between 15% and 25% (3–6). Although percutaneous coronary intervention of CTO (CTO-PCI)

is often a challenging procedure, the success rate continues to improve thanks to significant advancements in technology, techniques and operator experience. However, its clinical benefits have been debated for several years and the decision whether to treat patients should be weighted against technical challenges, significant radiation exposure, contrast dose, associated costs, and an overall lower success rate when compared to non-CTO-PCI.

Rationale of CTO Revascularization in Terms of Ischemia Relief, Symptom and Left Ventricular Function Improvement and Reduction of Major Adverse Cardiac Events

The aim of CTO-PCI is to improve myocardial perfusion of the corresponding territory and to relieve ischemia (7, 8). Indeed, viable myocardium subtended by a CTO is generally ischemic, regardless of the extent of collateralization (9, 10). Myocardial ischemia relief after successful CTO revascularization has several positive effects for patients that are discussed below.

With regard to angina and quality of life (QoL), only the DECISION CTO study failed to demonstrate superiority of PCI compared with pharmacological treatment (11). However, several limitations of the trial should be acknowledged including slow and early termination of enrollment, high percentage of cross-over in both arms, high frequency of PCI for non-CTO lesions and inclusion of patients with mild or absent symptoms (11). In contrast, the EuroCTO study (12) and the IMPACTOR CTO study (13) showed, at 1-year follow-up, advantages of percutaneous revascularization in reducing angina and improving QoL assessed with the Seattle Angina Questionnaire (SAQ). Further confirmation of the efficacy of percutaneous revascularization in terms of improvement of symptoms comes from a recent study conducted by Hirai et al. In 1,000 consecutive patients with high-grade refractory angina, they showed that successful CTO-PCI led to higher improvement in the SAQ Angina Frequency and SAQ Summary Scores compared with unsuccessful PCI (14). This suggests that patients who may receive greater benefit from CTO-PCI are those with the highest level of ischemia. Refractory angina in patients with CTO may cause psychological distress and a depressive state. In this regard, the OPEN-CTO registry demonstrated a better QoL due to improvement of the depression-related symptoms (15). In conclusion, most of the available data indicate that CTO-PCI carries advantages in terms of symptom improvement compared with drug therapy alone. In patients without symptoms, ischemic burden evaluation is recommended, and CTO recanalization is indicated if ischemia is present in $\geq$10% of the left ventricle (LV) mass (8, 16).

One of the most investigated aspects of CTO-PCI is the possible improvement of LV systolic function. The REVASC trial showed no differences at 1 year between CTO-PCI and medical therapy in terms of changes in segmental wall thickening (SWT) in the CTO territory (17). However, several factors could have influenced these results. First, the revascularization of non-CTO lesions in the group treated with medical therapy may have increased the collateral flow, leading to recovery of areas of dysfunctional myocardium subtended by the occluded coronary artery in the group of patients without CTO-PCI. This speculation derives from a subgroup analysis showing that improvement in SWT occurred only in patients undergoing CTO revascularization who had less complex CAD (SYNTAX score $<$13). Second, another trial limitation could have been the lack of myocardial viability assessment with cardiac magnetic resonance (CMR) imaging. Indeed, a previous study demonstrated that SWT improved significantly only in patients with $<$75% transmural myocardial infarction (MI) at CMR indicating a significant remaining viable myocardium (18). Third, the mean LV ejection fraction (LVEF) of patients included in the REVASC study was normal (17). In this regard, a recent meta-analysis of 34 studies with 2,804 patients showed that a successful CTO-PCI is associated with a significant improvement of LVEF, especially in patients with lower baseline values (19).

A higher risk of ventricular arrhythmia or appropriate ICD shock has been reported in patients with CTO of an infarct-related coronary artery (IRA) (20). Ventricular arrhythmias in patients with a previous MI arise in the myocardial area surrounding the fibrous scar (21). In patients with CTO, hypoperfusion in this area could represent an arrhythmic substrate that may favor the occurrence of life-threatening arrhythmias. Indeed, a recent meta-analysis that assessed ventricular arrhythmias in patients with CTO has shown that an occluded vessel is associated with an increased risk of ventricular arrhythmia and all-cause mortality (22). Therefore, revascularization of IRA-CTO may generate positive electrical remodeling and reduce the arrhythmic risk by restoring blood flow in the viable myocardium close to the fibrotic scar.

There is a great discordance in the literature regarding hard end points such as mortality and major adverse cardiac events (MACE) between observational studies and randomized clinical trials. In the DECISION CTO trial, which assessed all-cause mortality, MI, revascularization, stroke and MACE, no advantages were found between the PCI group and patients treated only with drugs (11). However, a further limitation of the study, in addition to those already mentioned, was the exclusion of patients with a LVEF $<$30% who are those likely benefitting more from revascularization (23). In contrast, data from several registries showed an increase in survival in patients undergoing successful CTO recanalization compared with those with unsuccessful PCI (24, 25). A meta-analysis of 25 studies including 28,486 patients (26) showed a lower incidence of death, stroke, coronary artery bypass grafting and recurrent angina associated with CTO-PCI as compared to failed procedures. Similarly, in a more recent meta-analysis Li et al. reported possible benefits in terms of all-cause mortality, cardiac death and MACE in patients undergoing CTO revascularization in comparison with those treated with medical therapy (27). Similarly, although not powered for clinical end points, the REVASC study showed that at 12 months the CTO- PCI group had a lower risk of MACE, defined as total mortality, MI and any clinically driven repeat revascularization compared to the group with medical therapy alone (17). In addition, a recent study suggested that patients with no residual ischemia and extensive

ischemic burden reduction after CTO-PCI had lower risk of all-cause death and non-fatal MI with a follow up of 2.8 years (28). Finally, Taek Kyu Park et al. (29) observed that CTO- PCI might reduce a 10-year rate of cardiac and all-cause death compared with optimal medical therapy, as well as that of acute MI and any revascularization.

IMAGING MODALITIES

Echocardiography

Echocardiography for Pre-procedural Assessment

In patients with coronary artery disease (CAD) and in particular in those with CTOs, echocardiography provides important information on global LV function and regional wall motion abnormalities at rest. In order to make a correct indication for CTO revascularization, it is essential to differentiate transmural infarcted myocardium, which cannot benefit from reperfusion, from areas of hibernating but viable myocardium. In this context, transthoracic echocardiography is usually the first technique for myocardial viability assessment. Rosner et al. (30) demonstrated that evidence of normokinetic or slightly hypokinetic myocardium by means of wall motion scores and longitudinal strain measurement has a good negative predictive value for excluding transmural scar, even without the use of dobutamine stress echocardiography. Accordingly, in the latest consensus document for the management of CTO (3) it was agreed that the presence of normal myocardial function or hypokinesia in the CTO territory should be interpreted as a sign of myocardial viability and therefore, when symptoms are present despite optimal medical therapy, the revascularization procedure is indicated. Of note, the Rosner et al. study also showed that severe regional myocardial dysfunction by stress echocardiography is not always a manifestation of a transmural scar, suggesting that akinesia in a myocardial area subtended by a CTO should be further evaluated with other imaging techniques to detect viability and to guide therapeutic decisions. Dobutamine echocardiography is an accurate and reproducible method for detecting hibernating myocardium that may predict functional recovery after PCI (31). Myocardial segments hibernating at rest can improve contractility, showing the so-called "contractile reserve," with low doses of intravenous dobutamine (5–10 micrograms/kg/min), while high doses of dobutamine (up to 40 micrograms/kg/min) can cause LV function worsening due to reduced coronary flow reserve. This biphasic response to dobutamine infusion is frequent in case of hibernating myocardium and seems to predict LV function improvement with high predictive value, as shown by Afridi et al. (32). In a systematic review of 37 studies that looked at different techniques that can predict regional and global improvement of function after revascularization in chronic CAD, Bax et al. reported that low dose dobutamine echocardiography showed the highest predictive accuracy (33). Transesophageal and transthoracic echocardiography may also play a role in the direct identification of CTOs. High sensitivity and specificity of transesophageal echocardiography were demonstrated in the detection of stenotic and occlusive coronary lesions using a modified continuity equation (34). In a study of 110 patients, occlusions of the left anterior descending (LAD) coronary artery and the right coronary artery (RCA), but not of the circumflex (CFX) coronary artery were demonstrated by transthoracic echocardiography with high sensitivity and specificity using retrograde flow in the epicardial and intramyocardial collaterals (35). One of the factors that may predict the success of CTO-PCI is the presence of well-developed collaterals, even if this condition does not seem to guarantee an advantage on survival and prognosis (36). Pizzuto et al. (37) measured in 51 patients the collateral flow reserve in occluded arteries with transthoracic coronary Doppler echocardiography. The measurement of collateral flow reserve (the ratio between hyperemic, during venous adenosine infusion, and baseline diastolic velocity of the stenotic vessel) was feasible and correlated directly with the angiographic evaluation of collaterals and the number of diseased vessels and was found to be inversely related to stenosis of the non-occluded arteries that provide the collaterals. Myocardial contrast echocardiography (MCE) is also a potentially useful method for estimating the microcirculation. Myocardial blood flow measured by MCE and in particular the plateau acoustic intensity, which represents the volume of myocardial flow, and the wall motion score index appear to correlate well with the flow of collateral vessels assessed by coronary angiography (38).

Echocardiography for the Detection of Procedural Complications

Transthoracic echocardiography provides a valid support for a rapid and easy identification of possible complications during and immediately after the revascularization procedure. Coronary perforation represents one of the most feared complications of CTO-PCI with an estimated incidence of 3% (39, 40). It can be responsible for pericardial effusion and tamponade, requiring emergency pericardiocentesis, and in some cases cardiac surgery. Echocardiography plays a key role in the evaluation of pericardial effusion and provides a prompt diagnosis of a life-threatening tamponade. Another well-known complication of CTO-PCI is perforation of a collateral vessel that can occur in 3–7% of cases (39, 40). Some perforations can progress to become septal hematomas, which in turn, can cause hemodynamic compromise through left-sided or biventricular outflow obstruction that can be promptly identified by transthoracic echocardiogram providing operators with detailed information needed for the correct management of the complication (41).

Echocardiography for Post-procedural Evaluation of LV Function

A successful percutaneous treatment of a CTO can improve LV systolic function (42). In a study of 43 patients with CTO treated with PCI, global longitudinal strain assessed with two- dimensional speckle tracking echocardiography (2D-STE) improved from the first day after the procedure, while LVEF tended to improve 3–6 months after the procedure (43). Meng et al. in a recent study of 63 patients with a single CTO demonstrated that at 2-year follow-up only global longitudinal strain and LV systolic function assessed with 2D-STE showed a statistically significant improvement in the group treated with PCI compared to the group receiving medical therapy only (44).

Future Perspective

The introduction of three-dimensional speckle tracking echocardiography (3D STE) may overcome some of 2D STE limitations, such as the need to acquire multiple images and out-of-plane speckle motion (45) improving reproducibility and accuracy. Furthermore, software improvements allowing tissue characterization and identification of myocardial scars may increase the use of transthoracic echocardiography for diagnostic and prognostic evaluation of patients with CTOs (46).

Coronary Computed Tomography Angiography

Coronary Computed Tomography Angiography (CCTA) is emerging as an essential tool in the management of CTOs, from pre-procedural assessment, intraprocedural guidance to follow-up. When compared to other imaging modalities, it is the only non-invasive tool playing a crucial role in the practical guidance of revascularization procedures. Indeed, it is considered as the most comprehensive non-invasive imaging modality for CTO pre-procedural assessment and treatment planning that can dramatically increase the likelihood of successful PCI, especially in case of complex coronary lesions and previous unsuccessful attempts of revascularization.

CCTA for Pre-procedural Assessment

In the pre-procedural assessment of CTOs, CCTA is a potential "one stop shop" to assess anatomy, perfusion and viability in one single examination (47). It allows visualization and evaluation of the entire coronary tree including the CTO lesion, which appears as a "missing segment" when using dual injection at invasive coronary angiography. This is particularly useful in long and tortuous CTOs and in ostial occlusions, in which the definition of the course and the features of the occluded segment are key information for PCI success (48). A precise mapping of lesion tortuosity and distal vessel anatomy may be assessed using 2- and 3-dimensional reconstructions from any arbitrary angle, allowing an accurate measurement of the length, cross-sectional area and diameter of the CTO. Moreover, CCTA provides anatomical details of the atherosclerotic plaque, being highly accurate in defining the presence, location and extent of calcifications and in the description of the morphology of the proximal and distal CTO caps. These anatomical features strongly influence treatment strategy and materials selection for the interventional procedure. In case of heavily calcified lesions, the need for additional lesion pre-treatment such as rotational atherectomy or intravascular lithotripsy can be anticipated. Therefore, the anatomic information provided by CCTA before getting into the catheterization laboratory allow adequate procedural planning, potentially reducing procedural time and contrast dose, which are the most frequent reasons for stopping a CTO-PCI attempt.

A pitfalls of CCTA is the limited spatial resolution that may lead to inaccuracy in differentiating a CTO from an artery subocclusion and inability to visualize collateral vessels, which can be seen only with high-quality exams if the collateral diameter is >1.0 mm. The identification of a CTO could be increased by integrating multiple parameters, including ≥9-mm lesion length (49), presence of an adjacent side branch (most CTOs are imaged as "inter-bifurcation disease"), bridging collaterals and a blunt stump. Intracoronary attenuation-based analyses of CCTA may provide non-invasive functional and anatomical assessment of coronary collateral flow and may detect flow direction, predicting angiographically well-developed collateral vessels, refining the evaluation of complex coronary circulation in patients with CTO (50).

In addition to coronary anatomy evaluation, CCTA could also perform functional assessment of myocardial perfusion and viability by application of appropriate scanner protocols. However, routine use of CCTA for this purpose is not currently available.

CCTA and Prognosis

The detection of CTO at CCTA, which occurs in 6.2% of CAD patients undergoing this non-invasive imaging exam, is associated with a 2-year mortality similar to moderate-to-severe CAD (51). The success rate of CTO-PCI was until recent times about 75–80% (48); nowadays, the marked technological advances in terms of devices, techniques and operator experience have increased the procedural success over 90% but obviously there remains a gap between non-CTO and CTO procedures. Unsuccessful attempts of revascularization are associated with worse outcome (30-day MACE: 14.8 vs. 5.5%), mainly due to a significantly higher rate of MACE in the immediate period following the procedure (52). Therefore, careful selection of patients who are most likely to benefit from revascularization and have a good chance of a successful PCI is essential. CCTA offers the unique opportunity to non-invasively assess anatomical features of CTO that have been shown to predict PCI failure. Calcifications, a well-known hallmark of complex CTO, can be easily detected, localized and quantified by CCTA. Cross-sectional calcium area ≥50% of the vessel area, rather than calcium length, is a strong predictor of lesion crossing difficulty (53). The best cut-off value proposed is ≥54% (54). However, calcium length may influence the subsequent technical steps that follow each other during a contemporary recanalization procedure. The location of calcifications, whether at the proximal or distal cap, could influence the choice of the technical approach and material used. However, a study by Ehara et al. (55) demonstrated that the most prominent independent predictor of guidewire crossing failure was bending (defined as an angle >45° either at the occlusion site or proximal to the occluded segment), which can be missed on coronary angiography and is easily identified on CCTA. With respect to the predictive value of anatomical features, bending is followed by vessel shrinkage, i.e., an abrupt narrowing (<1-mm cross-sectional diameter) of the occluded segment that is indicative of negative remodeling and predictive of failure using an anterograde approach (55). In addition, a blunt stump morphology and the presence of multiple occlusions hampers successful guidewire crossing and passage into the distal true lumen.

Two computed tomography (CT)-based scoring systems, CT-RECTOR and KCCT, combine the previously described anatomical features with clinical characteristics to estimate the complexity of CTO-PCI and to predict the probability of successful guidewire crossing within 30 min. Both scores showed

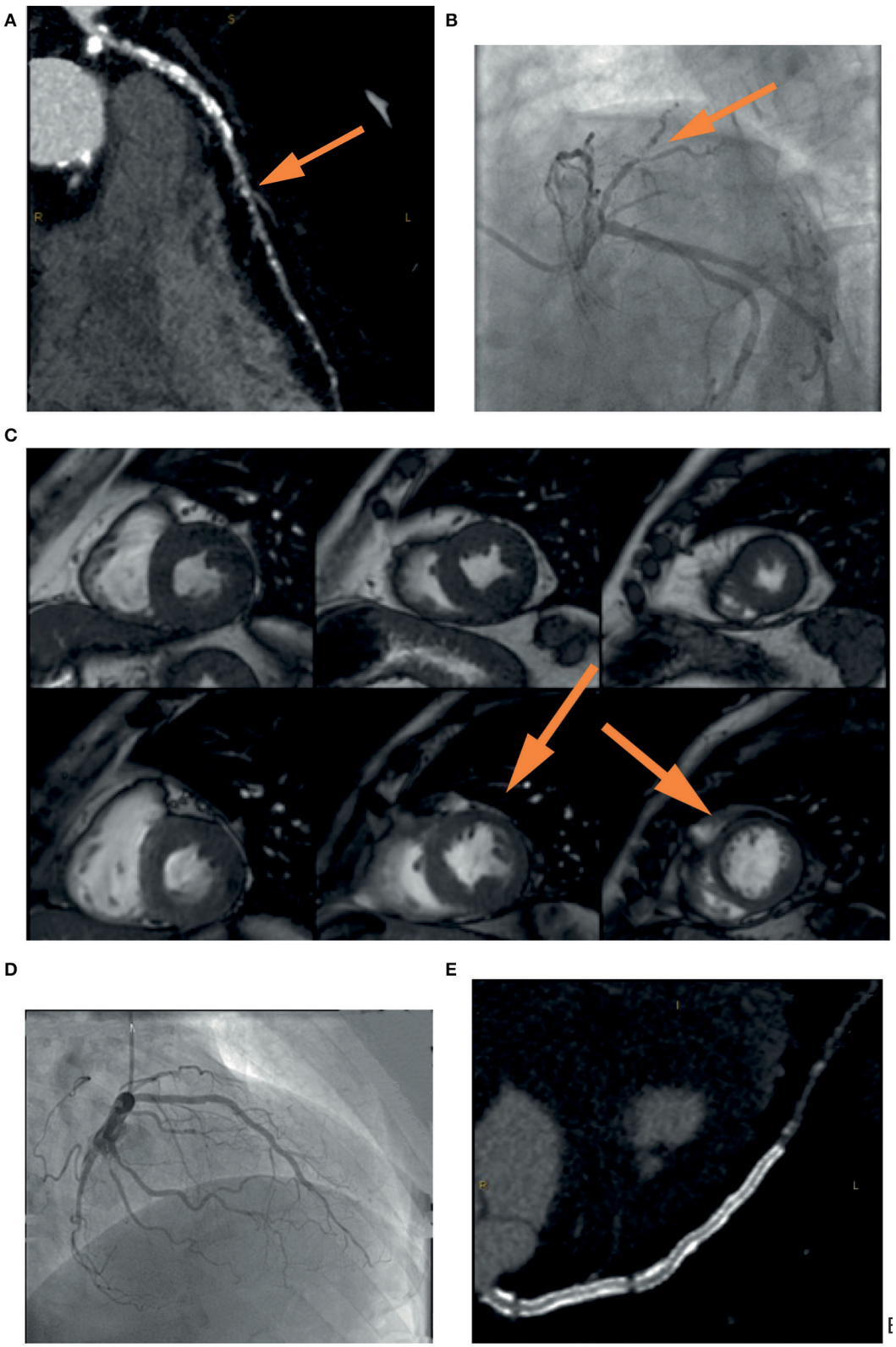

FIGURE 1 | Example of the usefulness of multi-modality imaging in placing a correct indication for CTO percutaneous treatment. A 72-year-old patient performed a coronary computed tomography angiography (CCTA) **(A)** that showed severe three-vessel disease with occlusion (*yellow arrow*) of the left anterior descending (LAD)

(Continued)

FIGURE 1 | coronary artery. Coronary angiography **(B)** confirmed the presence of a calcified lesion occluding the LAD (*yellow arrow*) that was filled by means of collateral circulation. In consideration of the lack of symptoms and the unfavorable anatomy, it was decided not to proceed with a procedure without first assessing ischemia in the territory of the vessel. Cardiac stress magnetic resonance **(C)** showed inducible ischemia and myocardial viability in the mid-apical segment of the anterior wall and the interventricular septum (*yellow arrow*). Coronary angioplasty was then performed with implantation of a drug-eluting stent in the left main and LAD with an excellent result **(D)**. Vessel patency without restenosis was confirmed by coronary CCTA at follow-up **(E)**.

better predictive value than the J-CTO angiographic score (56, 57).

CCTA in PCI Guidance and Future Perspective

The new frontier is the application of CCTA directly in the catheterization laboratory for real time PCI guidance. Advancements in software for identification of centerline and vessel contour allow the fusion of 3D reconstructed CCTA images onto live fluoroscopy images during coronary angiography. To compensate for breathing and heart beating, the extracted CCTA images of the coronary vessels are matched to the diastolic images of the invasive series using bifurcation points as markers. The co-registration helps the identification of projections that minimize foreshortening of the coronary segment of interest and vessel overlap. Moreover, it allows the visualization of the CTO morphological features and the geometry of the luminal path to indicate guidewire direction and advancement. This approach resulted is a significantly higher success rate of CTO-PCI compared with procedures performed without CCTA (58). A more technologically complex approach with continuous co-registration is now possible thanks to dynamic 4D roadmap acquired from multiple phases during the cardiac cycle. Integration of 4D multi-slice data, however, is only achievable off-line for a single respiratory phase. Respiratory gating requires the integration of dedicated sensors using small magnetic fields, such as those employed in the MPS-system from Mediguide (Haifa, Israel) (59). Another innovative technology to guide CTO-PCI is based on precise stereotactic localization and control of the guidewire tip using magnetically enabled guidewire while crossing the lesion. The magnetic navigation technology developed by Stereotaxis, the Niobe® Magnetic Navigation System (MNS, Stereotaxis, Inc., St. Louis, MO, USA) is based on the creation of a uniform magnetic field of 0.08 Tesla within the patient chest by two permanent external magnets placed on either side of the fluoroscopy table. In this magnetic field, the tip of the guidewire, provided with a tiny magnet, can be precisely directed with a full 360° omni-rotation. A virtual roadmap of the coronary tree acquired from 3D volume-rendered CCTA images displays the changes of the magnetic vector as the guidewire is advanced and indicate its position. This technology, in limited experiences, has been shown to increase safety and effectiveness of CTO-PCI, along with a reduction in contrast dose (60). Recently, a novel technology uses a more complex CT approach, which relies on the integration of flat panel detectors positioned on the C-arm of the X-ray machine. Therefore, image acquisition and reconstruction are possible directly during PCI, without the need of patient transfer.

The main limitation of the intra-procedural application of CCTA consists in the need of additional radiation dose and contrast use in patients undergoing PCI. However, the latest CT-scanners have dramatically reduced the amount of radiation and contrast and, at the same time, improved image quality. Since CCTA-guided PCI resulted in reductions of procedural time and complication rates, it could be hypothesized that the net sum of radiation and contrast during these procedures is equal or even lower than that of patients not undergoing CCTA. Future studies will be needed to prove this hypothesis. Moreover, stress myocardial CT perfusion (CT-MPI) and fractional flow reserve derived from CCTA (FFRCT) have been introduced in clinical practice as new tools for evaluating the functional relevance of coronary stenoses, with the possibility to overcome the main CCTA drawback, i.e., anatomical assessment only (61). Conventional CT scanners can be applied for stress myocardial perfusion imaging to diagnose inducible myocardial ischemia, although better image quality can be achieved with more contemporary technology. As for the other stress myocardial imaging modalities, during pharmacologically induced myocardial hyperemia (adenosine, regadenoson, dipyridamol), obstructive CAD causes relative hypoperfusion, which can be visualized through injection of contrast agent. In the specific field of CTO, CT-MPI seems particularly useful, by combining anatomical information on lesion characteristics from CCTA with the presence and extension of ischemia from perfusion assessment and demonstrated high and similar diagnostic performance vs. other non-invasive stress tests to identify flow-limiting coronary lesions at invasive FFR (62–64). Finally, some group of researchers are developing a dedicated tool for a full, real-time integration of anatomical (calcium and atherosclerosis) and functional (FFRCT) CCTA-derived information into the cath lab for the guidance of PCI (65).

Cardiac Magnetic Resonance

Cardiac Magnetic Resonance (CMR) is a high-resolution non-invasive imaging technique that can assess regional and global LV function, as well as detect the presence and the extent of MI and ischemic burden before PCI. CMR could also provide a careful post-procedural evaluation to assess CTO-PCI efficacy.

CMR for Pre-procedural Assessment

CMR is the non-invasive gold standard for the measurement of LV volume and LVEF, showing very high reproducibility, and low intra- and inter-observer variability (66). CMR is also an excellent tool for the evaluation of myocardial viability by means of late gadolinium enhancement (LGE) extent and the response to inotropic drug such as low-dose dobutamine. Moreover, CMR can easily assess ischemia by evaluating perfusion defects and wall motion abnormalities, which are important to define the indication for a revascularization procedure in the presence of a CTO (67).

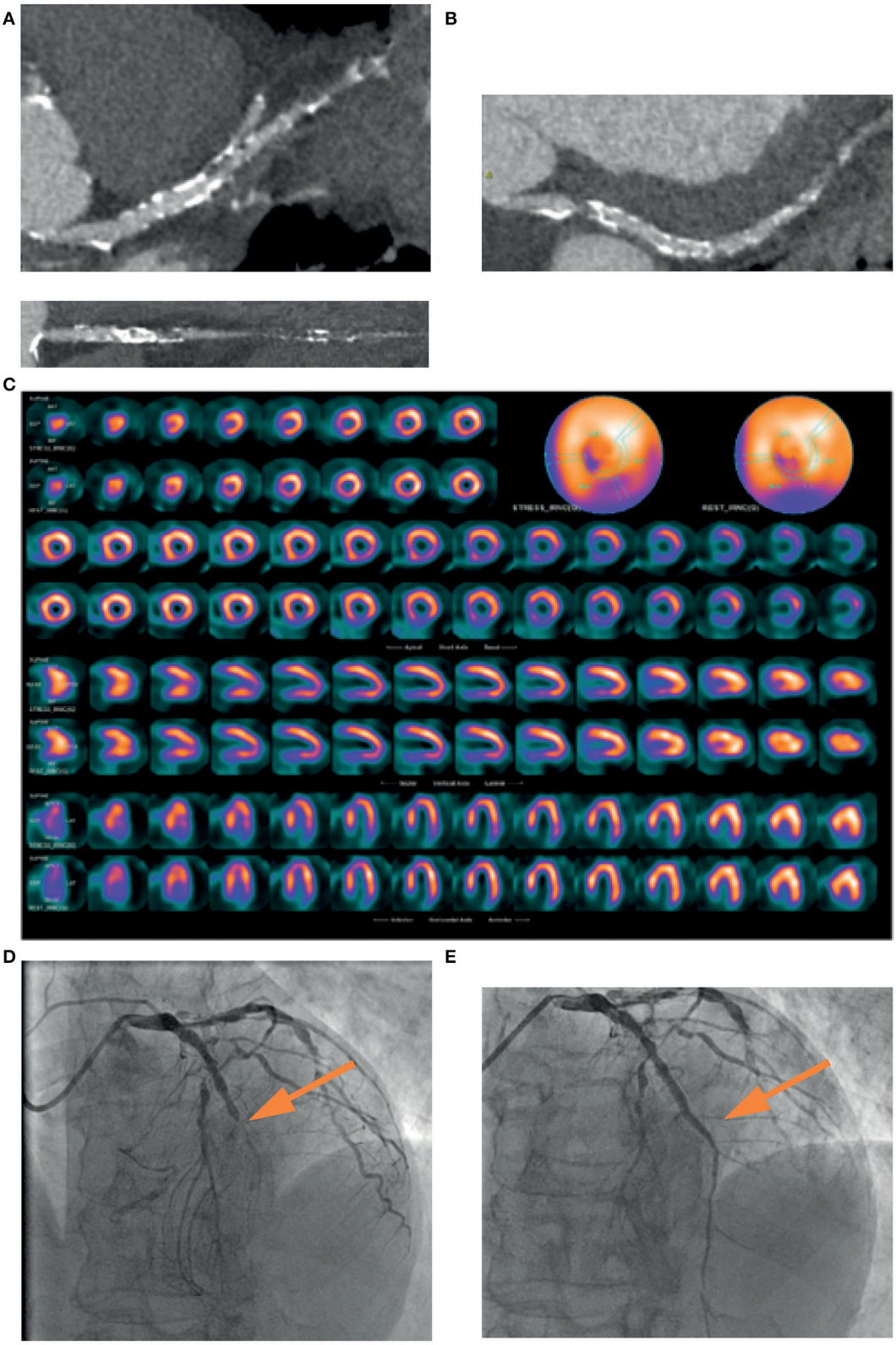

FIGURE 2 | A 74-years-old patient, symptomatic for chest pain, performed a coronary CT, which showed a mild stenosis of left main and a diffuse severe stenosis of mid-distal left anterior descending (LAD) coronary artery **(A)**. Circumflex artery had a significant ostial stenosis, with sub-occlusion of mid-distal portion **(B)** and right artery was occluded at the mid portion **(C)**. SPECT showed perfusion defect at the apical septum and at infero-lateral mid-basal wall **(D)**. Coronary angiography confirmed the presence of sub-occlusion (*yellow arrow*) of the middle section of the LAD coronary artery **(E)**, treated with coronary angioplasty and placement of a medicated stent (*yellow arrow*), with a good final angiographic result **(F)**.

According to the CARISMA-CTO study (67), viability can be defined as <50% of LGE in the region of interest or as an improvement in segment function >1 grade during low-dose dobutamine infusion. LGE has become the most widely used technique for tissue characterization and is considered the cornerstone of myocardial viability assessment. The gadolinium-based contrast agents used for LGE may differentiate viable myocardium from scar in different clinical settings, including MI. The degree of LGE transmurality is related to the time of myocardial ischemia and to the potential functional recovery following revascularization (68). Generally, a transmural extent of 50% is considered a cut-off value to predict contractile function recovery in patients who undergo coronary revascularization. Nakachi et al. showed that, in the CTO territory, longitudinal circumferential strain significantly improved in segments with a LGE extent <50% after CTO-PCI, but not in segments with a transmural extent of LGE >50% (69). However, poor data are available regarding the optimal cut-off value of the transmural extent of LGE at CMR to detect myocardial segments that will functionally recover after CTO recanalization. Although LGE has high sensitivity to detect scar tissue, a study including 71 patients with 122 CTO showed that about one third of segments showing a transmural scar had inside them hibernating myocardium detected by ^{99m}Tc-sestamibi and ^{18}F-FDG imaging. Therefore, CMR seems to be less accurate than CT scan in terms of hibernating myocardium detection (70).

Several CMR parameters have been evaluated to predict LV functional recovery after CTO-PCI. Among them, extracellular volume (ECV) fraction proved to be superior to both LGE and rim thickness for predicting the improvement of regional and global LV function improvement 6 months after revascularization in patients with CTO (71). In addition, novel T1 relaxation time maps ("T1 mapping") offer a quantitative evaluation of diffuse myocardial fibrosis, hence overcoming the limitation of traditional LGE sequences when myocardial abnormalities are present (72).

Regarding the diagnosis of reversible ischemia, stress CMR represents an excellent alternative to other non-invasive stress tests to detect perfusion defects and regional wall motion abnormalities (WMA). Adenosine and high-dose dobutamine stress CMR allows to identify perfusion anomalies and to quantify ischemic burden in CAD patients, especially in those with CTO. Stress CMR is accurate in detecting inducible ischemia due to flow-limiting stenosis of the epicardial coronary arteries (73–75), showing perfusion defects and WMA, and in characterizing hibernating myocardium. Dobutamine stress CMR may also predict recovery of function after revascularization in patients with chronic regional WMA. Functional improvement of hypokinetic or akinetic segments during low-dose dobutamine (5–20 μg/kg/min) has been shown to be more specific than LGE assessment, especially when LGE transmurality is intermediate (<75%) (76). Some groups use a low- and high-dose dobutamine protocol to assess the presence of a biphasic response that may indicate hibernating myocardium. However, most clinicians would use either type of response as a sign of viability to maximize the test sensitivity.

CMR and Prognosis

Several CMR studies have evaluated patients undergoing CTO-PCI, in order to identify which patients may benefit the most from the procedure. In patients undergoing PCI with evidence of ischemia and viability on MRI, an improvement in LVEF and volume have been observed. In patients with CTO, Baks et al. (77) and Kirschbaum et al. (18) demonstrated that after PCI there were both early and late improvements in regional LV function in the perfusion territory of CTO that were related to the transmural extent of MI (LGE extent) on pretreatment CMR imaging. Bellanger et al. (78) showed a significant correlation between the number of viable segments within the infarct zone and end-systolic volume and LVEF improvement at follow-up. Fiocchi et al. (79) showed that segmental contractility improvement during low-dose dobutamine might predict LV function recovery at 6 months after PCI in a small cohort of patients. Bucciarelli-Ducci et al. (80) in 32 patients selected for CTO-PCI based on myocardial viability (LGE <75%) and myocardial ischemia, demonstrated that revascularization significantly reduced inducible ischemia, favored reverse remodeling and improved quality of life. Cardona et al. (81) showed that one third of their patients with successful CTO-PCI also underwent PCI of non-occlusive coronary stenoses. No difference in the degree of LVEF improvement was seen when this group was compared with patients who did not undergo non-CTO-PCI, suggesting that changes in LV function parameters after successful CTO-PCI were derived from CTO recanalization. Rossello et al. (82) proposed a novel CMR ischemic burden index based on the characteristics of perfusion defects. High scores were associated with a greater improvement in exercise tolerance. In contrast, the REVASC trial showed that after successful CTO-PCI there were no improvements in CMR parameters even though there was a reduction in clinical

TABLE 1 | Main features of each imaging modality.

	Low-dose dobutamine echocardiography	CCTA	CMR	PET	SPECT
Radiation exposure (mSv) (91)	0	2–4 mSv	0	^{18}FDG: 5-7 mSv $^{13}NH_3$: 4 mSv	^{99}TC: 20 mSv
Cost	+	++	+++	+++	++
Operator dependency	+++	+	+	+	+
Ischemia quantification (92)	YES	NO	YES	YES	YES
Viability sensitivity (95%CI) (91–93)	81% (80-82)	-	95% (93-97)	93% (91-95)	81% (78-84)
Viability specificity (95%CI) (91)	80% (79-81)	-	51% (40-62)	58% (54-62)	66% (63-69)

end points compared to medical therapy (17). The CARISMA study (67) proposed a multi-parameter CMR protocol tailored on patients suitable for CTO-PCI to evaluate viability with LGE and ischemia with a perfusion and stress study with low- and high-dose dobutamine for identifying those who could most benefit from CTO-PCI.

Future Prospective

The introduction of 3D CMR perfusion imaging represents a promising tool for measurement of myocardial blood flow and an alternative technique to single photon emission computed tomography (SPECT) or positron emission tomography (PET). Compared to the conventional 2D multislice perfusion imaging, 3D CMR allows quantification of the percentage of ischemic myocardium and reduces the scan time by a simultaneous acquisition of all slices at the same point of the cardiac cycle (83). The strain technique was recently applied to CMR in the field of myocardial deformation assessment, facilitating the accurate identification of patients at high risk of future cardiac events who may be candidate of revascularization procedures (84).

Nuclear Cardiac Imaging

Nuclear cardiac imaging can be useful for CTO pre-procedural assessment in terms of evaluation of myocardial viability and ischemia by myocardial perfusion imaging (MPI) and scintigraphy (MPS) studies during stress or rest. MPS can be obtained by two main techniques: single photon emission computed tomography (SPECT) and positron emission tomography (PET). During the tests, a radioactive isotope tracer administered intravenously reaches the viable myocardial cells. Subsequently, photons or positrons are emitted from the myocardium in proportion to the extent of tracer uptake, which correlates with perfusion. Several studies demonstrated that myocardial perfusion defects, found in SPECT MPI, might predict MACE (85). At present, during a SPECT acquisition it is preferred to use a technetium-based tracer instead of the older thallium-201-chloride. The use of technetium, coupled with high count rates gated SPECT allows LV function and myocardial perfusion to be assessed with superior image quality and lower radiation dose (86).

For CTO evaluation, Wright et al. demonstrated that evidence of ischemia on MPI by SPECT with Technetium (^{99m}Tc) sestamibi accurately predicted MACE (death, MI, unstable angina), whereas the demonstration of distal collateralization at angiography alone failed to predict freedom from ischemia and MACE (87).

Moreover, SPECT is a very effective imaging technique for distinguishing viable from non-viable myocardium and for predicting contractile function recovery following revascularization with a mean sensitivity of 84% and mean specificity of 77% (88). This led to a better selection of patients who may derive the higher benefit in terms of both LV function and prognosis.

In PET studies, N-13 ammonia and rubidium-82 are tracers used for rest MPI evaluation, whereas 15O-labeled water and 18F-labeled are agents used to test cardiac glucose metabolism. Preserved glucose metabolism is a sign of cardiac viability in regions without normal resting perfusion. The absence of 18F-FDG uptake, on the other hand, implies a non-viable myocardium.

Compared with SPECT, PET MPI carries various technological advantages, including better space resolution, accurate attenuation correction, a technique that removes soft tissue artifacts, and lower radiation exposure. These benefits are especially important in viability studies because they help identify the existence, amount, and severity of myocardial scars. Moreover, PET MPI is considered the gold standard for non-invasive MPI since it can obtain a quantitative analysis of myocardial blood flow (MBF) and coronary flow reserve using a pharmacological stress (89). These findings allow assessing the condition of both the epicardial and microvascular circulation, providing an absolute quantification of myocardial perfusion.

Using $[^{15}O]H_2O$ PET performed prior and after successful PCI of CTO or non-CTO lesions in patients with preserved LVEF, Schumacher et al. demonstrated that, although myocardial perfusion findings were slightly more hampered in CTO patients before and after PCI, CTO-PCI improved absolute myocardial perfusion and reduced the extent of the perfusion defect similarly to PCI of hemodynamically significant non-CTO lesions, emphasizing that this a useful diagnostic tool in CTO patient selection (90).

Future Perspective

The introduction of hybrid PET/CCTA allows for the precise identification and assessment of myocardial ischemia and viability in conjunction with the evaluation of coronary morphology. As a result, hybrid imaging will be helpful in the clinical work-up of CTO patients to better identify eligibility and plan the strategy of revascularization.

DISCUSSION AND CONCLUSION

At the present time, there are no clear indications from the literature on the preferred imaging method or on the steps to be followed in the pre-procedural evaluation of patients with CTOs (**Figures 1**, **2**). This suggests that knowledge of the limits and advantages of each method represents the starting point for a correct approach and appropriate management.

Stress echocardiogram is an easily accessible and low-cost technique that does not require the administration of contrast or radiation. On the other hand, it is operator-dependent and requires good image quality, even though it is likely that in the near future its accuracy could increase also favored by regional strain evaluation.

Cardiac CT, which requires the administration of radiation and contrast medium, is particularly indicated in the pre-procedural study of complex coronary anatomy. Of note, the latest scan generation has reduced the estimated radiation dose to 2–4 mSv. Stress myocardial computed tomography perfusion (CTP) allows an assessment of the functional relevance of coronary stenoses and could therefore provide information on myocardial viability. However, at present there are no specific studies of its application in patients with CTO.

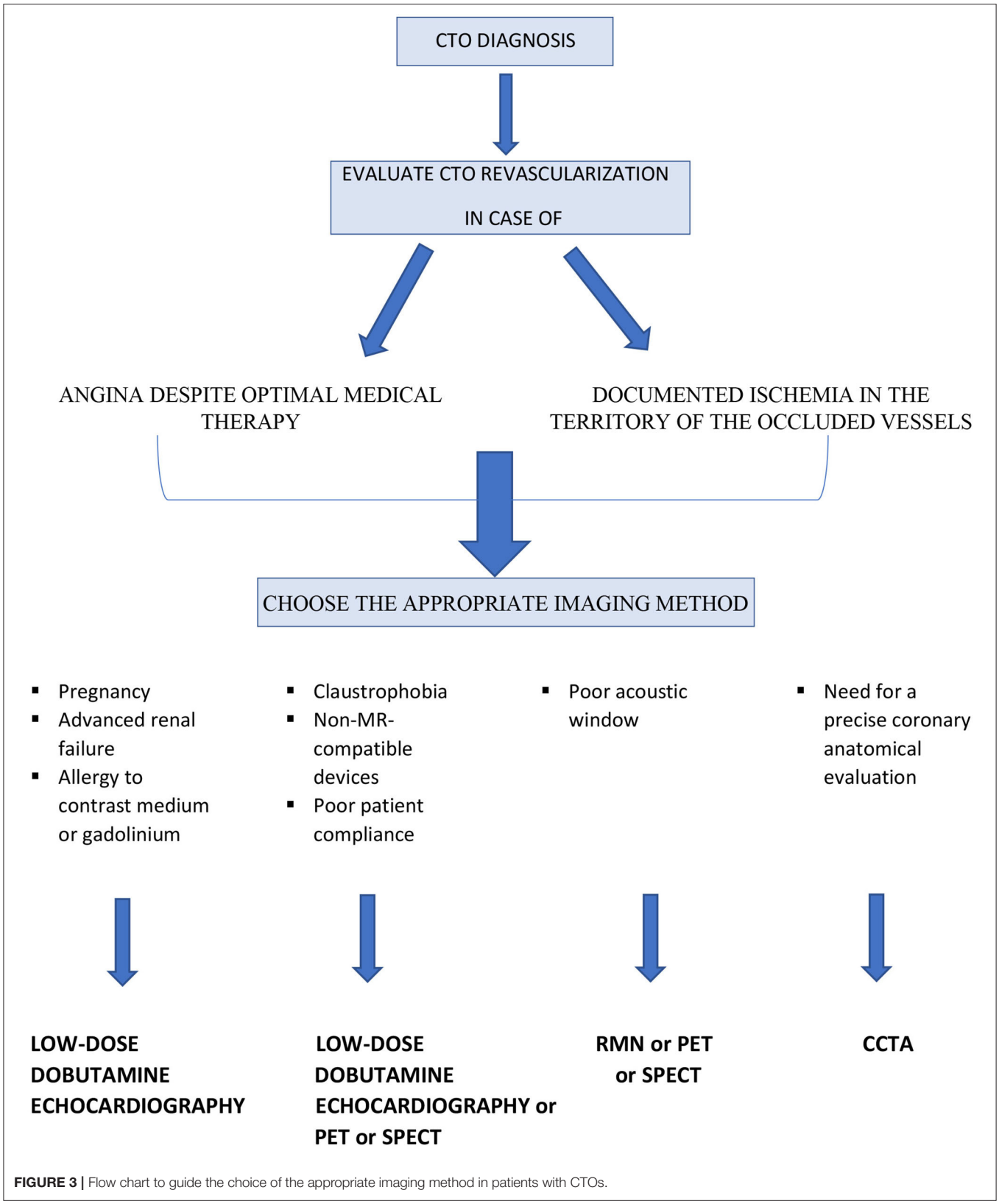

FIGURE 3 | Flow chart to guide the choice of the appropriate imaging method in patients with CTOs.

Cardiac MRI does not use ionizing radiation and has good spatial resolution, sensitivity and specificity in the evaluation of myocardial viability. However, it has significant costs and may have lower sensitivity for hibernating myocardium identification.

SPECT imaging allows measuring LV function and simultaneously evaluating myocardial ischemia but it does not clearly differentiate between non-viable and hibernating myocardium. On the other hand, PET, thanks to the measurement of absolute myocardial flow and coronary flow reserve, has excellent diagnostic accuracy and high sensitivity in the evaluation of myocardial viability, with the limitation of 2–5 mSv radiation exposure and high cost.

Table 1 summarizes the main characteristics of each imaging method. The authors also propose a simple flow chart to guide the clinicians and the interventional cardiologist for selecting the more appropriate imaging modality in patients with CTOs (**Figure 3**).

In conclusion, coronary CTOs represent a diagnostic and therapeutic challenge for the cardiologist. Multimodality imaging and a multidisciplinary team approach are essential for an individualized decision-making and effective treatment planning.

AUTHOR CONTRIBUTIONS

All authors listed have made a substantial, direct, and intellectual contribution to the work and approved it for publication.

REFERENCES

1. Di Mario C, Werner GS, Sianos G, Galassi AR, Büttner J, Dudek D, et al. European perspective in the recanalisation of chronic total occlusions (CTO): consensus document from the EuroCTO Club. *EuroIntervention*. (2007) 3:30–43.
2. Sianos G, Werner GS, Galassi AR, Papafaklis MI, Escaned J, Hildick-Smith D, et al. Recanalisation of chronic total coronary occlusions: 2012 consensus document from the EuroCTO club. *EuroIntervention.* (2012) 8:139–45. doi: 10.4244/EIJV8I1A21
3. Galassi AR, Werner GS, Boukhris M, Azzalini L, Mashayekhi K, Carlino M, et al. Percutaneous recanalisation of chronic total occlusions: 2019 consensus document from the EuroCTO Club. *EuroIntervention.* (2019) 15:198–208. doi: 10.4244/EIJ-D-18-00826
4. Tomasello SD, Boukhris M, Giubilato S, Marza F, Garbo R, Contegiacomo G, et al. Management strategies in patients affected by chronic total occlusions: results from the Italian Registry of Chronic Total Occlusions. *Eur Heart J.* (2015) 36:3189–98. doi: 10.1093/eurheartj/ehv450
5. Azzalini L, Jolicoeur EM, Pighi M, Millan X, Picard F, Tadros VX, et al. Epidemiology, management strategies, and outcomes of patients with chronic total coronary occlusion. *Am J Cardiol.* (2016) 118:1128–35. doi: 10.1016/j.amjcard.2016.07.023
6. Jeroudi OM, Alomar ME, Michael TT, El Sabbagh A, Patel VG, Mogabgab O, et al. Prevalence and management of coronary chronic total occlusions in a tertiary Veterans Affairs hospital. *Catheter Cardiovasc Interv.* (2014) 84:637–43. doi: 10.1002/ccd.25264
7. Azzalini L, Vo M, Dens J, Agostoni P. Myths to debunk to improve management, referral, and outcomes in patients with chronic total occlusion of an epicardial coronary artery. *Am J Cardiol.* (2015) 116:1774–80. doi: 10.1016/j.amjcard.2015.08.050
8. Safley DM, Koshy S, Grantham JA, Bybee KA, House JA, Kennedy KF, et al. Changes in myocardial ischemic burden following percutaneous coronary intervention of chronic total occlusions. *Catheter Cardiovasc Interv.* (2011) 78:337–43. doi: 10.1002/ccd.23002
9. Werner GS, Surber R, Ferrari M, Fritzenwanger M, Figulla HR. The functional reserve of collaterals supplying long-term chronic total coronary occlusions in patients without prior myocardial infarction. *Eur Heart J.* (2006) 27:2406–12. doi: 10.1093/eurheartj/ehl270
10. Sachdeva R, Agrawal M, Flynn SE, Werner GS, Uretsky BF. Reversal of ischemia of donor artery myocardium after recanalization of a chronic total occlusion. *Catheter Cardiovasc Interv.* (2013) 82:E453–8. doi: 10.1002/ccd.25031
11. Lee SW, Lee PH, Ahn JM, Park DW, Yun SC, Han S, et al. Randomized trial evaluating percutaneous coronary intervention for the treatment of chronic total occlusion. *Circulation.* (2019) 139:1674–83. doi: 10.1161/CIRCULATIONAHA.118.031313
12. Werner GS, Martin-Yuste V, Hildick-Smith D, Boudou N, Sianos G, Gelev V, et al. A randomized multicentre trial to compare revascularization with optimal medical therapy for the treatment of chronic total coronary occlusions. *Eur Heart J.* (2018) 39:2484–93. doi: 10.1093/eurheartj/ehy220
13. Obedinskiy AA, Kretov EI, Boukhris M, Kurbatov VP, Osiev AG, Ibn Elhadj Z, et al. The IMPACTOR-CTO Trial. *JACC Cardiovasc Interv.* (2018) 11:1309–11. doi: 10.1016/j.jcin.2018.04.017
14. Hirai T, Grantham JA, Sapontis J, Cohen DJ, Marso SP, Lombardi W, et al. Quality of life changes after chronic total occlusion angioplasty in patients with baseline refractory angina. *Circ Cardiovasc Interv.* (2019) 12:e007558. doi: 10.1161/CIRCINTERVENTIONS.118.007558
15. Yeh RW, Tamez H, Secemsky EA, Conte E, Collet C, Sonck J. et al. Depression and Angina Among Patients Undergoing Chronic Total Occlusion Percutaneous Coronary Intervention: The OPEN-CTO Registry. *JACC Cardiovasc Interv.* (2019) 12:651–8. doi: 10.1016/j.jcin.2018.12.029
16. Galassi AR, Brilakis ES, Boukhris M, Tomasello SD, Sianos G, Karmpaliotis D, et al. Appropriateness of percutaneous revascularization of coronary chronic total occlusions: an overview. *Eur Heart J.* (2016) 37:2692–700. doi: 10.1093/eurheartj/ehv391
17. Mashayekhi K, Nuhrenberg TG, Toma A, Gick M, Ferenc M, Hochholzer W, et al. A randomized trial to assess regional left ventricular function after stent implantation in chronic total occlusion: the REVASC trial. *JACC Cardiovasc Interv.* (2018) 11:1982–91. doi: 10.1016/j.jcin.2018.05.041
18. Kirschbaum SW, Baks T, van den Ent M, Sianos G, Krestin GP, Serruys PW, et al. Evaluation of left ventricular function three years after percutaneous recanalization of chronic total coronary occlusions. *Am J Cardiol.* (2008) 101:179–85. doi: 10.1016/j.amjcard.2007.07.060
19. Megaly M, Saad M, Tajti P, Burke MN, Chavez I, Gössl M, et al. Meta-analysis of the impact of successful chronic total occlusion percutaneous coronary intervention on left ventricular systolic function and reverse remodeling. *J Interv Cardiol.* (2018) 31:562–71. doi: 10.1111/joic.12538
20. Nombela-Franco L, Mitroi CD, Fernández-Lozano I, García-Touchard A, Toquero J, Castro-Urda V, et al. Ventricular arrhythmias among implantable cardioverterdefibrillator recipients for primary prevention: impact of chronic total coronary occlusion (VACTO Primary Study). *Circ Arrhythm Electrophysiol.* (2012) 5:147–54. doi: 10.1161/CIRCEP.111.968008
21. Tse G. Mechanisms of cardiac arrhythmias. *J Arrhythm.* (2016) 32:75–81. doi: 10.1016/j.joa.2015.11.003
22. Chi WK, Gong M, Bazoukis G, Yan BP, Letsas KP, Liu T, et al. Impact of coronary artery chronic total occlusion on arrhythmic and mortality outcomes: a systematic review and meta-analysis. *JACC Clin Electrophysiol.* (2018) 4:1214–23. doi: 10.1016/j.jacep.2018.06.011
23. Galassi AR, Boukhris M, Toma A, Elhadj Z, Laroussi L, Gaemperli O, et al. Percutaneous coronary intervention of chronic total occlusions in patients with low left ventricular ejection fraction. *JACC Cardiovasc Interv.* (2017) 10:2158–70. doi: 10.1016/j.jcin.2017.06.058
24. Choi IJ, Koh YS, Lim S, Choo EH, Kim JJ, Hwang BH, et al. Impact of percutaneous coronary intervention for chronic total occlusion in non-infarct-related arteries in patients with acute myocardial infarction

(from the COREA-AMI Registry). *Am J Cardiol.* (2016) 117:1039–46. doi: 10.1016/j.amjcard.2015.12.049
25. Park JY, Choi BG, Rha SW, Kang TS, Choi CU, Yu CW, et al. Chronic total occlusion intervention of the non-infarct-related artery in acute myocardial infarction patients: the Korean multicenter chronic total occlusion registry. *Coron Artery Dis.* (2018) 29:495–501. doi: 10.1097/MCA.0000000000000630
26. Christakopoulos GE, Christopoulos G, Carlino M, Jeroudi OM, Roesle M, Rangan BV, et al. Meta-analysis of clinical outcomes of patients who underwent percutaneous coronary interventions for chronic total occlusions. *Am J Cardiol.* (2015) 115:1367–75. doi: 10.1016/j.amjcard.2015.02.038
27. Li KHC, Wong KHG, Gong M, Liu T, Li G, Xia Y, et al. Percutaneous coronary intervention versus medical therapy for chronic total occlusion of coronary arteries: a systematic review and meta-analysis. *Curr Atheroscler Rep.* (2019) 21:42. doi: 10.1007/s11883-019-0804-8
28. Schumacher SP, Stuijfzand WJ, de Winter RW, van Diemen PA, Bom MJ, Everaars H, et al. Ischemic Burden Reduction and Long-Term Clinical Outcomes After Chronic Total Occlusion. *Percutaneous.* (2021) 14:1407–18. doi: 10.1016/j.jcin.2021.04.044
29. Park TK, Lee SH, Choi KH, Lee JM, Yang JH, Song YB, et al. Late survival benefit of percutaneous coronary intervention compared with medical therapy in patients with coronary chronic total occlusion: a 10-year follow-up study. *J Am Heart Assoc.* (2021) 10:e019022. doi: 10.1161/JAHA.120.019022
30. Rosner A, Avenarius D, Malm S, Iqbal A, Bijnens B, Schirmer H. Severe regional myocardial dysfunction by stress echocardiography does not predict the presence of transmural scarring in chronic coronary artery disease. *Eur Heart J Cardiovasc Imaging.* (2015) 16:1074–81. doi: 10.1093/ehjci/jev096
31. Wijns W, Vatner SF, Camici PG. Hibernating myocardium. *N Engl J Med.* (1998) 339:173–81. doi: 10.1056/NEJM199807163390307
32. Afridi I, Kleiman NS, Raizner AE, Zoghbi WA. Dobutamine echocardiography in myocardial hibernation. Optimal dose and accuracy in predicting recovery of ventricular function after coronary angioplasty. *Circulation.* (1995) 91:663–70. doi: 10.1161/01.CIR.91.3.663
33. Bax JJ, Wijns W, Cornel JH, Visser FC, Boersma E, Fioretti PM. Accuracy of currently available techniques for prediction of functional recovery after revascularization in patients with left ventricular dysfunction due to chronic coronary artery disease: comparison of pooled data. *J Am Coll Cardiol.* (1997) 30:1451–60. doi: 10.1016/S0735-1097(97)00352-5
34. Vrublevsky AV, Boshchenko AA, Karpov RS. Diagnostics of main coronary artery stenoses and occlusions: multiplane transoesophageal Doppler echocardiographic assessment. *Eur J Echocardiogr.* (2001) 2:170–7. doi: 10.1053/euje.2001.0092
35. Boshchenko AA, Vrublevsky AV, Karpov RS. Transthoracic echocardiography in the detection of chronic total coronary artery occlusion. *Eur J Echocardiogr.* (2009) 10:62–8. doi: 10.1093/ejechocard/jen159
36. Allahwala UK, Kott K, Bland A, Ward M, Bhindi R. Predictors and prognostic implications of well-matured coronary collateral circulation in patients with a chronic total occlusion (CTO). *Int Heart J.* (2020) 61:223–30. doi: 10.1536/ihj.19-456
37. Pizzuto F, Voci P, Puddu PE, Chiricolo G, Borzi M, Romeo F. Functional assessment of the collateral-dependent circulation in chronic total coronary occlusion using transthoracic Doppler ultrasound and venous adenosine infusion. *Am J Cardiol.* (2006) 98:197–203. doi: 10.1016/j.amjcard.2006.01.075
38. Cho JS, Her SH, Youn HJ, Kim CJ, Park MW, Kim GH, et al. Usefulness of the parameters of quantitative myocardial perfusion contrast echocardiography in patients with chronic total occlusion and collateral flow. *Echocardiography.* (2015) 32:475–82. doi: 10.1111/echo.12663
39. Patel VG, Brayton KM, Tamayo A, Mogabgab O, Michael TT, Lo N, et al. Angiographic success and procedural complications in patients undergoing percutaneous coronary chronic total occlusion interventions: a weighted meta-analysis of 18,061 patients from 65 studies. *JACC Cardiovasc Interv.* (2013) 6:128–36. doi: 10.1016/j.jcin.2012.10.011
40. Patel Y, Depta JP, DeMartini TJ. Complications of chronic total occlusion percutaneous coronary intervention. *Interv Cardiol.* (2013) 5:567–75. doi: 10.2217/ica.13.48
41. Doshi D, Hatem R, Masoumi A, Karmapaliotis D. A case report of right ventricular compression from a septal haematoma during retrograde coronary intervention to a chronic total occlusion. *Eur Heart J Case Rep.* (2019) 3:ytz089. doi: 10.1093/ehjcr/ytz089
42. Sirnes PA, Myreng Y, Molstad P, Bonarjee V, Golf S. Improvement in left ventricular ejection fraction and wall motion after successful recanalization of chronic coronary occlusions. *Eur Heart J.* (1998) 19:273–81. doi: 10.1053/euhj.1997.0617
43. Wang P, Liu Y, Ren L. Evaluation of left ventricular function after percutaneous recanalization of chronic coronary occlusions: The role of two-dimensional speckle tracking echocardiography. *Herz.* (2019) 44:170–4. doi: 10.1007/s00059-017-4663-1
44. Meng S, Qiu L, Wu J, Huang R, Wang H. Two-year left ventricular systolic function of percutaneous coronary intervention vs optimal medical therapy for patients with single coronary chronic total occlusion. *Echocardiography.* (2021) 38:368–73. doi: 10.1111/echo.14976
45. Collier P, Phelan D, Klein A. A test in context: myocardial strain measured by speckle-tracking echocardiography. *J Am Coll Cardiol.* (2017) 69:1043–56. doi: 10.1016/j.jacc.2016.12.012
46. Gaibazzi N, Bianconcini M, Marziliano N, Parrini I, Conte MR, Siniscalchi C, et al. Scar detection by pulse-cancellation echocardiography: validation by CMR in patients with recent STEMI. *JACC Cardiovasc Imaging.* (2016) 9:1239–51. doi: 10.1016/j.jcmg.2016.01.021
47. Opolski MP, Achenbach S, CT. Angiography for revascularization of CTO: crossing the borders of diagnosis and treatment. *JACC Cardiovasc Imaging.* (2015) 8:846–58. doi: 10.1016/j.jcmg.2015.05.001
48. Estevez-Loureiro R, Ghione M, Kilickesmez K, Agudo P, Lindsay A, Di Mario C. The role for adjunctive image in pre-procedural assessment and peri-procedural management in chronic total occlusion recanalisation. *Curr Cardiol Rev.* (2014) 10:120–6. doi: 10.2174/1573403X10666140331143731
49. von Erffa J, Ropers D, Pflederer T, Schmid M, Marwan M, Daniel WG, et al. Differentiation of total occlusion and high-grade stenosis in coronary CT angiography. *Eur Radiol.* (2008) 18:2770–5. doi: 10.1007/s00330-008-1068-9
50. Choi JH, Kim EK, Kim SM, Song YB, Hahn JY, Choi SH, et al. Noninvasive evaluation of coronary collateral arterial flow by coronary computed tomographic angiography. *Circ Cardiovasc Imaging.* (2014) 7:482–90. doi: 10.1161/CIRCIMAGING.113.001637
51. Opolski MP, Gransar H, Lu Y, Achenbach S, Al-Mallah MH, Andreini D, et al. Prognostic value of chronic total occlusions detected on coronary computed tomographic angiography. *Heart.* (2019) 105:196–203. doi: 10.1136/heartjnl-2017-312907
52. Hoye A, van Domburg RT, Sonnenschein K, Serruys PW. Percutaneous coronary intervention for chronic total occlusions: the Thoraxcenter experience 1992–2002. *Eur Heart J.* (2005) 26:2630–6. doi: 10.1093/eurheartj/ehi498
53. Mollet NR, Hoye A, Lemos PA, Cademartiri F, Sianos G, McFadden EP, et al. Value of preprocedure multislice computed tomographic coronary angiography to predict the outcome of percutaneous recanalization of chronic total occlusions. *Am J Cardiol.* (2005) 95:240–3. doi: 10.1016/j.amjcard.2004.09.009
54. Cho JR, Kim YJ, Ahn CM, Moon JY, Kim JS, Kim HS, et al. Quantification of regional calcium burden in chronic total occlusion by 64-slice multi-detector computed tomography and procedural outcomes of percutaneous coronary intervention. *Int J Cardiol.* (2010) 145:9–14. doi: 10.1016/j.ijcard.2009.05.006
55. Ehara M, Terashima M, Kawai M, Matsushita S, Tsuchikane E, Kinoshita Y, et al. Impact of multislice computed tomography to estimate difficulty in wire crossing in percutaneous coronary intervention for chronic total occlusion. *J Invasive Cardiol.* (2009) 21:575–82.
56. Yu CW, Lee HJ, Suh J, Lee NH, Park SM, Park TK, et al. Coronary computed tomography angiography predicts guidewire crossing and success of percutaneous intervention for chronic total occlusion: Korean multicenter CTO CT registry score as a tool for assessing difficulty in chronic total occlusion percutaneous coronary intervention. *Circ Cardiovasc Imaging.* (2017) 10:e005800. doi: 10.1161/CIRCIMAGING.116.005800
57. Tan Y, Zhou J, Zhang W, Zhou Y, Du L, Tian F, et al. Comparison of CT-RECTOR and J-CTO scores to predict chronic total occlusion difficulty for percutaneous coronary intervention. *Int J Cardiol.* (2017) 235:169–75. doi: 10.1016/j.ijcard.2017.02.008
58. Rolf A, Werner GS, Schuhback A, Rixe J, Mollmann H, Nef HM, et al. Preprocedural coronary CT angiography significantly improves success rates

of PCI for chronic total occlusion. *Int J Cardiovasc Imaging.* (2013) 29:1819–27. doi: 10.1007/s10554-013-0258-y
59. Jeron A, Fredersdorf S, Debl K, Oren E, Izmirli A, Peleg A, et al. First-in-man (FIM) experience with the magnetic medical positioning system (MPS) for intracoronary navigation. *EuroIntervention.* (2009) 5:552–7. doi: 10.4244/EIJV5I5A90
60. Ramcharitar S, Pugliese F, Schultz C, Ligthart J, de Feyter P, Li H, et al. Integration of multislice computed tomography with magnetic navigation facilitates percutaneous coronary interventions without additional contrast agents. *J Am Coll Cardiol.* (2009) 53:741–6. doi: 10.1016/j.jacc.2008.10.050
61. Conte E, Sonck J, Mushtaq S, Collet C, Mizukami T, Barbato E, et al. FFRCT and CT perfusion: a review on the evaluation of functional impact of coronary artery stenosis by cardiac CT. *Int J Cardiol.* (2020) 300:289–96. doi: 10.1016/j.ijcard.2019.08.018
62. Takx RA, Blomberg BA, El Aidi H, Habets J, de Jong PA, Nagel E, et al. Diagnostic accuracy of stress myocardial perfusion imaging compared to invasive coronary angiography with fractional flow reserve meta-analysis. *Circ Cardiovasc Imaging.* (2015) 8:e002666. doi: 10.1161/CIRCIMAGING.114.002666
63. Mushtaq S, Conte E, Pontone G, Baggiano A, Annoni A, Formenti A, et al. State-of-the-art-myocardial perfusion stress testing: static CT perfusion. *J Cardiovasc Comput Tomogr*. (2019).
64. Andreini D, Mushtaq S, Pontone G, Conte E, Collet C, Sonck J, et al. CT perfusion versus coronary ct angiography in patients with suspected in-stent restenosis or cad progression. *J Am Coll Cardiol Img*. (2020) 13:732–42. doi: 10.1016/j.jcmg.2019.05.031
65. Collet C, Sonck J, Leipsic J, Monizzi G, Buytaert D, Kitslaar P, et al. Implementing coronary computed tomography angiography in the catheterization laboratory. *JACC Cardiovasc Imaging.* (2021) 14:1846–55. doi: 10.1016/j.jcmg.2020.07.048
66. Bellenger NG, Burgess MI, Ray SG, Lahiri A, Coats AJ, Cleland JG, et al. Comparison of left ventricular ejection fraction and volumes in heart failure by echocardiography, radionuclide ventriculography and cardiovascular magnetic resonance; are they interchangeable? *Eur Heart J.* (2000) 21:1387–96. doi: 10.1053/euhj.2000.2011
67. Pica S, Di Giovine G, Bollati M, Testa L, Bedogni F, Camporeale A, et al. Cardiac magnetic resonance for ischaemia and viability detection. Guiding patient selection to revascularization in coronary chronic total occlusions: The CARISMA_CTO study design. *Int J Cardiol.* (2018) 272:356–62. doi: 10.1016/j.ijcard.2018.08.061
68. Eitel I, de Waha S, Wohrle J, Fuernau G, Lurz P, Pauschinger M, et al. Comprehensive prognosis assessment by CMR imaging after ST-segment elevation myocardial infarction. *J Am Coll Cardiol.* (2014) 64:1217–26. doi: 10.1016/j.jacc.2014.06.1194
69. Nakachi T, Kato S, Kirigaya H, Iinuma N, Fukui K, Saito N, et al. Prediction of functional recovery after percutaneous coronary revascularization for chronic total occlusion using late gadolinium enhanced magnetic resonance imaging. *J Cardiol.* (2017) 69:836–42. doi: 10.1016/j.jjcc.2017.01.002
70. Wang L, Lu MJ, Feng L, Wang J, Fang W, He ZX, et al. Relationship of myocardial hibernation, scar, and angiographic collateral flow in ischemic cardiomyopathy with coronary chronic total occlusion. *J Nucl Cardiol.* (2019) 26:1720–30. doi: 10.1007/s12350-018-1241-8
71. Chen Y, Zheng X, Jin H, Deng S, Ren D, Greiser A, et al. Role of myocardial extracellular volume fraction measured with magnetic resonance imaging in the prediction of left ventricular functional outcome after revascularization of chronic total occlusion of coronary arteries. *Korean J Radiol.* (2019) 20:83–93. doi: 10.3348/kjr.2018.0069
72. Haaf P, Garg P, Messroghli DR, Broadbent DA, Greenwood JP, Plein S. Cardiac T1 mapping and extracellular volume (ECV) in clinical practice: a comprehensive review. *J Cardiovasc Magn Reson.* (2016) 18:89. doi: 10.1186/s12968-016-0308-4
73. Pennell DJ, Underwood SR, Manzara CC, Swanton RH, Walker JM, Ell PJ, et al. Magnetic resonance imaging during dobutamine stress in coronary artery disease. *Am J Cardiol.* (1992) 70:34–40. doi: 10.1016/0002-9149(92)91386-I
74. Hundley WG, Hamilton CA, Thomas MS, Herrington DM, Salido TB, Kitzman DW, et al. Utility of fast cine magnetic resonance imaging and display for the detection of myocardial ischemia in patients not well suited for second harmonic stress echocardiography. *Circulation.* (1999) 100:1697–702. doi: 10.1161/01.CIR.100.16.1697
75. Nagel E, Lehmkuhl HB, Bocksch W, Klein C, Vogel U, Frantz E, et al. Noninvasive diagnosis of ischemia-induced wall motion abnormalities with the use of high-dose dobutamine stress MRI: comparison with dobutamine stress echocardiography. *Circulation.* (1999) 99:763–70. doi: 10.1161/01.CIR.99.6.763
76. Arai AE. The cardiac magnetic resonance (CMR) approach to assessing myocardial viability. *J Nucl Cardiol.* (2011) 18:1095–102. doi: 10.1007/s12350-011-9441-5
77. Baks T, van Geuns RJ, Duncker DJ, Cademartiri F, Mollet NR, Krestin GP, et al. Prediction of left ventricular function after drug-eluting stent implantation for chronic total coronary occlusions. *J Am Coll Cardiol.* (2006) 47:721–5. doi: 10.1016/j.jacc.2005.10.042
78. Bellenger NG, Yousef Z, Rajappan K, Marber MS, Pennell DJ. Infarct zone viability influences ventricular remodelling after late recanalisation of an occluded infarct related artery. *Heart.* (2005) 91:478–83. doi: 10.1136/hrt.2004.034918
79. Fiocchi F, Sgura F, Di Girolamo A, Ligabue G, Ferraresi S, Rossi R, et al. Chronic total coronary occlusion in patients with intermediate viability: value of low-dose dobutamine and contrast-enhanced 3-T MRI in predicting functional recovery in patients undergoing percutaneous revascularisation with drug-eluting stent. *Radiol Med.* (2009) 114:692–704. doi: 10.1007/s11547-009-0426-2
80. Bucciarelli-Ducci C, Auger D, Di Mario C, Locca D, Petryka J, O'Hanlon R, et al. CMR guidance for recanalization of coronary chronic total occlusion. *JACC Cardiovasc Imaging.* (2016) 9:547–56. doi: 10.1016/j.jcmg.2015.10.025
81. Cardona M, Martin V, Prat-Gonzalez S, Ortiz JT, Perea RJ, de Caralt TM, et al. Benefits of chronic total coronary occlusion percutaneous intervention in patients with heart failure and reduced ejection fraction: insights from a cardiovascular magnetic resonance study. *J Cardiovasc Magn Reson.* (2016) 18:78. doi: 10.1186/s12968-016-0287-5
82. Rossello X, Pujadas S, Serra A, Bajo E, Carreras F, Barros A, et al. Assessment of inducible myocardial ischemia, quality of life, and functional status after successful percutaneous revascularization in patients with chronic total coronary occlusion. *Am J Cardiol.* (2016) 117:720–6. doi: 10.1016/j.amjcard.2015.12.001
83. Motwani M, Kidambi A, Sourbron S, Fairbairn TA, Uddin A, Kozerke S, et al. Quantitative three-dimensional cardiovascular magnetic resonance myocardial perfusion imaging in systole and diastole. *J Cardiovasc Magn Reson.* (2014) 16:19. doi: 10.1186/1532-429X-16-19
84. Korosoglou G, Gitsioudis G, Voss A, Lehrke S, Riedle N, Buss SJ, et al. Strain-encoded cardiac magnetic resonance during high-dose dobutamine stress testing for the estimation of cardiac outcomes: comparison to clinical parameters and conventional wall motion readings. *J Am Coll Cardiol.* (2011) 58:1140–9. doi: 10.1016/j.jacc.2011.03.063
85. Mowatt G, Brazzelli M, Gemmell H, Hillis GS, Metcalfe M, Vale L, et al. Systematic review of the prognostic effectiveness of SPECT myocardial perfusion scintigraphy in patients with suspected or known coronary artery disease and following myocardial infarction. *Nucl Med Commun.* (2005) 26:217–29. doi: 10.1097/00006231-200503000-00006
86. Berman DS, Kiat H, Maddahi J. The new 99mTc myocardial perfusion imaging agents: 99mTc-sestamibi and 99mTc-teboroxime. *Circulation.* (1991) 84:I7–21.
87. Wright S, Lichtenstein M, Grigg L, Sivaratnam D. Myocardial perfusion imaging (MPI) is superior to the demonstration of distal collaterals in predicting cardiac events in chronic total occlusion (CTO). *J Nucl Cardiol.* (2013) 20:563–8. doi: 10.1007/s12350-013-9678-2
88. Camici PG, Prasad SK, Rimoldi OE. Stunning, hibernation, and assessment of myocardial viability. *Circulation.* (2008) 117:103–14. doi: 10.1161/CIRCULATIONAHA.107.702993
89. Murthy VL, Naya M, Foster CR, Hainer J, Gaber M, Di Carli G, et al. Improved cardiac risk assessment with noninvasive measures of coronary flow reserve.

Circulation. (2011) 124:2215–24. doi: 10.1161/CIRCULATIONAHA.111.050427

90. Schumacher SP, Driessen RS, Stuijfzand WJ, Raijmakers PG, Danad I, Dens J, et al. Recovery of myocardial perfusion after percutaneous coronary intervention of chronic total occlusions is comparable to hemodynamically significant non-occlusive lesions. *Catheter Cardiovasc Interv*. (2019) 93:1059–66. doi: 10.1002/ccd.27945
91. Almeida AG, Carpenter JP, Cameli M, Donal E, Dweck MR, Flachskampf FA, et al. Multimodality imaging of myocardial viability: an expert consensus document from the european association of cardiovascular imaging (EACVI). *Eur Heart J Cardiovasc Imaging*. (2021) 22:e97–125. doi: 10.1093/ehjci/jeab053
92. Allahwala UK, Brilakis ES, Kiat H, Ayesa S, Nour D, Ward M, et al. The indications and utility of adjunctive imaging modalities for chronic total occlusion (CTO) intervention. *J Nucl Cardiol*. (2020). doi: 10.1007/s12350-020-02381-0
93. Romero J, Xue X, Gonzalez W, Garcia MJ. CMR imaging assessing viability in patients with chronic ventricular dysfunction due to coronary artery disease: a meta-analysis of prospective trials. *JACC Cardiovasc Imaging*. (2012) 5:494–508. doi: 10.1016/j.jcmg.2012.02.009

Conflict of Interest: The authors declare that the research was conducted in the absence of any commercial or financial relationships that could be construed as a potential conflict of interest.

The reviewer FC declared a shared affiliation, though no other collaboration, with one of the authors DN to the handling Editor.

Advantages of publishing in Frontiers

OPEN ACCESS
Articles are free to read for greatest visibility and readership

FAST PUBLICATION
Around 90 days from submission to decision

HIGH QUALITY PEER-REVIEW
Rigorous, collaborative, and constructive peer-review

TRANSPARENT PEER-REVIEW
Editors and reviewers acknowledged by name on published articles

Frontiers
Avenue du Tribunal-Fédéral 34
1005 Lausanne | Switzerland

Visit us: www.frontiersin.org
Contact us: frontiersin.org/about/contact

REPRODUCIBILITY OF RESEARCH
Support open data and methods to enhance research reproducibility

DIGITAL PUBLISHING
Articles designed for optimal readership across devices

FOLLOW US
@frontiersin

IMPACT METRICS
Advanced article metrics track visibility across digital media

EXTENSIVE PROMOTION
Marketing and promotion of impactful research

LOOP RESEARCH NETWORK
Our network increases your article's readership